Terms and Conditions of Use of Digitised Theses from Trinity College Library Dublin

Copyright statement

All material supplied by Trinity College Library is protected by copyright (under the Copyright and Related Rights Act, 2000 as amended) and other relevant Intellectual Property Rights. By accessing and using a Digitised Thesis from Trinity College Library you acknowledge that all Intellectual Property Rights in any Works supplied are the sole and exclusive property of the copyright and/or other IPR holder. Specific copyright holders may not be explicitly identified. Use of materials from other sources within a thesis should not be construed as a claim over them.

A non-exclusive, non-transferable licence is hereby granted to those using or reproducing, in whole or in part, the material for valid purposes, providing the copyright owners are acknowledged using the normal conventions. Where specific permission to use material is required, this is identified and such permission must be sought from the copyright holder or agency cited.

Liability statement

By using a Digitised Thesis, I accept that Trinity College Dublin bears no legal responsibility for the accuracy, legality or comprehensiveness of materials contained within the thesis, and that Trinity College Dublin accepts no liability for indirect, consequential, or incidental, damages or losses arising from use of the thesis for whatever reason. Information located in a thesis may be subject to specific use constraints, details of which may not be explicitly described. It is the responsibility of potential and actual users to be aware of such constraints and to abide by them. By making use of material from a digitised thesis, you accept these copyright and disclaimer provisions. Where it is brought to the attention of Trinity College Library that there may be a breach of copyright or other restraint, it is the policy to withdraw or take down access to a thesis while the issue is being resolved.

Access Agreement

By using a Digitised Thesis from Trinity College Library you are bound by the following Terms & Conditions. Please read them carefully.

I have read and I understand the following statement: All material supplied via a Digitised Thesis from Trinity College Library is protected by copyright and other intellectual property rights, and duplication or sale of all or part of any of a thesis is not permitted, except that material may be duplicated by you for your research use or for educational purposes in electronic or print form providing the copyright owners are acknowledged using the normal conventions. You must obtain permission for any other use. Electronic or print copies may not be offered, whether for sale or otherwise to anyone. This copy has been supplied on the understanding that it is copyright material and that no quotation from the thesis may be published without proper acknowledgement.

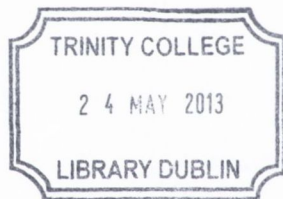# Modulation of microglial phenotypes
by CD200

Stephanie Denieffe

Thesis submitted to University of Dublin for the degree of

Doctorate in Philosophy

Supervisor: Professor Marina A. Lynch

Department of Physiology

Trinity College Dublin

2012

Declaration of Authorship

This thesis is submitted by the undersigned for the degree of Doctor of Philosophy at the University of Dublin, Trinity College. I declare that this thesis is entirely my own work with the following exceptions; certain results were produced in collaboration with Tara Browne and Justin Yssel. This work has not been submitted, in whole or in part, to this or any other university for any other degree. The author gives permission to the library to lend or copy this work upon request.

Stephanie Denieffe

Acknowledgements

I would like to firstly thank my supervisor Professor Marina Lynch for being so supportive throughout my PhD. Your continued support and guidance throughout the last 3 years has been invaluable and I have thoroughly enjoyed working under your supervision. I'd also like to thank the physiology department as well as my funding providers HRB.

I'd like to thank MAL lab members, past and present, for their help and support in the lab and for the friendships which I have gained. A special and huge thank you to the FACS god that is Barry Moran, your help and guidance in the last year has been so appreciated.

To my family and friends you have put up with the rollercoaster of PhD life and I couldn't have done it without you. Mum and Dad you have made so many sacrifices over the years to get me to where I am and I thank you so much for your endless support, you are both an inspiration to me and I could never thank you enough for the opportunities you've given me, the help and the belief in me that I could do it. My godmother Maire, you are absolutely incredible thank you so much for everything. To all my friends, I am so lucky to have the incredible friends I do and without you're support I may not have got to this point, I owe you everything.

Abstract

Microglia are the principal immune cells of the CNS continually surveying their micro-environment for endogenous and exogenous stimuli which may threaten the immunological balance. Recent studies have suggested that activated microglia, like macrophages, adopt different phenotypes depending on the stimulus; IFNγ induces classical activation of microglia, whereas IL-4 induces an alternative activation state. A deactivation state has been described in which the interaction between ligand-receptor pairs, for example CD200-CD200R, suppress the immune response. The focus of this study was to investigate the modulatory role of CD200 on different microglial phenotypes.

IFNγ enhanced the expression of TNFα, IL-6 and NOS2 by microglia while it inhibited the expression of the alternative activation marker, mannose receptor. Mannose receptor, and 2 other markers of alternative activation, arginase I and chitinase 3-like 3, were increased when cells were incubated in the presence of IL-4 but IL-4 inhibited the expression of the classical activation markers, TNFα and NOS2. These results demonstrate the ability of microglia to respond to adaptive as well as innate immune signals in a similar fashion to that of macrophages. Cells prepared from CD200$^{-/-}$ mice demonstrated exaggerated responses to activating stimuli LPS and IFNγ. In addition increased cell surface expression of TLR4 and IFNGR1, and increased activation of NFκB and STAT1, respectively, meant the regulatory systems which control LPS- and IFNγ-induced inflammation were altered in cells prepared from CD200$^{-/-}$ mice. Furthermore, CD200Fc suppressed IFNγ-induced TNFα and IL-6 mRNA and supernatant concentration from cells prepared from wildtype mice; this suggests that CD200-related deactivation of microglia may specifically modulate the classically-activated pathway.

In vivo analysis revealed that CD200$^{-/-}$ mice demonstrated increased expression of CD11b, CD40 and MHC class II in the hippocampus. These results demonstrate the important homeostatic role of CD200 on microglial function. IFNγ, which is a potent activator of microglia, was significantly increased in the hippocampus of CD200$^{-/-}$ mice. Since resident cells produce little IFNγ, the infiltration of IFNγ-producing peripheral cells was investigated and the findings showed that there was a significant increase in CD4$^+$ and CD8$^+$ T cells, and MHC class II$^+$ macrophages in the brains of CD200$^{-/-}$, compared with wildtype, mice. The data indicate that infiltration of peripheral immune cells was associated with increased BBB permeability and increased chemokine concentration in the hippocampus of CD200$^{-/-}$ mice.

The data indicate the importance of the interaction between CD200 and CD200R as a regulator of microglial inflammatory responses both in vitro and in vivo. The loss of CD200 has been implicated in many neurodegenerative disorders including Alzheimer's disease (AD) and multiple sclerosis (MS). Importantly, CD200-deficiency alters control of inflammation even under resting conditions resulting in dysfunctional regulation of immune homeostasis in the brain. This may be significant in the development and progression of age-related neurodegenerative diseases since an age-related decrease in CD200 has been reported. Upregulation of CD200 presents a potential approach for therapeutic intervention in disorders associated with inflammatory alterations and immune cell infiltration such as AD and MS.

Abbreviations

ANOVA	Analysis of variance
APC	Antigen presenting cell
BCA	Bicinchoninic acid
BSA	Bovine serum albumin
CD	Cluster of differentiation
CD200Fc	CD200 Fusion protein
cDNA	Complimentary deoxyribonucleic acid
CIA	Collagen-induced arthritis
CNS	Central nervous system
DMEM	Dulbecco's modified Eagle's medium
DNase	Deoxyribonuclease
dNTP	Deoxyribonucleotide triphosphate
DOK	Docking protein
EAE	Experimental Allergic Encephalomyelitis
ELISA	Enzyme linked immunosorbent assay
ERK	Extracellular signal-regulated kinase
FBS	foetal bovine serum
FIZZ1	Found in inflammatory zone 1
HMGB1	High mobility group protein B1
HSV	Herpes simplex virus
IFNγ	Interferon-γ
IgSF	Immunoglobulin superfamily
IKK	IκB kinase
IL-10	Interleukin-10
IL-1β	Interleukin-1β
IL-4	Interleukin-4
IL-6	Interleukin-6
IRAK	Interleukin-1 receptor associated kinase
IκB	Inhibitor of κB
JAK	Janus tyrosine kinase
LBP	Lipopolysaccaride-binding protein
LPS	Lipopolysaccaride
LTA	Lipoteichoic acid

MAL	MyD88 adaptor-like protein
MAPK	Ras/Mitogen-activated protein kinase
MD-2	Myeloid differentiation-2
MHC II	Major histocompatibility complex class II
mRNA	Messenger RNA
MS	Multiple sclerosis
MyD88	Myeloid differentiation primary response gene 88
NCAM	Neural cell adhesion molecule
NEMO	NF-kappa-B essential modulator
NFκB	Nuclear factor kappa-light-chain-enhancer of activated B cells
NK cells	Natural Killer cells
NOS	Nitric oxide synthase
Pam_3	Pam_3Cys_4
PAMP	Pathogen-associated molecular pattern
PCR	Polymerase reaction chain
PRR	Pattern recognition receptor
RasGAP	Ras GTPase activating protein
RNA	Ribonucleic acid
RNase	Ribonuclease
SEM	Standard error of mean
SHIP	Sh2-containing inositol phosphatase
SOCS	Suppressor of cytokine signaling
SphK	Spingosine phosphate kinase
STAT	Signal transducer and activator of transcription
Strep-HRP	Streptavidin-horseradish peroxidise linked
TAK1	TGF-β activated kinase 1
TGF-β	Transforming growth factor β
Th1	T helper 1
Th2	T helper 2
Thy-1	Tymus cell antigen 1
TIR domain	Toll/Interleukin-1 domain
TIRAP	TIR-domain containing adaptor protein
TLR	Toll-like receptor
TNFα	Tumor necrosis factor alpha

TRAM	TRIF-related adapter molecule
TRIF	TIR-domain containing adapter-inducing interferon β
TYK	Tyrosine kinase

Table of Contents

Chapter 1 Introduction

Chapter 2 Methods

Chapter 3

Chapter 4

Chapter 5

Chapter 6

Chapter 7

List of Figures

Chapter 1

Chapter 2

Chapter 3

Chapter 4

List of Tables   XV

Chapter 1

Introduction

1.1. Innate and adaptive immune responses

The microorganisms that are encountered daily in the life of a normal healthy individual rarely cause observable illness. Most are detected and destroyed within minutes or hours by defence mechanisms that do not require a prolonged period of induction because they do not rely on the clonal expansion of antigen-specific lymphocytes, these are the mechanisms of innate immunity. Innate immunity relies on the recognition of pathogens by germline-encoded receptors on the surface of antigen presenting cells (APCs) such as macrophages and dendritic cells, with ligation of many of these receptors resulting in phagocytosis of the pathogen. If the infectious agent breaches these early lines of defence an adaptive immune response ensues mediated by T cells or antibodies. The adaptive immune response uses a large repertoire of receptors encoded by rearranging gene segments to recognize a large variety of antigens (Matyszak 1998).

1.1.1. Antigen Presentation

Antigen presentation is the fundamental link between the innate and adaptive immune response. The ability of the immune system to recognize and defend against foreign antigen is partially dependent upon the ability of the host's major histocompatability complex (MHC), which presents peptides degraded in intracellular vesicles to circulating T cells (Nabavi, Freeman et al. 1992). Macrophages continuously phagocytose self proteins and cells in normal tissue repair, these are processed and the antigen is presented on the cell surface through MHC molecules. These self-proteins however do not activate T cells, because in the absence of an infectious agent macrophages express low levels of MHC and co-stimulatory molecules. Bacterial agents such as lipopolysaccaride (LPS) signal macrophages to release proinflammatory cytokines and up-regulate expression of MHC class II, and co-stimulatory molecules CD80/CD86 and CD40, which results in them becoming strong antigen-presenting cells and increasing their ability to interact with T cells (Mosser 2003).

T cell precursors migrate from the bone marrow to the thymus where the T cell receptor (TCR) genes are arranged. T lymphocytes can be divided into CD4- and

1

CD8-positve T cells, hereafter referred to as CD4 and CD8 T cells. To initiate an antigen-specific immune response, naive T cells must physically interact with APCs, such as macrophages, dendritic cells or B cells (Friedl and Gunzer 2001). This physical interaction allows engagement of surface receptors including the TCR-MHC-peptide complex and the CD4 or CD8 co-receptor which transmits a signal to the T cell that antigen has been encountered. A second signal is required, the co-stimulatory signal, delivered by the same APC. APCs express co-stimulatory molecules CD80 and CD86, which bind to the T cell CD28 (Figure 1.1) (Lang, Nguyen et al. 2002). Naive CD4 T cells respond to their specific antigen-MHC class II complex on the surface of APCs by making interleukin (IL)-2, leading to their proliferation and differentiation into T helper (Th) cells to become effector T cells. Effector T cells can be divided into Th1, Th2 and Th17 cells, which differ in the cytokines they produce and hence their function (Woodland and Dutton 2003). Th1 cells classically produce their signature cytokine, IFNγ, whereas Th2 cells produce IL-4 and IL-13 (Friedl and Gunzer 2001). Naive CD8 T cells are already predestined to become cytotoxic cells and respond to their specific antigen-MHC class I complex. Once the cells have differentiated into effector T cells any encounter with specific antigen triggers their effector actions.

While such an inflammatory response is typical in non-central nervous system (CNS) tissue, the CNS, which exhibits limited regenerative capacity, is invariably susceptible to damage initiated by inflammation. Based on a number of observations including limited to minimal MHC expression found in the CNS, no classical lymphatic drainage system and the presence of the blood-brain-barrier (BBB), the early description of the CNS as an immune privileged site emerged as a suggested mechanism by which the brain prevents damage and maintains neural health (Rezai-Zadeh, Gate et al. 2009).
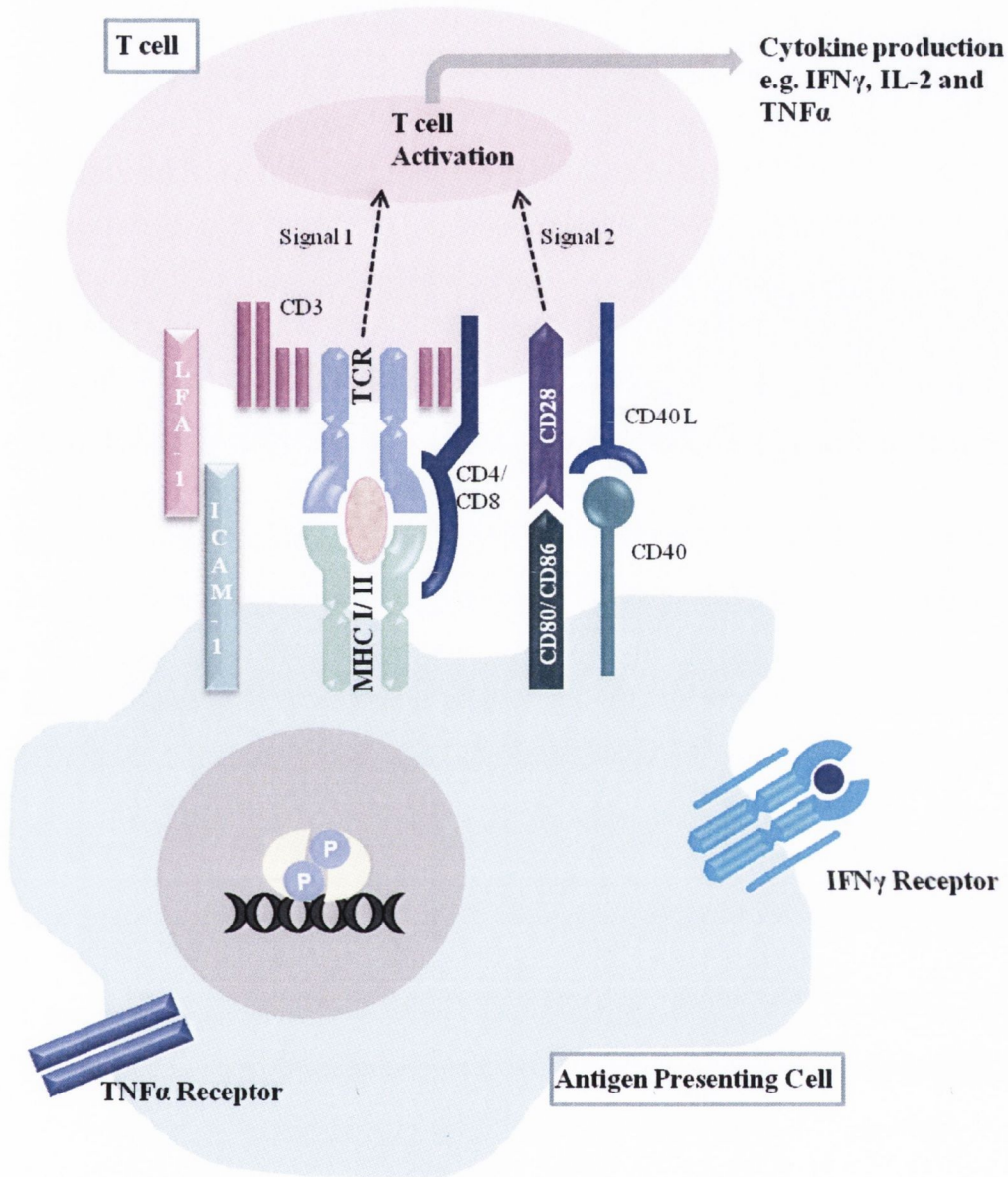
Figure 1.1. Antigen-specific immune response. *Naive CD4$^+$ T cell receive an antigen-specific signal (signal 1) through its clonally derived TCR, which interacts with antigenic peptides presented by MHC class II molecules expressed on the surface of APCs. Signal 2 is delivered by co-stimulatory molecules expressed by activated APCs, such as CD80 and/or CD86, which interact with the CD28 co-receptor that is constitutively expressed by CD4$^+$ T cells, resulting in T-cell proliferation, cytokine production and increased adhesion molecules necessary for trafficking.*

1.2. Immune privilege

The concept of immune privilege in the CNS has a long history, years before Billingham and Boswell coined the term in 1953 (Billingham and Boswell 1953). In Japan in 1921, Shirai observed that a rat sarcoma grew well when transplanted into the mouse brain parenchyma, however the same was not observed when implanted intramuscularly or subcutaneously (Shirai 1921). Another study in 1923 by Murphy and Sturm, found that by co-transplanting recipient spleen with the foreign tumour into the brain parenchyma an inhibition of tumour growth was observed (Murphy 1923). The evidence suggested that survival of a foreign tumour within the CNS occurred as a result of disconnection from the systemic immune system. Since then many studies have confirmed these original observations by experiments involving tissue grafts (Medawar 1948), bacteria (Matyszak and Perry 1995), viruses and vectors (Byrnes, MacLaren et al. 1996; Wood, Charlton et al. 1996; Stevenson, Hawke et al. 1997), all of which evaded immune recognition when implanted into the brain parenchyma.

1.2.1. Compartmentalized CNS

The CNS is organised into different compartments; the parenchyma, the ventricles containing the choroid plexus and CSF, and the meninges. Murphy and Sturm's experiments in 1923 apart from finding that co-transplantation of recipient spleen with the foreign tumor resulted in tumor rejection also discovered that rejection of the foreign tumour within the brain occurred if it approached the ventricles (Murphy 1923). These observations were corroborated in the case of other antigens, an intracerebroventricular (i.c.v.) injection of foreign tissue grafts was rejected and influenza virus elicited hormonal and cytotoxic T cell responses (Galea, Bechmann et al. 2007). These findings suggested that immune privilege is compartmentalised, confined to the CNS parenchyma, and is not applicable to the meninges or ventricles.

While the theory of the "immunologically privileged" CNS was being developed the discovery of the blood-brain-barrier (BBB) was made with the emergence of the view that immune privilege of the brain was wholly attributed to the BBB,

isolating the CNS (Galea, Bechmann et al. 2007; Forrester, Xu et al. 2008). More recent data demonstrate the essential nature of the immune-privileged brain as a quality relative to other organs but does not imply an organ lacking in immunological components, but rather a tightly-regulated structure (Bechmann, Galea et al. 2007; Galea, Bechmann et al. 2007)

1.3. The blood-brain-barrier (BBB)

The BBB encompasses the capillaries and postcapillary venules in the brain and spinal cord. Tight junctions between the epithelium of the choroid plexus and the vascular endothelial cells severely restrict the entry of macromolecules from the blood into the CSF or from the blood into the CNS; they also provide an obstacle to cellular egress (Prendergast and Anderton 2009). The BBB is composed of specialised non-fenestrated endothelial cells connected by tight junctions of high electrical resistance composed of occludin, junctional adhesion molecules (JAMs) and claudins (Figure 1.2) (Wilson, Weninger et al. 2010). In the healthy CNS, the BBB express low levels of adhesion molecules and tight junctions seal the endothelial cells forming an effective barrier occluding diffusion of specific factors and solutes, including >98% of antibodies and small molecules from the blood into the parenchyma (Wilson, Weninger et al. 2010).
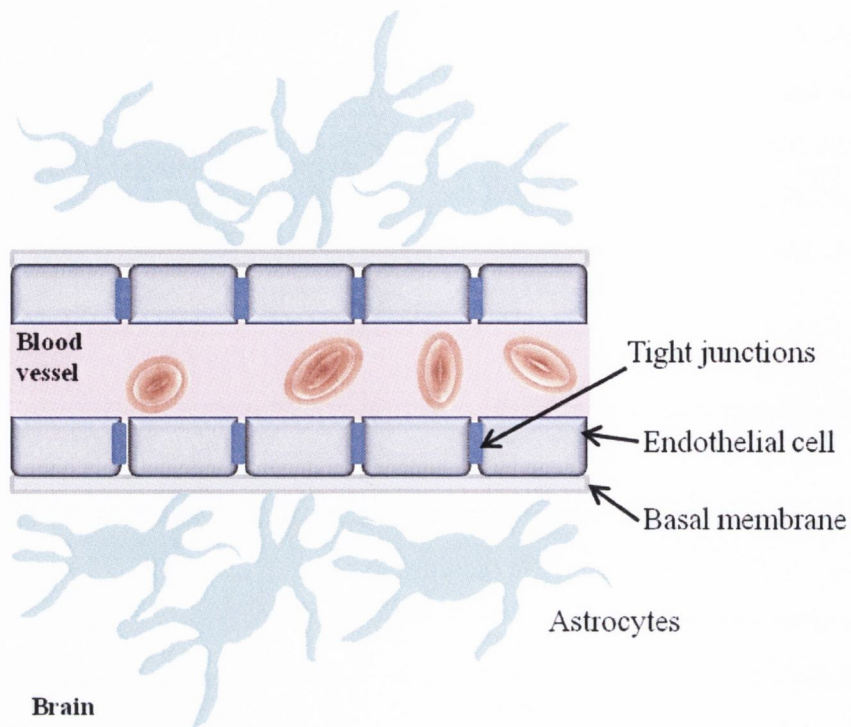
Figure 1.2. The blood-brain-barrier (BBB). *The BBB is created by non-fenestrated endothelial cells connected by tight junctions with high electrical resistance, forming a barrier between the circulation and the brain parenchyma. The endothelial cells are surrounded by a basal lamina, pericytes and astrocytic end-feet.*

1.3.1. Leukocyte entry to the CNS

It was once believed that there was no routine immunological surveillance of the brain by peripheral immune cells because of undetectable levels of T cells by immunohistochemistry in the healthy CNS associated with negligible levels of MHC required for antigen presentation to T cells (Hickey, Hsu et al. 1991). However peripheral leukocyte migration and infiltration into the brain parenchyma can occur but is a tightly-regulated process at the level of the BBB (Rezai-Zadeh, Gate et al. 2009).

There are two sites of entry for lymphocytes into the CNS from the blood: across the blood-cerebrospinal fluid (CSF) barrier of the choroid plexus and across the BBB into the brain parenchyma. The brain has three membranes which enclose the brain parenchyma: the dura matter is the outermost membrane, the arachnoid membrane and the inner membrane known as the pia membrane. The CSF, made

6

primarily by the choroid plexus, is contained within the sub-arachnoid space (SAS) created between the pia mater, arachnoid membrane and dura mater. The CSF circulates around the SAS with the fluid turning over three to four times a day. The epithelium of the choroid plexus constitutes the blood-CSF barrier (Prendergast and Anderton 2009). Entry of T cells in the CSF across the blood-CSF barrier results from migration across the fenestrated capillary bed and consequent crossing of the tight junctions of the epithelial layer and appears to be important in immune-surveillance (Prendergast and Anderton 2009).

The passage of cells across the BBB involves active trans-endothelial migratory processes, a complex process regulated at every step (Forrester, Xu et al. 2008). The initial interaction is thought to be mediated by adhesion molecules on the surface of the endothelial cells; an initial low affinity interaction results in tethering of the lymphocytes, facilitating rolling along the endothelial surface. The next signal comes from chemokines and activation of chemokine receptors on the lymphocytes; this can result in inhibited movement into the parenchyma or promote infiltration. The lymphocyte extravagates across the endothelial layer negotiating the tight junctions, this occurs in an intracellular adhesion molecule-1 (ICAM-1)- and ICAM-2-dependent manner (Prendergast and Anderton 2009).

Under normal circumstances the entry of lymphocytes across the BBB is low. However the integrity of the BBB is challenged under certain physiological and pathological states. Following immune activation within the CNS, cytokines and chemokines diffuse into the blood stream attracting infiltrating leukocytes to the site of inflammation, however the vast majority of recruited leukocytes are not re-stimulated within the CNS and never penetrate the astrocytic end feet of the BBB (Rezai-Zadeh, Gate et al. 2009), allowing the endogenous immune cells of the CNS to mount a controlled response to infection while also acting as supportive cells to fragile neurons (Streit 2002).

1.4. Immune cells of the CNS

The brain resident innate immune cells are microglia, traditionally referred to as the resident macrophage of the CNS, and astrocytes.

1.4.1. Astrocytes

Astrocytes are the most numerous of glial cells in the CNS. Discovered by Ramon y Cajal, their name arises from their star-shaped appearance (Somjen 1988). The diverse range of functions of astrocytes in the CNS has lead to their description as "multifunctional housekeeping cells" (Nedergaard, Ransom et al. 2003). They are involved in the physical structuring of the brain, this idea originating back in the 1840's when glia were first described as glue-like substance (Volterra and Meldolesi 2005). They provide metabolic support to neurons delivering nutrients such as glucose, and, as discussed, play a critical role in the BBB helping form the impermeable lining in the brain's capillaries and venules, preventing toxic substances in the blood from entering the brain (Derouiche and Frotscher 2001). They play a vital role in neurotransmitter reuptake and release through plasma membrane transporters and regulate ion concentration in the extracellular space (Tritsch and Bergles 2007).

In addition, recent *in vivo* data have highlighted their central role in regulating neuroinflammation (Brambilla, Bracchi-Ricard et al. 2005; Farina, Aloisi et al. 2007). Transgenic mice were generated in which nuclear factor kappa-light-chain-enhancer of activated B cells (NFκB), a fundamental transcription factor in innate immune responses, was specifically inactivated in astrocytes. The results demonstrated that the selective inactivation of astroglial NFκB lead to a dramatic improvement in functional recovery 8 weeks after contusive spinal cord injury correlating with a drop in leukocyte recruitment to the lesioned area and a decrease in IP-10 and MCP-1, chemokines produced by astrocytes (Brambilla, Bracchi-Ricard et al. 2005; Farina, Aloisi et al. 2007). These results show that the NFκB pathway in astrocytes is a key regulator of inflammation in the CNS and demonstrate the role of astrocytes in initiating adaptive immune responses in recruitment of leukocytes.

8

1.4.2. Microglia

Franz Nissl, in the late 19th century, was the first to consider microglia in the pathologically-altered brain and noted that the various stages and states of neurodegeneration were accompanied by notable glial reactions (Theele and Streit 1993). However even more pertinent to modern day science, is his insight into microglia as key cells of the immune system in the brain: "it is highly likely that glial cells, in addition to producing intracellular substances, have a second task which is approximately the same as the role leukocytes have in other tissues" (Nissl 1899) (Theele and Streit 1993). It is really only in the last twenty years that studies have supported this role for microglia as the "defense cells" of the CNS replacing the long-standing notion that the brain is an immunologically-privileged organ (Streit 2002; Graeber and Streit 2010).

Although microglia were originally described by F. Nissl and F. Robertson it was Pio Del Rio-Hortega, a student of Santiago Ramon y Cajal, who is regarded as the "father of microglia" (Theele and Streit 1993). Del Rio-Hortega was the first to recognize microglia as a distinct population of cells (Rio-Hortega 1932). He established the fundamental characteristics of microglia utilizing silver staining methods and light microscopy (Theele and Streit 1993). From the moment these discoveries were made, there has been controversy over their differential phenotypic expression, embryonic development and their overall functioning in the CNS. Originally it was suggested that microglia may have arisen from blood mononuclear cells due to their shared phagocytic function (Theele and Streit 1993). More recent theories suggest that microglia are initially derived from mesodermal precursor cells that are related to the monocyte/macrophage lineage derived from embryonic hematopoietic organs (Theele and Streit 1993; Liu and Hong 2003).

1.4.3. Microglial "Activation"

From Del Rio-Hortega's original studies utilizing the Nissl stain, it was concluded that fully differentiated "resting" microglia take on a ramified morphology (Rio-Hortega 1932). Experiments on a stab wound model led to the conclusion that the

ramified microglia were capable of phenotypic differentiation into a migratory amoeboid or "activated" form (Theele and Streit 1993). Recent studies have highlighted a need for a more definitive definition of microglial activation. A study in 2005 using *in vivo* two-photon microscopy investigated the behavior of resting microglia in the neocortex of intact adult brains, it was concluded that microglial cells were highly dynamic in their resting state (Nimmerjahn, Kirchhoff et al. 2005). Resting microglia displayed highly motile filopodia-like profusions which sample the extracellular environment; this serves a housekeeping function enabling the microglial cells to effectively control their microenvironment and is likely to facilitate prompt reactions to danger signals which may threaten the immunological balance of the CNS (Nimmerjahn, Kirchhoff et al. 2005). It has been suggested that "resting" microglia may be more appropriately described as "surveying" microglia due to their extensive housekeeping functions as they actively search for and read signals in the brain environment (Hanisch and Kettenmann 2007).

Further, the original description of activated microglia was described as a change in the morphology from ramified to amoeboid. Recent data demonstrate that treatment of a microglial cell line BV2 cells with a range of pro-inflammatory and anti-inflammatory cytokines, including IFNγ, IL-4 and IL-10, and staining with Coomassie blue to distinguish gross morphology established that cells displayed a mixture of branched, bipolar and amoeboid cells and were indistinguishable based on treatment (Colton and Wilcock 2010). These results signify that while changes in morphology may signal a change in functional state, morphology alone cannot be used to predict functional outcome (Colton and Wilcock 2010). Thus activated microglia can be identified based on combined morphological and functional changes disguising them from their resting phenotype (Graeber and Streit 2010).

1.5. Heterogeneity of microglial activation

Much of what is known in regard to microglial function was derived from initial work on macrophages. The primary function of macrophages is to sense danger and eliminate the threat. Recent developments have questioned how these cells participate in host defense and have highlighted the remarkable plasticity and

complex nature of macrophage responses (Mosser and Edwards 2008). A review in 2008 defined three primary macrophage populations based on their function: host defense, wound healing and immune regulatory macrophages (Mosser and Edwards 2008). Even more interesting was the comparison of these populations to the three primary colours of the colour wheel resulting in a 'spectrum' of macrophage populations and allowing for the development of macrophages which may contain characteristics of two populations (Mosser and Edwards 2008).

In a similar fashion CNS-resident microglia develop distinct patterns of functional outcome depending on the stimulus and the context of the microenvironment (Hanisch and Kettenmann 2007). The mode of activation crucially affects their fate, and so, the fate of the neurons surrounding them. Macrophages and microglia are capable of responding to both endogenous and exogenous stimuli and it is the amount and the duration of a stimulus which dictates the inflammatory state that will ensue. For example the production of interferon (IFN)-γ by natural killer (NK) cells is generally transient initiating an acute response from macrophages and is not sustained; in contrast production of IFNγ in an antigen-specific fashion results in sustained macrophage activation (Hanisch and Kettenmann 2007). The importance of defining microglial plasticity becomes apparent when trying to identify individual populations in disease.
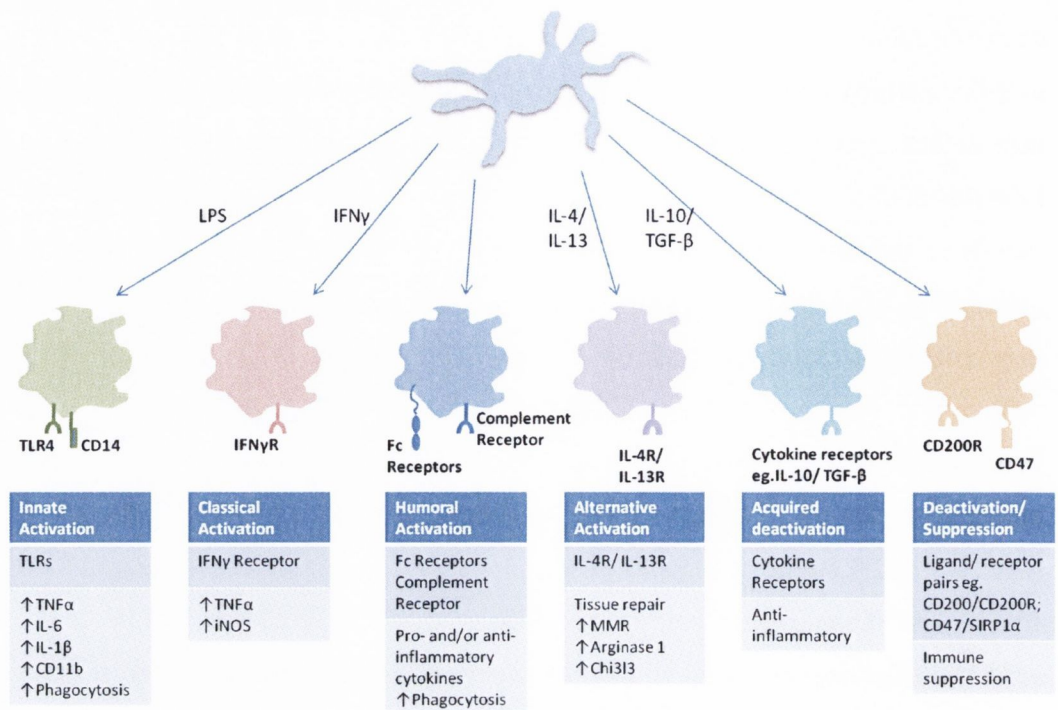
Figure 1.3. Microglial/macrophage plasticity. *Microglia can be stimulated by both endogenous and exogenous stimuli, from both innate and adaptive immune responses, displaying remarkable plasticity developing distinct patterns of functional outcome depending on the stimulus and the context of it microenvironment.*

1.6. Innate Immune activation

The innate immune system provides the initial protection against an insult. Host cells express pattern recognition receptors (PRRs) that sense diverse pathogen-associated molecular patterns (PAMPs). Activation of PRRs trigger intracellular signaling cascades which culminate in the induction and release of cytokines, chemokines, reactive oxygen species, IFNs and many other inflammatory mediators (Kawai and Akira 2007).
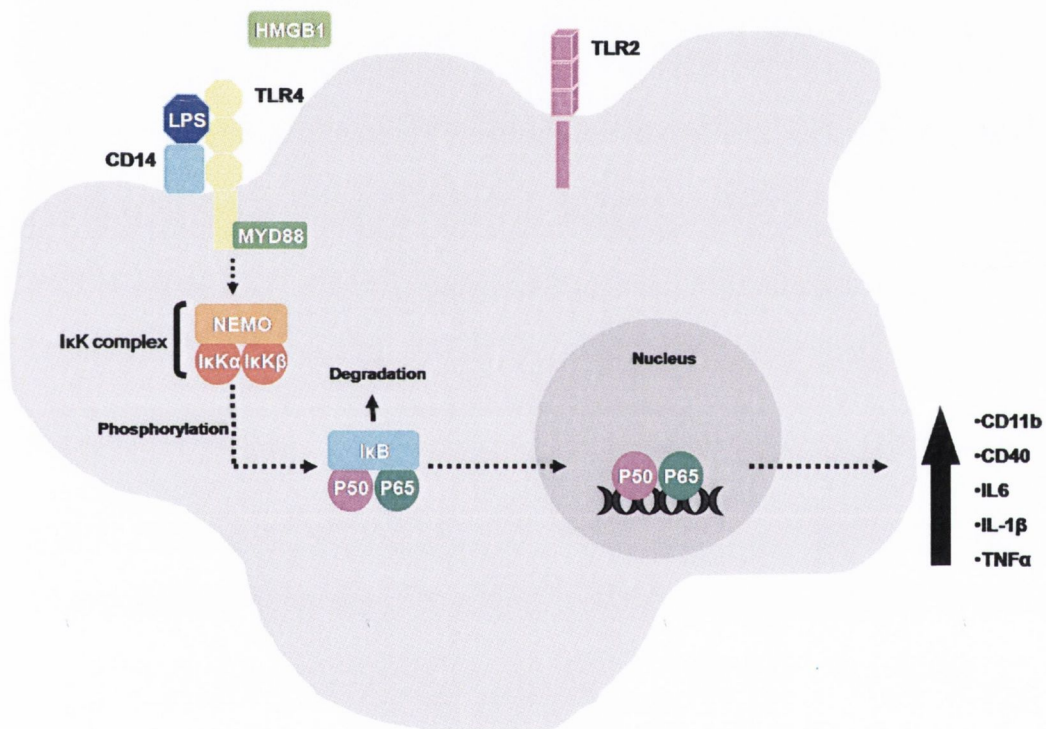
Figure 1.4. TLRs: A central role in the induction of the immune response. *TLRs are expressed on APCs and utilize different combinations of adaptor molecules, which activate different transcription factors to elicit specific innate immune responses.*

1.6.1. TLRs

Toll-like receptors (TLRs) are expressed on APCs, macrophage, dendritic cells and in the brain, on microglial cells (Figure 1.4). TLRs are type I membrane proteins characterized by an ectoderm composed of leucine rich repeats that are responsible for recognition of PAMPs and a cytoplasmic domain known as a

Toll/Interleukin 1 receptor domain, or TIR domain, which is required for downstream signaling. TLRs utilize different combinations of adaptor molecules, which activate different transcription factors to elicit specific innate immune responses. Eleven human TLRs and thirteen mouse TLRs have been identified to date, with each appearing to recognize distinct PAMPs from bacteria, viruses, protozoa and fungi (Kawai and Akira 2007). TLRs 1, 2, 4 and 6 recognize lipids; TLR 5 and 11 recognize protein ligands; TLR 3, 7, 8, and 9 are localized internally and are responsible for the detection of nucleic acids derived from viruses and bacteria (Kawai and Akira 2007).

TLR2 is regarded as being quite promiscuous for its ability to recognize the most diverse set of pathogen-associated motifs including components of gram-positive bacteria such as lipoproteins, lipoteichoic acid (LTA), peptidoglycan, as well as different lipopolysaccaride (LPS) from certain gram-negative bacteria, fungi and yeast (Triantafilou, Gamper et al. 2006). Its response to such a wide range of stimuli is accounted for by its ability to heterodimerize with TLR1 and 6. TLR2/6 heterodimer responds to diacylated lipoproteins and TLR2/1 heterodimer responds to triacylated lipoproteins; thus it is the formation of receptor clusters that allows TLR2 to respond to a wide range of microbial products (Triantafilou, Gamper et al. 2006). Pam_3Cys_4 (tripalmitoyl-cysteinylseryl-(lysyl)3-lysine) is a synthetic peptide commonly used as an experimental ligand for TLR2 (Akira and Sato 2003).

The activation of microglial cells by LPS, a major component of the cell wall of gram-negative bacteria, is mediated by TLR4 and is by far the best described TLR response (Garden and Moller 2006). LPS is recognized by TLR4 which interacts with 3 different extracellular proteins; LPS-binding protein (LBP), CD14 and myeloid differentiation protein-2 (MD-2), to induce a signalling cascade leading to the activation of NFκB and, subsequent pro-inflammatory cytokine production (Figure 1.5). Although TLR4 activation can occur without CD14 and LBP, their presence increases the sensitivity of the receptor for LPS (Triantafilou and Triantafilou 2002).
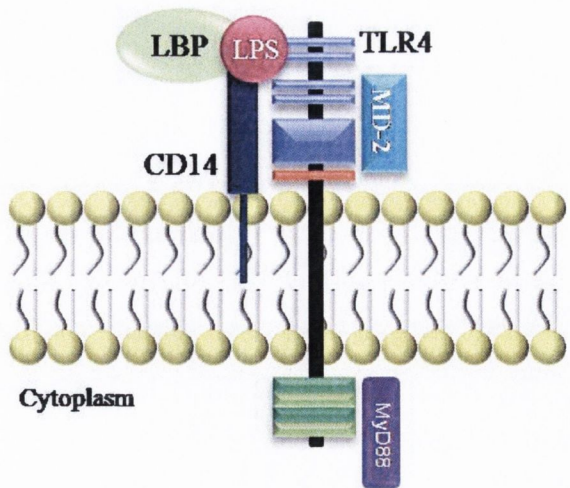
Figure 1.5. TLR4 receptor complex. *LPS forms binds to LBP, the LPS binding protein, which conveys LPS to cell surface CD14; this brings LPS in contact with TLR4 and associative MD-2 completing the receptor complex and resulting in the activation on downstream signalling.*

1.61.1. Endogenous ligands for TLRs

Cell surface TLRs respond to endogenous ligands in addition to microbial ligands. A number of endogenous ligands have been identified including heat shock proteins (HSPs), extracellular matrix degradation products and high mobility group protein B1 (HMGB1) (Miyake 2007). Many of these molecules are released during an inflammatory response or in response to tissue damage and are potent activators of the innate immune system capable of inducing proinflammatory cytokine production by macrophages and initiate an adaptive immune response (Tsan and Gao 2004).

HMGB1 is an abundant nuclear and cytoplasmic protein present in mammalian cells (Yang, Wang et al. 2002). Originally described as a DNA-binding protein that stabilizes nucleosomes and facilitates transcription, it is also described as an endogenous danger signal released passively from necrotic cells or actively released in response to inflammatory stimuli (Park, Svetkauskaite et al. 2004). HMGB1 may signal through receptor for advanced glycation end products (RAGE) and TLR2 and TLR4, inducing activation of NFκB (Park, Svetkauskaite et al. 2004). The direct pro-inflammatory effects of HMGB1 have not been reproduced consistently in the literature with some reports suggesting

proinflammatory cytokine release was as a result of LPS contamination (Tsan and Gao 2004; Tsan and Gao 2007), however evidence has pointed to the formation of complexes with TLR ligands, such as LPS, and cytokines, including IL-1β, resulting in amplification of the inflammatory response (Sha, Zmijewski et al. 2008). Further to this, HMGB1 can promote inflammation indirectly due to its chemotactic activity on monocytes, macrophages, neutrophils and dendritic cells (Degryse and de Virgilio 2003; Bianchi and Manfredi 2007; Dumitriu, Bianchi et al. 2007). Availability of endogenous ligands is tightly controlled, as is surface expression of TLRs, in order to avoid excessive activation.

1.6.2. TLR-mediated signaling

Signal transduction through TLRs originates from their cytoplasmic TIR-domain. Recognition of microbial products by TLRs stimulates the recruitment of a set of intracellular TIR-domain-containing adaptors; these include myeloid differentiation primary response gene 88 (MyD88) and TIR-domain containing adaptor protein (TIRAP) also known as MAL. TIRAP mediates the activation of a MyD88-dependent pathway downstream of TLR2 and TLR4. TIR-domain containing adapter-inducing interferon β (TRIF) and TRIF-related adapter molecule (TRAM) are recruited to TLR4 initiating a MyD88-independent pathway. The MyD88-dependent pathway is shared by all TLRs except TLR3 which signals via a TRIF-dependent pathway (Kawai and Akira 2007).

1.6.2.1. MyD88-dependent pathway

The association of TLRs with MyD88 leads to the recruitment of members of the interleukin-1 receptor associated kinase (IRAK) family of proteins, namely IRAK1 and 4. Upon phosphorylation, IRAKs dissociate from MyD88 and interact with TRAF6, leading to the activation of TAK1. TAK1 in combination with TAB1, 2 and 3 leads to the activation of the IκB kinase (IKK) complex (Kawai and Akira 2007). IKK complex is composed of IKKα and IKKβ, and a regulatory subunit non-enzymatic scaffold protein (NEMO) (Hayden and Ghosh 2004). Activation of the β subunit of the IKK complex leads to the phosphorylation of

IκB which is necessary for its degradation and subsequently the freed NFκB translocates to the nucleus where it modulates gene activation typically resulting in the expression of tumor necrosis factor alpha (TNFα), IL-1β, IL-6 proteins as well as chemokines and redox proteins (Figure 1.6) (Hayden and Ghosh 2004; Kawai and Akira 2007; Colton 2009).
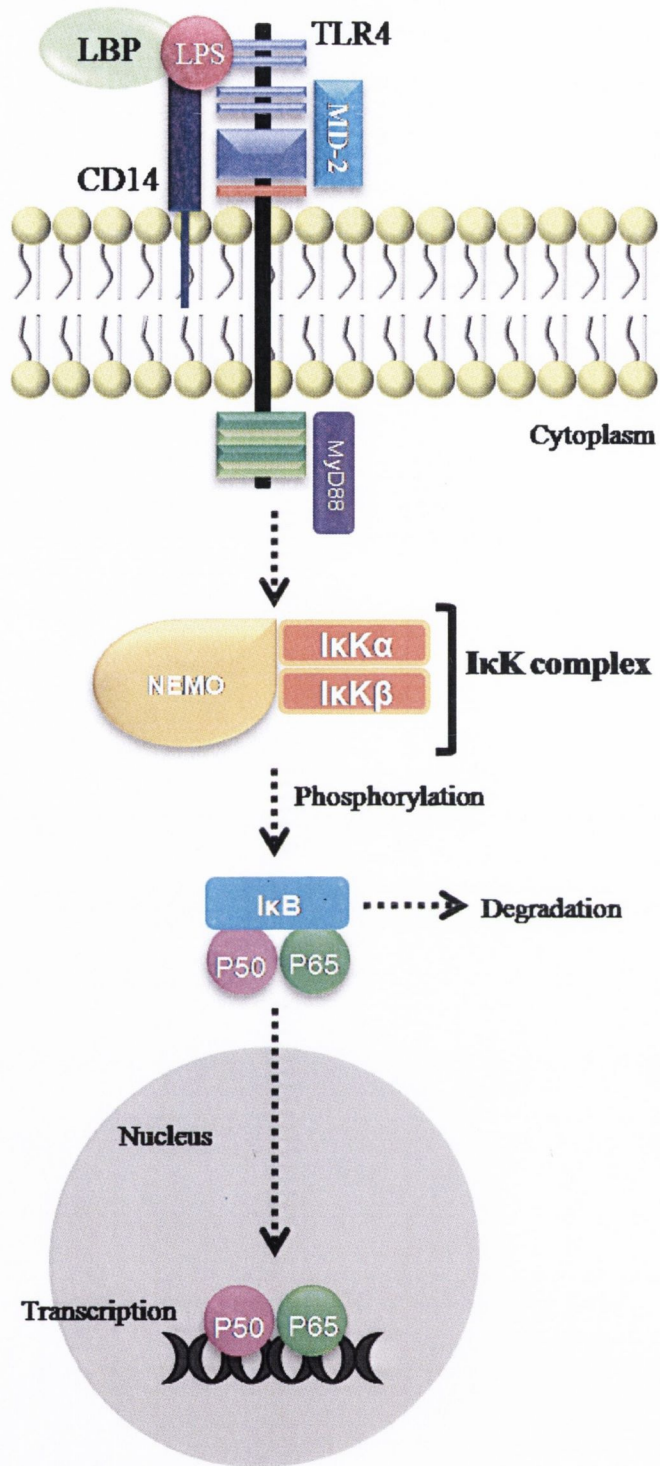
Figure 1.6. TLR4 signalling cascade. *LPS signals via TLR4 and co-receptor CD14 resulting in NFκB activation and an up-regulation of NFκB responsive genes including proinflammatory cytokines IL-1β, TNFα and IL-6.*

1.7. Classical activation pathway

Release of IFNγ, originally known as macrophage-activating factor, leads to a rapid reinforcement of the initial immune response leading to classical activation of macrophages or microglia (Colton 2009).
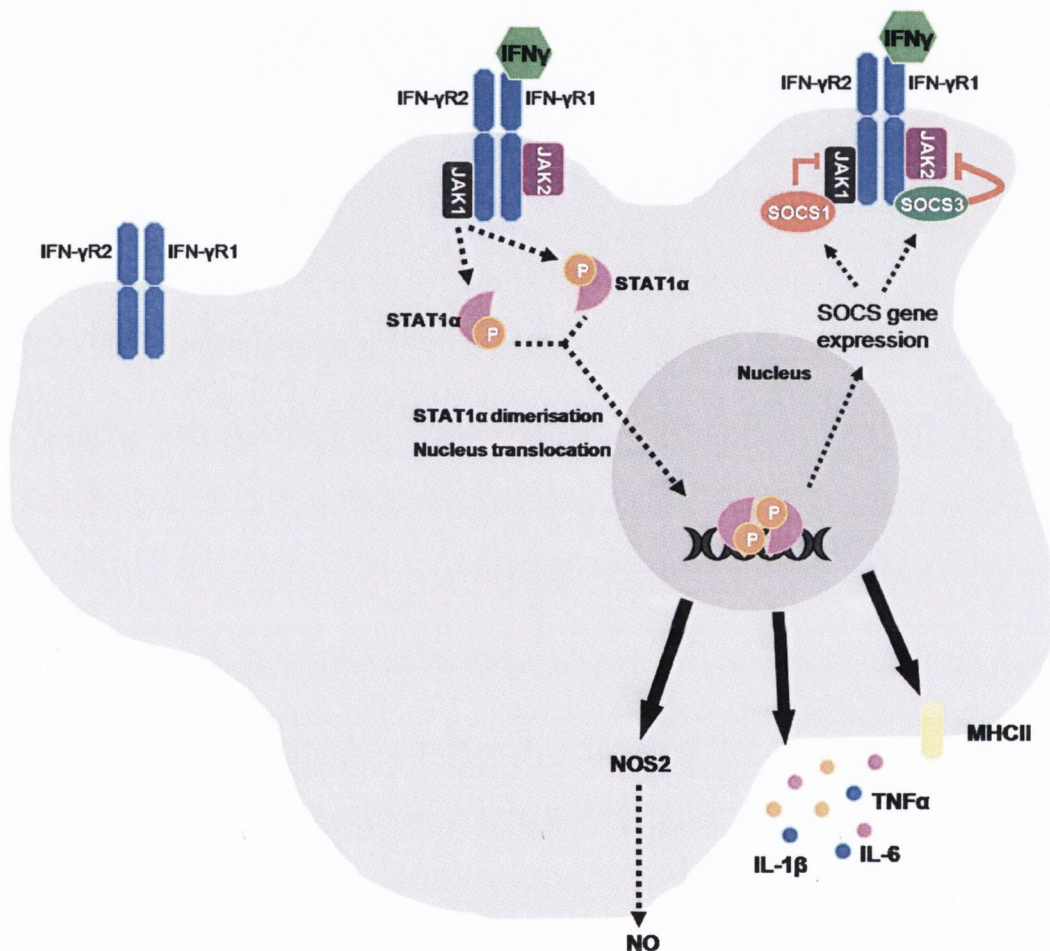
Figure 1.7. IFNγ-induced classical activation pathways. *Th1 cytokine, IFNγ, induces classically-activated microglia through its actions at the IFNGR and signals via JAK/STAT pathway resulting in a response characterized by the upregulation of TNFα and NOS2. SOCS1 and SOCS3 are inhibitors for JAKs and block the interaction of the JAK catalytic domain with STAT, terminating the signal.*

In the presence of IFNγ, macrophages are triggered to become effector cells and classically activated macrophages are highly microbicidal and proinflammatory (Figure 1.7) (Ma, Chen et al. 2003). Classical activation was initially reported to require two activating stimuli in the form of IFNγ and TNFα. However in

response to TLR activation, TNFα is induced in a MyD88-dependent manner, which can then cooperate with IFNγ, activating this macrophage population (Mosser and Edwards 2008). These cells are identified by a pronounced production of inducible nitric oxide synthase (iNOS) and TNFα (Ma, Chen et al. 2003; Mosser 2003), and induction of MHC class II which promotes peptide specific activation of CD4$^+$ T cells (Schroder, Hertzog et al. 2004).

1.7.1. IFNγ

IFNs are classified into type I and Type II IFNs according to their receptor specificity and sequence homology (Schroder, Hertzog et al. 2004). IFNγ is the sole type II IFN; it is structurally related to the type I IFNs but binds to a different receptor. It was originally thought that CD4$^+$ Th1 cells, CD8$^+$ cytotoxic T cells and NK cells were the exclusive producers of IFNγ (De Simone, Levi et al. 1998), however recent evidence has suggested APCs such as monocytes, macrophage and dendritic cells may be a source of IFNγ in the early defence mechanisms of the innate immune response (Schroder and Jaster 2004). IFNγ production is controlled by cytokines secreted by APCs, including IL-12 and IL-18. Macrophages release IL-12 and chemokines upon pathogenic challenge resulting in the recruitment of T cells and NK cells, where IL-12 secretion promotes IFNγ production from these cells (Schroder and Jaster 2004).

1.7.1.1. IFNγ receptor signalling

The IFNγ receptor (IFNγR) is comprised of two IFNγ receptor 1 (IFNGR1) and two IFNγ receptor 2 (IFNGR2) subunits. The IFNGR1 subunit is the ligand-binding subunit and its intracellular domain contains binding motifs for the Janus tyrosine kinase (JAK) 1 and the signal transducer and activator of transcription (STAT) 1 (Schroder, Hertzog et al. 2004). The intracellular domain of IFNGR2 contains a non-contiguous binding motif for recruitment of JAK2 (Schroder, Hertzog et al. 2004).
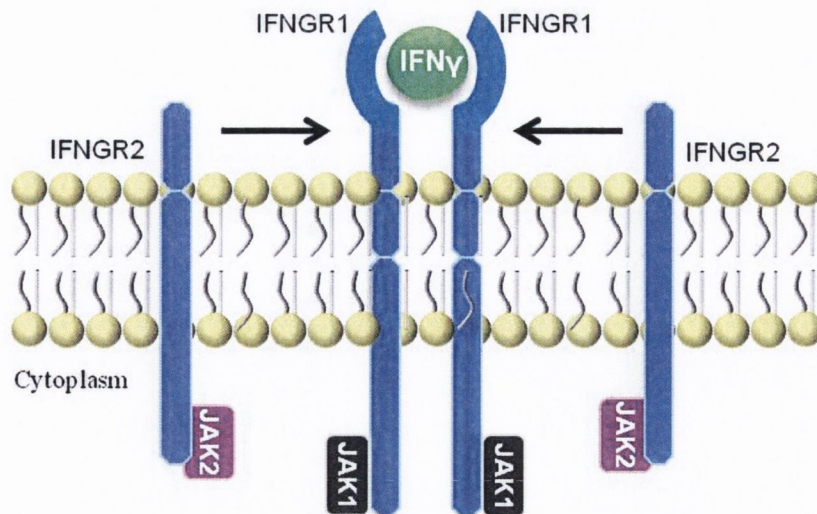
Figure 1.8. The IFNγ receptor complex. *The IFNγ receptor has 2 subunits; IFNGR1, ligand-binding subunit, and IFNGR2, the signal transducing chain. IFNγ binds 2 IFNGR1 chains leading to dimerisation and subsequent association with 2 IFNGR2 chains completing the IFNGR complex. Following signalling the IFNGR1 chains are internalized limiting IFNγ signalling.*

Upon ligation, the IFNGR undergoes a conformational change such that the inactive JAK2 kinase undergoes autophosphorylation and activation, allowing JAK1 transphosphorylation by JAK2 (Figure 1.8). JAK1 phosphorylates tyrosine residues on the intracellular domain of each IFNGR1 resulting in two adjacent docking sites for the Src homology (SH) 2 domains of latent STAT1 (Igarashi, Garotta et al. 1994). STAT1 pair is phosphorylated leading to the formation of a homodimer and dissociation of the homodimer from the receptor complex resulting in translocation to the nucleus and upregulation of IFNγ responsive genes (Figure 1.9) (Schroder, Hertzog et al. 2004). Following IFNγ-treatment the phosphorylation of the four critical tyrosine residues, contained by JAK1, JAK2, IFNGR1 and STAT1, occurs within 1 minute (Greenlund, Farrar et al. 1994). Suppressor of cytokine signalling (SOCS) proteins are inhibitory endogenous regulators of the JAK/STAT pathway of cytokine receptor signalling (Figure 1.7) (Dimitriou, Clemenza et al. 2008).
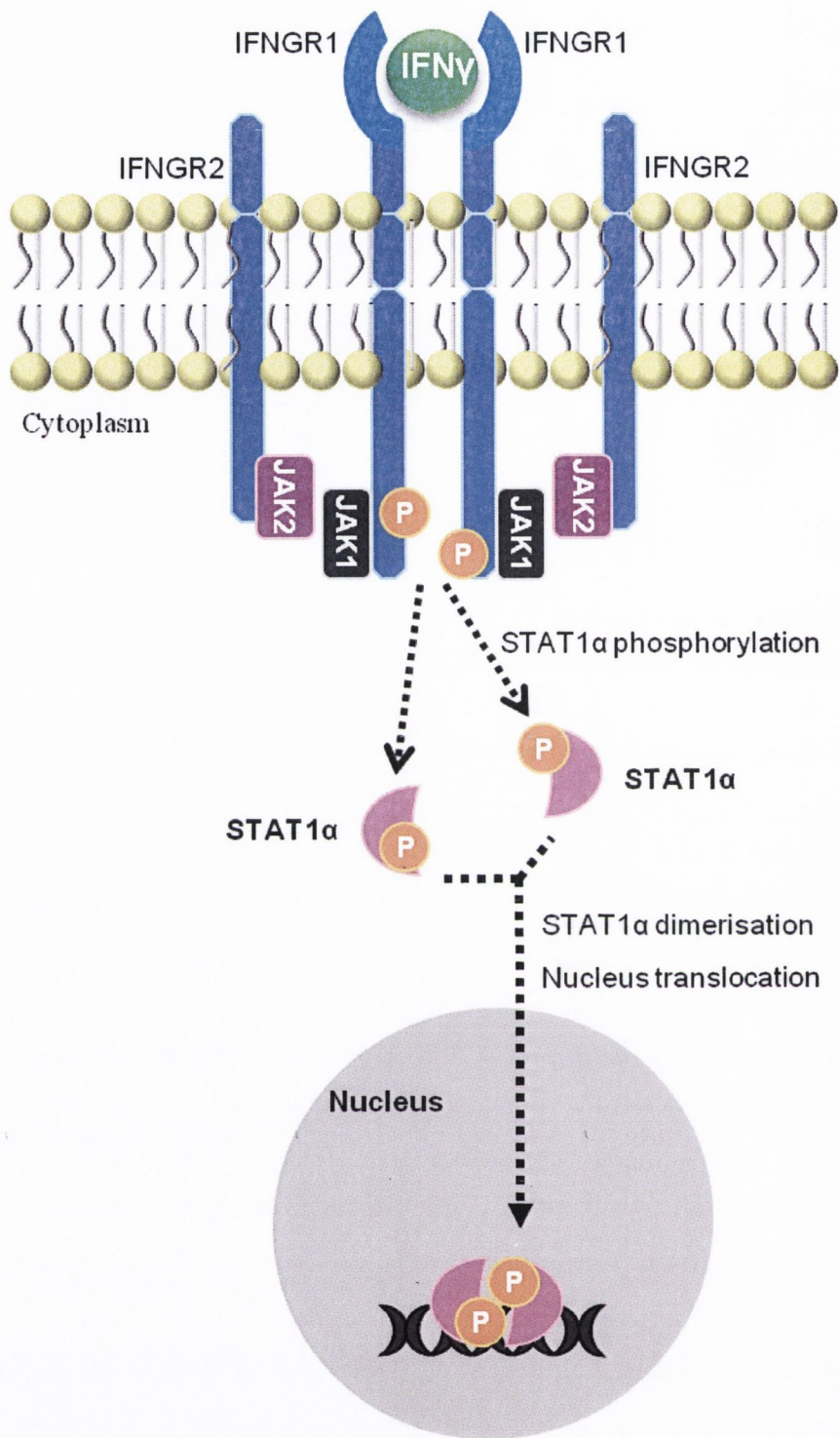
Figure 1.9. IFNγ Receptor signaling. *Ligand binding induces JAK2 autophosphorylation and activation allowing JAK1 transphosphorylation by JAK2. Activated JAK1 phosphorylates tyrosine residues on the intracellular domain of the IFNGR1 subunits, leading to recruitment and phosphorylation of STAT1. The formation of a homodimer results in translocation to the nucleus and upregulation of IFNγ responsive genes.*

1.7.2. Deficiencies in IFNγ and IFNγR

Deficiencies in IFNγ or the IFNγR, in mice and humans, have highlighted the importance of this system in host defence showing susceptibility to various bacterial, protozoal or viral infections (Dorman and Holland 1998). Mendelian susceptibility to mycobacterial diseases (MSMD) is a rare and life threatening congenital syndrome that was first described in 1951 in an otherwise healthy child with disseminated disease caused by bacillus Calmette-Guerin (BCG) vaccine. Disease causing mutations have been found in IFNGR1, IFNGR2 and STAT1 activation (Filipe-Santos, Bustamante et al. 2006). Individuals with defective IFNγR expression or function have a widespread defect in macrophage activation, resulting in reduced production of TNFα and other proinflammatory cytokines in response to IFNγ, defective MHC class II expression in response to IFNγ, and reduced ability to present antigen to T cells (Dorman and Holland 1998).

The classical activation pathway is clearly beneficial for the survival of an organism, however in order to resolve the infection or injury, the innate immune response requires replacement of lost and damaged cells and re-modeling of damaged extracellular matrix (Colton 2009).

1.8. Alternative activation pathway

The term "alternative activation" was first coined in the 1990's as a pathway distinct from both the IFNγ-mediated classical pathway, and from the direct effects of microbial stimuli such as LPS (Stein, Keshav et al. 1992). These cells fail to make NO and so are inefficient "killing" cells, although they up-regulate MHC class II they are not efficient antigen presenting cells and in fact inhibit T cell proliferation (Mosser 2003). These macrophages are described as regulatory macrophages and are involved in shutting down the production of pro-inflammatory cytokines and increasing factors involved in wound healing and tissue repair (Colton, Mott et al. 2006). It was proposed that Th2 cytokines, IL-4 (Stein, Keshav et al. 1992) and IL-13 (Doyle, Herbein et al. 1994), induce alternative activation in macrophages.
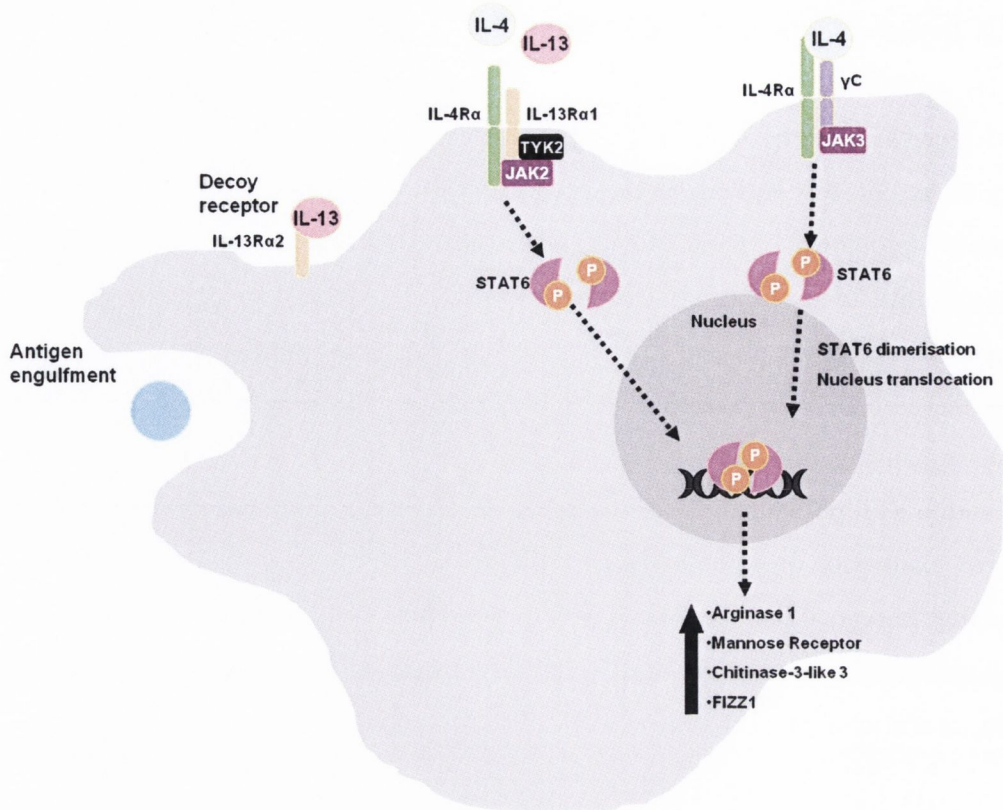
Figure 1.10 IL-4- and IL-13-induced alternative activation pathways. *IL-4- and IL-13-induced alternative activation is mediated through type I and type II receptor complexes resulting in the upregulation of arginase 1, mannose receptor, chitinase 3-like 3 and FIZZ1.*

Alternative activation is identified by the up-regulation of genes that produce arginase I, mannose receptor, and genes associated with tissue remodelling such as found in inflammatory zone 1 (FIZZ1) and chitinase 3-like 3 however the exact functions of many of the protein products of these genes are still unclear (Figure 1.10) (Colton, Mott et al. 2006). Mannose receptor is a transmembrane glycoprotein that mediates Ca^{2+}-dependent endocytosis and phagocytosis of mannosylated ligands (Gordon 2003; Colton, Mott et al. 2006). Arginase 1 has been well studied in peripheral macrophages and is believed to have a role in the production of polyamines and proline; polyamines such as spermine are known to alter cell proliferation, and proline is an important component of collagens which is involved in repair of the extracellular matrix (Mosser 2003; Colton, Mott et al. 2006). Both arginase 1 and inducible NOS, a key component in classical activation pathway, are dependent on arginine and so must compete for arginine explaining the inverse relationship between the two enzymes (Colton 2009). Both

FIZZ1 and chitinase 3-like 3 are believed to play a role in repair processes after infection and injury (Colton, Mott et al. 2006).

1.8.1. IL-4 and IL-13 receptor signalling
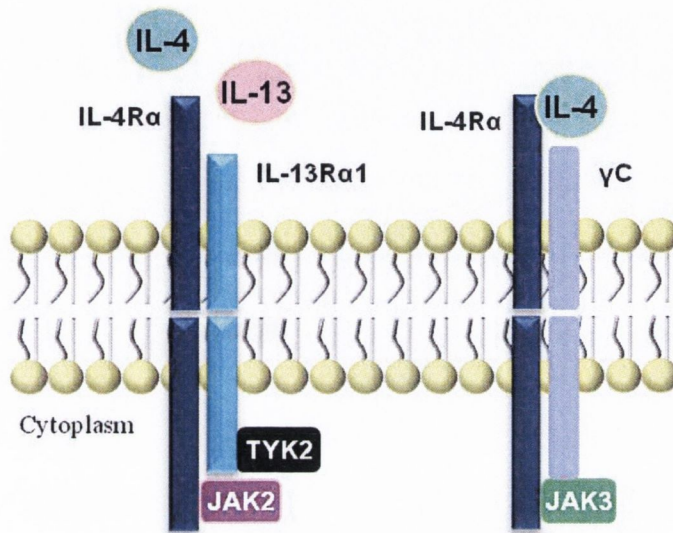
Figure 1.11. IL-4 and IL-13 receptor complexes. *Il-4 binds to the IL-4Rα subunit of both type I (IL-4Rα: γc complex) and type II (IL-4Rα: IL-13Rα1 complex) receptors. IL-13 is recognized by the IL-13Rα1 subunit of the type II receptor complex. Activation of type I receptor complex results in activation of JAK3, while IL-13Rα1 activates TYK2 and JAK2; activated JAKS recruit STAT6 resulting in dimerisation, translocation to the nucleus and upregulation of IL-4 and IL-3 responsive genes.*

IL-4 mediates its effects through type I and type II receptor complexes (Martinez, Helming et al. 2009). The type I receptor complex consists of IL-4Rα subunit and a γc subunit; IL-4 binds to the IL-4Rα subunit of the receptor complex and leads to the γc activation of JAK3. Both IL-13 and IL-4 can bind to the type II receptor complex consisting of IL-4Rα and IL-13Rα1 subunits; IL-4 binds through the IL-4Rα subunit whereas, IL-13 binds through the IL-13Rα1 subunit, leading to the activation of two tyrosine kinases, tyrosine kinase 2 (TYK2) and JAK2 (Martinez, Helming et al. 2009; Oh, Geba et al. 2010). IL-13 can also bind to IL-13Rα2 receptor; however its function is not known (Figure 1.11) (Martinez, Helming et al. 2009). Activated JAKs mediate the phosphorylation of the cytoplasmic tail of IL-4R on conserved tyrosine residues which serve as docking sites for proteins

containing SH2 domains, and serve as docking sites for STAT6 (Oh, Geba et al. 2010). The phosphorylation of STAT6 leads to STAT6 dimerisation and translocation to the nucleus where it binds to the promoters of IL-4 and IL-13 responsive genes (Oh, Geba et al. 2010).

It appears that both in the normal CNS and the diseased brain, immune cells display distinct gene profiles resulting in functional phenotypes ranging from the characteristic pro-inflammatory profile resulting from classical activation state to an alternative activation state resulting in tissue repair and extracellular matrix remodelling (Colton, Mott et al. 2006).

1.9. Deactivation of the immune response
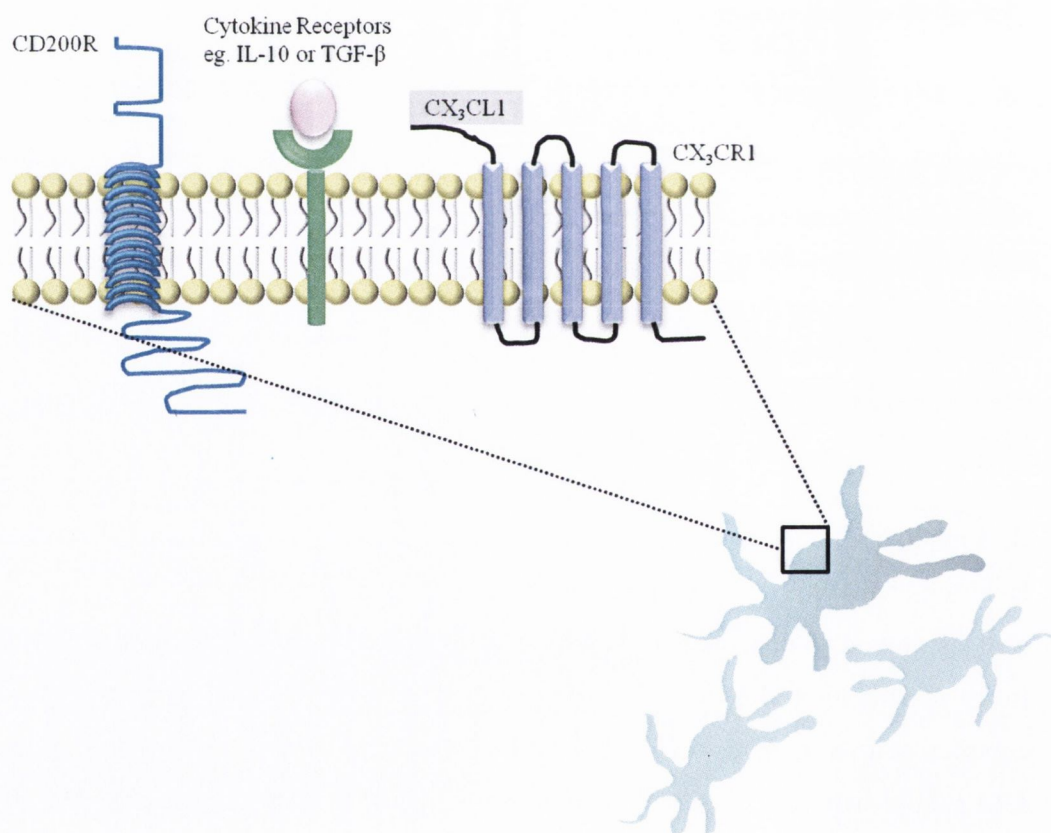
Figure 1.12. Maintenance of microglia in a quiescent state. *Microglia express CD200R and CX$_3$CR1, receptors for neuronal CD200 and Fractalkine, both suggested to suppress the activation of microglia. Further, neurons, astrocytes and microglia all produce cytokines IL-10 and TGFβ which shift microglial activation to a strong immunosuppressive state.*

1.9.1 Acquired deactivation

Acquired deactivation, like alternative activation, is associated with the down-regulation of the innate immune response, with both displaying similar but not identical gene profiles. The induction of acquired deactivation is mediated by immunosuppressive cytokines TGFβ and/or IL-10 (Figure 1.12) (Colton 2009). Astrocytes and microglia, and in some cases neurons, are capable of producing and releasing IL-10 and TGFβ when stimulated (Colton and Wilcock 2010). TGFβ and IL-10 have been shown to repress the production of IL-1β, TNFα, iNOS and MHCII gene expression, in macrophage and microglia, all characteristic of a proinflammatory classical immune response. Furthermore, increased levels of TGFβ promote IL-10 production and both cytokines can feed back in an autocrine or paracrine fashion to raise their own levels (Colton and Wilcock 2010). Acquired deactivation shifts cells towards a strong immunosuppressive state and is often initiated in response to apoptotic cells; the interaction between microglia and apoptotic cells increases the expression of spingosine phosphate kinase (SphK), an enzyme that catalyses the phosphorylation of spinogosine to form sphingosine 1-phosphate, leads to intacellular signalling cascades and subsequent upregulation of anti-apototic proteins, SphK is regarded as a candidate for a marker of acquired deactivation (Colton and Wilcock 2010). Due to its anti-inflammatory role, IL-10 has been targeted as a potential therapy for neuroinflammatory diseases (Colton and Wilcock 2010). Other substances such as glucocorticoids are immune-suppressive in high concentrations and inhibit MHC I and II and antigen processing (Ma, Chen et al. 2003).

1.9.2. Cell-cell contact: maintaining microglia in a quiescent state

In addition to the role of soluble secreted factors, deactivation/suppression has been described in response to cell-cell contact in which the interaction between ligand-receptor pairs plays a role in the down-regulation of macrophage activation (Figure1.12) (Barclay, Wright et al. 2002). Fractalkine (CX₃CL1) is the sole member of the CX₃C chemokine family of proteins and has demonstrated modulatory effects on microglial activation attenuating LPS-induced microglial

activation *in vitro* and the age-related increase *in vivo* (Lyons, **Lynch** et al. 2009). Signalling induced by microglial receptors CD172, CD200R and CD45 following interaction with neuronal CD47, CD200 and CD22, respectively, has also been reported to inhibit microglial activity (Saijo and Glass 2011).

1.10. Modulation of microglial activity: CD200-CD200R interaction

1.10.1. CD200

CD200, originally referred to as OX2, is a type I transmembrane glycoprotein with two immunoglobulin superfamily (IgSF) domains and a short cytoplasmic domain. Barclay and colleagues sequenced the CD200 antigen deducing a N-terminal domain which fit best with Ig V domain, while the C terminal part was like a C domain (Clark, Gagnon et al. 1985; Preston, Wright et al. 1997). The V-set is the variable domain and contains the antigen-binding properties, where the C-domain mediates the effector function, C-domains are distinguished by being shorter than V-domains, the C2-set found in CD200, has a similar sequence to V-domains but is closer in size to C-domains (Barclay 2003). Cell surface markers containing Ig-like domains are among the most abundant protein classes expressed in the mammalian genome (Wright, Cherwinski et al. 2003). Members of the IgSF include cell surface antigen receptors, co-receptors and co-stimulatory molecules of the immune system, molecules involved in antigen presentation to lymphocytes, cell adhesion molecules, certain cytokine receptors and intracellular muscle proteins. CD200 belongs to a group of leukocyte IgSF glycoproteins that includes NCAM, which plays a role in cell-cell adhesion, Thy-1, the smallest member of the IgSF, and the L1 family of cell adhesion molecules, all of which are expressed on both lymphoid and neuronal tissue (Webb and Barclay 1984; Preston, Wright et al. 1997; Wright, Puklavec et al. 2000).

CD200, first described in the thymus and brain (McMaster and Williams 1979), has been shown to be expressed on a variety of cells types including neurons (Webb and Barclay 1984), follicular dendritic cells and endothelium (Barclay 1981; Webb and Barclay 1984; Clark, Gagnon et al. 1985), and more recently its

expression on astrocytes has been shown (Costello, Lyons et al. 2011). Its broad pattern of distribution and short cytoplasmic domain, devoid of any known signaling motifs, make identification of its function difficult, however based on its localisation, IgSF sequence and its structural and genetic relationship with co-stimulatory molecules B7-1 and B7-2, it seemed likely it would interact with another cell surface protein (Wright, Puklavec et al. 2000). In 1997, a cell surface ligand for CD200 was identified on macrophage using a soluble chimeric protein from the extracellular region of CD200 engineered onto domains 3 + 4 of rat CD4 antigen (Preston, Wright et al. 1997).

1.10.2. CD200R

CD200 receptor, or OX2R, highly expressed on myeloid cells, is closely related to CD200 and it is thought they probably evolved by gene duplication (Barclay, Wright et al. 2002). Structurally, CD200 and CD200R also resemble each other. Both the receptor and ligand contain the same V/C2 IgSF domains, interestingly both contain unusual and characteristic additional cysteine residues in their V-like domains which distinguish them from their closely related B7 molecules (Wright, Puklavec et al. 2000). One interesting feature of the CD200R is a high content of N-linked glycosylation sites, six potential sites have been identified in mouse (Barclay 2003). Variable levels of glycosylation is a feature of IgSF domains these carbohydrates are believed to provide a shield to prevent unwanted interactions with other proteins at the surface or with soluble proteins, they are also believed to assist in restricting the movement of the membrane glycoprotein, optimising access to the binding site (Barclay 2001; Barclay 2003).

CD200 and CD200R are believed to interact via their N-terminal IgSF V set domains (Figure 1.13) (Preston, Wright et al. 1997). The 67 amino acid cytoplasmic region of CD200R was found to contain three tyrosine residues as potential phosphorylation sites, the membrane distal tyrosine is located within a NPXY signaling motif, which is known to interact with the phosphotyrosine-binding (PTB) domains present in several signaling adaptor molecules (Wright, Puklavec et al. 2000).
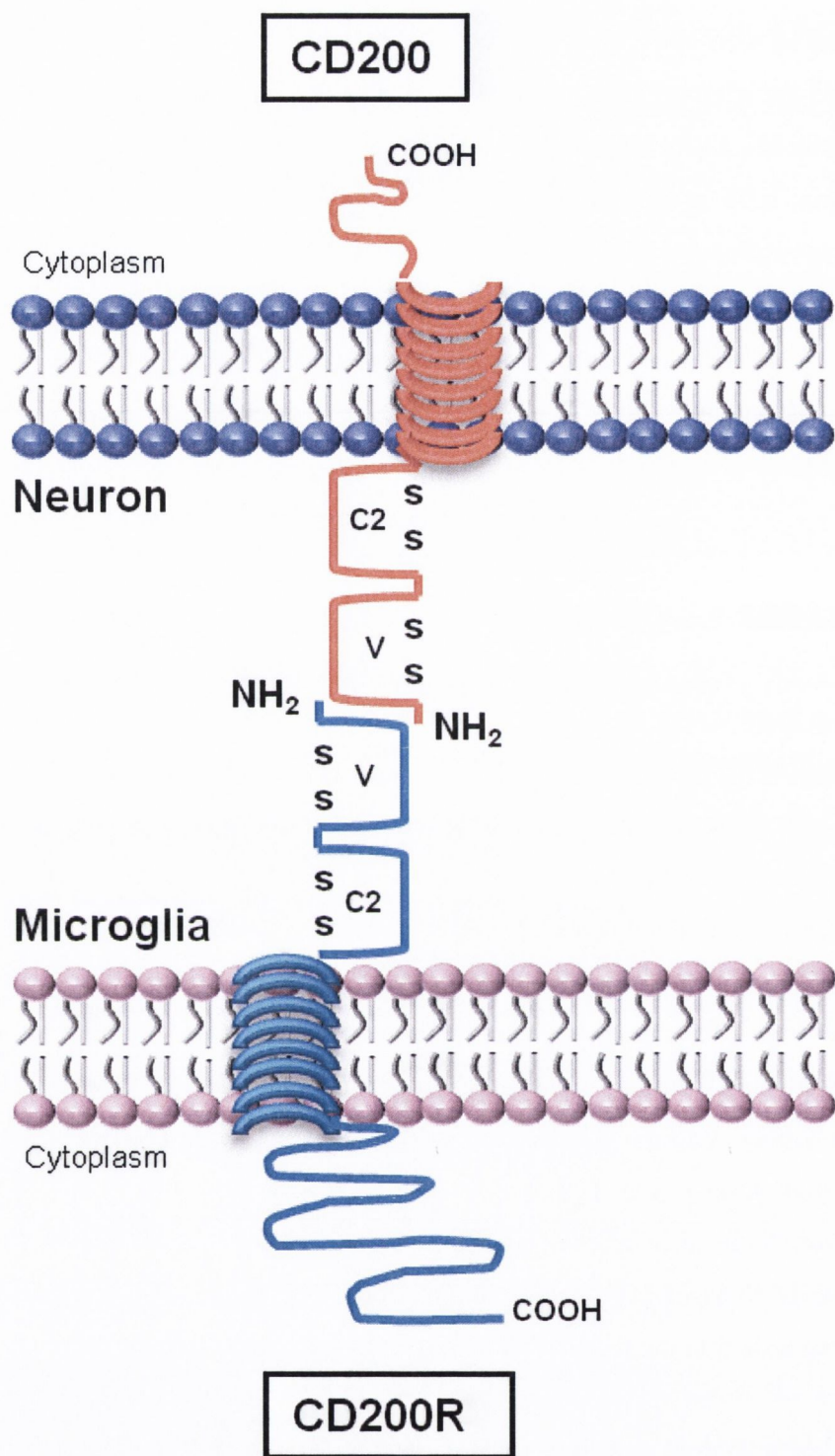
Figure 1.13. CD200-CD200R interaction. *Structurally related CD200, expressed on neurons, and CD200R, expressed on microglia, contain the same V/C2 IgSF domains and interacts through their N-terminal IgSF V domain.*

1.10.2.1. CD200R signalling

A study in U937 cells expressing wildtype or mutant human CD200R, determined CD200R signaling was dependent on the most distal tyrosine residue, the second tyrosine residue appeared to have no functional dependence, and phosphorylation of the proximal tyrosine may function to stabilize interactions with the third (Mihrshahi, Barclay et al. 2009). Ligation of the receptor and tyrosine phosphorylation of the distal tyrosine leads to recruitment of adaptors downstream of tyrosine kinase 1 (DOK1) and DOK2, and recruitment of RAS p21 protein activator 1 (RasGAP) and the phosphatase SH2-containing inositol phosphatase (SHIP) which leads to inhibition of Ras and ERK activation and the ras/mitogen-activated protein kinase (MAPK) pathway (Figure 1.14) (Barclay, Wright et al. 2002; Snelgrove, Goulding et al. 2008; Mihrshahi, Barclay et al. 2009). Recent evidence indicates that the interaction between CD200R and DOK2 is crucial in initiating signaling, it is likely that DOK1 is recruited to CD200R via DOK2 rather than by a direct association with the receptor due to its high affinity for phosphorylated DOK2 and relatively low affinity for CD200R (Mihrshahi, Barclay et al. 2009); furthermore the suppressive effects of CD200Fc on Aβ-induced pro-inflammatory release were blocked in cells that were incubated in the presence of Dok2 siRNA (Lyons, Downer et al. 2012). Phosphorylated SHIP binds to DOK1 in response to CD200R ligation in mast cells, a sub population of leukocytes that are implicate in a variety of inflammatory disorders (Zhang, Zhang et al. 2004; Cherwinski, Murphy et al. 2005); recent experiments carried out in a human system demonstrated SHIP knockdown had no effect on CD200R signaling (Mihrshahi, Barclay et al. 2009). Although the full pathway remains to be elucidated evidence suggests that CD200R signaling is reliant on recruitment and activation of DOK1/DOK2 and RasGAP for the ability to inhibit Ras-ERK signaling offering a potential biochemical mechanism for initiating signal transduction as a consequence of CD200-CD200R interaction.
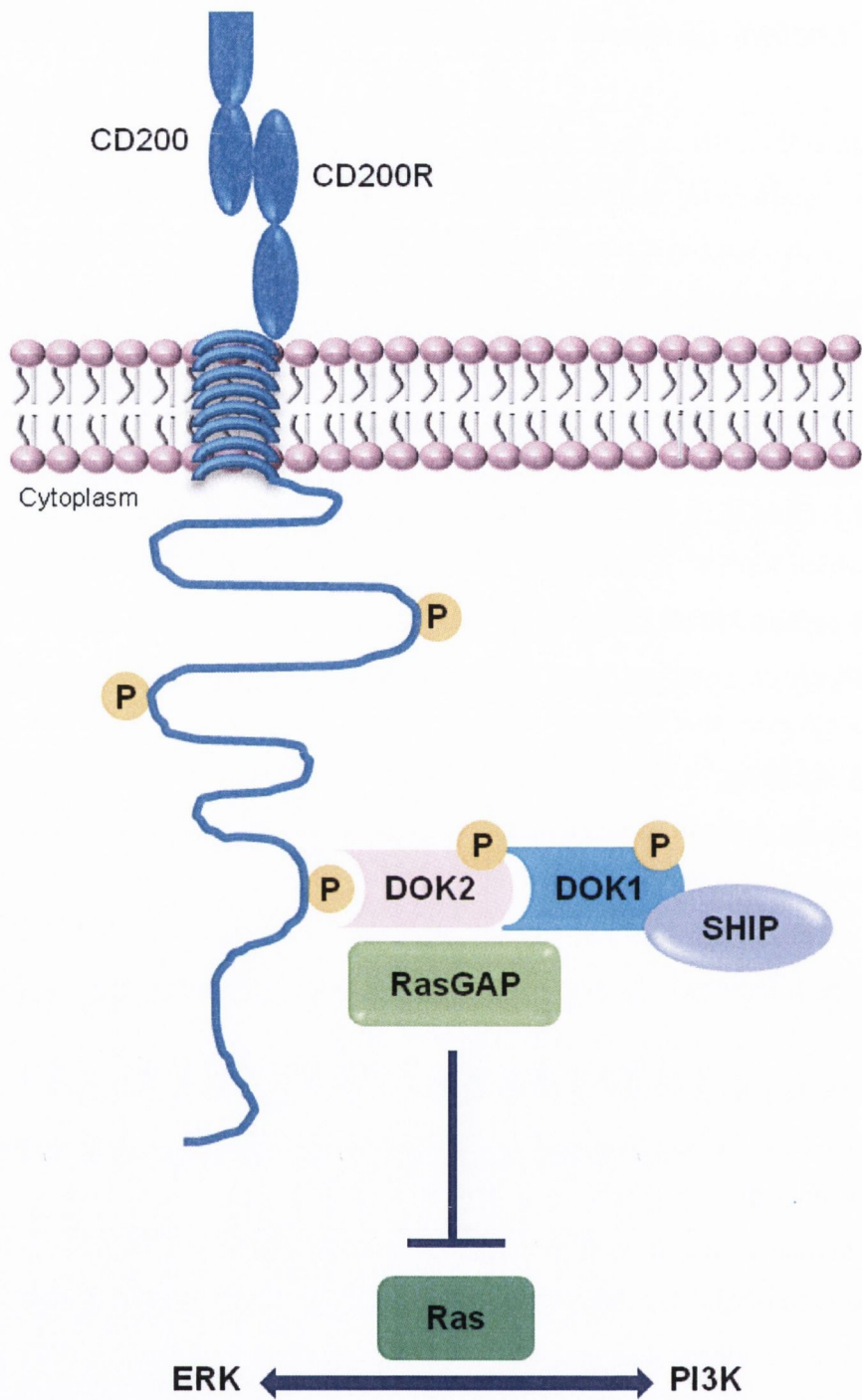
Figure 1.14. A model for CD200 receptor signaling. *Ligation of CD200R results in DOK2 binding the distal phosphotyrosine in the cytoplasmic tail; DOK2 phosphorylation leads to the recruitment and activation of DOK1, RasGAP and SHIP resulting in inhibition of Ras and ERK activation and the ras/mitogen-activated protein kinase (MAPK) pathway*

1.11. The role of CD200-CD200R interaction in the regulation of inflammation

The first clues towards understanding a function for the CD200-CD200R interaction came with the discovery that CD200 contains two IgSF domains and a single transmembrane domain common in proteins mediating cell-cell interactions. At the leukocyte cell surface almost half the proteins with IgSF domains only contain two domains and this may be important in ensuring the right distance for interactions between two cells. In addition, while the distribution of CD200 at first seemed unusual, the discovery of the CD200R and its restricted expression to cells of the myeloid lineage provides points of control for myeloid cells in a variety of tissues (Barclay, Wright et al. 2002). However, it is the development of CD200-deficient mice that has led to the most significant advances being made on understanding the possible functions of the CD200-CD200R interaction.

1.11.1 CD200$^{-/-}$ mice

Mice lacking in functional CD200 were developed from C57BL/6 embryonic stem cells transfected with a construct lacking an Eco-47III-Sal 1 fragment of a CD200 genomic clone and microinjected into BALB/c blastocysts. Chimeras were mated with C57BL/6 mice and CD200$^{-/-}$ offspring generated by crossbreeding offspring expressing the deleted germ-line DNA (Hoek, Ruuls et al. 2000; Minas and Liversidge 2006). CD200 Heterozygous (+/-) and homozygous (-/-) mice were normal in appearance, bred normally, and exhibited normal life span with no obvious behavioral differences when compared with CD200$^{+/+}$ (wildtype) mice (Hoek, Ruuls et al. 2000). However, on closer inspection CD200$^{-/-}$ mice expressed increased numbers CD11b^{+} myeloid cells in the spleen compared with wildtype mice (Hoek, Ruuls et al. 2000). A defect in the organization of the mesenteric lymph nodes was also reported (Barclay, Wright et al. 2002) along with an expanded and activated population of macrophages (Hoek, Ruuls et al. 2000). Microglia from CD200$^{-/-}$ mice displayed a highly activated phenotype, including a less ramified morphology, shorter glial processes, a disordered arrangement and increased levels of markers of microglial activation including CD11b and CD45,

and increased expression of CD68 and NOS2. Interestingly the microglia form aggregates more readily and appear clustered in the spinal cord, this is rarely seen in healthy CNS and is often associated with inflammation and neurodegeneration (Hoek, Ruuls et al. 2000; Nathan and Muller 2001).

As an absence of CD200 resulted in an increase in cells that express the CD200R and a higher expression of cell surface markers CD11b and CD45, it was hypothesized that CD200$^{-/-}$ mice display a state of myeloid cell tonic activation (Hoek, Ruuls et al. 2000). In the facial nerve transection injury model, CD200$^{-/-}$ mice showed an accelerated microglial response, with microglial activation detected 2 days after transection peaking at 4 days, as opposed to that seen in wildtype mice, where microglial activation was detected at 4 days and peak at 7 days (Hoek, Ruuls et al. 2000; Wang, Ye et al. 2007). Experimental Autoimmune Encephalomyelitis (EAE), a model of human disease multiple sclerosis (MS), results from the activation of peripheral T lymphocytes, macrophages and granulocytes, which are believed to migrate to the CNS where they cause microglial activation, tissue damage and neurological deficits. EAE can be induced in mice by injecting myelin oligodendrocyte glycoprotein (MOG), *mycobacterium tuberculosis* and pertussis toxin (Nathan and Muller 2001). MOG-induced EAE was earlier in CD200$^{-/-}$, compared with wildtype mice (Hoek, Ruuls et al. 2000). Similarly, CD200$^{-/-}$ animals showed an increased susceptibility to collagen-induced arthritis (CIA), an autoimmune model of rheumatoid arthritis, induced by injection of chicken collagen and *M. tuberculosis*, developing moderate to severe arthritis with synovial inflammation and cartilage and bone degradation compared with C57BL/6 mice which are normally resistant to CIA (Hoek, Ruuls et al. 2000; Nimmerjahn, Kirchhoff et al. 2005).

The first reported CD200R knock out mouse was described by Boudakov et al. in 2007, and confirmed the phenotype observed in CD200$^{-/-}$ mice. Similar to that observed with CD200-deficient mice, they were found to have normal appearance, fertility and lifespan. However multiple tests of immunological function in these animals demonstrated that they were quite unlike their wildtype counterparts. Stimulation of splenic TNFα production by LPS was enhanced in these CD200R (-/-) mice relative to control (+/+) mice and further, was not suppressed by addition of exogenous CD200Fc (Boudakov, Liu et al. 2007). These data further

establish the role of CD200-CD200R interaction in attenuation of inflammation and regulation of immune responses.

1.12. Manipulation of the CD200-CD200R interaction – therapeutic potential?

CD200 fusion protein (CD200Fc), a synthetic activator of the CD200R, has shown potential for use as a therapeutic agent in a number of animal models of disease and inflammation (Barclay, Wright et al. 2002). In murine induced CIA, associated with activation of T cells producing type I cytokines IFNγ and IL-2 and increased TNFα, infusion of CD200Fc was effective at decreasing induction of the disease and this was associated with decreased serum levels of IFNγ and TNFα (Gorczynski, Chen et al. 2001). The immunosuppressive nature of CD200Fc has also been observed in a transplant model (Gorczynski, Chen et al. 2004), resulting in prolonged tissue graft survival and, in a model of tumor rejection, where it reversed the protective effects of prior immunization with tumor cells expressing CD80 (Barclay, Wright et al. 2002). A recent study investigated the therapeutic value of CD200Fc administration to control the severity of ocular lesions caused by herpes simplex virus (HSV) infection, although complete reversal of the lesion was not achieved, CD200Fc demonstrated potential for the treatment of viral-induced inflammatory disease (Barclay, Wright et al. 2002; Sarangi, Woo et al. 2009).

Airway macrophages are located at the interphase between the air and lung tissue and provide the first line of defense following inhalation of airborne pathogens (Tate, Pickett et al. 2010). Interestingly these macrophages have higher basal levels of CD200R relative to other tissue macrophages linked with the constitutive expression of IL-10 and TGFβ. Epithelial cells which line the lumenal aspect of the airway express CD200 and thus have the ability to regulate the site specific macrophage creating an immune-suppressed population. The importance of homeostatic maintenance mediated by the CD200-CD200R interaction in airway macrophages is highlighted in CD200$^{-/-}$ mice infected with influenza which resulted in enhanced macrophage activity, delayed resolution of inflammation and ultimately, death (Snelgrove, Goulding et al. 2008). Thus the absence of CD200

35

primed these macrophages to respond to activating stimuli. The administration of fusion protein or agonists that bind CD200R restored inflammatory control and cleared the virus offering a potential therapeutic strategy. The current evidence cements the role of the CD200-CD200R interaction as an immunomodulatory pathway with direct delivery of immunosuppressive responses after antigen challenge (Nimmerjahn, Kirchhoff et al. 2005).

Due to the relationship between neuronal CD200 and glial CD200R and the important role of microglial activation in the progression of neurodegenerative diseases, it has been proposed that CD200-CD200R signaling is closely correlated to microglial activation (Wang, Ye et al. 2007). The *Wld* mouse is a spontaneously-occurring mutant with the unique phenotype of protection against several forms of axonal injury (Chitnis, Imitola et al. 2007). A reduced susceptibility to EAE in the *wld* mutant mouse strain compared with wildtype mice, has been reported, characterized by delayed onset and an attenuated disease course; this is associated with enhanced neuronal expression of CD200 which was pivotal in suppression of CNS inflammation (Chitnis, Imitola et al. 2007; Walker, Dalsing-Hernandez et al. 2009). Blocking CD200 in *Wld* mice with antibodies restored EAE pathology to control levels (Walker, Dalsing-Hernandez et al. 2009). Using this model it has been demonstrated that increased expression of CD200 is capable of protecting neurons and axons from microglia-induced damage *in vitro* and *in vivo* (Chitnis, Imitola et al. 2007). As progressive forms of MS are associated with diffuse axonal damage and microglial activation, enhanced levels of CD200 demonstrates potential as a therapeutic strategy in the treatment of the neurodegenerative disorder MS.

A recent study has found both a deficiency in CD200 and CD200R in human AD brains suggesting reduced efficacy of the CD200-CD200R system to control inflammation (Walker, Dalsing-Hernandez et al. 2009). It was suggested that increasing expression of CD200 and CD200R therapeutically may provide a method of enhancing the efficacy of the system. Interestingly, data have indicated that IL-4 can increase CD200 expression in cultured neurons from mice and that IL-4$^{-/-}$ mice have lower levels of CD200 (Lyons, Downer et al. 2007). This has been strengthened by the recent discovery that CD200R mRNA expression was strongly increased in microglia and macrophage by IL-4 treatment in a dose-

dependent manner (Walker, Dalsing-Hernandez et al. 2009). This reinforces the evidence suggesting that strategies which enhance the CNS expression of CD200 or which trigger CD200R activation may suppress inflammatory mediated neurodegeneration.

1.13. Glial dysfunction in aging and disease

The brain is very sensitive to even the most subtle inflammatory changes and the balance between pro- and anti-inflammatory influences in the microenvironment has profound effects on neuronal function. Chronic inflammation is a pathological hallmark of many age-related neurodegenerative diseases including AD (Walker, Dalsing-Hernandez et al. 2009), however how such an inflammatory cascade ensues is still beyond our knowledge. What has become clear is that much of the regulatory systems that are in place in the CNS to control the inflammatory response lose effectiveness during aging and indeed AD pathogenesis resulting in an imbalance between inflammatory mediators and inflammatory regulators (Walker, Dalsing-Hernandez et al. 2009). Thus, microglia can become dysregulated in the context of age and neurodegeneration and thereby may contribute to disease progression and severity. Age-related inflammatory changes include increased MHC class II and proinflammatory cytokine expression including IFNγ, a potent activator of microglia, and a decrease in CD200 (Frank, Barrientos et al. 2006), this may prime the microglia and play a role in the development of age-related inflammatory diseases.

1.14. Objectives

It is clear that microglia can adopt multiple activation states in response to different stimuli. It was predicted that the loss of CD200 would result in alterations in the inflammatory phenotypes of microglial cells. Thus, the objectives of this study were to investigate the role of CD200 in modulating microglial activity with respect to innate, classical and alternative activation states *in vitro* and *in vivo*.

Specifically, the aims of this thesis were:

- To assess the inflammatory responses of glia prepared from wildtype and CD200$^{-/-}$ mice to TLR4 agonist, LPS; and to assess the impact of CD200-CD200R interaction on these responses

- To assess the activation states of mixed glia and purified microglia prepared from wildtype and CD200$^{-/-}$ mice to IFNγ and IL-4, and assess whether modulating the CD200-CD200R interaction could alter the different activation states

- To assess how CD200-deficiency in vivo may alter control of inflammation at basal levels resulting in dysfunctional regulation of immune homeostasis in the brain

Chapter 2
Methods

2.1. *In vitro* studies

2.1.1. Preparation of primary cultures

Mixed glia were prepared from cortices of 1-day old C57/BL6 mice (wildtype) and CD200$^{-/-}$ mice (BioResources Unit, Trinity College, Dublin, Ireland). Mice were decapitated and brain cerebral cortices were dissected, bi-directionally chopped using a sterile scalpel and placed in a 15ml falcon tube (Sarstedt; Ireland) in Dulbecco's modified Eagle's medium (DMEM; 2ml; Invitrogen, Ireland) supplemented with 10% foetal bovine serum (FBS) (Gibco, UK) and 1% penicillin and streptomycin (Gibco; UK), from now on this will be referred to as supplemented DMEM. Samples were triturated and passed through a sterile nylon mesh cell strainer, centrifuged (2000xg, 5 minutes, 20°C), and the pellets resuspended in supplemented DMEM. Cells were plated (1 x 10^6 cells/ml) in 6-well plates (Sarstedt; Ireland) and incubated for 2 hours before the addition of warmed supplemented DMEM (1.5ml). Cells were grown at 37°C in a humidified environment (5% CO$_2$: 95% air) for 12 days prior to treatment and the medium was replaced every 3 days.

2.1.2. Preparation of cultured microglia and astrocytes

Primary cortical microglia and astrocytes were prepared from 1-day old wildtype and CD200$^{-/-}$ mice using the same method for primary cortical glia cells described in section 2.1.1, with the exception that the resulting pellet was resuspended in 5ml supplemented DMEM and seeded in separate T25 flasks (Sarstedt, Germany). Glia were left for 48 hours (5% CO$_2$, 95% air, 37°C) allowing cells to adhere before adding cultured media (5ml) enriched with 2x mononuclear phagocyte colony stimulating factor (M-CSF; 20ng/ml; R&D Systems; US) and 2x granulocyte macrophage colony stimulating factor (GM-CSF; 10ng/ml; R&D Systems; US). On day 5 the enriched cultured media was removed and replaced with enriched cultured media (6ml) and every 3 days following. On day 10 flasks were wrapped with parafilm (Alcan, US), making an air tight seal around the cap and neck of the flask, and placed on an orbital shaker (110rpm) for 2 hours at RT.

Flasks were returned to the hood and the supernatant containing suspended microglia was poured into a 50ml falcon tube and centrifuged (2000rpm; 5 minutes; 20°C). The resulting pellet was resuspended and plated in 6-well plates (2 x 10^5 cells/ml).

Astrocytes, which remain adhered to the flask, were incubated in trypsin-ethylenediaminetetraacetic acid (1.5ml; Trypsin-EDTA; Sigma Alrich; UK), for 10 minutes at 37°C before the flask was tapped and the contents poured off into a 50ml falcon tube and centrifuged (2000rpm; 5 minutes; 20°C). The resulting pellet was resuspended in supplemented DMEM and plated at the appropriate density.

Both the microglia and astrocytes were plated in supplemented DMEM (1ml) and allowed to adhere, the following day supplemented DMEM (0.5ml) was added and cells were allowed rest for a further 24 hours before treatment.

2.1.2.1. Cell counting

Cell counts were performed by diluting cells in trypan blue (1:10; Sigma Alrich, UK). An aliquot of cell suspension (approximately 10µl) was loaded onto the haemocytometer. Viable cells were visualised as white under the light microscope and counted before plating at the desired density, as described above.

2.1.3. Cell treatments

All agents used to treat cells were diluted to required concentrations in pre-warmed supplemented DMEM and all solutions were filter-sterilised through a 0.2µm cellulose acetate membrane filter.

Lipopolysaccaride (LPS; Sigma, UK) was diluted to a final concentration of 10-100ng/ml in supplemented DMEM. A time course was carried out to establish the ideal treatment period for specific experiments.

IFNγ (R&D Systems; UK) was prepared as a stock solution in sterile phosphate-buffered saline (PBS) and 1% BSA and diluted to the desired concentration of 50ng/ml in supplemented DMEM. Cells were treated for 24 hours with IFNγ.

A stock solution of IL-4 (R&D systems, UK) was prepared in sterile PBS and 1% BSA and diluted to the desired concentration in supplemented DMEM (200ng/ml). Cells were treated for 24 hours.

CD200Fc (R&D systems, UK) was prepared as a stock solution in sterile PBS and 1% BSA. Cells were pre-treated with CD200Fc (2.5µg/ml; 1 hour) and co-incubated in the presence or absence of IFNγ (50ng/ml; R&D systems, UK) for a further 24 hours.

HMGB1 (Sigma Aldrich; UK) was prepared as a stock solution in sterile H_2O, and stored in working aliquots at -80°C. Cells were challenged with HMGB1 (100ng/ml) alone or in combination with LPS (100ng/ml). HMGB1 diluted in PBS was incubated with LPS at 37°C for 30 minutes before addition to cell cultures.

Following the indicated treatments, supernatants were removed and stored in 1.5ml tubes at -80° (Fisher Scientific; UK) for later cytokine and chemokine analysis. Cells used for polymerase chain reaction (PCR) were harvested by washing in sterile 1x PBS and lysed in RA1 buffer (Macherey-Nagel; US) containing β-mercaptoethanol (1:100 dilution; Sigma Alrich; UK) and stored at -80°C in RNase free tubes (Medical Supply Company, Ireland) for later analysis of messenger ribonucleic acid (mRNA) expression. Cells used for western immunoblotting were harvested by washing once in sterile PBS and lysed in ice-cold lysis buffer (100µl; 10mM Tris HCl, 50mN NaCl, 10mM $Na_4P_2O_7.H_2O$, 50mM NaF, 1% Igepal, 1:100 dilution phosphatase inhibitor cocktail I and II, 1:100 dilution protease inhibitor cocktail; Sigma, UK), scraped off and stored at -80°C in 1.5ml tubes.

2.2. Analysis of mRNA expression

RNA was isolated and cDNA synthesised from hippocampal tissue from wildtype and CD200$^{-/-}$ mice. Quantitative real-time PCR (RT-PCR) was carried out to analyse the gene expression of proinflammatory cytokines IL-β, TNFα and IL-6, and markers of microglia which reflected the innate immune response as well as markers of classically- and alternatively-activated microglia.

2.2.1. RNA Isolation

Messenger RNA (mRNA) was extracted from snap-frozen hippocampus. Tissue was washed 3 times in Krebs buffer, placed in 2ml RNase free tubes (NucleoSpin® RNA II – MACHEREY-NAGEL) and homogenised in Cell Lysis Mastermix (350µl RA1 + 3.5µl β-mercaptoethanol) in the fume hood with 2x 5sec pulses of the polytron mixer. The resulting lysate was filtered through NucleoSpin® Filter units (violet) into a new collecting tube and centrifuged (11,000 g; 1 minutes). In the case of cultured cells, up to 5x10^6 cultured cells were collected, lysed in RA1 buffer and β-mercaptoethanol (1:100 dilution) and added to the membranes of NucleoSpin® filters and centrifuged (11,000 g; 1 minute). The NucleoSpin® Filter units were discarded and 70% ethanol (350µl; prepared using DEPC-H$_2$O) was added to the homogenized lysate. NucleoSpin® column units (light blue), which bind the RNA, were placed in 2ml centrifuge tubes and the lysate was loaded and the samples were centrifuged (8,000 g; 30 seconds). The columns were placed in new collecting tubes, and the membrane desalting buffer was applied (350µl; NucleoSpin® RNA II – MACHEREY-NAGEL), and the samples were centrifuged (11,000 g; 1 minute). In order to digest the DNA, rDNase reaction mixture (95µl) was added directly to the centre of the silica membrane of the column and left at room temperature for 15 minutes. The silica membrane was washed and dried. RA2 buffer (200µl) was added to the NucleoSpin® columns and centrifuged (8,000 g; 30 seconds). The column was placed in a new collecting tube and washed with RA3 buffer (600µl) and centrifuged (8,000 g; 30 seconds). The flow-through was discarded and the column placed back in the same collecting tube. RA3 buffer (250µl) was added to the NucleoSpin® columns and centrifuged (11,000 g; 2 minutes), following which

the column was placed in a new pre-labelled nuclease free 1.5ml micro centrifuge tube (NucleoSpin® RNA II). The RNA was eluted using RNase-free water (40μl x 2) and centrifuged (11,000 g; 1 minute) and the NucleoSpin® columns discarded. RNA concentration was quantified using the Nanodrop Spectrophotometer ND-1000 and samples were equalised to 1μg total RNA with RNase-free water.

2.2.2. cDNA Synthesis

RNA was reverse-transcribed into cDNA using high-capacity cDNA archive kit (Applied Biosystems, UK). The master mix was prepared from the components of the high-capacity cDNA archive kit (10X Reverse transcription buffer; 25X dNTPs; 10X random primers; MultiScribe reverse transcriptase (50U/μl); nuclease-free water) the amounts of which were scaled depending on how much cDNA was needed. Mastermix and RNA were added in a 1:1 ratio. The appropriate quantity of Mastermix was added to each PCR tube (Starstedt; Ireland) and the same quantity of RNA was added. The contents were mixed and tubes were placed in the mini centrifuge to eliminate any bubbles, and then placed in the thermal cycler (10 minutes at 25°C; 120 minutes at 37°C). cDNA was stored at -20°C until needed for PCR.

2.2.3. RT-PCR

Real-time PCR primers were delivered as Taqman® Gene Expression Assays containing forward and reverse primers, and a FAM-labelled MGB Taqman probe for each gene (Table 2.1; Applied Biosystems, US). A 1:4 dilution of cDNA with RNase-free water was prepared and real-time PCR performed using Applied Biosystems 7300 Real-time PCR system. cDNA was mixed with qPCR Mastermix (Applied Biosystems; US) containing a thermostable DNA polymerase, Taq, (12.5μl) and the respective gene assay (1.25μl). Mouse β-actin was used as an endogenous control. Forty cycles were run as follows: stage 1, 50°C for 2 minutes; stage 2, 95°C for 10 minutes; stage 3, 95°C for 15 seconds and; stage 4, 60°C for 1 minute. After 40 cycles the plate was removed and the

data analysed using 7500 Fast system V1.3.1 relative quantitative study. Gene expression was calculated relative to the endogenous control and samples were calibrated to a control sample, where the baseline was established on the linear amplification plot. Analysis was performed using the $2^{-\Delta\Delta Gt}$ method. Data were analysed using GraphPad Prism 5.

Gene Name	TaqMan Gene Expression Assay Number
IL-1β	Mm00434228_m1
TNFα	Mm0043258_m1
IL-6	Mm00446191_m1
CD68	Mm03047340_m1
CD40	Mm0041895_m1
CD11b (Itgam)	Mm01271263_m1
TLR2	Mm00442346_m1
TLR4	Mm00445273_m1
TLR6	Mm02529782_s1
CD14	Mm00438094_g1
Mannose Receptor (Mrc1)	Mm00485148_m1
Arginase 1	Mm00475988_m1
Chitinase-3-like 3	Mm04213363_u1
Fizz1	Mm00488611_m1
NOS2	Mm00440502_m1
B-actin	Mm00607939_s1
IFNγ	Mm00801778_m1
IFNγ receptor	Mm00599890_m1
MHC class II	Mm00439221_m1
MCP1	Mm00441242_m1
IP-10	Mm00445235_m1
Claudin 5	Mm00727012_ml

Table 2.1. Gene expression assay numbers of PCR primers

2.3. Analysis of cytokine concentration

The concentrations of IL-1β, IL-6 and TNFα were assessed by ELISA in supernatant samples obtained from cultured mixed glia prepared from wildtype and CD200$^{-/-}$ mice (R&D systems, UK). Capture antibody (100μl; anti-mouse IL-1β, 4μg/ml; anti-mouse TNF-α, 0.8μg/ml; anti-mouse IL-6, 1μg/ml) was used to coat 96-well plates. Plates were incubated overnight at 4°C, and washed 4 times in wash buffer (250μl Tween-20 in 500ml PBS) and, for IL-1β, were incubated for 1 hour at room temperature in assay diluent (100μl; 0.1% BSA in filtered TBS). In the case of TNF-α and IL-6 plates were incubated at room temperature for 2 hours in assay diluent (100μl; 1% BSA in PBS). Plates were washed and samples (100μl) in duplicate, as well as standards (100μl; 0-2000pg/ml recombinant mouse IL-1β, IL-6 or TNFα) added to the plate and incubation continued at room temperature for 2 hours. Plates were washed 4 times with wash buffer and incubated at room temperature for 2 hours in the presence of detection antibody (100μl; 108μg/ml biotinylated anti-mouse IL-1β; biotinylated anti-mouse TNF-α; or biotinylated anti mouse IL-6). Plates were washed 4 times and, for IL-1β, were incubated in the dark at room temperature for 20 minutes with horseradish peroxidase-conjugated streptavidin (Strep-HRP; 100μl; 50μl Strep-HRP in 10ml IL-1β assay diluent). In the case of TNF-α and IL-6, samples were incubated at room temperature for 30 minutes with Strep-HRP (100μl; 50μl Strep-HRP in 10ml TNF-α or IL-6 assay diluent). Plates were washed 4 times in wash buffer and incubated with substrate solution (100μl; 3,3',5,5' Tetramethybenzidine (TMB) liquid substrate; Sigma, UK), for 20-30 minutes in the dark at room temperature or until colour developed. The reaction was stopped using ELISA stop solution (50μl; 1M H$_2$SO$_4$) and the absorbance was read using Labsystem Genesis v3.03 at a wavelength of 450nm. Cytokine concentrations were estimated from standard curves and expressed as pg/ml; data were analysed using Graph Pad Prism v5.0.

2.4. Protein quantification

Hippocampal tissue was homogenised in lysis buffer (100μl; 10mM Tris HCl, 50mM NaCl, 10mM Na$_4$P$_2$O$_7$.H$_2$0, 50mM NaF, 1% Igepal, 1:100 dilution

phosphatase inhibitor cocktail I and II, 1:100 dilution protease inhibitor cocktail; Sigma, UK). In the case of cultured cells, cells were harvested in 60μl lysis buffer. The protein concentrations were assessed using bicinchoninic acid (BCA) protein assay kit (Pierce, The Netherlands). Standards (0mg/ml-1mg/ml; BSA), and samples (diluted 1:10) were added to the 96-well plate in triplicate and duplicate respectively (25μl/well). Pierce BCA reagent (200μl/well; 1:50 Reagent B to Reagent A) was added to the plate and samples were incubated for 30 minutes at 37°C. The optical density was determined by measuring the absorbance at 565nm. Protein concentrations were calculated relative to the standard curve and were equalised in samples using lysis buffer and 4x Tris-glycine sample buffer (0.5M Tris-HCl pH 6.8, 25% SDS solution, glycerol, dH_20, bromophenol blue, 1:100 dilution β-mercaptoethanol).

2.4.1. Western Blotting

Samples, equalised for protein (20μg), were heated at 70-95°C for 3 minutes and separated on 7%, 10% or 12% Tris-glycine gels (composition; 30% acrylamide; $H20$; 4x SPA buffer: 1.5M Tris/SDS 0.2%, pH 8.8, 10% APS and Temed). MagicMark™ XP protein standard (Invitrogen, Ireland) and SeeBlue® Plus2 Prestained Standard 1x (Invitrogen, Ireland) were loaded on the gel to allow direct visualisation of protein standard bands on the blot with and without chemiluminescence respectively. Proteins were transferred to 0.2 or 0.4μM nitrocellulose membrane and blocked in Tris-buffered-saline containing 0.05% Tween 20 (TBS-T) (composition; 20mM Tris-HCl, 150mM NaCl, 0.05% Tween 20) and 5% dried milk at room temperature. Membranes were incubated overnight at 4°C with primary antibody (see table 2.2), washed, and incubated with the appropriate peroxidase-conjugated secondary antibody for 1 hour at room temperature (see table 2.2). Immunoreactive bands were detected using enhanced chemiluminescence. Blots were stripped (Re-blot plus; Chemicon, US) and reprobed for β-actin (see table 2.2; Sigma, UK). Images were captured using the Fijifilm LAS-4000 system and the image reader LAS-4000 package.

Target	Supplier	Mol. weight	Primary antibody	Secondary antibody (Sigma, UK)
Phospho-IκBα (ser32)	Cell Signalling #2859	40kDa	1:1000 dilution in 2.5% milk/TBS-T	1:5000 dilution anti-rabbit in 2.5% milk/TBS-T
Phospho-IκK	Cell Signalling #2697	85-87kDa	1:1000 dilution in 2.5% milk/TBS-T	1:5000 dilution anti-rabbit in 2.5% milk/TBS-T
IκK	Cell Signalling #2684	87kDa	1:1000 dilution in 2.5% milk/TBS-T	1:5000 dilution anti-rabbit in 2.5% milk/TBS-T
HMGB1	Abcam ab18256	29kDa	1:1000 dilution in 2.5% milk/TBS-T	1:5000 dilution anti-rabbit in 2.5% milk/TBS-T
SOCS1	Cell Signalling #3950	23kDa	1:1000 dilution in 2.5% milk/TBS-T	1:5000 dilution anti-rabbit in 2.5% milk/TBS-T
SOCS3	Cell Signalling #2923	26kDa	1:1000 dilution in 2.5% milk/TBS-T	1:5000 dilution anti-rabbit in 2.5% milk/TBS-T
IFNGR1	Santa cruz	80-95kDa	1:1000 dilution in 2.5% milk/TBS-T	1:5000 dilution anti-rabbit in 2.5% milk/TBS-T
pSTAT1	Cell Signalling		1:1000 dilution in 2.5% milk/TBS-T	1:5000 dilution anti-rabbit in 2.5% milk/TBS-T
β-actin	Sigma, UK	40kDa	1:10,000 dilution in 2.5% milk/TBS-T	1:10000 dilution anti-mouse in 2.5% milk/TBS-T

Table 2.2. Western immunoblotting protocols

2.5. Animals

Male and female, young (2-4 months) and aged (18-22 months), wildtype mice and CD200$^{-/-}$ mice were supplied by Harlan UK Ltd. (Bicester, UK) and the Bioresources unit, Trinity College, respectively. Animals were maintained in the Bio-resources Unit, Trinity College Dublin, under veterinary supervision and were housed in a controlled environment (12-hour light-dark cycle at an ambient temperature of 22-23°C). All animals used in these studies had access to normal laboratory chow and water on an *ad libitum* basis. Experiments were performed under license from the Department of Health and Children (Ireland) and with ethical approval from the local ethics committee in Trinity College Dublin, in compliance with the Cruelty to animals act, 1876 and the European Community Directive, 86/609/EC. Every effort was made to minimise stress to the animals at all stages of the study.

2.5.1. Tissue isolation from CNS

Wildtype and CD200$^{-/-}$ mice were anaesthetised with urethane (1.5g/kg; Sigma Aldrich; IRE), deep anaesthesia was confirmed by the absence of a pedal reflex, following which the animals were perfused intracardially with ice-cold PBS (20ml). The brain was rapidly removed and placed on ice, the cerebellum and olfactory bulbs were removed and the brain was bisected along the midline. A quarter of the hippocampus of the right hemisphere was snap-frozen in liquid nitrogen for later analysis by PCR, a section of cortex was snap-frozen for analysis of IFNγ concentration and mononuclear cells were isolated from the remaining tissue for analysis by flow cytometry.

2.5.1.1 Mononuclear cell isolation from CNS tissue

The section of brain taken for analysis by flow cytometry was cross-chopped and placed in a 5ml glass potter tube containing 3ml medium A (1x HBSS supplemented with 45% glucose and 1M HEPES). The potter was gently moved up and down to dissociate the tissue. Fire polished glass Pasteur pipettes of

decreasing diameters (3x) were used to triturate the sample. Tissue was dissociated through a sterile nylon-mesh filter (70μm), following each trituration the pipette was flushed through the filter with medium A to ensure no cell material was lost. The cell suspension was applied to the 70μm filter and medium A was added to give a total volume of 25ml, samples were centrifuged with no brake (10 minutes; 200 g; 4°C). The resulting pellet was resuspended in 1.088g/ml Percoll (9ml; Sigma Aldrich; UK). This was underlaid with 1.122g/ml Percoll (5ml), and overlaid with 1.072g/ml Percoll (9ml), 1.030g/ml Percoll (9ml), and 1x PBS (9ml). The samples containing the percoll gradients were centrifuged (1250 g; 45 minutes; 20°C). Mononuclear cells were removed from the 1.088:1.072 and 1.072:1.030 g/ml interfaces and washed in medium A (30ml) (Figure 2.1). Cells were stained for flow cytometric analysis.
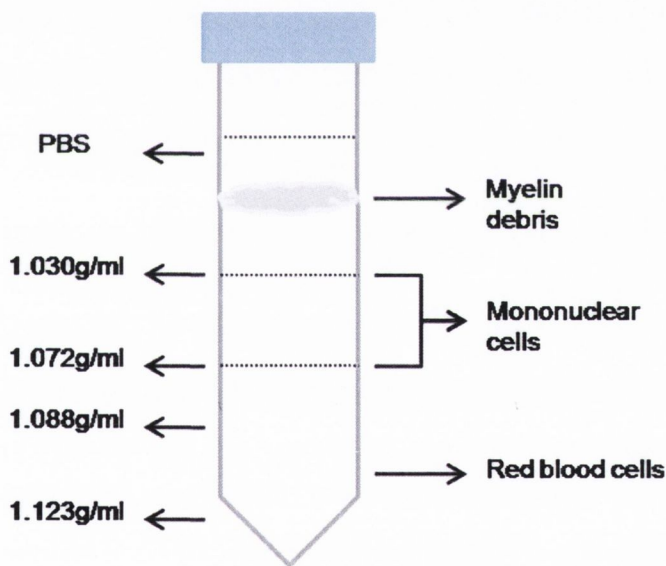
Figure 2.1. Mononuclear cell isolation.

2.6 Fluorescently activated cell sorting- FACS

Surface marker expression on cells prepared from the brain, and on cultured microglia and astrocytes, were analysed by flow cytometry using the Dako Cyan$_{ADP}$ (Advanced Digital Processing) flow cytometer. This instrument is equipped with 488nm (blue) and 633nm (red) solid state lasers, for which nine

parameters are available including Forward Scatter (FSC), Side Scatter (SSC), and seven fluorescent channels (FL1-FL5; FL8-FL9) (Table 2.3).

Channel	Wavelength	Fluorescent label
FL1	490-570nm	FITC/ ALEXA 488
FL2	550-600nm	PE
FL3	593-633nm	PI/ PE-Texas Red
FL4	650-710nm	PerCP/ PECy 5
FL5	<750nm	PeCy7
FL8	655-675nm	APC/ ALEXA 647
FL9	<750nm	APC-Cy7/ ALEXA-750

Table 2.3. Dako Cyan$_{ADP}$ flow cytometer. *Florescent labels and emission spectra for the blue argon laser (488nm) and red diode laser (635nm).*

Mononuclear cells were resuspended in FACS buffer (200µl; composition 500ml PBS, 10ml foetal bovine serum (FBS) and 0.5g sodium azide). Cultured cells were harvested by washing with PBS followed by addition of trypsin-EDTA (150µl; Sigma-Aldrich: UK). Cultured cells were incubated with trypsin and placed in the incubator at 37°C for 5 minutes to remove cells; the trypsin was inactivated by placing the cells in supplemented DMEM (2ml). Cells were washed twice in FACS buffer and centrifuged (1,200 rpm; 5 minutes; 20°C). The low-affinity IgG receptors (FcγRIII) were blocked by incubating with CD16/CD32 FcγRIII block (1:100 dilution; BD Biosciences; UK) for 15 minutes at room temperature. The cells were washed in FACS buffer (2ml/tube) and resuspended in FACS buffer (100µl); the antibodies were added at optimised concentrations (see table 2.4) and incubation proceeded for 30 minutes at RT in the dark. Conjugated antibodies were chosen that emitted florescence at suitable channels for the blue argon laser (488nm) and red diode laser (635nm) (Table 2.3). Cells were washed twice in ice-cold FACS buffer (1,200rpm; 5 minutes; 20°C) and resuspended in FACS buffer (400µl) for data acquisition using Summit v3.4

software (Dako, Denmark). Results were analysed using FlowJo software (Tree Star, US).

2.6.1 Experimental design

As well as experimental samples, unstained cells were used in order to display to the background or autofluorescence of the system. This sample was also required for adjusting voltage and gain of side scatter (SS; intensity proportional to granularity and structural complexity) and gain of forward scatter (FS; intensity proportional to size) in order to isolate the cell population. Setting voltages for fluorescent channels in use allowed for the identification of negative populations.

Polystyrene microparticles were used to optimise florescence compensation settings for multicolour experiments (anti-rat and anti-hamster Ig κ/ negative control (FBS) compensation Particles set; BD Biosciences, UK), appropriate single colour microparticles each conjugated antibody used must have a single colour micro-particles were used for each coloured antibody used in the experiment.

Fluorescence minus one (FMO) samples were used to determine gating boundaries. FMO controls contain every stain in the experiment except the one you are controlling for in that sample, for example, a FITC FMO would contain all fluorochromes except FITC.

Target	Fluorochrome	Supplier	Conc.
CD3	APC	BD Pharmingen (UK) Cat# 557869	1:50
CD4	Pe-Cy7	BD Pharmingen (UK) Cat# 552775	1:200
CD8a	PerCP	BD Pharmingen (UK) Cat# 553036	1:200
CD11b	APC-Cy7	BD Pharmingen (UK) Cat# 557657	1:200
CD40	FITC	BD Pharmingen (UK) Cat# 553723	1:200
CD45	Pe-Cy7	BD Pharmingen (UK) Cat# 552848	1:100
CD68	FITC	AbD Serotec (UK) Cat# MCA1957A488	1:200
CD80	APC	BD Pharmingen (UK) Cat# 560016	1:200
CD86	PerCP	Biolegend (UK) Cat# 105028	1:200
CD119	PE	eBioscience (UK) Cat# 12-1191	1:200
CD124	PE	BD Pharmingen (UK) Cat# 552509	1:200
NKp46	PE	BD Pharmingen (UK) Cat# 560757	1:200
MHC II (I-A)	PE-Cy5	eBioscience (UK) Cat# 15-5322	1:200
TLR4	FITC	Hycult Biotech (US) Cat# HM1029F	1:200
GLAST	APC	Miltenyi Biotec (IR) 130-098-803	1:200

Table 2.4. Conjugated antibodies for flow cytometry

2.7. Generation of T cells – preparation of spleen cell culture

Wildtype mice (3-6 months) were sacrificed by cervical dislocation and spleens were harvested to 50 ml falcon tubes containing x-vivo media (2 ml; Lonza, Belgium) containing penicillin (100 µg/ml), L-glutamine (100 mM; Gibco, UK) and β-mercaptoethanol (2 µl). Spleens were homogenized and passed through 40 µm sterile nylon mesh filters to obtain a single cell suspension. Cells were centrifuged at 1,200 rpm for 5 minutes and resuspended in x-vivo media (2 ml). For the generation of specific T cells, x-vivo media (9 ml) was added and cells were counted by diluting cells (1:10) in trypan blue. The cell suspension (10 µl) was loaded into a disposable haemocytometer (Hycor Biomedical, UK). Viable cells which did not stain (trypan blue method) were counted under a light microscope (trypan blue method). Cells were centrifuged at 1,200 rpm for 5 minutes and supernatants removed. CD4$^+$ T cells were isolated using a magnetic activated cell sorter (MACS) column (Miltenyi Biotec, UK) and a CD4$^+$ T cell isolation kit (Miltenyi Biotec, UK). Cells were resuspended in MACS buffer (40 µl/per 10^7 cells; PBS containing 0.5 % bovine serum albumen (BSA) and 2 mM EDTA; Sigma-Aldrich, UK) and incubated in antibody cocktail (10 µl/per 10^7 cells; Miltenyi Biotec, UK) for 10 minutes at 4 °C. Cells were flooded with MACS buffer (30 µl/per 10^7 cells) and incubated with beads (20 µl/per 10^7 cells; Miltenyi Biotec, UK) for 15 minutes at 4 °C. Cells were flooded in MACS buffer (20 x volume of antibody added), centrifuged at 1,200 rpm for 5 minutes and resuspended in Macs buffer (500 µl). The MACS column was flooded with MACS buffer (3 ml) and cells were transferred to the MACS column for magnetic sorting. T cells were centrifuged at 1,200 rpm for 5 minutes and resuspended in x-vivo media (2 ml). Cells were counted and plated in 24-well plates (200 µl/well, 2 x 10^6 cells/ml).

2.7.1. Generation of Th1, Th2 and Th17 cell lines

T cell lines were cultured for 5 days at 37 °C in a humidified 5 % CO$_2$ environment. All T cell lines were developed in the presence of anti cluster of differentiation 3/28 (αCD3/CD28; 4 µg/ml, BD Biosciences, US) at the beginning of the culture. Th1 cell lines were developed in the presence of IL-12 (500 ng/ml,

R&D Systems), Th2 cell lines in the presence of IL-4 (10 ng/ml, R&D Systems) and anti-IFN-γ (5 μg/ml, BD Biosciences US) and Th17 cell lines in the presence of IL-1β (25 ng/ml, R&D Systems), IL-23 (50 ng/ml), anti-IFN-γ (5 μg/ml) and TGFβ (5 ng/ml, R&D Systems). On the 3rd day of the culture media was changed on the T cell lines and cytokines were added in fresh x-vivo media without αCD3/CD28. T cell lines were harvested on the 5th day for co-culture with glia.

2.7.2. Co-culture and treatment of specific T cell lines and glia

Supernatants were removed from T cell lines and stored at -20 $^{\circ}$C for later cytokine analysis. T cells were transferred from the 24-well plates to 50 ml falcon tubes by pipetting up and down. Tubes were centrifuged at 1,200 rpm for 5 minutes and resuspended in DMEM (500 μl). Cells were counted and resuspended in DMEM allowing for 1.5 x 10^5 cells/ml. T cells were cultured at a 1:2 ratio with microglia (300 μl/well) for 24 hours at 37 $^{\circ}$C in a humidified 5 % CO_2 environment. Supernatants were removed for cytokine analysis by enzyme linked immunosorbent assay (ELISA) and cells were harvested for flow cytometry.

2.8 Statistical analysis

Statistical analysis was performed using the computer-based statistical package GraphPad Prism (GraphPad, US). Data were assessed using a two-tailed Student's *t* test for independent means, 1-way analysis of variance (ANOVA) followed by post hoc comparisons using Newman-Keuls test, or 2-way ANOVA followed by Bonferroni post test. All data were expressed as mean $\pm$ standard error of mean (SEM).

Chapter 3

Analysis of the effect of TLR4 agonist, LPS,
on glial cells prepared from CD200$^{-/-}$ mice

3.1. Introduction

Astrocytes and microglia are two major glial populations in the CNS. Microglia are the immune cells of the CNS and express a large number of cell surface and nuclear receptors which play a critical role in both the initiation and modulation of their immune response (Garden and Moller 2006). Like microglia, astrocytes can also act as immune competent cells and are capable of producing cytokines and chemokines *in vitro* and *in vivo* and are thought to play a pivotal role in the type and extent of the inflammatory response (Dong and Benveniste 2001).

The innate immune system provides the initial protection against an insult. Host cells express pattern recognition receptors (PRRs) that sense diverse pathogen-associated molecular patterns (PAMPs); activation of PRRs trigger intracellular signaling cascades which culminate in the induction and release of cytokines, chemokines, reactive oxygen species and other inflammatory mediators (Kawai and Akira 2007). TLRs are expressed on APCs, including macrophages and in the brain, microglial cells. The most studied TLR is TLR4. The activation of microglial cells by LPS is initiated by TLR4 to induce a signaling cascade leading to the activation of NFκB and subsequent pro-inflammatory cytokine production. Further, an endogenous danger signal, HMGB1 is believed to interact with both TLR2 and TLR4 and induces activation of NFκB during acute inflammatory responses (Park, Svetkauskaite et al. 2004).

CD200 is a type I transmembrane glycoprotein which has been identified as having immune-suppressive function (Wright, Puklavec et al. 2000) and has been shown to be expressed on a number of cell types including neurons, endothelial cells and oligodendrocytes (Barclay, Wright et al. 2002). CD200 interacts with a structurally related receptor, CD200R, expressed on cells of the myeloid lineage, and has been identified on microglia in the brain (Hoek, Ruuls et al. 2000). The development of CD200$^{-/-}$ mice has led to significant advances being made on understanding the inflammatory implications of the CD200-CD200R interaction. CD200$^{-/-}$ animals showed an increased susceptibility to CIA (Hoek, Ruuls et al. 2000; Nimmerjahn, Kirchhoff et al. 2005). Furthermore, Hoek and colleagues observed that the onset of MOG-induced EAE was earlier in CD200$^{-/-}$, compared with wildtype, mice (Hoek, Ruuls et al. 2000). A recent study found a deficiency

in both CD200 and CD200R in the brain of patients with AD suggesting reduced efficacy of the CD200-CD200R system to control inflammation (Walker, Dalsing-Hernandez et al. 2009).

The interaction of CD200 with CD200R provides a mechanism for controlling myeloid cell activity and while several studies have investigated the effect of CD200 deficiency in macrophages little is known about the effects on microglia.

Therefore, the objectives of the following set of experiments were;

- To assess the inflammatory responses of primary mixed glia, purified microglia and purified astrocytes prepared from wildtype and CD200$^{-/-}$ mice in response to TLR4 agonist LPS
- And, to investigate the impact of the CD200-CD200R interaction on these responses.

3.2. Methods

Mixed glia, purified microglia and purified astrocytes were prepared from cortices of 1-day old wildtype and CD200$^{-/-}$ mice, and cultured for 12 days before treatment (see section 2.1 for details). Cells were incubated in the presence or absence of LPS (100ng/ml; Sigma, UK) for 24 hours. Purified astrocytes were challenged with HMGB1 (100ng/ml) alone or in combination with LPS (100ng/ml); HMGB1 (100ng/ml) diluted in PBS was incubated with LPS (100ng/ml) at 37°C for 30 minutes before addition to cell cultures. Supernatant cytokine concentrations were determined by ELISA and expression of cytokine and TLR mRNA was assessed by PCR in harvested cells (see section 2.2-2.3). Western immunoblotting was used to examine the NFκB signalling pathway and HMGB1 expression in mixed glia prepared from wildtype and CD200$^{-/-}$ mice (see section 2.4). Flow cytometry was used to assess CD200 (BD Bioscience; UK), CD200R (BD Bioscience; UK) and TLR4 (Hycult Biotech; UK) expression on GLAST^{+} cells from a purified astrocyte culture (see section 2.6). For PCR, values are expressed as a relative quantity (RQ) calculated with respect to endogenous control, β-actin. Protein concentration was calculated from the standard curve and expressed in pg/ml. Protein expression established using western immunoblotting, was calculated using densitometric analysis to calculate mean data. All data are expressed as means ± SEM. 1-way ANOVA using Neumann Keuls post-test and 2-way ANOVA with Bonferroni post-test, were used to extrapolate the data, where appropriate the students t test for independent means was performed to determine whether significance existed between treatment groups. Statistical analysis was performed using the computer-based statistical package, GraphPad prism (GraphPad, US).

3.3. Results

Glia prepared from CD200$^{-/-}$ mice respond more profoundly to TLR4 agonist LPS

It has been previously shown that microglia from CD200$^{-/-}$ mice display an activated phenotype, with cells showing a less ramified morphology and increased expression of markers of microglial activation including CD11b and CD45 (Hoek, Ruuls et al. 2000). The aim of this set of experiments was to investigate the responses of glia prepared from CD200$^{-/-}$ mice to TLR4 agonist, LPS, compared with that of wildtype mice.

LPS (100ng/ml) stimulated a significant increase in mRNA expression (A) and supernatant concentration (B) of IL-1β in mixed glia prepared from wildtype and CD200$^{-/-}$ mice (***$p<0.001$; 2-way ANOVA; Figure 3.1) and this LPS-induced increase was enhanced in mixed glia prepared from CD200$^{-/-}$, compared with wildtype, mice ($^+p<0.05$; $^{+++}p<0.001$; 2-way ANOVA; Figure 3.1); further analysis revealed a significant interaction between treatment and genotype (***$p<0.001$; 2-way ANOVA). In a similar fashion, LPS induced an increase in TNFα (Figure 3.2) and IL-6 (Figure 3.3) mRNA expression (A) and supernatant concentration (B) in mixed glia prepared from wildtype and CD200$^{-/-}$ mice (***$p<0.001$; 2-way ANOVA); the LPS-induced increases were enhanced in mixed glia prepared from CD200$^{-/-}$ mice ($^{++}p<0.01$; $^{+++}p<0.001$; 2-way ANOVA). This indicates that CD200 has a modulatory role on TLR4 induced inflammatory responses in glia.

As a possible explanation for the increased responsiveness of glia from CD200$^{-/-}$ mice to LPS, the expression of the LPS multi-receptor components CD14 and TLR4 were assessed. TLR4 mRNA expression (A) was significantly increased in mixed glia prepared from CD200$^{-/-}$, compared with wildtype, mice (*$p<0.05$; Student's t test for independent means; Figure 3.4); however no genotype associated change in CD14 mRNA expression was observed (B; Student's t test for independent means). In order to assess whether this effect was specific to TLR4 the expression of other TLRs were assessed. TLR2, which mediates an

inflammatory response to the most diverse set of pathogen-associated motifs including components of gram-positive bacteria such as lipoproteins, lipoteichoic acid (LTA), peptidoglycan, as well as different LPS from certain gram-negative bacteria, fungi and yeast (Triantafilou, Gamper et al. 2006), was assessed. TLR2 mRNA (C) was significantly increased in mixed glia prepared from CD200$^{-/-}$, compared with wildtype, mice (*p<0.05; Students t test for independent means; Figure 3.4). TLR2 in some cases can occur in a heterodimer with TLR6 however, TLR6 mRNA (D) was similar in mixed glia prepared from wildtype and CD200$^{-/-}$ mice (Figure 3.4).

HMGB1 is a cytokine mediator of inflammation and is an endogenous activator of TLR2 and TLR4. The sample immunoblot (shown in Figure 3.6) indicates that HMGB1 was increased in mixed glia prepared from CD200$^{-/-}$, compared with wildtype, mice, and mean data from densitometric analysis reveal a significant genotype-related difference (*p<0.05; Student's t test for independent means; Figure 3.6).

Signalling through TLR is up-regulated in glia prepared from CD200$^{-/-}$ mice

Stimulation of TLRs leads to the activation of NFκB (Akira and Sato 2003), which is initiated by the degradation of inhibitory protein IκBα primarily through the activation of IκB Kinase (IκK). IκK exists as a heterodimer of IκKα and IκKβ, and the regulatory subunit NEMO. LPS-induced a significant increase in IκKβ phosphorylation in glia prepared from wildtype and CD200$^{-/-}$ mice (***p<0.001; 2-way ANOVA; Figure 3.7); this effect was further increased in cells prepared from CD200$^{-/-}$, compared with wildtype, mice ($^{++}$p<0.01; 2-way ANOVA). IκB kinase phosphorylates IκB on 2 serine residues resulting in its ubiquitination and consequently its degradation. Following this, the NFκB subunits can translocate to the nucleus triggering expression of NFκB-specific genes. A sample immunoblot (Figure 3.8) indicates that LPS induced an increase in IκBα phosphorylation in glia prepared from wildtype mice (***p<0.001; 2-way ANOVA); this effect was further enhanced in cells prepared from CD200$^{-/-}$, compared with wildtype, mice ($^{+++}$p<0.001; 2-way ANOVA); further analysis of the data revealed a significant interaction between treatment and genotype (**p<0.01; 2-way ANOVA; Figure

3.7). Mean phosphorylated IκKβ (A) and pIκBα (B), assessed by densitometric analysis, were increased in cells prepared from CD200$^{-/-}$, compared with wildtype, mice (*p<0.05; Student's t test for independent means; Figure 3.9), indicating that NFκB signalling is up-regulated in cells obtained from CD200$^{-/-}$ mice.

Analysis of the effect of LPS on purified microglia from wildtype and CD200$^{-/-}$ mice

Having examined the effects of LPS on mixed glia, the effects in purified microglia were assessed. Purified microglia prepared from CD200$^{-/-}$ mice expressed increased TLR4 mRNA (A) and TLR2 mRNA (B) (***p<0.001; student's *t* test for independent means; Figure 3.10), compared with wildtype mice. However, analysis of the effect of LPS on cytokine release from purified microglia prepared from wildtype and CD200$^{-/-}$ mice revealed no significant genotype-related change in the cytokine concentration of IL-1β (Figure 3.11), IL-6 (Figure 3.12) and TNFα (Figure 3.13). In the brain, CD200 is expressed on neurons and endothelial cells, but not microglia (Barclay, Wright et al. 2002). CD200R is restricted to cells of the myeloid lineage and in the brain is expressed on microglia. In Figure 3.14, flow cytometry was used to assess CD200 and CD200R expression on GLAST^{+} cells in a purified astrocytic culture from wildtype mice; the results demonstrate that GLAST^{+} cells express high levels of CD200, but not CD200R (Figure 3.14). Thus isolated microglia prepared from wildtype and CD200$^{-/-}$ mice display an equally activated phenotype as a result of loss of the interaction between CD200 on astrocytes and CD200R on microglia.

Analysis of the effect of LPS on purified astrocytes prepared from wildtype and CD200$^{-/-}$ mice

Astrocytes can act as immune effector cells responding to an imbalance in their local environment, releasing cytokines and chemokines, and performing antigen presenting functions (Dong and Benveniste 2001). In order to further explore the genotype-related difference in responsiveness to LPS, the effect of LPS on purified astrocytes prepared from wildtype and CD200$^{-/-}$ mice was assessed. LPS

(100ng/ml) stimulated a significant increase in mRNA expression (A) and supernatant concentrations (B) of IL-1β (Figure 3.16) and IL-6 (Figure 3.17) in purified astrocytes prepared from wildtype and CD200$^{-/-}$ mice (***p<0.001; 2-way ANOVA); this LPS-induced increase was enhanced in purified astrocytes prepared from CD200$^{-/-}$, compared with wildtype, mice ($^{+}$p<0.05; $^{+++}$p<0.001; 2-way ANOVA; Figure 3.16 and 3.17). In a similar fashion, LPS induced an increase in TNFα (Figure 3.19) mRNA expression (A) and supernatant concentration (B) in purified astrocytes prepared from wildtype and CD200$^{-/-}$ mice (***p<0.001; 2-way ANOVA); TNFα supernatant concentration was further enhanced in purified astrocytes prepared from CD200$^{-/-}$ mice ($^{+++}$p<0.001; two-way ANOVA). The enhanced responsiveness of the purified astrocytes prepared from CD200$^{-/-}$ mice to LPS was associated with increased expression of TLR4 on GLAST^{+} cells (*p<0.05; 2-way ANOVA; Figure 3.15).

Activated astrocytes have been shown to release HMGB1 (Chen, Ward et al. 2004). Furthermore, HMGB1 has been shown to form an inflammatory complex with LPS, acting at the TLR4 receptor (Bianchi 2009). Here, the possibility that the increase in HMGB1 observed in glia prepared from CD200$^{-/-}$ mice may contribute to the enhanced response to LPS in purified astrocytes prepared from CD200$^{-/-}$ mice was examined. LPS (100ng/ml) induced a significant increase in supernatant concentrations of IL-6 (Figure 3.18) and TNFα (Figure 3.20) in astrocytes prepared from wildtype mice (***p<0.001; 1-way ANOVA); HMGB1 (100ng/ml) alone had no effect on either IL-6 or TNFα release, however, the combination of LPS and HMGB1 (ratio 1:1) significantly enhanced IL-6 and TNFα when compared with LPS alone ($^{+}$p<0.05; $^{++}$p<0.01; 1-way ANOVA). Coupled with the increased expression of TLR4, observed on purified astrocytes prepared from CD200$^{-/-}$ mice compared with wildtype mice, these results represent a plausible explanation for increased responsiveness to LPS.

A

B

Figure 3.1. LPS-induced increase in IL-1β was enhanced in glia prepared from CD200$^{-/-}$ mice

LPS induced a significant increase in IL-1β mRNA expression (A) and supernatant concentration (B) in mixed glia prepared from wildtype and CD200$^{-/-}$ mice (*p<0.05; ***p<0.001; 2-way ANOVA); analysis of the data revealed that there was a significant interaction between treatment and genotype ($^{+}$p<0.05; $^{+++}$p<0.001; 2-way ANOVA). mRNA is expressed as a relative quantity (RQ) calculated with respect to the endogenous control, β-actin. Cytokine concentration was calculated from the standard curve and expressed in pg/ml. Values are presented as means ± SEM.

A. 2-way ANOVA: LPS $_{effect}$ $F_{(1,13)}$=549.4; ***p<0.001, Genotype $_{effect}$ $F_{(1,13)}$=8.821; *p=0.01, Interaction $_{effect}$ $F_{(1,13)}$=8.821; *p<0.0001
B. 2-way ANOVA: LPS $_{effect}$ $F_{(1,24)}$=37.75; ***p<0.0001, Genotype $_{effect}$ $F_{(1,24)}$=29.76; ***p<0.0001, Interaction $_{effect}$ $F_{(1,24)}$=29.53; ***p<0.0001
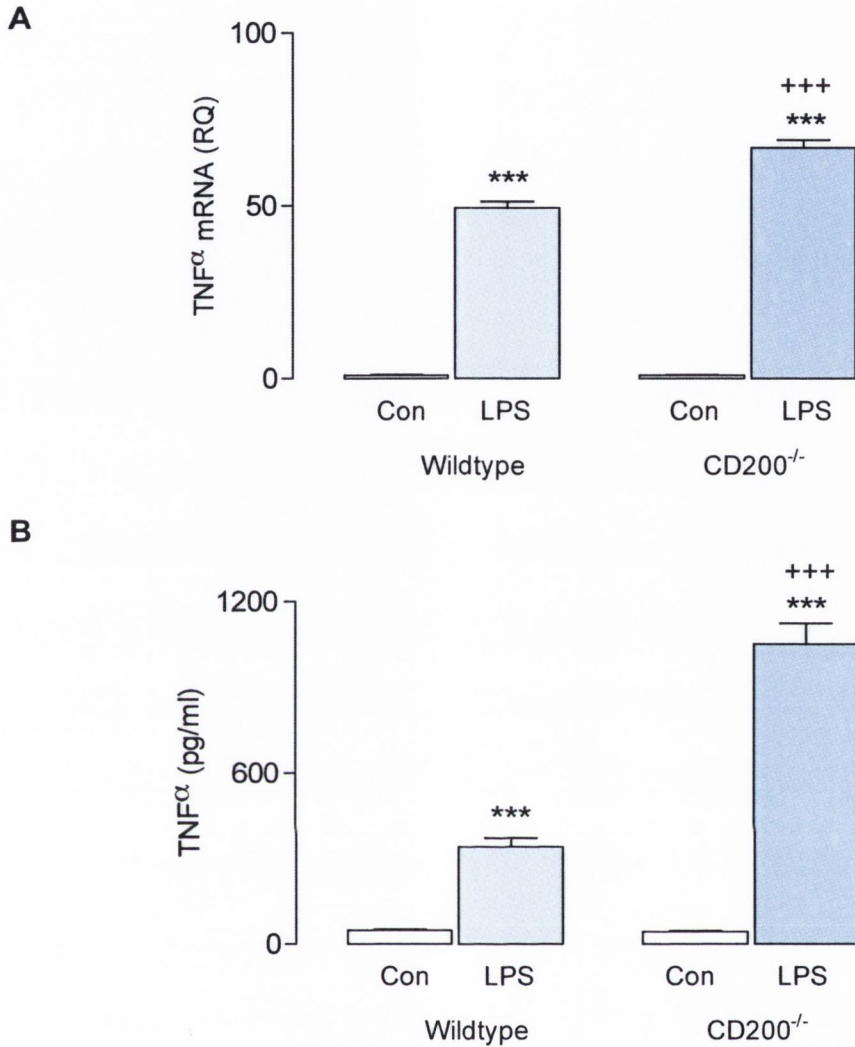
Figure 3.2. LPS-induced increase in TNFα was enhanced in glia prepared from CD200$^{-/-}$ mice

LPS induced a significant increase in TNFα mRNA expression (A) and supernatant concentration (B) in mixed glia prepared from wildtype and CD200$^{-/-}$ mice (***p<0.001; 2-way ANOVA); analysis of the data revealed that there was a significant interaction between treatment and genotype ($^{+++}$p<0.001; 2-way ANOVA). mRNA is expressed as a relative quantity (RQ) calculated with respect to endogenous control, β-actin. Cytokine concentration was calculated from the appropriate standard curve and expressed in pg/ml. Values are presented as means ± SEM.

A. 2-way ANOVA: LPS $_{effect}$ $F_{(1,13)}$=1450; ***p<0.0001, Genotype $_{effect}$ $F_{(1,13)}$=33.52; ***p=0.0001, Interaction $_{effect}$ $F_{(1,13)}$=33.75; ***p<0.0001

B. 2-way ANOVA: LPS $_{effect}$ $F_{(1,16)}$=352.8; ***p<0.0001, Genotype $_{effect}$ $F_{(1,16)}$=102.8; ***p<0.0001, Interaction $_{effect}$ $F_{(1,16)}$=106.2; ***p<0.0001
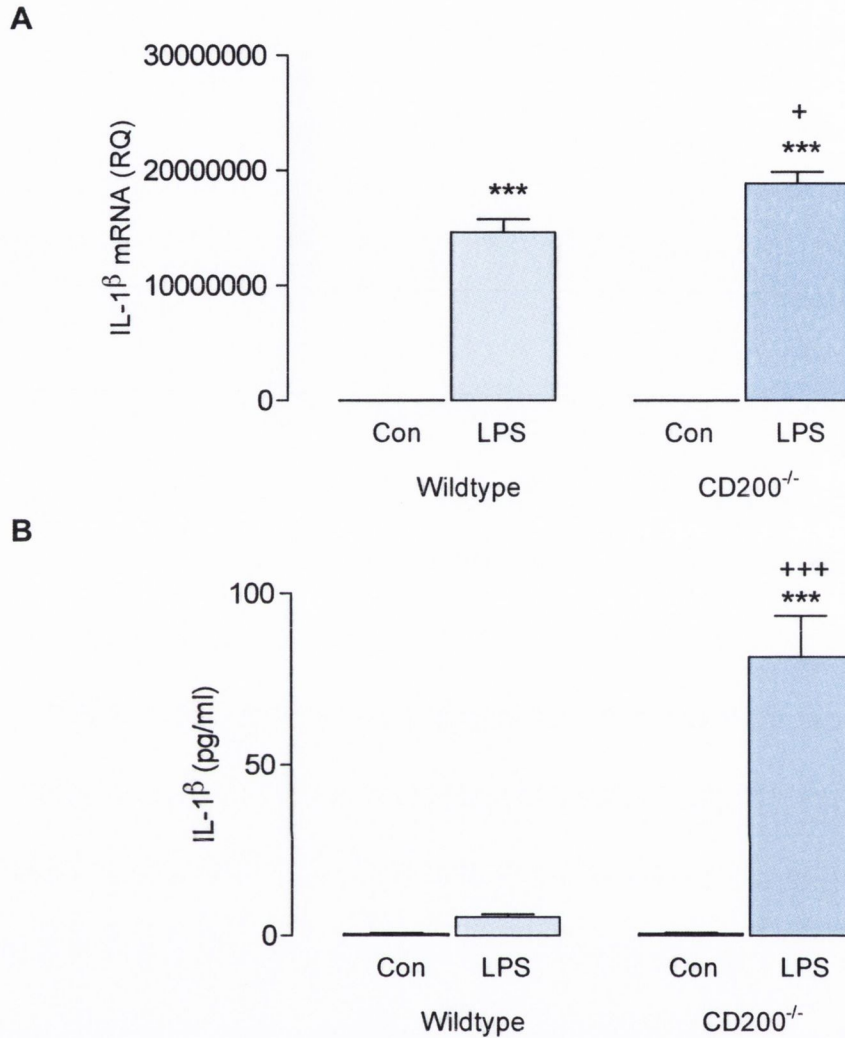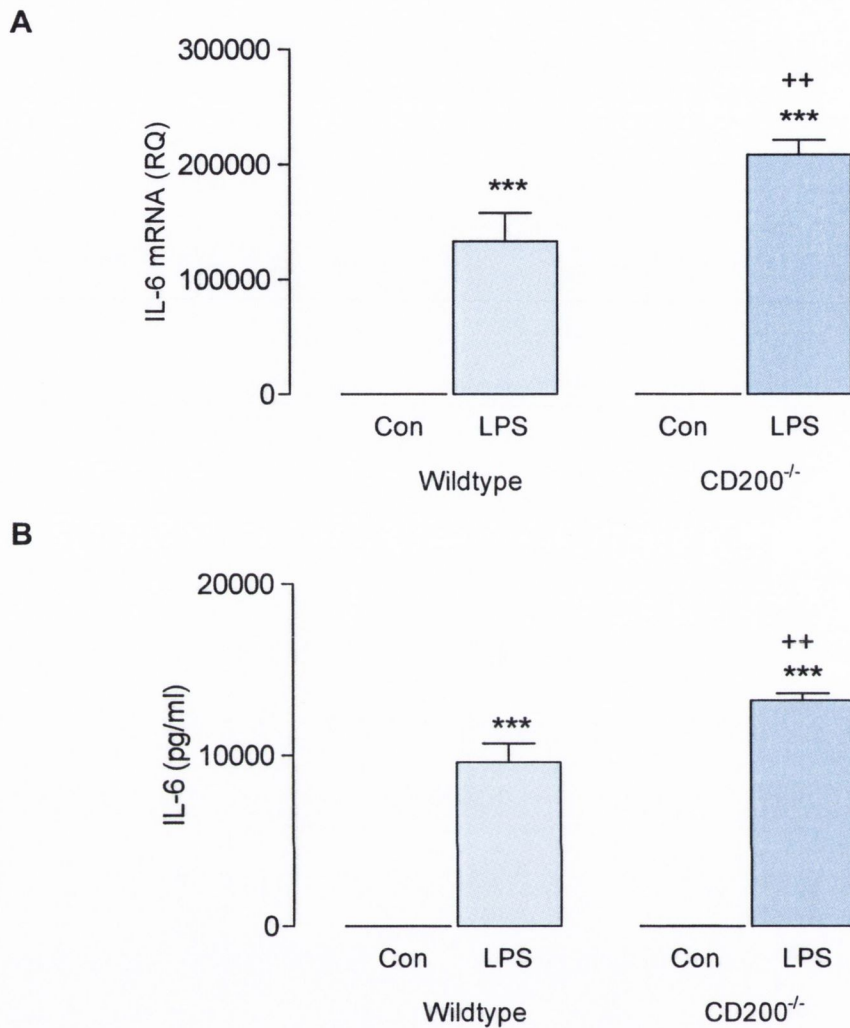
Figure 3.3. LPS-induced increase in IL-6 was enhanced in glia prepared from CD200$^{-/-}$ mice

LPS induced a significant increase in IL-6 mRNA expression (A) and supernatant concentration (B) in mixed glia prepared from wildtype and CD200$^{-/-}$ mice (***p<0.001; 2-way ANOVA); analysis of the data revealed that there was a significant interaction between treatment and genotype ($^{++}$p<0.01; 2-way ANOVA). mRNA is expressed as a relative quantity (RQ) calculated with respect to endogenous control, β-actin. Cytokine concentration was calculated from the appropriate standard curve and expressed in pg/ml. Values are presented as means ± SEM.

A. 2-way ANOVA: LPS $_{effect}$ $F(1,13)=224.7$; ***p<0.0001, Genotype $_{effect}$ $F(1,13)=10.97$; **p=0.0056, Interaction $_{effect}$ $F(1,13)=10.97$; **p=0.0056

B. 2-way ANOVA: LPS $_{effect}$ $F(1,16)=518.7$; ***p<0.0001, Genotype $_{effect}$ $F(1,16)=13.02$; **p=0.0024, Interaction $_{effect}$ $F(1,16)=12.88$; **p=0.0025
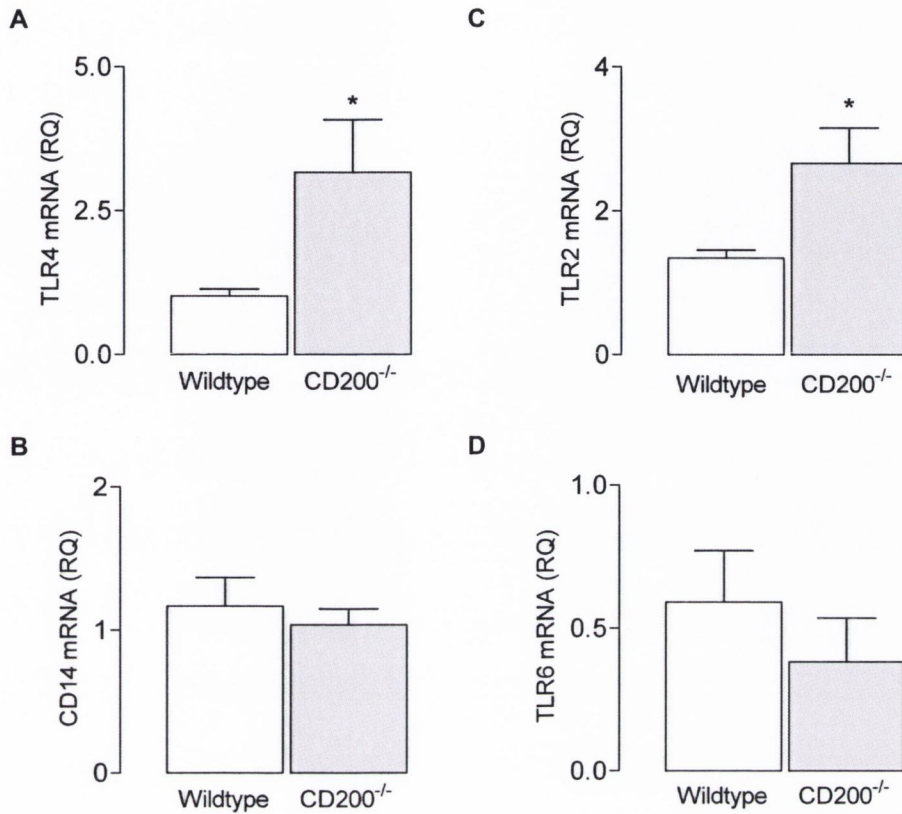
Figure 3.4. Expression of TLR2 and TLR4 was increased in mixed glia prepared from CD200$^{-/-}$ mice

mRNA expression of TLR4 (A), but not CD14 (B), was significantly increased in mixed glia prepared from CD200$^{-/-}$ mice compared with wildtype mice (*p<0.05; 1.015 ± 0.1225; n=5 vs. 3.163 ± 0.9190; n=4; Student's t test for independent means). mRNA expression of TLR2 (C), but not TLR6 (D), was significantly increased in mixed glia prepared from CD200$^{-/-}$ mice compared with wildtype mice (*p<0.05; 1.343 ± 0.1097; n=5 vs. 2.658 ± 0.4922; n=5; Student's t test for independent means). mRNA is expressed as a relative quantity (RQ) calculated with respect to endogenous control, β-actin. Values are presented as means ± SEM.
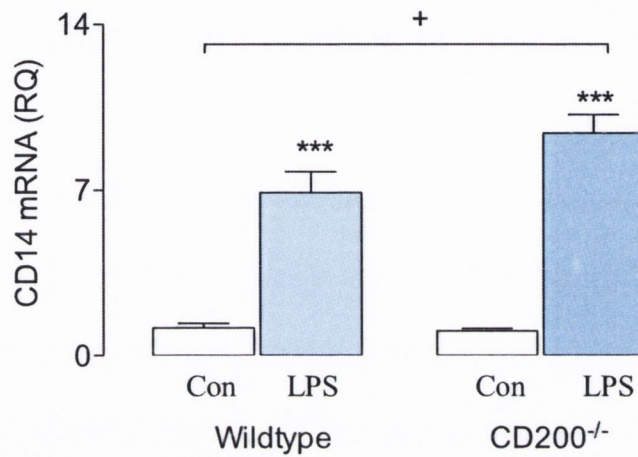
Figure 3.5. LPS-induced increased in CD14 mRNA was enhanced in mixed glia prepared from CD200$^{-/-}$ mice

LPS significantly increased CD14 mRNA in cells prepared from wildtype and CD200$^{-/-}$ mice (***p<0.001; 2-way ANOVA); further analysis revealed a significant interaction between treatment and genotype was observed ($^+$p<0.01; 2-way ANOVA). Values are presented as means ± SEM expressed relative to β-actin.

2-way ANOVA: LPS $_{effect}$ F(1,16)=138.3; ***p<0.0001, Genotype $_{effect}$ F(1,16)=3.929; p=0.0649, Interaction $_{effect}$ F(1,16)=4.842; *p=0.0428
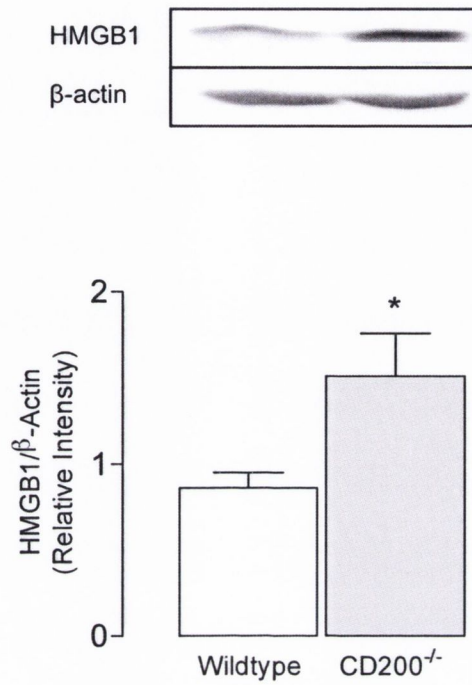
Figure 3.6. HMGB1 expression was increased in mixed glia prepared from CD200$^{-/-}$ mice

A sample immunoblot indicates that HMGB1 expression was increased in mixed glia prepared from CD200$^{-/-}$, compared with wildtype, mice; mean data from densitometric analysis revealed a significant genotype-related difference (*$p<0.05$; 0.8628 ± 0.08747; n=7 vs. 1.510 ± 0.2489; n=4; Student's t test for independent means). Values are presented as means ± SEM.
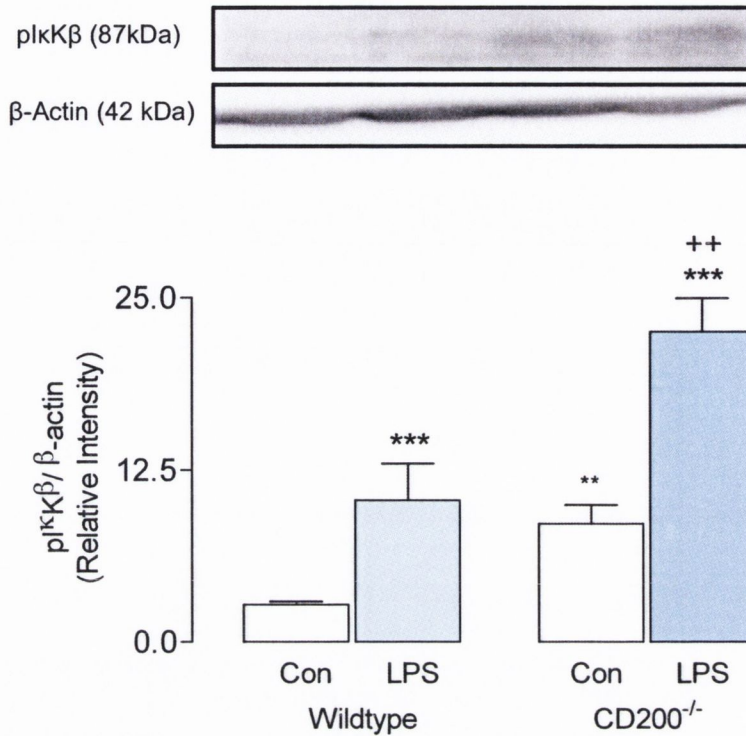
Figure 3.7. IκKβ phosphorylation was increased in mixed glia prepared from CD200$^{-/-}$ mice

LPS significantly increased IκKβ phosphorylation in cells prepared from wildtype and CD200$^{-/-}$ mice (***$p<0.001$; 2-way ANOVA); this effect was further increased in cells prepared from CD200$^{-/-}$, compared with wildtype, mice (++$p<0.01$; 2-way ANOVA). Densitometric analysis was used to calculate the mean data and values are presented as means ± SEM expressed relative to β-actin.

2-way ANOVA: LPS $_{effect}$ F(1,9)=25.22; ***$p=0.0007$, Genotype $_{effect}$ F(1,9)=17.83; **$p=0.0022$, Interaction $_{effect}$ F(1,9)=2.202; $p=0.1720$
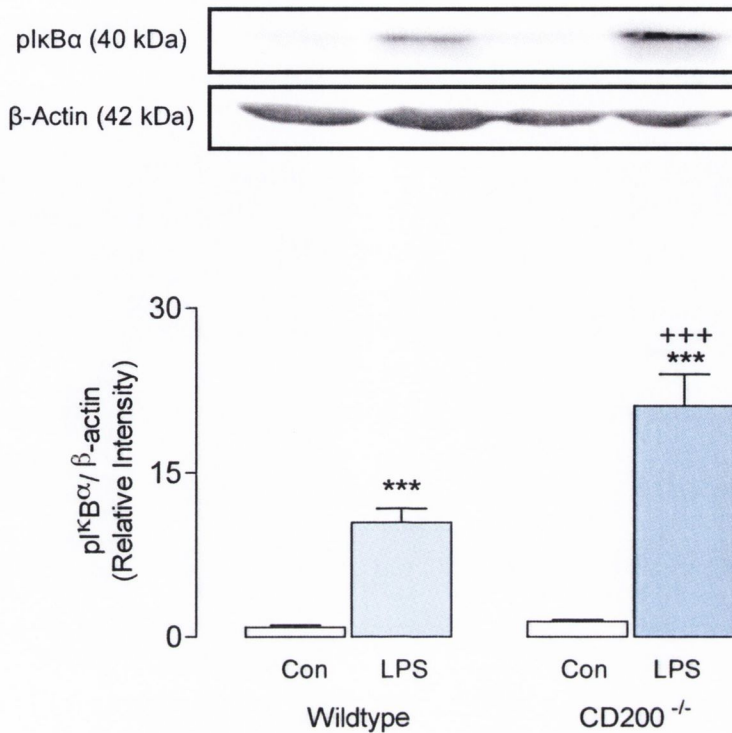
Figure 3.8. IκBα phosphorylation was increased in mixed glia prepared from CD200^{-/-} mice

A sample immunoblot indicates that LPS increased IκBα phosphorylation in cells prepared from wildtype and CD200^{-/-} mice (***p<0.001; 2-way ANOVA); this effect was significantly increased in cells prepared from CD200^{-/-}, compared with wildtype, mice ([+++]p<0.001; 2-way ANOVA); further analysis of the data revealed a significant interaction between treatment and genotype (**p<0.01; 2-way ANOVA). Densitometric analysis was used to calculate the mean data and values are presented as means ± SEM expressed relative to β-actin.

2-way ANOVA: LPS $_{effect}$ $F(1,14)=124.7$; ***p<0.0001, Genotype $_{effect}$ $F(1,14)=18.18$; ***p=0.0008, Interaction $_{effect}$ $F(1,14)=14.92$; **p=0.0017
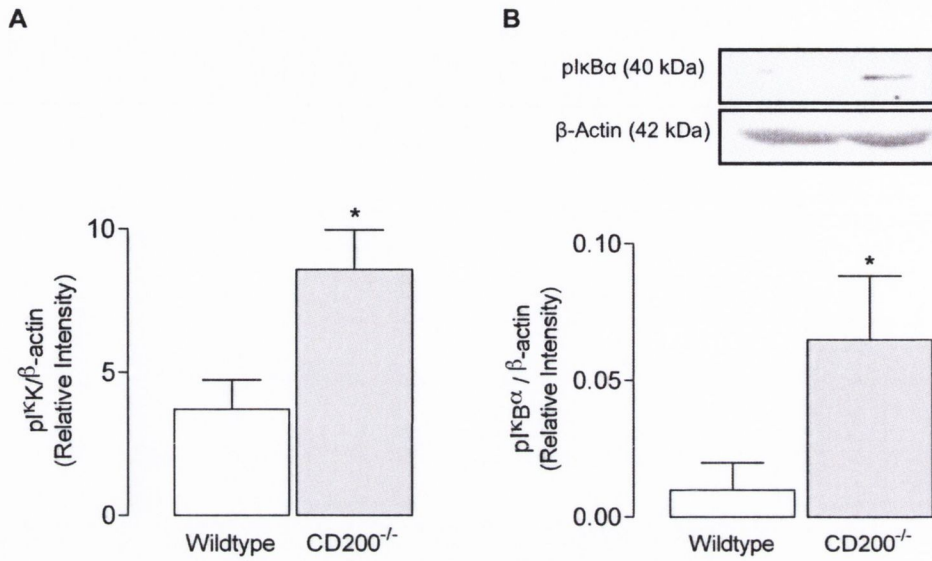
Figure 3.9. Phosphorylated IκKβ and IκBα were increased in mixed glia prepared from CD200$^{-/-}$ mice

Phosphorylated IκKβ (A) was increased in mixed glia prepared from CD200$^{-/-}$, compared with wildtype, mice (*p<0.05; 3.7 ± 1.0; n=4 vs. 8.6 ± 1.4; n=3; Student's *t* test for independent means). Phosphorylated IκBα (B) was increased in mixed glia prepared from CD200$^{-/-}$, compared with wildtype, mice (*p<0.05; 0.01 ± 0.01; n=6 vs. 0.065 ± 0.023; n=4; Student's *t* test independent means). Densitometric analysis was used to calculate the mean data and values are presented as means ± SEM expressed relative to β-actin.
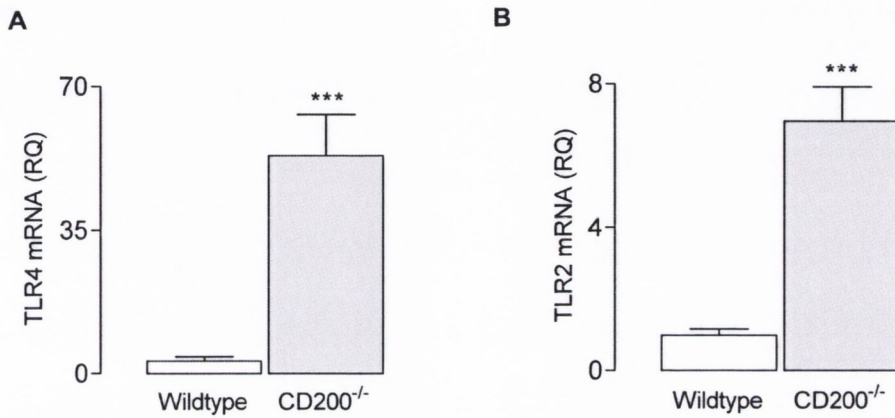
Figure 3.10. Expression of TLR2 and TLR4 was increased in purified microglia prepared from CD200$^{-/-}$ mice

Expression of TLR4 (A) and TLR2 (B) was significantly increased in purified microglia prepared from CD200$^{-/-}$, compared with wildtype, mice (***p<0.001; A; 3.106 ± 1.075; n=10 vs. 53.18 ± 10.03; n=10; B; 0.98 ± 0.1799; n=10 vs. 6.962 ± 0.9507; n=10; Student's *t* test for independent means). mRNA is expressed as a relative quantity (RQ) calculated with respect to endogenous control, β-actin. Values are presented as means ± SEM.
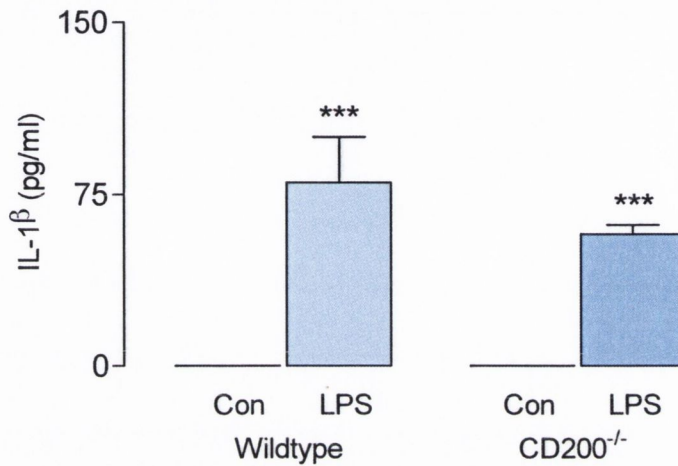
Figure 3.11. LPS-induced IL-1β release was increased in purified microglia prepared from wildtype and CD200^{-/-} mice

LPS induced a significant increase in IL-1β supernatant concentrations in purified microglia prepared from wildtype and CD200$^{-/-}$ mice (***p<0.001; 2-way ANOVA); but there was no significant interaction between treatment and genotype. Protein concentration was calculated from the standard curve and expressed in pg/ml. Values are presented as means ± SEM.

2-way ANOVA: LPS $_{effect}$ F(1,38)=61.26; ***p<0.0001, Genotype $_{effect}$ F(1,38)=1.637; p=0.2085, Interaction $_{effect}$ F(1,38)=1.637; p=0.2085
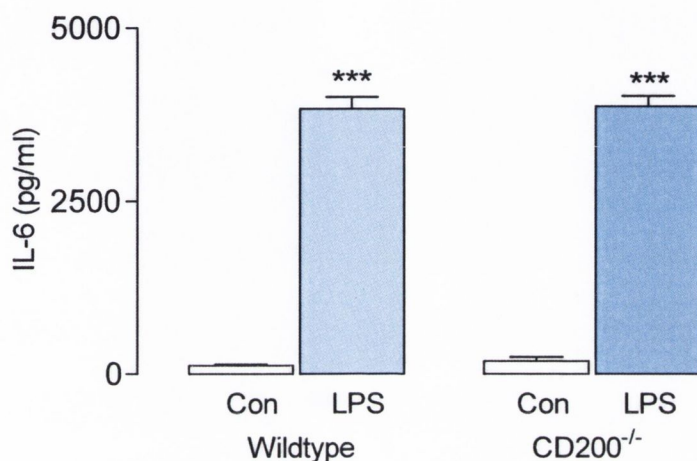
Figure 3.12. LPS-induced IL-6 release was increased in purified microglia prepared from wildtype and CD200$^{-/-}$ mice

LPS induced a significant increase in IL-6 supernatant concentrations in purified microglia prepared from wildtype and CD200$^{-/-}$ mice (***p<0.0001; 2-way ANOVA); but there was no significant interaction between treatment and genotype. Protein concentration was calculated from the standard curve and expressed in pg/ml. Values are presented as means ± SEM.

2-way ANOVA: LPS $_{effect}$ F(1,40)=1008; ***p<0.0001, Genotype $_{effect}$ F(1,40)=0.2064; p=0.6520, Interaction $_{effect}$ F(1,40)=0.01712; p=0.8966
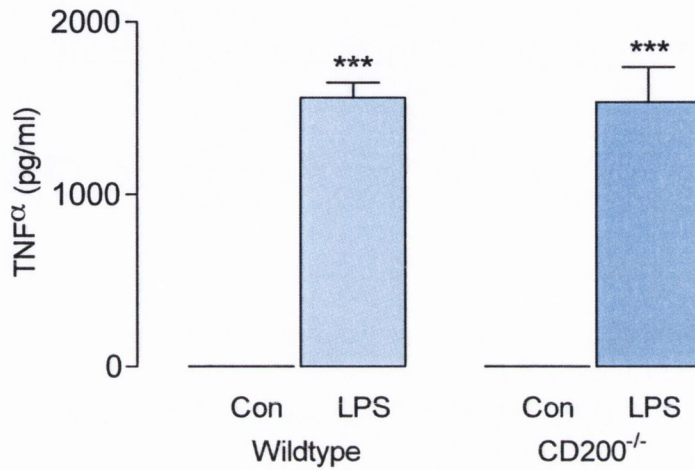
Figure 3.13. LPS-induced TNFα release was increased in purified microglia prepared from wildtype and CD200$^{-/-}$ mice

LPS induced a significant increase in TNFα supernatant concentrations in purified microglia prepared from wildtype and CD200$^{-/-}$ mice; however there was no significant interaction between treatment and genotype. Protein concentration was estimated from the appropriate standard curve and expressed in pg/ml. Values are presented as means ± SEM.

2-way ANOVA: LPS $_{effect}$ $F(1,40)=1008$; ***$p<0.0001$, Genotype $_{effect}$ $F(1,40)=0.2064$; $p=0.6520$, Interaction $_{effect}$ $F(1,40)=0.01712$; $p=0.8966$
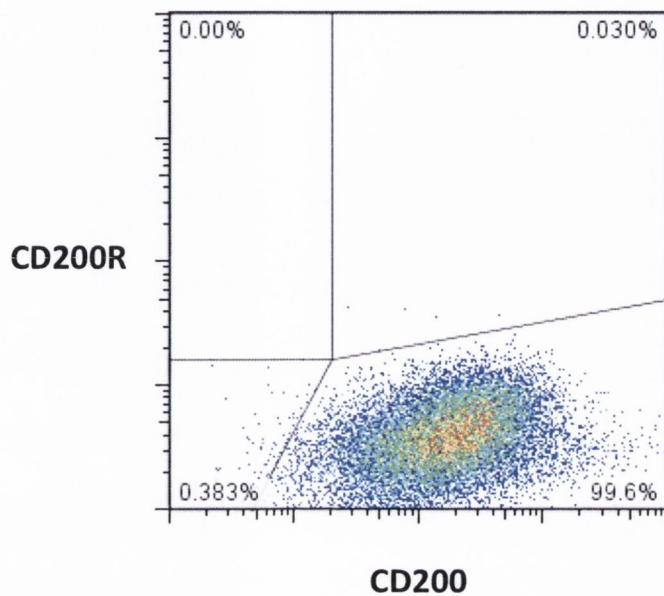
Figure 3.14. GLAST$^+$ cells prepared from purified astrocytes express CD200, but not CD200R

GLAST$^+$ cells prepared from a purified astrocyte culture stained positively for CD200, but not CD200R. A representative FACS plot is shown of 3 independent experiments.
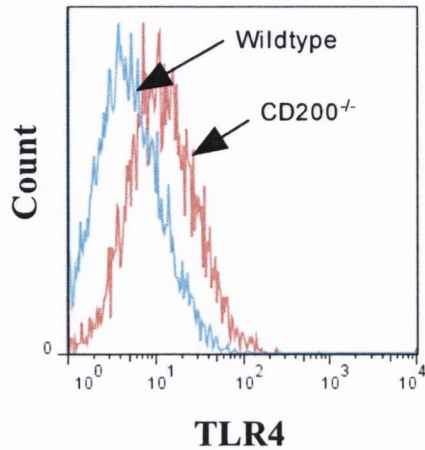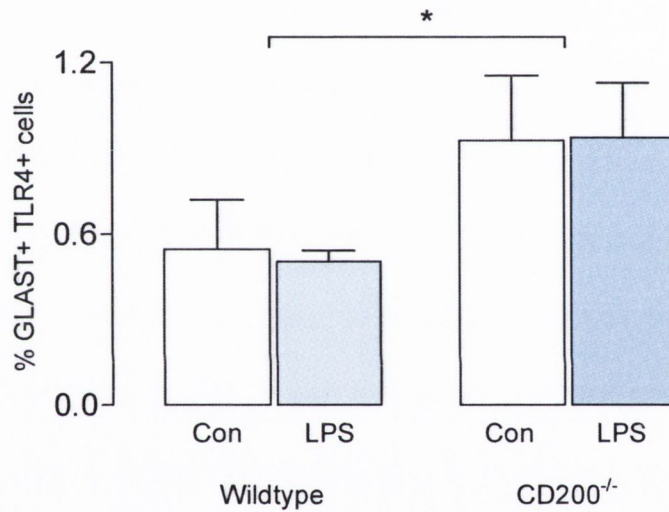
Figure 3.15. Expression TLR4 on GLAST$^+$ cells was increased in purified astrocytes prepared from CD200$^{-/-}$ mice

The number of GLAST$^+$ cells that stained positively for TLR4 is presented in (A). The mean percentage of cells expressing TLR4 was significantly increased on GLAST$^+$ cells from CD200$^{-/-}$, compared with wildtype, mice (*p<0.05; 2-way ANOVA). Values are presented as means ± SEM.

2-way ANOVA: LPS $_{effect}$ F(1,8)=0.009; p=0.9252, Genotype $_{effect}$ F(1,8)=5.582; *p=0.045, Interaction $_{effect}$ F(1,8)=0.024; p=0.8807
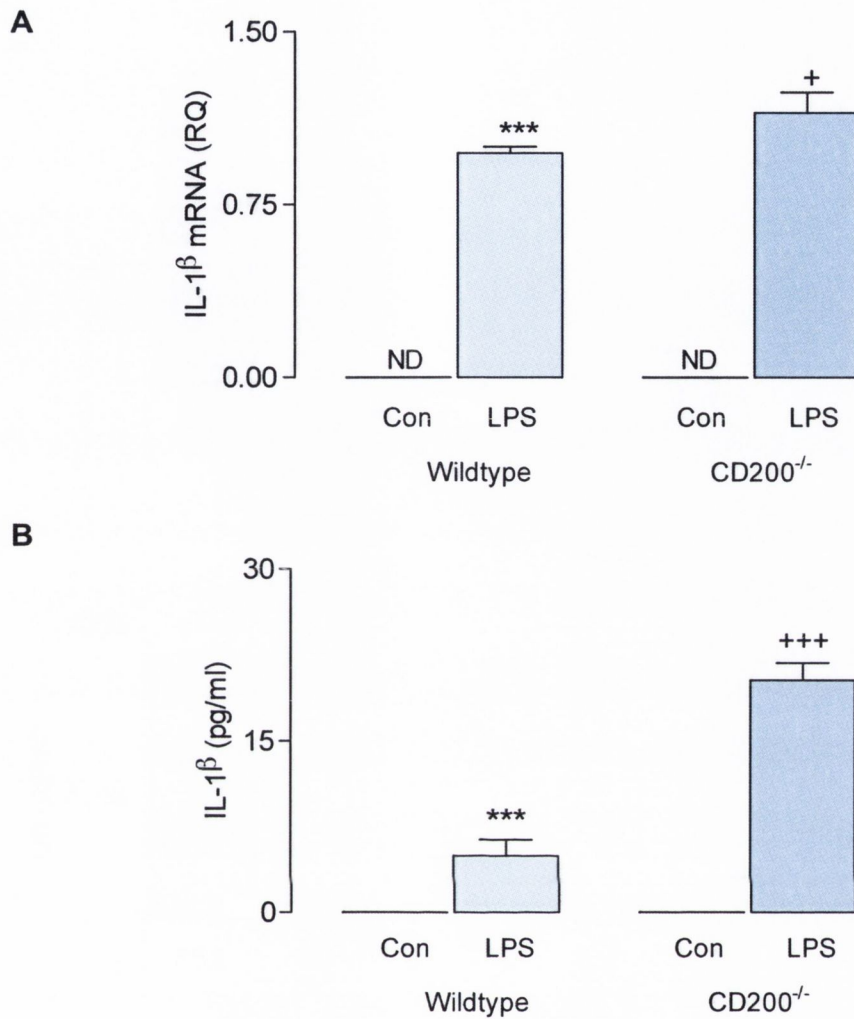
Figure 3.16. LPS-induced IL-1β was enhanced in isolated astrocytes prepared from CD200$^{-/-}$ mice

LPS induced a significant increase in IL-1β mRNA expression (A) and supernatant concentration (B) in isolated astrocytes prepared from wildtype and CD200$^{-/-}$ mice (***p<0.0001; ANOVA); this response was further enhanced in astrocytes prepared from CD200$^{-/-}$, compared with wildtype, mice ($^+$p<0.05; $^{+++}$p<0.0001; ANOVA). mRNA is expressed as a relative quantity (RQ) calculated with respect to endogenous control, β-actin. Cytokine concentration was calculated from the standard curve and expressed in pg/ml. Values are presented as means ± SEM.

A. 2-way ANOVA: LPS $_{effect}$ F(1,35)=494.6; ***p<0.0001, Genotype $_{effect}$ F(1,35)=3.371; p=0.0748, Interaction $_{effect}$ F(1,35)=3.371; p=0.0748
B. 2-way ANOVA: LPS $_{effect}$ F(1,18)=125.9; ***p<0.0001, Genotype $_{effect}$ F(1,18)=46.98; ***p<0.0001, Interaction $_{effect}$ F(1,18)=46.98; ***p<0.0001
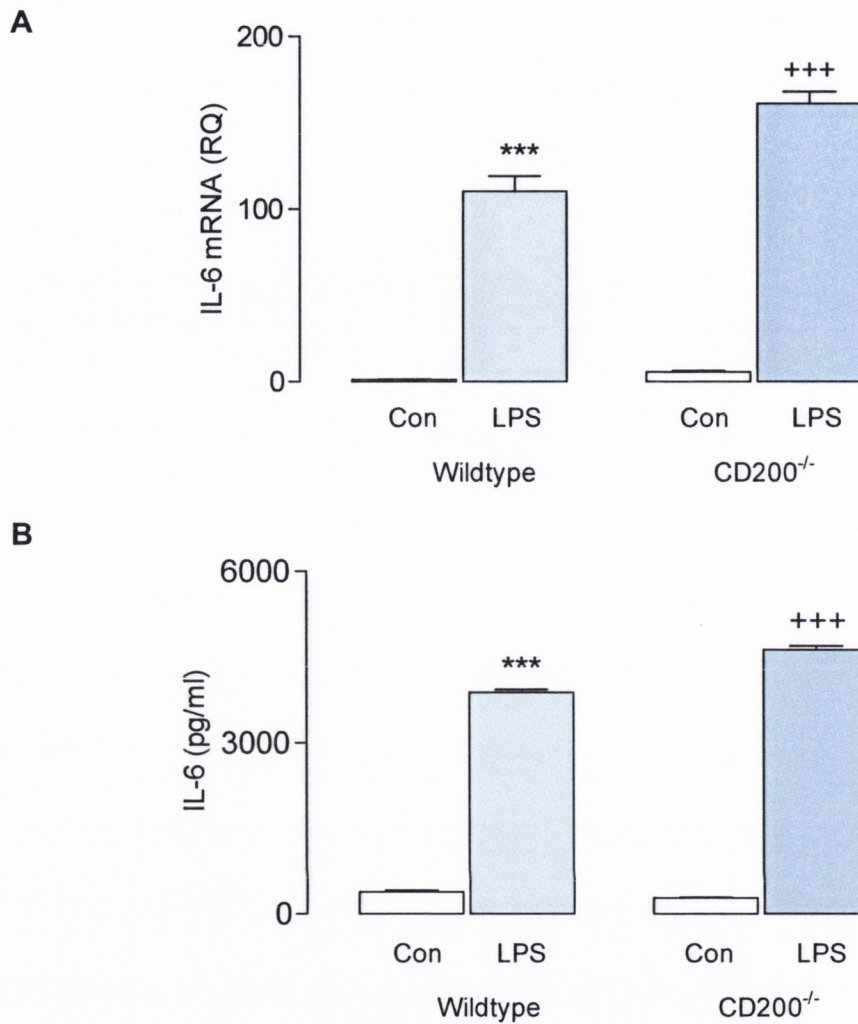
Figure 3.17. LPS-induced IL-6 was enhanced in isolated astrocytes prepared from CD200$^{-/-}$ mice

LPS induced a significant increase in IL-6 mRNA expression (A) and supernatant concentration (B) in isolated astrocytes prepared from wildtype and CD200$^{-/-}$ mice (***$p<0.001$; ANOVA); this response was further enhanced in astrocytes prepared from CD200$^{-/-}$, compared with wildtype, mice ($^{+++}$$p<0.0001$; ANOVA). mRNA is expressed as a relative quantity (RQ) calculated with respect to endogenous control, β-actin. Cytokine concentration was calculated from the standard curve and expressed in pg/ml. Values are presented as means ± SEM.

A. 2-way ANOVA: LPS $_{effect}$ $F(1,40)=561.7$; ***$p<0.0001$, Genotype $_{effect}$ $F(1,40)=24.59$; ***$p<0.0001$, Interaction $_{effect}$ $F(1,40)=17.32$; ***$p=0.0002$
B. 2-way ANOVA: LPS $_{effect}$ $F(1,20)=7250$; ***$p<0.0001$, Genotype $_{effect}$ $F(1,20)=47.66$; ***$p<0.0001$, Interaction $_{effect}$ $F(1,20)=85.00$; ***$p<0.0001$
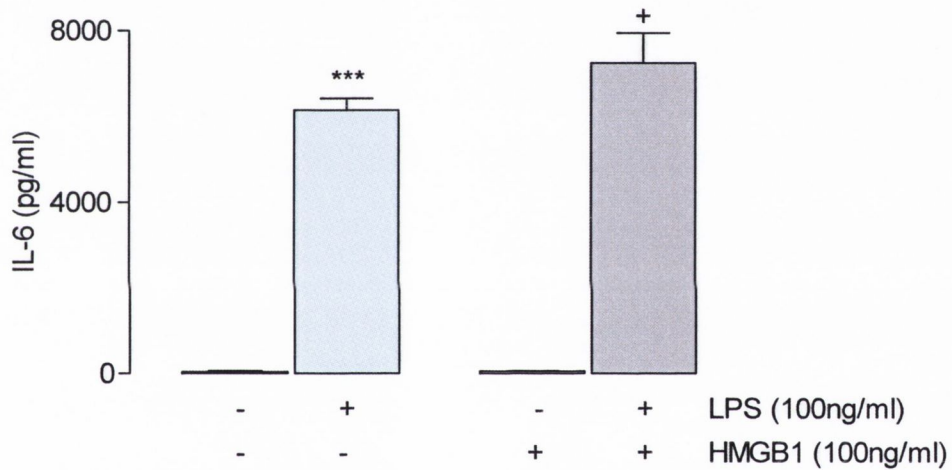
Figure 3.18. HMGB1 exacerbated the LPS-induced IL-6 release from astrocytes

LPS (100ng/ml) induced a significant increase in IL-6 concentrations in purified astrocytes prepared from wildtype mice (***p<0.001; ANOVA; n=4); HMGB1 (100ng/ml) alone had no effect on TNFα release; but the combination of LPS and HMGB1 significantly enhanced IL-6 concentration when compared with LPS alone (⁺p<0.05; ⁺⁺p<0.01; ANOVA; n=4). Cytokine concentration was calculated from the standard curve and expressed in pg/ml. Values are presented as means ± SEM.

A

B
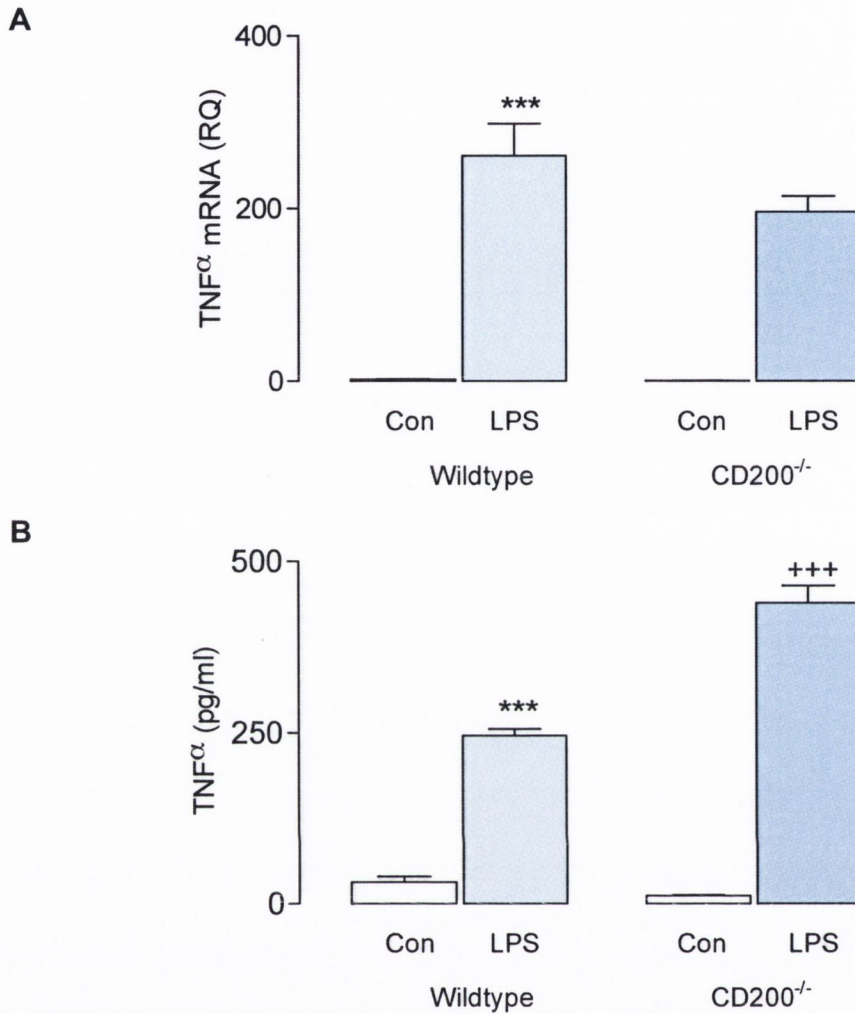
Figure 3.19. LPS-induced TNFα was enhanced in isolated astrocytes prepared from CD200$^{-/-}$ mice

LPS induced a significant increase in TNFα mRNA expression (A) and supernatant concentration (B) in isolated astrocytes prepared from wildtype and CD200$^{-/-}$ mice (***$p<0.001$; ANOVA); supernatant concentration of TNFα was further enhanced in astrocytes prepared from CD200$^{-/-}$, compared with wildtype, mice (B; $^{+++}p<0.0001$; ANOVA). mRNA is expressed as a relative quantity (RQ) calculated with respect to endogenous control, β-actin. Cytokine concentration was calculated from the standard curve and expressed in pg/ml. Values are presented as means ± SEM.

A. 2-way ANOVA: LPS $_{effect}$ $F(1,35)=115.5$; ***$p<0.0001$, Genotype $_{effect}$ $F(1,35)=2.495$; $p=0.1232$, Interaction $_{effect}$ $F(1,35)=2.264$; $p=0.1414$
B. 2-way ANOVA: LPS $_{effect}$ $F(1,19)=375.4$; ***$p<0.0001$, Genotype $_{effect}$ $F(1,19)=27.36$; ***$p<0.0001$, Interaction $_{effect}$ $F(1,19)=41.55$; ***$p<0.0001$
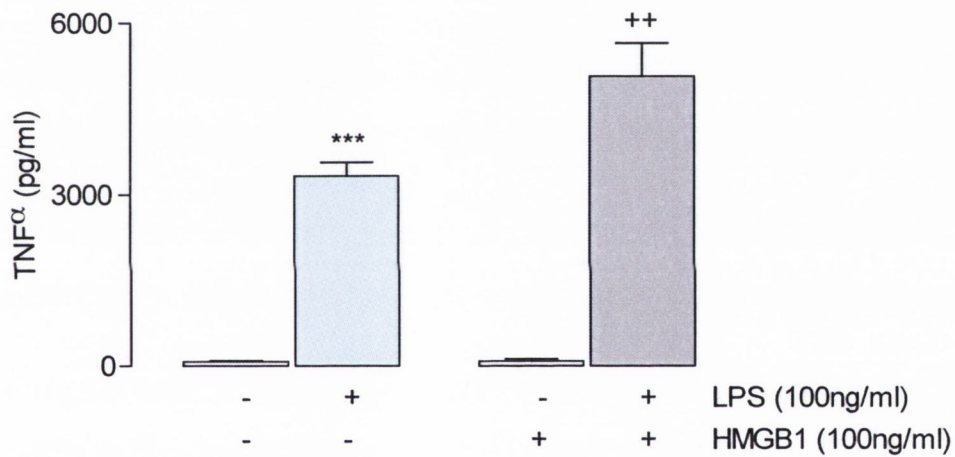
Figure 3.20. HMGB1 exacerbated the LPS-induced TNFα release from astrocytes

LPS (100ng/ml) induced a significant increase in TNFα concentrations in purified astrocytes prepared from wildtype mice (***$p<0.001$; ANOVA; n=4); HMGB1 (100ng/ml) alone had no effect on TNFα release; but the combination of LPS and HMGB1 significantly enhanced TNFα concentration compared with LPS alone (++$p<0.01$; ANOVA; n=4). Cytokine concentration was calculated from the standard curve and expressed in pg/ml . Values are presented as means ± SEM.

3.4. Discussion

The loss of CD200 has a significant impact on the activation of microglia. The present findings demonstrate that glia from CD200$^{-/-}$ mice have a greater response to LPS; it is proposed that increased expression of TLR4 could account for the increased sensitivity of CD200$^{-/-}$ mice. Furthermore, HMGB1, known to amplify the inflammatory responses of LPS, was increased in cells prepared from CD200$^{-/-}$ mice presenting a potential novel mechanism for the magnification of the LPS-induced changes in cells prepared from CD200$^{-/-}$ mice.

LPS increased the gene expression and protein release of proinflammatory cytokines IL-1β, TNFα and IL-6, from mixed glia prepared from wildtype mice consistent with previously-described effects (Kong, McMillian et al. 1997; Lyons, McQuillan et al. 2009; Watson, Costello et al. 2010). This effect was greater in mixed glia prepared from CD200$^{-/-}$ mice, compared with wildtype mice. It has been suggested that CD200, present on neurons, is responsible for keeping microglia in a quiescent state due to its interaction with the CD200R present on microglia (Neumann 2001; Jurgens and Johnson 2010). In the mixed glial preparation used in this study, it is astrocytic CD200 that is responsible for modulating microglial inflammatory responses to stimuli (Koning, Swaab et al. 2009; Costello, Lyons et al. 2011). Taken together these data suggest the interaction between CD200 and the CD200R modulates TLR4-induced proinflammatory cytokine production and release. This is broadly consistent with previous data which indicated that loss of this interaction, i.e. in CD200$^{-/-}$ mice, was associated with exacerbated inflammation; thus these mice exhibit a more rapid onset of EAE and CIA (Hoek, Ruuls et al. 2000). CD200$^{-/-}$ mice also show exacerbated microglial activation following facial nerve transection (Hoek, Ruuls et al. 2000).

Although previous studies have demonstrated that disruption of the CD200-CD200R interaction can lead to excessive inflammation in response to a stimulus (Deckert, Sedgwick et al. 2006), the underlying mechanism for this has yet to be elucidated. LPS is captured by LBP and delivered to the LPS multi-component cell surface receptor consisting of CD14 and TLR4, where it initiates the signaling process leading to LPS-induced activation (Takeuchi, Hoshino et al. 1999;

Triantafilou and Triantafilou 2002). In this study, the expression of the LPS receptor, and TLR2 and TLR6, were investigated. Under resting conditions an increase in the expression of both TLR2 and TLR4 was observed in mixed glia prepared from CD200$^{-/-}$, compared with wildtype, mice, which may account for the increased susceptibility of CD200$^{-/-}$ mice to LPS. It has been shown that TLR4 activation can occur without CD14 and LBP; however their presence increases the sensitivity of the receptor for LPS (Triantafilou and Triantafilou 2002). The present data demonstrate that mixed glia prepared from CD200$^{-/-}$ show enhanced CD14 mRNA in response to LPS and thus may enhance the delivery of LPS to the receptor. TLR2 and TLR4 activation lead to NFκB activation, evaluated in this study by assessing phosphorylated IκKβ and IκBα. The data indicate that phosphorylation of both was increased in response to LPS in mixed glia prepared from wildtype mice and this effect was greater in cells prepared from CD200$^{-/-}$ mice. Furthermore, mixed glia prepared from CD200$^{-/-}$ mice showed increased phosphorylated IκKβ and IκBα compared with wildtype mice, indicating that NFκB activation was increased in cells prepared from CD200$^{-/-}$ mice, even in the absence of stimulation.

HMGB1 is reported to be a ligand for both TLR2 and TLR4 (Lotze and Tracey 2005). It is a high mobility nuclear protein, which can influence transcription and function as an extracellular protein signaling tissue damage (Lotze and Tracey 2005; Qin, Dai et al. 2009). The data reveal that HMGB1 expression was increased in mixed glia prepared from CD200$^{-/-}$, compared with wildtype, mice. Activated macrophages have been shown to release HMGB1 following an inflammatory stimulus and it is believed to be a delayed mediator of inflammation (Lotze and Tracey 2005). Recent data have indicated that HMGB1 may act synergistically with LPS since HMGB1 and LPS physically interact and the complex elicits the release of inflammatory cytokines more effectively than either molecule alone (Castiglioni, Canti et al. 2011). Coupled with increased receptor expression and the associated NFκB activation, increased HMGB1 expression in cells from CD200$^{-/-}$ mice may contribute to the amplification of the LPS-induced response.

In the current experiments mixed glial cultures were used in order to investigate the importance of the interaction between astrocytes and microglia. Astrocytes

express CD200, but not CD200R, and thus in a mixed glial culture it is proposed that astrocytes are modulating the microglial inflammatory responses (Costello, Lyons et al. 2011). As hypothesized, purified microglia prepared from CD200^{-/-} mice displayed increased levels of TLR2 and TLR4 compared with wildtype mice; however purified microglia prepared from wildtype and CD200^{-/-} mice produced similar amounts of pro-inflammatory cytokines IL-1β, TNFα and IL-6 in response to LPS. These results highlight the importance of astrocyte CD200 in modulating the inflammatory responses of microglial cells prepared from wildtype mice.

Analysis of purified astrocytes prepared from wildtype and CD200^{-/-} mice resulted in a greater effect of LPS on astrocytes prepared from CD200^{-/-} mice, with increased mRNA and release of IL-1β, IL-6 and TNFα. Here we demonstrate one possible explanation for the enhanced LPS-induced responses of astrocytes from CD200^{-/-} mice, compared with wildtype, mice may be the genotype-related increase in expression of TLR4 on GLAST^{+} cells. In addition it has been previously shown that activated astrocytes have been shown to release HMGB1 (Chen, Ward et al. 2004). Here we demonstrated in purified astrocyte cultures, HMGB1 acts synergistically with LPS forming a complex, the complex elicits the release of inflammatory cytokines more effectively than either molecule alone, this is supported by previous data demonstrating HMGB1/LPS complex produced increased IL-6 release from PBMCs when compared to either stimulus alone (Hreggvidsdottir, Ostberg et al. 2009; Castiglioni, Canti et al. 2011).

The findings presented here concur with previous data indicating the role of CD200 as a negative regulator of inflammation. Furthermore the data suggest the increased sensitivity to LPS in cells prepared from CD200^{-/-} mice may be due to up-regulated TLR4, and increased activation of NFκB. In addition, increased expression of HMGB1, as a result of CD200 deficiency, may form a complex with LPS and deliver a stronger signal to the TLR4 receptor resulting in an enhanced inflammatory output.

Chapter 4

CD200-CD200R interaction-

A regulator of classical activation of microglia

4.1. Introduction

The identification of microglia as a unique and distinct cell type was first made by Del Rio-Hortega, whose original studies concluded that fully-differentiated resting microglia take on a ramified morphology (Rio-Hortega 1932). This was then elaborated on in experiments on a stab wound model which led to the discovery that ramified microglia were capable of phenotypic differentiation into a migratory amoeboid form or "activated" form (Theele and Streit 1993). Much research to date has focused on the phenotypic and functional activation states of macrophages highlighting a need for a more precise definition of microglial activation. Microglia are now believed to a markedly heterogeneous group of cells capable of adopting multiple activation states depending on the stimulus, each with a distinct gene expression profile.

IFNγ is a multifunctional cytokine that is involved in the initiation and establishment of inflammation, and participates in both innate and adaptive immune responses (Lee, Chanamara et al. 2012). IFNγ triggers macrophages to become effector cells; these are described as classically-activated macrophages which are highly microbicidal and proinflammatory, easily identified by their increased production of iNOS and TNFα (Ma, Chen et al. 2003; Mosser 2003). IFNγ is the sole type II interferon and exerts its effects on cells by interacting with the specific IFNγR composed of two IFNGR1 subunits and two IFNGR2 subunits. The IFNγ binds to two IFNGR1 ligand-binding subunits resulting in the association with two IFNGR2 signaling subunits (Ma, Chen et al. 2003). IFNGR1 is constitutively associated with JAK1, while the intracellular domain of IFNGR2 contains a noncontiguous binding motif for recruitment of JAK2 (Schroder, Hertzog et al. 2004). Ligation of the receptor results in a number of phosphorylation events, resulting in recruitment and activation of STAT1 and the upregulation of IFNγ responsive genes (Schroder, Hertzog et al. 2004). There are a number of regulatory mechanisms which control IFNγ signaling including SOCS proteins are inhibitory regulators of the JAK/STAT pathway of cytokine-associated receptor signaling and can be induced by IFNγ stimulating feedback inhibition to limit its own activity (Dimitriou, Clemenza et al. 2008). The classical activation pathway is necessary for the survival of an organism however in order to resolve the infection or injury, the innate immune response requires

replacement of lost and damaged cells and re-modeling of damaged extracellular matrix (Colton 2009).

Microglia can alter their functional phenotype promoting an alternative activation state reducing the pro-inflammatory response and promoting repair. Th2 cell-derived cytokines, like IL-4, induce an alternative activation state, which is key to repair, resolution of inflammation and reconstruction following tissue injury. IL-4 signals via the IL-4Rα subunit of type I and type II receptor complexes resulting in the consequent activation of JAK mediate phosphorylation and recruitment of STAT6 and up regulation of IL-4 responsive genes including mannose receptor, arginase 1 and chitinase 3-like 3 (Oh, Geba et al. 2010).

Mannose receptor is a transmembrane glycoprotein that mediates Ca^{2+}-dependent endocytosis and phagocytosis of mannosylated ligands (Gordon 2003; Colton, Mott et al. 2006). Arginase 1 is believed to have a role cell proliferation and repair of the extracellular matrix (Colton, Mott et al. 2006), while Chitinase 3-like 3 is believed to play a role in repair processes after infection and injury (Colton, Mott et al. 2006).

In addition to the role of soluble secreted factors in the resolution of an innate immune response a deactivation state has been described in response to cell-cell contact in which the interaction between ligand-receptor pairs, such as CD200-CD200R and CD47-CD172a, play a role in the downregulation of macrophage activation (Barclay, Wright et al. 2002). The interaction between CD200, expressed on neurons, endothelial cells and astrocytes, with CD200R, expressed on microglia, has been implicated in the direct delivery of immunosupressive responses after antigen challenge (Nimmerjahn, Kirchhoff et al. 2005; Costello, Lyons et al. 2011). A recent study has found both a deficiency in CD200 and CD200R in human AD brains suggesting reduced efficacy of the CD200-CD200R system and therefore decreased capacity to control inflammation (Walker, Dalsing-Hernandez et al. 2009). It has been suggested that increasing expression of CD200 and CD200R therapeutically may provide a highly focused method of controlling myeloid cell activity in response to stimuli at the site of action.

The objectives of this study were:

a) To assess the activation states of mixed glia and purified microglia prepared from wildtype and CD200$^{-/-}$ mice in response to IFNγ and IL-4

b) To investigate the role of the CD200-CD200R interaction on these activation states

c) To assess whether modulating this interaction could alter the different activation states

4.2. Methods

Mixed glia, purified microglia and purified astrocytes were prepared from cortices of 1-day old wildtype and CD200^{-/-} mice, and cultured for 12 days before treatment (see section 2.1 for details). Cells were incubated in the presence or absence of IFNγ (50ng/ml) and/or CD200Fc, a synthetic soluble activator of the CD200 receptor (2.5μg/ml; 30min pre-treatment), or IL-4 (200ng/ml), for 24 hours. Flow cytometry was used to assess mannose receptor (BD Bioscience; UK) expression on CD11b^{+} cells in response to IL-4 and IFNγ in a purified microglia culture. Supernatant cytokine concentrations were determined by ELISA and expression of markers of classical and alternative activation was assessed by PCR in harvested cells (see section 2.2-2.4). Western immunoblotting was used to examine the IFNγ receptor and its signalling pathway in mixed glia prepared from wildtype and CD200^{-/-} mice (see section 2.5). For PCR, values are expressed as a relative quantity (RQ) calculated with respect to endogenous control, β-actin. Protein concentration was calculated from the standard curve and expressed in pg/ml. Protein expression established using western immunoblotting was calculated using densitometric analysis to calculate mean data. All data are expressed as means $\pm$ SEM. 1-way ANOVA using Neumann Keuls post-test and 2-way ANOVA with Bonferroni post-tests, were used to statistically interrogate the data and where appropriate the student's t test for independent means was performed to determine whether significance existed between treatment groups. Statistical analysis was performed using the computer-based statistical package, GraphPad prism (GraphPad, US).

4.3. Results

Activated microglia initiate phagocytosis and inflammation in response to an immune challenge, promoting a killing phase followed by inflammatory resolution and repair to restore normal tissue homeostasis. This response is essential for host defense but needs to be tightly regulated to prevent damage to the host. Chronic inflammation is believed to be caused by uncontrolled inflammatory responses and has been highlighted as a key feature of most neurological pathology. It has become apparent that microglia, like macrophages, have the ability to respond to varying stimuli resulting in distinct functional activation states. The Th1 cell-derived cytokine, IFNγ, induces a classical activation state, whereas, Th2 cell-derived cytokines, like IL-4, induce an alternative activation state (Colton and Wilcock 2010). The aim of these experiments was to investigate whether microglia displayed the same relationship between classical and alternative activation as peripheral macrophages, and to establish whether CD200 had a modulatory effect on these activation states.

Microglia prepared from CD200$^{-/-}$ mice respond more profoundly to IFNγ

Classically-activated macrophages produce high concentrations of proinflammatory cytokines, nitric oxide and reactive oxygen species and serve to reinforce the initial innate immune response (Colton 2009). The responses of mixed glia and purified microglia prepared from wildtype and CD200$^{-/-}$ mice to IFNγ were assessed by investigating established markers of classical activation NOS2, TNFα and IL-6 (Colton and Wilcock 2010). IFNγ (50ng/ml) stimulated a significant increase in mRNA expression of NOS2 (Figure 4.1) in mixed glia (A) and purified microglia (B) prepared from wildtype and CD200$^{-/-}$ mice (*p<0.05; 2-way ANOVA); Bonferroni post-hoc analysis revealed the IFNγ-induced increase in NOS2 was enhanced in purified microglia prepared from CD200$^{-/-}$, compared with wildtype, mice (*p<0.05; 2-way ANOVA). In a similar fashion, IFNγ induced a significant increase in the expression of TNFα mRNA (Figure 4.2) in mixed glia (A) and purified microglia (B) prepared from wildtype and CD200$^{-/-}$ mice (*p<0.05; ***p<0.001; 2-way ANOVA). Further analysis of the data revealed a significant genotype effect in purified microglia prepared from CD200^{-}

$^{/-}$ mice ($^{++}$p<0.01; 2-way AONVA), the interaction between IFNγ treatment and CD200-deficiency was significant and therefore the expression of TNFα in purified microglia prepared from CD200$^{-/-}$ mice was greater than from wildtype mice ($^{++}$p<0.01; 2-way ANOVA). TNFα (Figure 4.3) and IL-6 (Figure 4.4) supernatant concentration was increased in response to IFNγ in mixed glia (A) and purified microglia (B) prepared from wildtype and CD200$^{-/-}$ mice (*p<0.05; **p<0.01; ***p<0.001; 2-way ANOVA). There was a significant genotype effect in cells prepared from CD200$^{-/-}$ mice ($^{+}$p<0.05; $^{+++}$p<0.001; 2-way ANOVA). Further analysis revealed a significant interaction between treatment and genotype for TNFα release from mixed glia (*p<0.05; 2-way ANOVA) and, purified microglia (***p<0.0001; 2-way ANOVA). Bonferroni post-hoc analysis revealed enhanced IL-6 concentration in the presence of IFNγ from mixed glia (A; ***p<0.001) and purified microglia (B; **p<0.01) prepared from CD200$^{-/-}$ mice. The data reveal CD200$^{-/-}$ mice display an enhanced response to IFNγ and suggest a role for CD200 in modulating the classical activation pathway.

IFNGR1 and STAT1 phosphorylation was increased in glia prepared from CD200$^{-/-}$ mice

As a possible explanation for the increased responsiveness of glia prepared from CD200$^{-/-}$ mice to IFNγ, the expression of the IFNγR was assessed. The IFNγR is a heterodimer of two chains, IFNGR1 and IFNGR2 subunits, JAK1 and JAK2 constitutively associate with IFNGR1 and IFNGR2, respectively. IFNγ binds to IFNGR1 and leads to receptor assembly resulting in a complete receptor complex containing two IFNGR1 and two IFNGR2 subunits (Schroder, Hertzog et al. 2004).

Microglial cells were prepared from wildtype and CD200$^{-/-}$ mice and labelled with CD11b as a marker of microglia. The percentage of IFNGR1^{+} CD11b^{+} cells was increased in microglial cells prepared from CD200$^{-/-}$, compared with wildtype, mice (**p<0.01; 2-way ANOVA; Figure 4.5), therefore CD200$^{-/-}$ mice had increased surface expression of IFNGR1 compared with wildtype mice. Following ligation of the IFNGR1 subunit, auto-phosphorylation of JAK1 and JAK2 and tyrosine phosphorylation of IFNGR1 leads to the recruitment of STAT1. Upon

activation by tyrosine phosphorylation, STAT1 forms a homodimer, translocates to the nucleus, and activates gene transcription (Schroder, Hertzog et al. 2004). Here, a sample immunoblot indicates that IFNγ significantly increased STAT1 phosphorylation in mixed glia prepared from CD200$^{-/-}$ mice (***$p<0.001$; 2-way ANOVA; Figure 4.6); a significant effect of CD200-deficiency was observed in the data ($^{+++}p<0.001$; 2-way ANOVA), resulting in a significant interaction between IFNγ treatment and CD200 deficiency (***$p<0.001$; 2-way ANOVA). Furthermore, STAT1 phosphorylation (B) was increased in unstimulated mixed glia prepared from CD200$^{-/-}$, compared with wildtype, mice (*$p<0.05$; Students t test for independent means). Thus, increased IFNGR1 and increased receptor signalling represent a plausible explanation for increased susceptibility to IFNγ observed in glia prepared from CD200$^{-/-}$ mice.

SOCS1: a regulator of IFNγ-induced signalling

SOCS1 inhibits IFNγ signalling because of its capacity to bind and inactivate JAK1 and JAK2 proteins thereby impeding STAT1 activation (Madonna, Scarponi et al. 2008). As the IFNγ signalling pathway appeared to be dysregulated in CD200$^{-/-}$ mice, SOCS1 expression was assessed as a known regulator of IFNγ signalling. SOCS1 mRNA (Figure 4.7) and protein (Figure 4.8) expression were both increased in response to IFNγ in mixed glia prepared from wildtype and CD200$^{-/-}$ mice (*$p<0.05$; ***$p<0.001$; 2-way ANOVA). A significant genotype effect was observed resulting in enhanced SOCS1 mRNA and protein in CD200$^{-/-}$ mice (**$p<0.01$; ***$p<0.001$; 2-way ANOVA). The data indicate that SOCS1 regulatory system is up-regulated in CD200$^{-/-}$ mice.

CD200Fc attenuates IFNγ-induced classical activation

The development of CD200$^{-/-}$ mice has led to significant advances in understanding the possible functions of the CD200-CD200R interaction and has highlighted its importance in modulating microglial activation (Wang, Ye et al. 2007). CD200Fc, a synthetic, soluble activator of the CD200R, has shown potential for use as a therapeutic agent in a number of animal models (Barclay,

Wright et al. 2002). In order to investigate the modulatory effects of CD200 on classical activation, mixed glia were cultured from wildtype mice and incubated in the presence or absence of IFNγ and/or CD200Fc. IFNγ increased the mRNA expression of NOS2 (A), TNFα (B) and IL-6 (C) in mixed glia prepared from wildtype mice (**p<0.01; ***p<0.001; 1-way ANOVA; Figure 4.9); CD200Fc significantly attenuated the IFNγ-induced increase in TNFα and IL-6 expression, but not NOS2 expression ([+]p<0.05; [++]p<0.01; 1-way ANOVA). In a similar fashion, IFNγ increased TNFα (A) and IL-6 (B) release from mixed glia prepared from wildtype mice (**p<0.01; ***p<0.001; 1-way ANOVA); CD200Fc significantly attenuated the IFNγ-induced increase in TNFα and IL-6 ([+]p<0.05; 1-way ANOVA; Figure 4.10). These results indicate that CD200Fc shows potential as a modulator of the classical activation pathway.

IL-4 induced alternative activation

Th2 cytokines IL-4 and IL-13 induce an alternative pathway distinct from the IFNγ-mediated classical pathway (Gordon and Martinez 2010). The alternative activation pathway described in macrophages is involved in shutting down the production of pro-inflammatory cytokines and increasing factors involved in wound healing and tissue repair and is characterized by the up-regulation of genes that produce arginase I, mannose receptor, and genes associated with tissue remodeling such as FIZZ1 and chitinase 3-like 3 however the exact functions of many of the protein products of these genes are still unclear (Colton, Mott et al. 2006).

IL-4 increased mannose receptor expression (A; figure 4.11) in mixed glia prepared from wildtype and CD200^{-/-} mice (**p<0.01; 2-way ANOVA); no genotype-related change was observed in response to IL-4. In addition IL-4, but not IFNγ, increased mannose receptor expression on the surface of CD11b^{+} cells prepared from wildtype mice (*p<0.05; 1-way ANOVA). IL-4 induced increased expression of arginase 1 (A; figure 4.13) and chitinase 3-like 3 (figure 4.14) in mixed glia prepared from wildtype and CD200^{-/-} mice (**p<0.01; ***p<0.001; 2-way ANOVA); however similar to that observed with mannose receptor, no genotype-related changes were observed. Interestingly, mRNA expression of

mannose receptor (B; figure 4.11) and arginase 1 (B; figure 4.13) was increased in unstimulated cells prepared from CD200$^{-/-}$, compared with wildtype, mice (*p<0.05; **p<0.01; student's t test for independent means).

IL-4 mediates its effects through a type I and type II receptor complex through the IL-4Rα subunit (Martinez, Helming et al. 2009; Oh, Geba et al. 2010). Here, the expression of the IL-4Rα subunit was assessed in purified microglia and astrocytes prepared from wildtype and CD200$^{-/-}$ mice. IL-4Rα was found to be expressed on both astrocytes and microglia prepared from wildtype mice, with microglia expressing three times the amount when compared with astrocytes (A; ***p<0.001; students t test for independent means; Figure 4.15). Further, IL-4Rα expression was found to be increased on purified microglia (B; ***p<0.001; students t test for independent means) and decreased on purified astrocytes (C; ***p<0.001; students t test for independent means) prepared from CD200$^{-/-}$, compared with wildtype, mice. The functional output of this phenotypic difference remains unclear at this point.

Alternative versus classical activation pathways

Alternative and classical activation are commonly viewed as two opposing activation states. Markers of classical activation, namely NOS2 and TNFα were decreased by IL-4 (**p<0.01; ***p<0.001; 2-way ANOVA; Figure 4.16). Interestingly, IL-4 decreased TNFα, but not IL-6, release from glia prepared from wildtype and CD200$^{-/-}$ mice (**p<0.01; 2-way AOVA; Figure 4.17). Mannose receptor expression was selectively down-regulated by IFNγ in mixed glia prepared from wildtype and CD200$^{-/-}$ mice (***p<0.001; 2-way ANOVA; Figure 4.18). These results demonstrate that IL-4 opposes the classical activation pathway through the selective down-regulation of TNFα and NOS2 gene expression, while IFNγ selectively down-regulates marker of alternative activation mannose receptor.
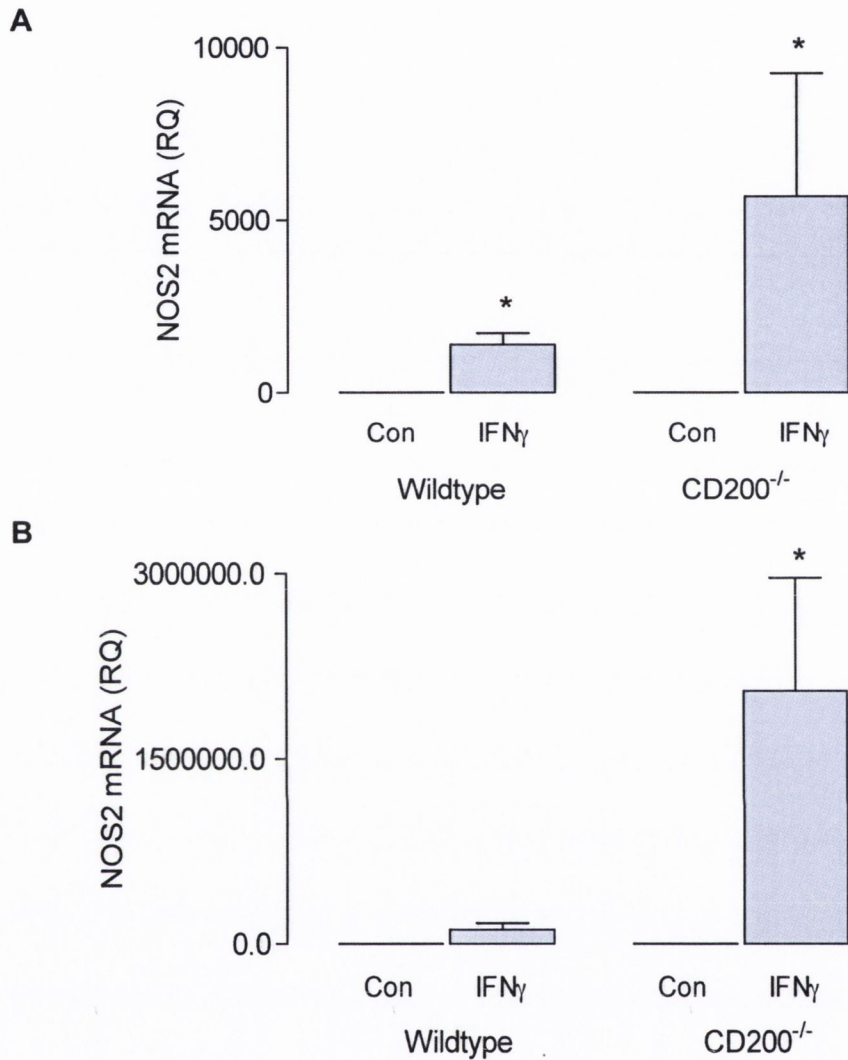
Figure 4.1. IFNγ increased NOS2 mRNA expression in mixed glia and purified microglia prepared from wildtype and CD200⁻/⁻ mice.

The expression of NOS2 was increased in response to IFNγ in mixed glia (A) and purified microglia (B) prepared from wildtype and CD200⁻/⁻ mice (*$p<0.05$; 2-way ANOVA); bonferroni post-hoc test analysis revealed this effect was greater in purified microglia prepared from CD200⁻/⁻, compared with wildtype, mice (*$p<0.05$; 2-way ANOVA). Values are presented as means ± SEM expressed as a relative quantity (RQ).

A. 2-way ANOVA: IFNγ $_{effect}$ $F(1,8)=10.55$; *$p=0.0117$, Genotype $_{effect}$ $F(1,8)=3.893$; $p=0.0840$, Interaction $_{effect}$ $F(1,8)=3.893$; $p=0.0840$

B. 2-way ANOVA: IFNγ $_{effect}$ $F(1,17)=14.37$; $p=0.0580$, Genotype $_{effect}$ $F(1,17)=11.49$; $p=0.0868$, Interaction $_{effect}$ $F(1,17)=11.49$; $p=0.0868$

A

B

Figure 4.2. IFNγ increased TNFα mRNA expression in mixed glia and purified microglia prepared from wildtype and CD200$^{-/-}$ mice.

The expression of TNFα was increased in response to IFNγ in mixed glia (A) and purified microglia (B) prepared from wildtype and CD200$^{-/-}$ mice (*p<0.05; ***p<0.001; 2-way ANOVA); this effect was greater in purified microglia prepared from CD200$^{-/-}$, compared with wildtype, mice (**p<0.01; 2-way ANOVA); further analysis revealed a significant interaction between treatment and genotype (**p<0.01; 2-way ANOVA). Values are presented as means ± SEM expressed as a relative quantity (RQ).

A. 2-way ANOVA: IFNγ $_{effect}$ $F_{(1,9)}=10.41$; *p=0.0104, Genotype $_{effect}$ $F_{(1,9)}=0.3753$; p=0.5553, Interaction $_{effect}$ $F_{(1,9)}=0.2499$; p=0.6291
B. 2-way ANOVA: IFNγ $_{effect}$ $F_{(1,20)}=150.3$; ***p<0.0001, Genotype $_{effect}$ $F_{(1,20)}=12.87$; **p=0.0018, Interaction $_{effect}$ $F_{(1,20)}=10.13$; **p=0.0047
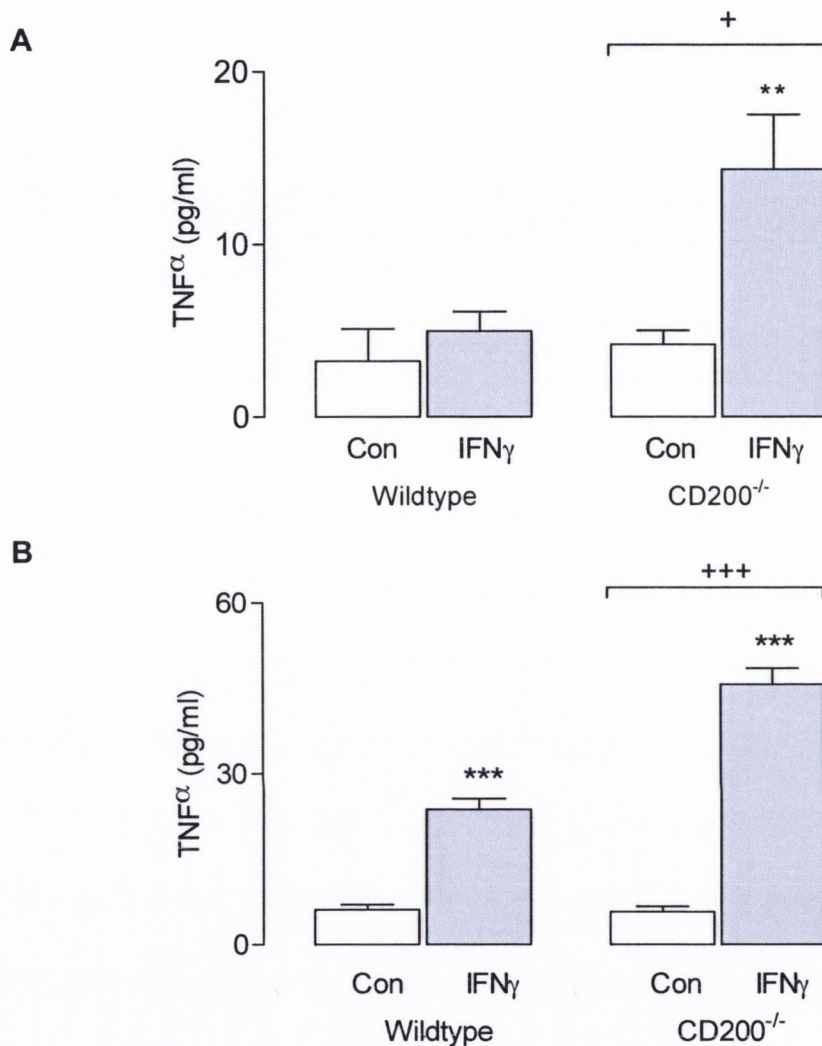
Figure 4.3. IFNγ-induced TNFα release was enhanced in mixed glia and purified microglia prepared from CD200$^{-/-}$ mice.

TNFα concentration was increased in supernatant from mixed glia (A) and purified microglia (B) prepared from wildtype and CD200$^{-/-}$ mice incubated in the presence of IFNγ (**$p<0.01$; ***$p<0.001$; 2-way ANOVA), this effect was significantly increased in mixed glia and purified microglia prepared from CD200$^{-/-}$ mice ($^+p<0.05$; $^{+++}p<0.001$; 2-way ANOVA); further analysis revealed a significant interaction between treatment and genotype was observed in mixed glia (*$p<0.05$; 2-way ANOVA) and, purified microglia (***$p<0.0001$; 2-way ANOVA). Values are presented as means ± SEM.

A. 2-way ANOVA: IFNγ $_{effect}$ $F(1,13)=10.14$; **$p=0.0072$, Genotype $_{effect}$ $F(1,13)=7.690$; *$p=0.0158$, Interaction $_{effect}$ $F(1,13)=5.086$; $p=0.0420$; *$p=0.0420$
B. 2-way ANOVA: IFNγ $_{effect}$ $F(1,20)=211.1$; ***$p<0.0001$, Genotype $_{effect}$ $F(1,20)=29.54$; ***$p<0.0001$, Interaction $_{effect}$ $F(1,20)=31.81$; ***$p<0.0001$
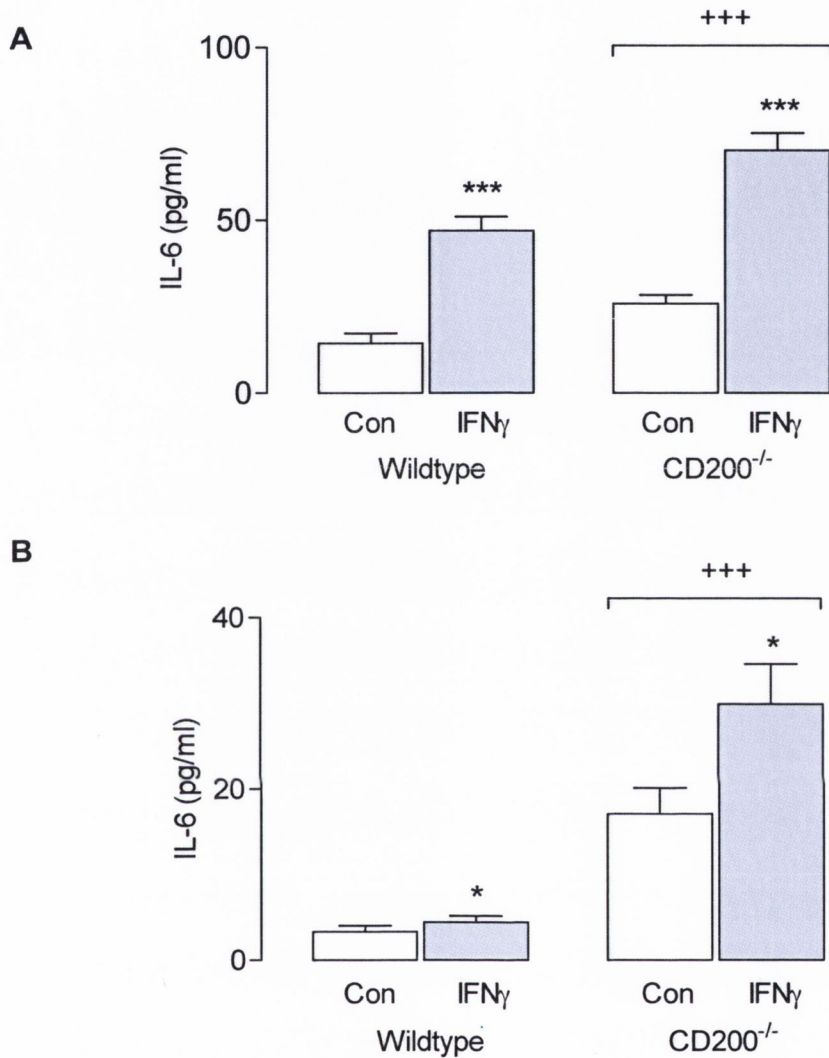
Figure 4.4. IFNγ-induced IL-6 release was enhanced in mixed glia and purified microglia prepared from CD200$^{-/-}$ mice.

IL-6 concentration was increased in supernatant from mixed glia (A) and purified microglia (B) prepared from wildtype and CD200$^{-/-}$ mice incubated in the presence of IFNγ (*$p<0.05$; ***$p<0.001$; 2-way ANOVA); there was a this significant genotype effect ($^{+++}$$p<0.001$; 2-way ANOVA); Bonferroni post-hoc analysis revealed this resulted in enhanced IL-6 release from mixed glia (***$p<0.001$) and purified microglia (**$p<0.01$) prepared from CD200$^{-/-}$ mice. Values are presented as means ± SEM.

    A. 2-way ANOVA: IFNγ $_{effect}$ F(1,12)=119.0; ***$p<0.0001$, Genotype $_{effect}$ F(1,12)=24.21; ***$p=0.0004$, Interaction $_{effect}$ F(1,12)=2.798; $p=0.1202$

    B. 2-way ANOVA: IFNγ $_{effect}$ F(1,14)=4.804; *$p=0.0458$, Genotype $_{effect}$ F(1,14)=38.13; ***$p<0.0001$, Interaction $_{effect}$ F(1,14)=3.4; $p=0.0865$

A

IFNGR1

B
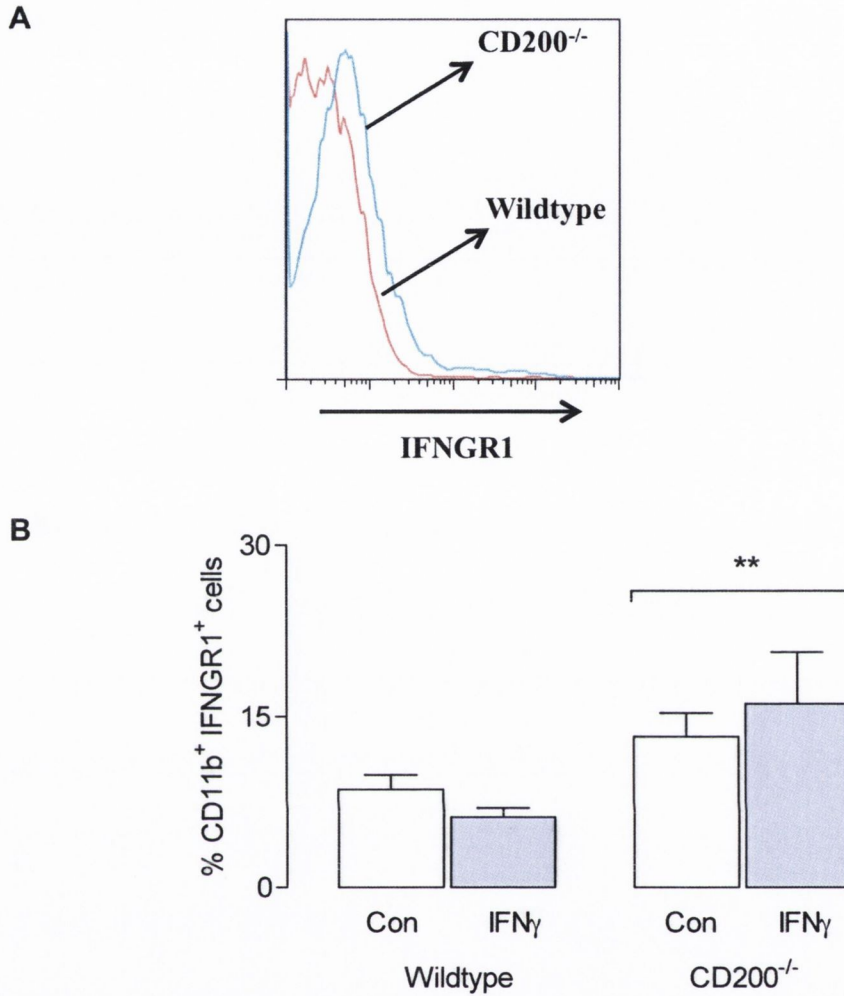
Figure 4.5. IFNγ receptor 1 was increased on CD11b$^+$ cells prepared from CD200$^{-/-}$ mice.

Microglial cells were prepared from wildtype and CD200$^{-/-}$ mice and labelled with CD11b as a marker of microglia. The percentage of CD11b$^+$ IFNGR1$^+$ cells was increased in cells prepared from CD200$^{-/-}$, compared with wildtype, mice (**p<0.01; 2-way ANOVA).

2-way ANOVA: IFNγ $_{effect}$ F(1,12)=0.01201; p=0.9146, Genotype $_{effect}$ F(1,12)=12.27; **p=0.0044, Interaction $_{effect}$ F(1,12)=1.637; p=0.225

A

B
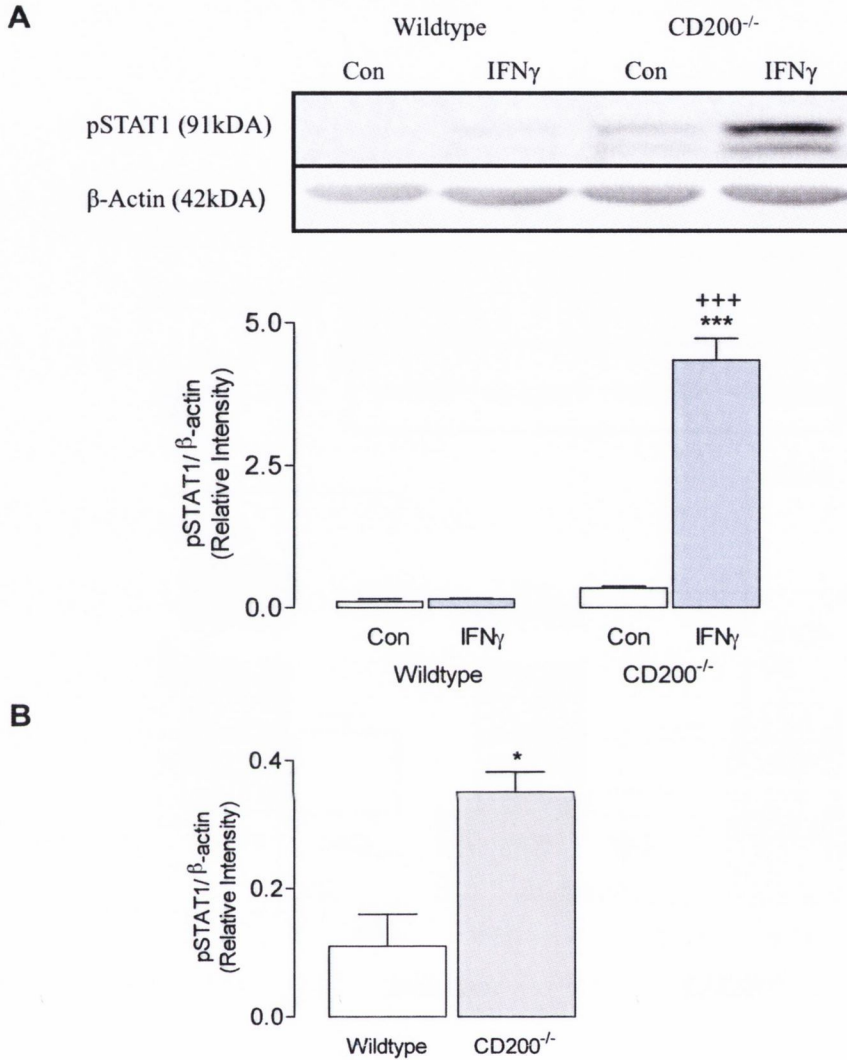
Figure 4.6. STAT1 phosphorylation was increased in mixed glia prepared from CD200$^{-/-}$ mice.

(A) A sample immunoblot indicates that IFNγ significantly increased STAT1 phosphorylation in mixed glia prepared from CD200$^{-/-}$ mice (***p<0.001; 2-way ANOVA); this effect was increased when compared to wildtype mice ($^{+++}$p<0.001; 2-way ANOVA); analysis revealed a significant interaction between treatment and genotype (***p<0.001; 2-way ANOVA). (B) STAT1 phosphorylation was increased unstimulated mixed glia prepared from CD200$^{-/-}$, compared with wildtype, mice (*p<0.05; students *t* test for independent means). Values are presented as means ± SEM expressed as a relative intensity.

2-way ANOVA: IFNγ $_{effect}$ F(1,9)=65.94; ***p<0.0001, Genotype $_{effect}$ F(1,9)=79.38; ***p<0.0001, Interaction $_{effect}$ F(1,9)=63.34; ***p<0.0001
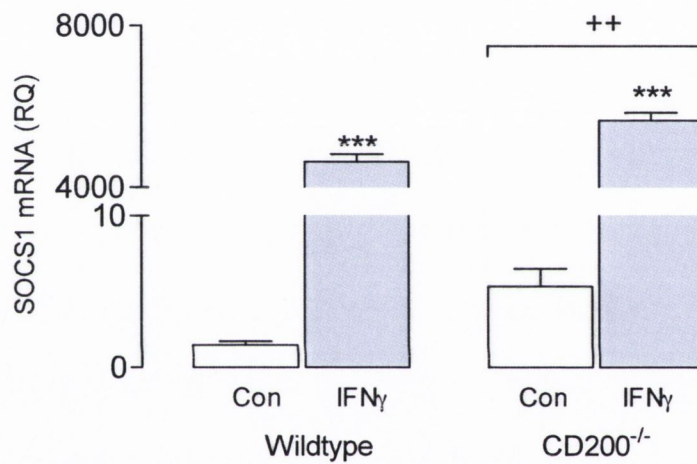
Figure 4.7. IFNγ-induced SOCS1 expression was increased in mixed glia prepared from CD200$^{-/-}$ mice.

IFNγ significantly increased SOCS1 mRNA expression in mixed glia prepared from wildtype and CD200$^{-/-}$ mice (***p<0.0001; 2-way ANOVA); this effect was enhanced in cells prepared from CD200$^{-/-}$ mice ($^{++}$p<0.01; 2-way ANOVA). Analysis of the data revealed that there was a significant interaction between treatment and genotype (**p<0.01; 2-way ANOVA). Values are presented as means ± SEM expressed relative to β-actin.

2-way ANOVA: IFNγ $_{effect}$ F(1,14)=1329; ***p<0.0001, Genotype $_{effect}$ F(1,14)=13.27; **p=0.0026, Interaction $_{effect}$ F(1,14)=13.07; **p=0.0028
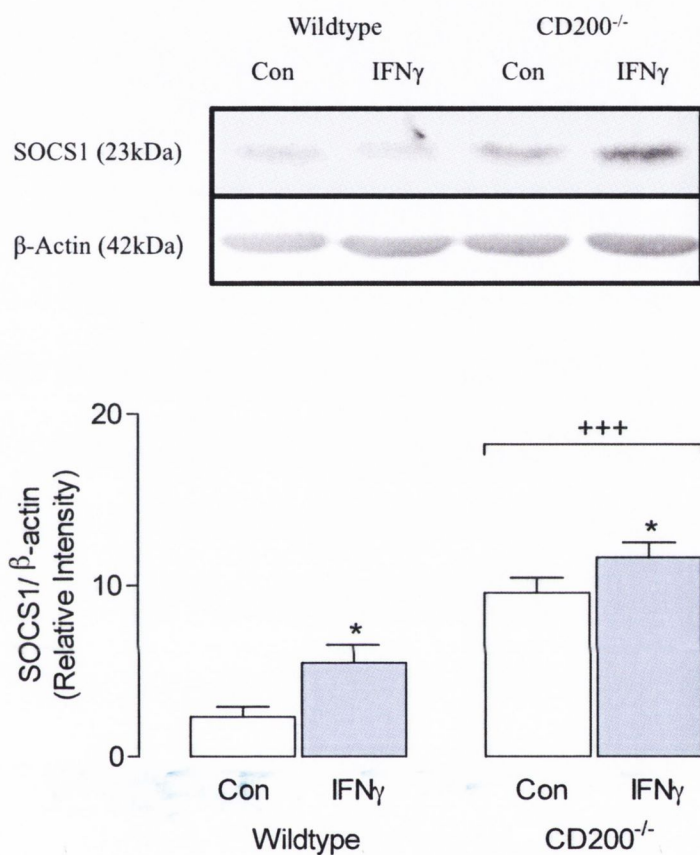
Figure 4.8. Protein expression of SOCS1 was increased in mixed glia prepared from CD200$^{-/-}$ mice.

A sample immunoblot indicates that IFNγ significantly increased SOCS1 expression in mixed glia prepared from wildtype and CD200$^{-/-}$ mice (*p<0.05; 2-way ANOVA); but CD200$^{-/-}$ mice expressed increased SOCS1 compared with wildtype mice (***p<0.001; 2-way ANOVA). Densitometric analysis was used to calculate the mean data and values are presented as means ± SEM expressed relative to β-actin.

2-way ANOVA: IFNγ $_{effect}$ F(1,8)=9.163; *p=0.0164, Genotype $_{effect}$ F(1,8)=60.05; ***p<0.0001, Interaction $_{effect}$ F(1,8)=0.4134; p=0.5382
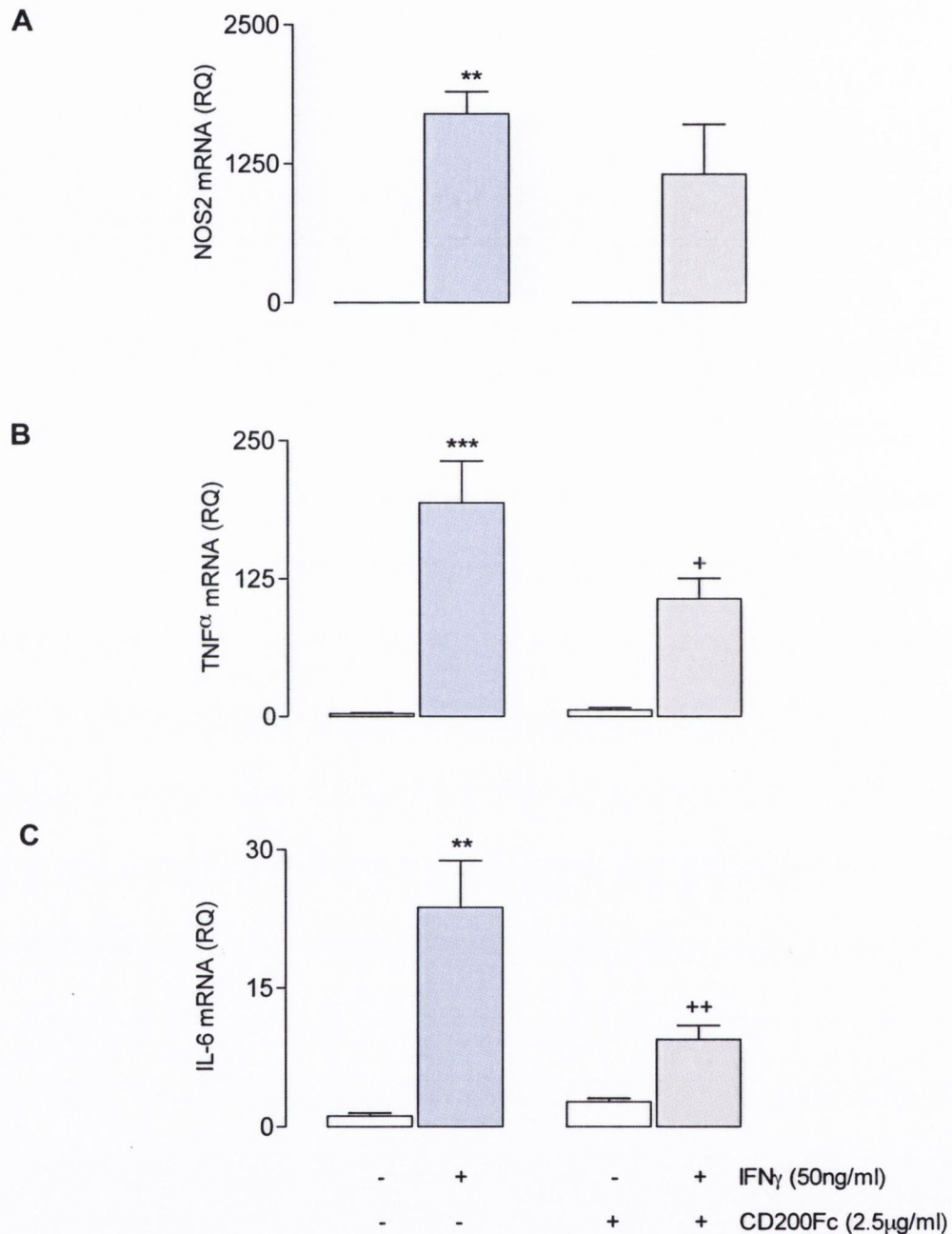
Figure 4.9. CD200Fc attenuated the IFNγ-induced increase in TNFα and IL-6 expression in mixed glia prepared from wildtype mice.

IFNγ increased NOS2 (A), TNFα (B) and IL-6 expression in mixed glia prepared from wildtype mice (**$p<0.01$; ***$p<0.001$; 1-way ANOVA; n=5); CD200Fc significantly attenuated the IFNγ-induced increase in TNFα and IL-6 mRNA, but not NOS2 mRNA (+$p<0.05$; ++$p<0.01$; 1-way ANOVA; n=5). Values are presented as means ± SEM and expressed as a relative quantity (RQ)
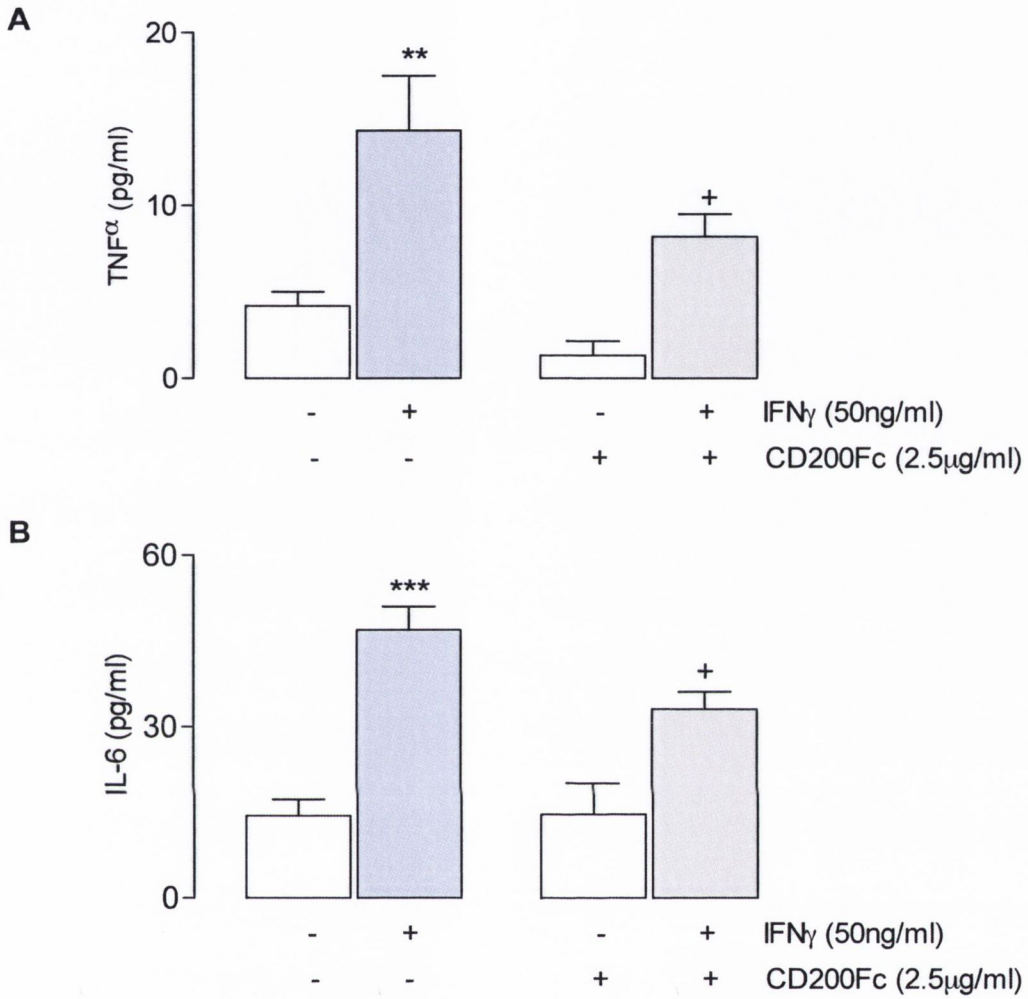
Figure 4.10. CD200Fc attenuated the IFNγ-induced increase in TNFα and IL-6 supernatant concentration in mixed glia prepared from wildtype mice.

IFNγ increased TNFα (A) and IL-6 (B) supernatant concentration from mixed glia prepared from wildtype mice (**p<0.01; ***p<0.001; 1-way ANOVA; n=4); CD200Fc significantly attenuated the IFNγ-induced effect ($^+$p<0.05; 1-way ANOVA; n=4). Values are presented as means ± SEM.
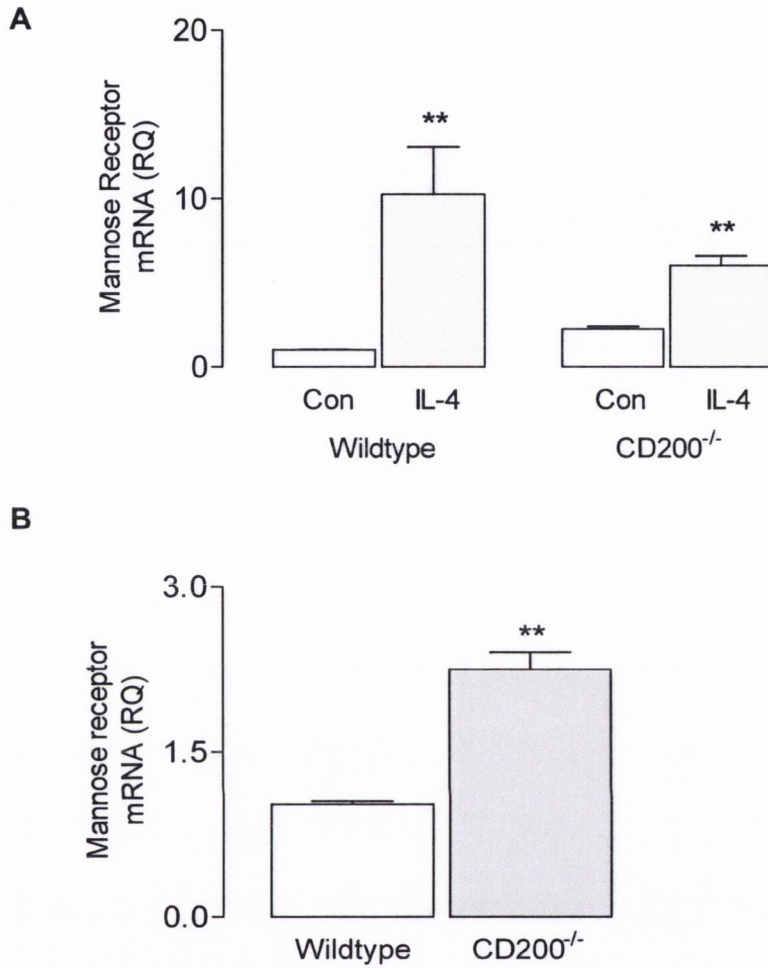
Figure 4.11. IL-4 increased mannose receptor expression in mixed glia prepared from wildtype and CD200$^{-/-}$ mice.

IL-4 increased mannose receptor (A) expression in mixed glia prepared from wildtype and CD200$^{-/-}$ mice (**p<0.01; 2-way ANOVA). (B) Mannose receptor was increased in mixed glia prepared from CD200$^{-/-}$, compared with wildtype, mice (*p<0.05; students t test for independent means). Values are presented as means ± SEM expressed as a relative quantity (RQ).

A. 2-way ANOVA: IL-4 $_{effect}$ F(1,9)=11.72; **p=0.0076, Genotype $_{effect}$ F(1,9)=0.6327; p=0.4468, Interaction $_{effect}$ F(1,9)=2.073; p=0.1838
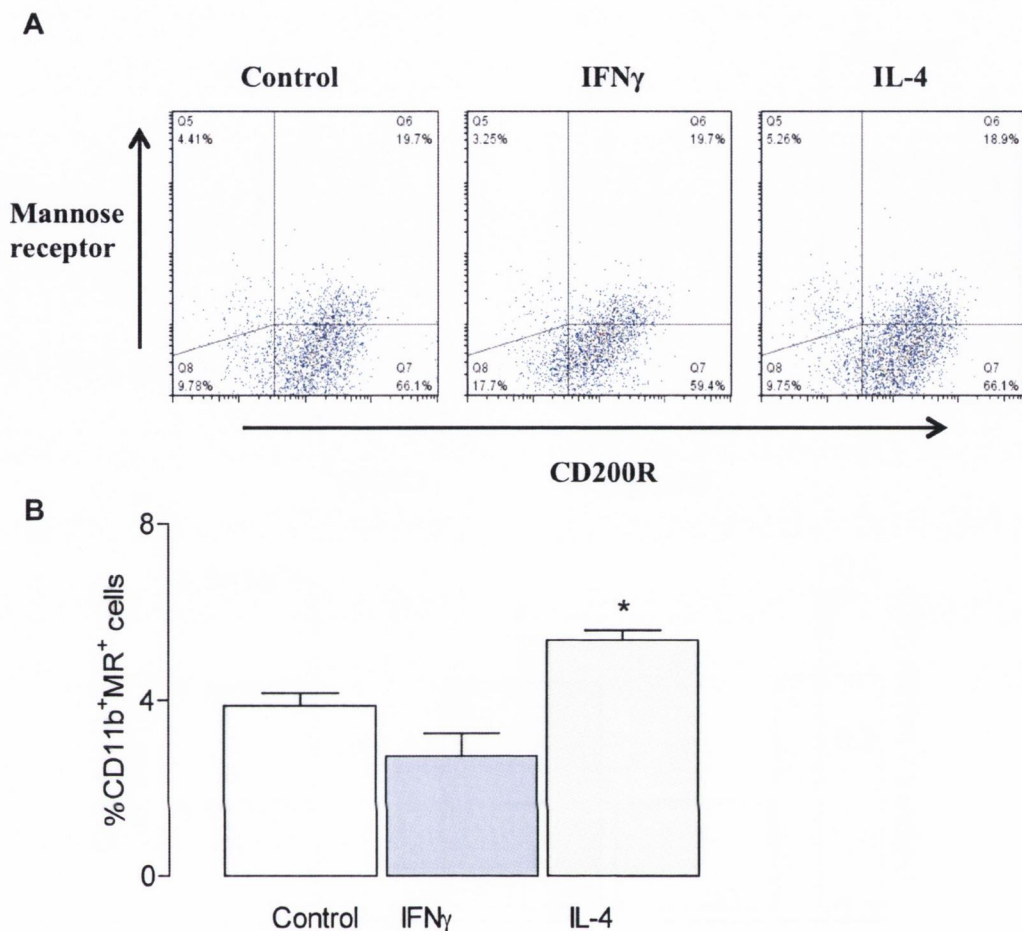
Figure 4.12. IL-4 increased mannose receptor expression on the surface of CD11b$^+$ cells prepared from wildtype mice.

Representative dot plots (A) are shown for mannose receptor expression on CD11b$^+$ cells for each treatment group described. IL-4, but not IFNγ, increased the percentage of CD11b$^+$ mannose receptor$^+$ cells in mixed glia prepared from wildtype mice (*p<0.05; 1-way ANOVA; n=3). Values are presented as means ± SEM and expressed as a percentage of CD11b$^+$ cells.
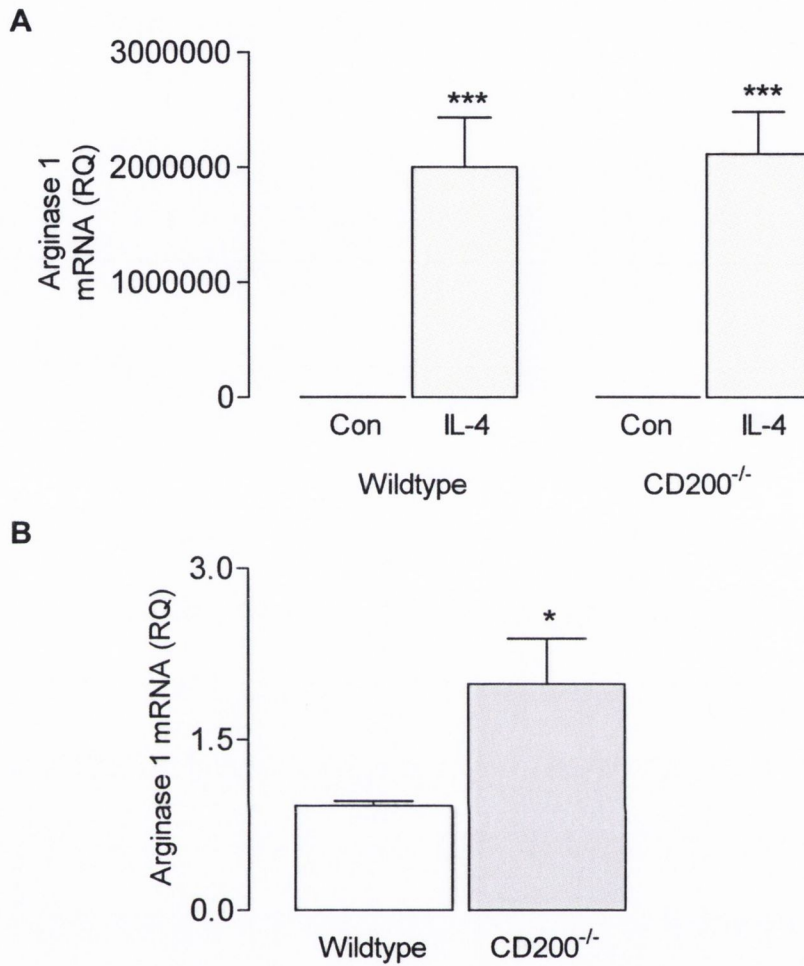
Figure 4.13. IL-4 increased arginase 1 expression in mixed glia prepared from wildtype and CD200$^{-/-}$ mice.

(A) IL-4 increased arginase 1 mRNA expression in mixed glia prepared from wildtype and CD200$^{-/-}$ mice (***p<0.001; 2-way ANOVA). (B) Arginase 1 expression was increased in mixed glia prepared from CD200$^{-/-}$, compared with wildtype, mice (*p<0.05; students *t* test for independent means). Values are presented as means ± SEM expressed as a relative quantity (RQ).

    A. 2-way ANOVA: IL-4 $_{effect}$ F(1,9)=29.79; ***p=0.0004, Genotype $_{effect}$ F(1,9)=0.02266; p=0.8837, Interaction $_{effect}$ F(1,9)=0.02266; p=0.8837
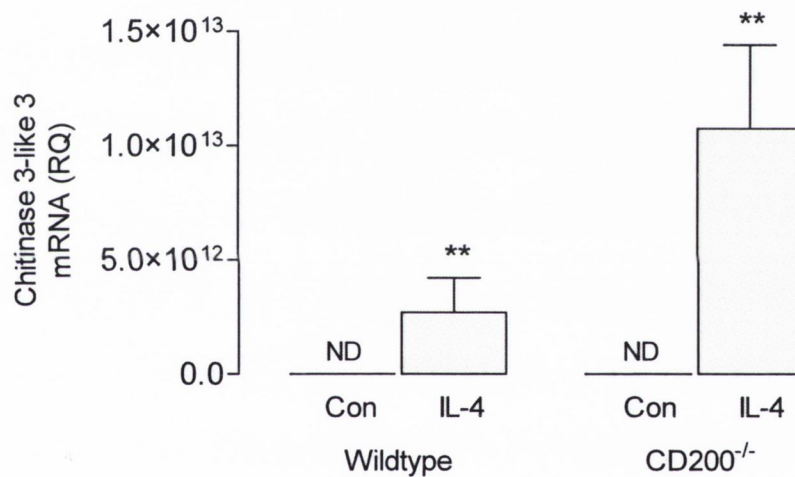
Figure 4.14. IL-4 increased Chitinase 3-like 3 expression in mixed glia prepared from wildtype and CD200$^{-/-}$ mice.

IL-4 increased chitinase 3-like 3 mRNA expression in mixed glia prepared from wildtype and CD200$^{-/-}$ mice (**$p<0.01$; 2-way ANOVA). Values are presented as means ± SEM expressed as a relative quantity (RQ).

2-way ANOVA: IL-4 $_{effect}$ F(1,11)=9.830; **$p=0.0095$, Genotype $_{effect}$ F(1,11)=3.521; $p=0.0874$, Interaction $_{effect}$ F(1,11)=3.521; $p=0.0874$
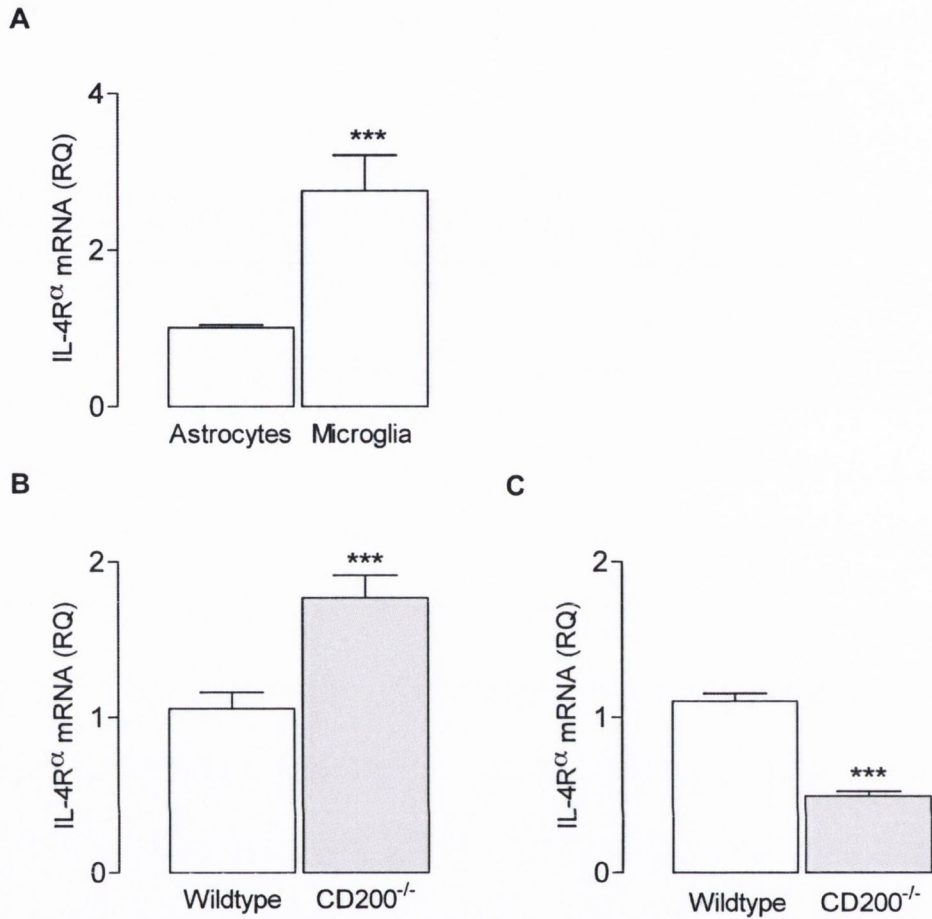
Figure 4.15. IL-4Rα, expressed on astrocytes and microglia, was increased on microglia prepared from CD200^{-/-} mice.

IL-4Rα was found to be expressed on both astrocytes and microglia prepared from wildtype mice, with microglia expressing three times the amount when compared with astrocytes (A; ***p<0.001; 1.009 ± 0.03615; n=15 vs. 2.756 ± 0.4553; n=10; student's t test for independent means). Furthermore, IL-4Rα expression was found to be increased on purified microglia (B; ***p<0.001; 1.056 ± 0.1057; n=10 vs. 1.770 ± 0.1446; n=10; student's t test for independent means) and decreased on purified astrocytes (C; ***p<0.001; 1.105 ± 0.048; n=15 vs. 0.4929 ± 0.03001; n=20; students t test for independent means) prepared from CD200^{-/-}, compared with wildtype mice. Values are presented as means $\pm$ SEM expressed as a relative quantity (RQ).
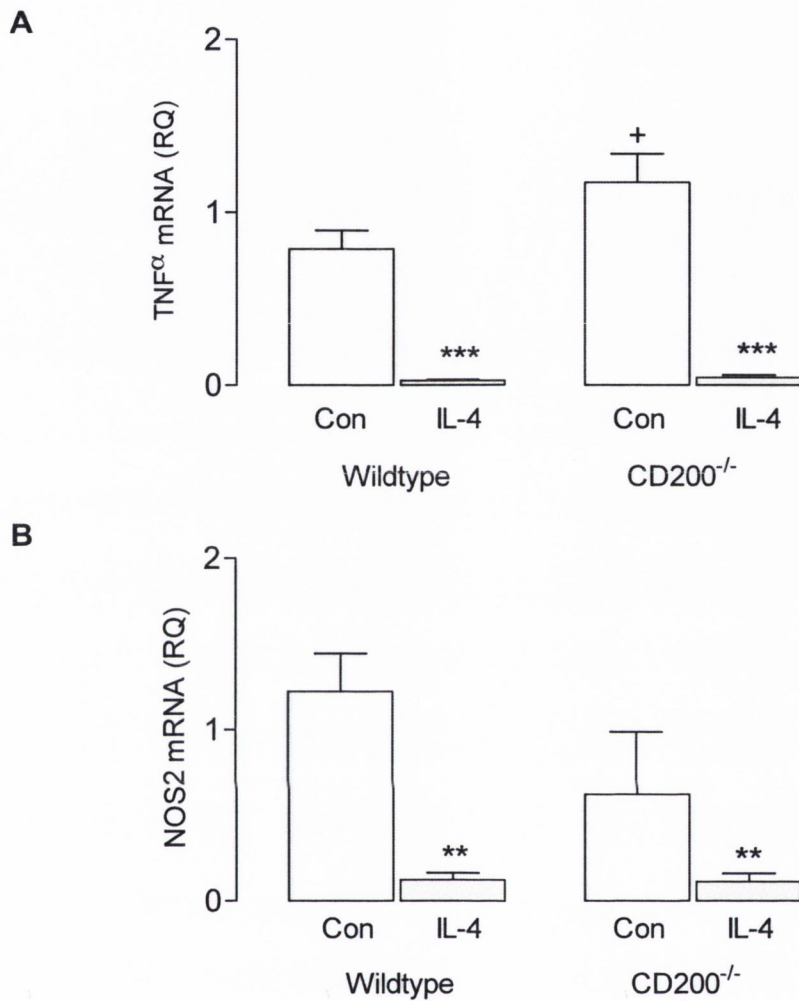
Figure 4.16. IL-4 attenuated the classical activation markers TNFα and NOS2 in mixed glia prepared from wildtype and CD200$^{-/-}$ mice.

IL-4 decreased TNFα (A) and NOS2 (B) mRNA expression in mixed glia prepared from wildtype and CD200$^{-/-}$ mice (**p<0.01; ***p<0.001; 2-way ANOVA). Values are presented as means ± SEM expressed as a relative quantity (RQ).

A. 2-way ANOVA: IL-4 $_{effect}$ $F(1,10)=129.2$; ***p<0.0001, Genotype $_{effect}$ $F(1,10)=5.818$; *p=0.0366, Interaction $_{effect}$ $F(1,10)=4.887$; p<0.0001
B. 2-way ANOVA: IL-4 $_{effect}$ $F(1,10)=15.92$; **p=0.004, Genotype $_{effect}$ $F(1,10)=2.297$; p=0.1681, Interaction $_{effect}$ $F(1,10)=2.111$; p=0.1843
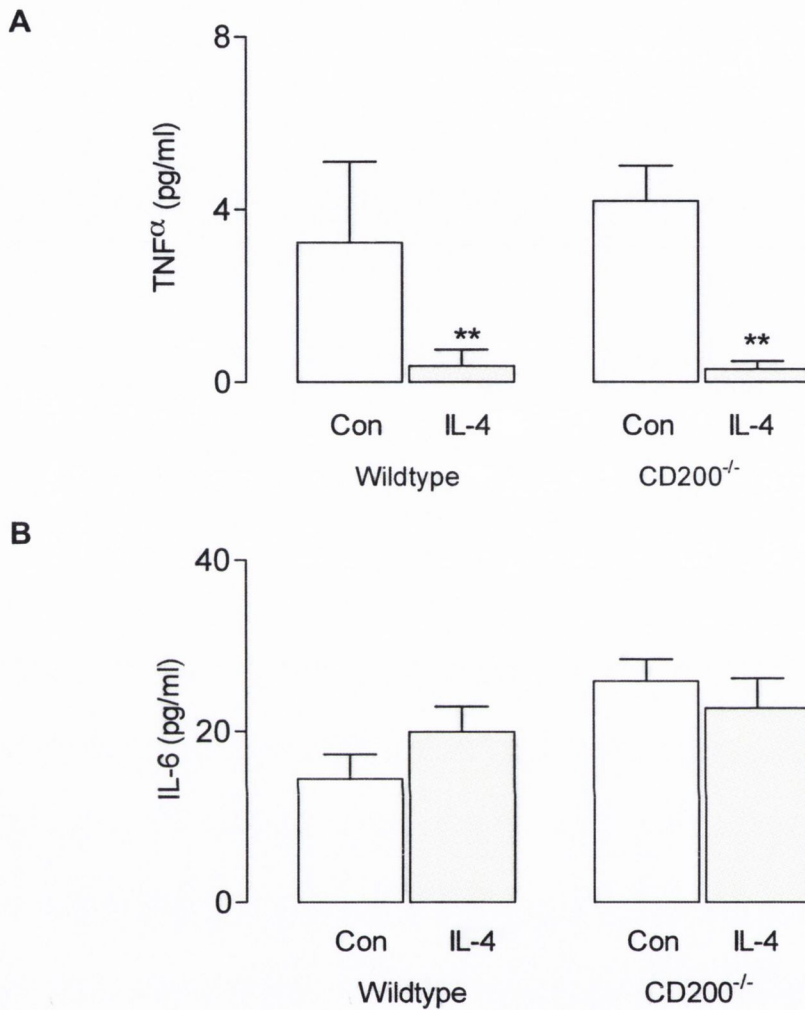
Figure 4.17. IL-4 decreased TNFα, but not IL-6, release from mixed glia prepared from wildtype and CD200$^{-/-}$ mice.

IL-4 decreased TNFα (A), but not IL-6 (B), supernatant concentration from mixed glia prepared from wildtype and CD200$^{-/-}$ mice (**$p<0.01$; 2-way ANOVA). Values are presented as means ± SEM expressed as a relative quantity (RQ).

A. 2-way ANOVA: IL-4 $_{effect}$ $F(1,13)=10.56$; **$p=0.0063$, Genotype $_{effect}$ $F(1,13)=0.1852$; $p=0.6740$, Interaction $_{effect}$ $F(1,13)=0.2502$; $p=0.0.6253$
B. 2-way ANOVA: IL-4 $_{effect}$ $F(1,14)=0.004$; $p=0.9481$, Genotype $_{effect}$ $F(1,14)=6.430$; *$p=0.0238$, Interaction $_{effect}$ $F(1,14)=2.773$; $p=0.1181$

110
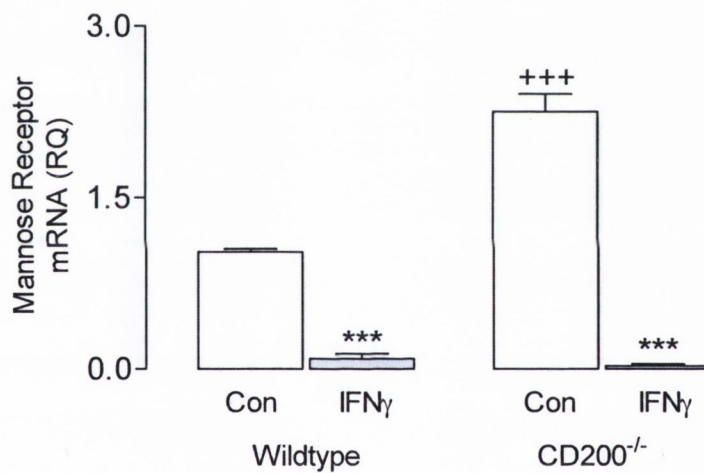
Figure 4.18. IFNγ attenuated the alternative activation marker, mannose receptor, in mixed glia prepared from wildtype and CD200$^{-/-}$ mice.

IFNγ decreased mannose receptor expression in mixed glia prepared from wildtype and CD200$^{-/-}$ mice (***p<0.001; 2-way ANOVA). Values are presented as means ± SEM expressed as a relative quantity (RQ).

2-way ANOVA: IFNγ $_{effect}$ F(1,9)=395.7; ***p<0.0001, Genotype $_{effect}$ F(1,9)=53.33; ***p<0.0001, Interaction $_{effect}$ F(1,9)=65.92; ***p<0.0001

4.4. Discussion

The data demonstrate that microglia from wildtype and CD200$^{-/-}$ mice respond to insults by differenatially altering their phenotypic state; like macrophages, IFNγ induces the characteristic pro-inflammatory profile indicative of classical activation, while IL-4 induces the alternative activation state. Cells obtained from CD200$^{-/-}$ mice displayed an enhanced response to IFNγ; it is proposed that increased expression of IFNGR1 and increased STAT1 phosphorylation could account for this increased sensitivity in cells from CD200$^{-/-}$ mice. Importantly, CD200Fc attenuated the IFNγ-induced increases in TNFα and IL-6 expression and release, suggesting CD200-related deactivation of microglia may specifically modulate the classically-activated pathway.

The Th1 cytokine IFNγ induces a distinct classical activation pathway in macrophages which serves to reinforce the initial response to a stimulus (Mosser 2003). One of the objectives of this study was to assess whether IFNγ induced similar changes in microglia. The data show that IFNγ increased NOS2, TNFα and IL-6 from mixed glia and purified microglia prepared from wildtype mice. This is consistent with previous data demonstrating classically activated murine macrophages are developed in response to IFNγ, these cells are easily identified by their production of NO and TNFα (Mosser 2003). Further, IFN-γ has been shown to induce various pro-inflammatory cytokines including, TNFα and IL-6, and NO in microglial cells (Benveniste and Benos 1995; Colton and Wilcock 2010). IFNγ produced a greater effect in microglia prepared from CD200$^{-/-}$ mice, compared with wildtype, mice. The data demonstrate the loss of CD200 leads to dysregulation of the IFNγ-induced classical activation pathway.

As microglia can respond to IFNγ, the expression of the IFNγ receptor was investigated on CD11b$^+$ cells prepared from wildtype and CD200$^{-/-}$ mice. Cell surface expression of IFNGR1, the ligand-binding subunit of the IFNγR, was increased on CD11b$^+$ cells prepared from CD200$^{-/-}$, compared with wildtype, mice. Ligation of the IFNγ receptor ultimately leads to activation of JAK1, JAK2 and STAT1 and consequently an increase in IFNγ-responsive genes (Benveniste and Benos 1995). Here, IFNγ increased phosphorylated STAT1 to a greater extent in mixed glia

prepared from CD200$^{-/-}$ mice. Moreover, the increased IFNGR1 expression observed in unstimulated mixed glia prepared from CD200$^{-/-}$ mice was associated with increased phosphorylated STAT1.

Several mechanisms negatively regulate IFNγ signaling; suppressor of cytokine signaling 1 (SOCS1) inhibits IFNγ receptor association with JAK1 and JAK2, and can be unregulated by IFNγ itself (Hu, Herrero et al. 2002; Baker, Akhtar et al. 2009). SOCS1-deficient mice develop multi-organ failure and death within 3 weeks of birth due to hypersensitivity to IFNγ. In addition, SOCS1-deficient macrophages are hyper-responsive to LPS and other toll-like receptor ligands, thus SOCS1 is believed to be a powerful regulator of IFN- and TLR-mediated responses in immune cells. Here SOCS1 expression was investigated in response to IFNγ in mixed glia prepared from wildtype and CD200$^{-/-}$ mice. SOCS1 mRNA expression and protein was found to be increased in response to IFNγ, consistent with previous experiments establishing IFNγ in regulating its own activity (Alexander, Starr et al. 1999). Interestingly, cells from CD200$^{-/-}$ mice expressed increased levels of SOCS1 mRNA and protein in both unstimulated and IFNγ-stimulated conditions compared with cells from wildtype mice. In a study by Hu and colleagues, the sensitivity of macrophages to IFNγ was shown to be regulated by interplay between STAT1 and SOCS; these proteins were expressed at different concentrations depending on the intensity or duration of an activating stimulus. It was concluded that high expression of STAT1 balanced the inhibition induced by SOCS proteins (Hu, Herrero et al. 2002). In this study, CD200-deficiency was associated with increased levels of SOCS1 but it is suggested that the concurrent increase in STAT1 activation may overcome the inhibitory effects of SOCS1 resulting in greater increases in IFNγ-responsive genes. Together these data present a novel mechanism by which the amplified response to IFNγ in cells from CD200$^{-/-}$ mice might be explained.

The evidence presented here, and to date in the literature, supports an immune-regulatory role for CD200 (Barclay, Wright et al. 2002; Minas and Liversidge 2006). Consistent with the proposed immunosuppressive role of CD200, CD200Fc, a chimeric protein that binds with CD200R, attenuated the IFNγ-induced increases in TNFα and IL-6 expression and release. This supports previous data in murine macrophages which indicated that CD200 may control inflammation *in vivo* via

inhibition of TNFα and IL-6 production following stimulation with IFNγ (Jenmalm, Cherwinski et al. 2006). In short, these results indicate that ligation of the CD200R modulates classical activation of microglia.

IL-4 induced a significant increase in mannose receptor expression in cells prepared from wildtype and CD200$^{-/-}$ mice. This is consistent with previous findings in macrophages in which mannose receptor was unregulated in response to IL-4 (Stein, Keshav et al. 1992). IL-4 also increased arginase 1 and chitinase 3-like 3 in cells prepared from wildtype and CD200$^{-/-}$ mice. These signature markers have been used in combination to define an alternative activation state (Loke, Nair et al. 2002; Gordon and Martinez 2010), but CD200 did not affect the response of microglia to IL-4. However unstimulated cells prepared from CD200$^{-/-}$ mice displayed higher expression of mannose receptor and arginase 1 compared with cells from wildtype mice.

The data demonstrate that both microglia and astrocytes express IL-4Rα, although microglial expression is greater. The presence of IL-4R on glial cells is controversial, a study by Sawada and colleagues demonstrated IL-4R expression on microglia but not astrocytes (Sawada, Itoh et al. 1993); although data from another study demonstrated IL-4R expression on astrocytes both at mRNA and protein level (Brodie, Goldreich et al. 1998). Microglia prepared from CD200$^{-/-}$ mice expressed increased IL-4Rα compared with wildtype mice, which may explain the increased expression of mannose receptor and arginase 1 in glia prepared from CD200$^{-/-}$ mice. Interestingly, CD200-deficiency resulted in decreased IL-4Rα expression on purified astrocytes. It is unclear whether this results in an altered functional output.

In addition to its ability to induce classical activation of microglia, IFNγ decreased mannose receptor expression which is consistent with data obtained previously in macrophages (Mokoena and Gordon 1985; Ma, Chen et al. 2003; Colton and Wilcock 2010; Gordon and Martinez 2010). In addition, IL-4 inhibited the expression of TNFα and NOS2 which supports previous findings demonstrating the antagonistic effects of IL-4 on macrophages effector cells (McBride, Economou et al. 1990). Interestingly, IL-4 inhibits TNFα release but not IL-6 release from mixed glia prepared from wildtype and CD200$^{-/-}$ mice; this is distinct from the effects of IL-10 and TGFβ,

which induce acquired deactivation and which decrease both TNFα and IL-6 release in macrophage (Colton 2009). This further establishes alternative activation as a distinct activation state. In summary alternative activation opposes the effects of the classically induced TNFα and NOS2 in mixed glia and is involved in increasing expression of mannose receptor and arginase 1, which leads to repair of the extracellular matrix (Nguyen and Benveniste 2000; Colton, Mott et al. 2006).

The current study highlights the complexity of the inflammatory response in the brain. Like macrophages, microglia are capable of adopting multiple activation states, each with a distinct gene expression profile. Functional dysregulation of TLR-induced activation and, classical and alternative pathways have been implicated in a variety of neurodegenerative and inflammatory disorders (Colton, Mott et al. 2006; Mukhopadhyay, Pluddemann et al. 2010). The significant finding of this study is that CD200-deficiency resulted in an enhanced response to IFNγ but not IL-4. CD200Fc suppressed IFNγ-induced cytokine expression and release. These findings suggest specificity for CD200R activation that may be exploited in specific neuroinflammatory or neurodegenerative conditions.

Chapter 5

Blood brain barrier permeability and infiltration of peripheral cells may contribute to microglial activation in CD200-deficient mice

5.1 Introduction

Neuroinflammation is a characteristic of many, if not all, neurodegenerative diseases, including AD, PD and MS (Liu and Hong 2003; Damani, Zhao et al. 2011). While much of the neuroinflammatory changes observed in neurodegenerative diseases have been attributed to inappropriate glia function, the role neuroinflammation has in the pathogenesis of these disorders still remains unclear. However, It has been demonstrated that advanced aging is the primary risk factor for a large number of neurodegenerative diseases and it is hypothesised that age-related changes in microglia may drive the pathogenic progression of such disorders as AD.

The observed age-related changes in microglia include upregulation of pro-inflammatory cytokine production (Godbout and Johnson 2004; Griffin, Nally et al. 2006), and increased markers of activation including MHC II, CD86 and CD40 (Godbout, Chen et al. 2005; Griffin, Nally et al. 2006). However the trigger(s) which lead to age-related increases in microglial activation remain unknown. Interestingly IFNγ, one of the most potent activators of microglia, has been found to be increased in the hippocampus of aged animals and is one possible molecule which may initiate microglial activation (Griffin, Nally et al. 2006). In the healthy brain, microglial interactions are important for maintaining homeostasis. Evidence from our laboratory has highlighted the role of the chemokine, fractalkine, on neurons, and its receptor on microglia in maintaining microglia in a quiescent state (Lyons, Lynch et al. 2009). In addition evidence has demonstrated the modulatory effect of the interaction between CD200, expressed on neurons, astrocytes and endothelial cells, with its receptor CD200R, expressed on microglia and macrophage. Interestingly, CD200 has been shown to be decreased in the hippocampus with age (Griffin, Nally et al. 2006).

The previous chapters established that glia prepared from CD200$^{-/-}$ mice have an enhanced response to TLR4 agonist, LPS, characterized by an increase in the proinflammatory cytokines IL-1β, IL-6 and TNFα (Costello, Lyons et al. 2011); and Th1 cell derived cytokine, IFNγ, indentified by an increase in TNFα and NOS2. From the data obtained it was proposed that increased expression of IFNGR1 and increased STAT1 phosphorylation, and increased expression of TLR4 and components of NFκB signaling, could account for the increased sensitivity of CD200$^{-/-}$ mice to IFNγ and

LPS, respectively. These findings are supportive of experiments carried out in CD200$^-$ $^{/-}$ mice which have shown an accelerated microglial response in the facial nerve transection model, compared with wildtype mice (Hoek, Ruuls et al. 2000; Wang, Ye et al. 2007); the symptoms in MOG-induced EAE appeared earlier in CD200$^{-/-}$, compared with wildtype mice (Hoek, Ruuls et al. 2000). Similarly, CD200$^{-/-}$ animals showed an increased susceptibility to collagen-induced arthritis (CIA) (Hoek, Ruuls et al. 2000; Nimmerjahn, Kirchhoff et al. 2005). However, despite the extensive evidence, both *in vitro* and *in vivo*, linking interaction between CD200 and CD200R with preservation of microglia in a quiescent state, it remains unclear what basal level alterations, if any, contribute to their profound responses to activating stimuli *in vivo*.

A recent study has found both a deficiency in CD200 and CD200R in human AD brains suggesting reduced efficacy of the CD200-CD200R system to control inflammation (Walker, Dalsing-Hernandez et al. 2009). For this reason understanding and modulating glial function still remains an attractive strategy for the treatment of neurodegenerative diseases. Here the focus was on how CD200-deficiency *in vivo* may alter control of inflammation at basal levels resulting in dysfunctional regulation of immune homeostasis in the brain.

Specifically, the objectives of this study were:
- To assess how CD200-deficiency *in vivo* may alter microglial activation
- And, to investigate whether IFNγ, a potent endogenous activator of microglia, may provide the stimulus for the observed microglial activation in CD200-deficient mice

5.2 Methods

Male and female, young (3 months), middle aged (12 months) and aged (17-24 months) wildtype and CD200$^{-/-}$ mice were anaesthetised with urethane (1.5g/kg; Sigma Aldrich; IRE), deep anaesthesia was confirmed by the absence of a pedal reflex. The animals were perfused intracardially with ice-cold PBS (20ml), the brain was rapidly removed and placed on ice, the cerebellum and olfactory bulbs were removed and the remaining brain was bisected along the midline. A quarter of the hippocampus was snap-frozen in liquid nitrogen for later analysis by PCR, further hippocampal samples were snap-frozen for analysis of IFNγ concentration and chemokine release, and mononuclear cells were isolated from the remaining tissue for analysis by flow cytometry for the investigation of infiltrating cells. Leukocyte common antigen (CD45) marker in combination with lineage specific markers, CD4 and CD8, were used to discriminate between T cell populations; macrophages were identified as CD11b^{+}CD45^{high} cells while microglia express low levels of CD45 (Tan, Town et al. 2000). Therefore the expression level of CD45 allowed phenotypes of CD45^{low} CD11b^{+} (microglia) and CD45^{high} CD11b^{+} (macrophage) to be identified (Streit, Walter et al. 1999; Guillemin and Brew 2004). Chemokine concentrations were determined by ELISA; protein concentration was calculated from the standard curve and expressed in pg/mg of protein. Expression of markers of microglial activation CD11b and MHC II were assessed by PCR (see section 2.2-2.4); values are expressed as a relative quantity (RQ) calculated with respect to endogenous control β-actin. In experiments with age as a parameter, 18S was used as an endogenous control as actin levels have been shown to alter with age. Western immunoblotting was used to examine IFNγ and IFNGR1 expression; protein expression established using western immunoblotting was calculated using densitometric analysis to calculate mean data. (see section 2.5).

In another experiment wildtype animals (n=6 per treatment group) received an i.c.v. injection of sterile saline or IFNγ (50ng/ml per mouse diluted in sterile saline); mononuclear cells were isolated from the cortex for analysis by flow cytometry and markers of microglial activation CD68 and CD86 were assessed on CD11b^{+} and CD11b^{negative} cells.

Statistical analysis was performed using the computer based statistical package GraphPad prism (GraphPad, US). Data were assessed using a two-tailed, or where specified one-tailed, Student's t test for independent means, 1-way ANOVA followed by post hoc comparisons using Newman-Keuls test, or 2-way ANOVA followed by post hoc comparisons using Bonferroni post test. All data were expressed as mean ± standard error of mean (SEM).

5.3 Results

The study of CD200$^{-/-}$ mice has provided significant insight into the role and function of CD200 *in vivo*, one of the first noteworthy observations regarding these animals was the discovery that the absence of CD200 resulted in an increase in the CD11b^{+} cell population in the spleen, but not CD4^{+} or CD8^{+} cells (Hoek, Ruuls et al. 2000). Furthermore, CD200$^{-/-}$ mice have shown increased susceptibility to autoimmune diseases with evidence of an unregulated inflammatory response (Hoek, Ruuls et al. 2000). Here we investigated the changes at basal level that may account for the susceptibility of CD200$^{-/-}$ mice to autoimmune diseases such as EAE, a disease driven by antigen-specific lymphocytes.

Microglial activation in CD200-deficient mice

In the normal CNS, microglial cells exist in a quiescent state expressing the macrophage cell marker CD11b, a low level of CD45, and low or negligible levels of MHC class II and co-stimulatory molecules CD40 and CD86 (Sedgwick, Schwender et al. 1991). In response to an activating stimulus, microglia up regulate the expression of CD45, MHC class II, CD40 and CD86 (Ponomarev, Shriver et al. 2005). Here under resting conditions, CD11b (A) and MHC II (B) mRNA expression was significantly increased in the hippocampus of CD200$^{-/-}$ mice compared with wildtype mice (*p<0.05; **p<0.01; Student's *t* test for independent means; Figure 5.1). In addition, there was an apparent increase in CD40 on CD11b^{+} cells prepared from CD200$^{-/-}$, compared with wildtype, mice (p=0.0687; One-tailed Student's *t* test for independent means; Figure 5.2). These results indicate a state of tonic activation in cells prepared from CD200$^{-/-}$ mice. Hence, as microglia, the resident macrophages of the CNS are CD200R^{+}, the lack of CD200, present on neurons and astrocytes, to regulate their function appears to be associated with a more activated phenotype.

IFNγ and IFNGR1 were increased in the hippocampus of CD200$^{-/-}$ mice

In the previous chapter the expression of the IFNγ receptor was investigated as a possible reason for the enhanced response of microglia prepared from CD200$^{-/-}$ to IFNγ. The ligand binding subunit of the receptor, IFNGR1, was found to be increased on CD11b$^+$ microglial cells prepared from CD200$^{-/-}$ mice. Here we investigated the expression of IFNγ (Figure 5.3) and IFNGR1 (Figure 5.4) in the hippocampus of wildtype and CD200$^{-/-}$ mice. A sample immunoblot indicates that IFNγ and IFNGR1 were increased in the hippocampus of CD200$^{-/-}$, compared with wildtype, mice, and mean data from densitometric analysis revealed a significant genotype-related difference (*p<0.05; Student's t test for independent means; Figure 5.3-5.4).

In order to investigate the effect of IFNγ on microglia and astrocytes *in vivo*, cells were prepared from the cortices of wildtype mice which received an i.c.v. injection of a pathophysiological concentration of IFNγ (50ng/ml) and from a cohort of saline-treated controls. Mean florescent intensity of CD11b (A) was increased in cells prepared from IFNγ-treated animals compared with saline-treated animals (*p<0.05; Student's t test for independent means; Figure 5.5). The co-stimulatory molecule CD86 (B) and the phagocytic marker of activation CD68 (C) were increased on CD11b$^+$ cells prepared from IFNγ-treated animals compared with saline-treated animals (*p<0.05;***p<0.001; Students t test for independent means; Figure 5.5). The expression of CD40 (A) was unchanged on CD11b$^-$ cells prepared from IFNγ-treated animals compared with saline-treated animals, however both CD86 (B) and CD68 (C) were increased on this CD11b$^-$ population of cells (**p<0.01; ***p<0.001; Students t test for independent means; Figure 5.6). This data demonstrate the profound activating effects of a physiologically-relevant dose of IFNγ on CNS resident cells.

Increased T cell and macrophage infiltration in CD200$^{-/-}$ mice

As Th1 CD4$^+$ T cells, CD8$^+$ T cells and NK cells are known to be the main producers of IFNγ (Benveniste and Benos 1995), infiltrating CD4$^+$ T cells and CD8$^+$ T cells were considered as a source IFNγ in the brain. CD45, in combination with CD4 and

CD8 was used to discriminate T cell populations in cells prepared from perfused brains of young (3 months), middle-aged (12 months) and aged (17-24 months) wildtype and CD200$^{-/-}$ mice. Representative FACS plots from each experimental group depict the CD45$^+$CD4$^+$ and CD45$^+$CD8$^+$ T cell populations (Figure 5.7). The percentage of CD45$^+$CD4$^+$ T cells was increased in CD200$^{-/-}$ compared with wildtype mice (**$p < 0.01$; 2-way ANOVA; Figure 5.7). Figure 5.8 demonstrates that Th1 CD4$^+$ T cells produce IFNγ compared with Th2 and Th17 CD4$^+$ T cells (***$p < 0.001$; 1-way ANOVA). It was also observed that Th1 cells induced increased MHC class II expression on mixed glia (A) and microglia (B) when co-incubated in a ratio of 1:2 for 24 hours (*$p < 0.05$; ***$p < 0.001$; Student's t test for independent means; Figure 5.9). The percentage of CD45$^+$CD8$^+$ T cell was increased with age in wildtype and CD200$^{-/-}$ mice (***$p < 0.001$; 2-way ANOVA); CD200$^{-/-}$ mice had increased CD45$^+$CD8$^+$ T cells were also increased in CD200$^{-/-}$, compared with wildtype, mice ($^{++}p < 0.01$; 2-way ANOVA; Figure 5.10).

The infiltration of macrophages defined as CD11b$^+$CD45^{high} cells was also investigated. The data show that macrophage infiltration was increased with age in wildtype and CD200$^{-/-}$ mice (***$p < 0.0001$; 2-way ANOVA; Figure 5.11); CD200$^{-/-}$ mice had increased macrophage infiltration compared with wildtype mice ($^{+++}p < 0.001$; 2-way ANOVA) and further analysis of the data revealed a significant interaction between age and genotype (*$p < 0.05$; 2-way ANOVA). Interestingly, the infiltrating macrophages observed in CD200$^{-/-}$ mice expressed increased MHC class II expression; representative FACS plots are shown (*$p < 0.05$; student's t test of independent means; Figure 5.12).

The increased T cell and macrophage infiltration in CD200$^{-/-}$ mice was associated with increased IFNγ expression across all ages in CD200$^{-/-}$ mice compared with wildtype mice (*$p < 0.05$; 2-way ANOVA). Additionally, mean florescent intensity of CD11b was increased with age in wildtype and CD200$^{-/-}$ mice (**$p < 0.01$; 2-way ANOVA) and cells from CD200$^{-/-}$ mice exhibited increased CD11b compared with wildtype mice (*$p < 0.05$; 2-way ANOVA; Figure 5.14).

Increased mononuclear cell infiltration was associated with decreased Claudin 5 and increased chemokine expression

The BBB is a network of continuous capillaries surrounded by basal lamina and astrocytic end feet that limits the entry of cells and macromolecules into the brain through several unique structural and functional attributes, the most distinct of which is the presence of tight junctions (Wen, Watry et al. 2004). Here the tight junction proteins of the BBB were investigated in CD200$^{-/-}$ mice as it is known that under inflammatory conditions or injury the integrity of the tight junctions can be altered facilitating leukocyte entry to the CNS (Capaldo and Nusrat 2009). Claudin 5 expression (A), but not expression of Claudin 12 (B) or occludin (C), was decreased in the hippocampus of CD200$^{-/-}$ mice compared with wildtype mice (*p<0.05; Students *t* test for independent means; Figure 5.15).

Activation of microglia during CNS disease leads to production of pro-inflammatory cytokines, such as IL-1β, IL-6 and TNFα, as well as particular chemokines (Murphy, Lalor et al. 2010). CXCR3 is the receptor for IP-10 and is predominantly expressed on Th1 cells while CCR2 is the receptor for MCP-1 is expressed not only on T cells, but also macrophages, microglia and dendritic cells. Here the expression and release of MCP-1 and IP-10 was investigated in the hippocampus of CD200$^{-/-}$ mice compared with wildtype mice. MCP-1 mRNA expression (A) and MCP-1 concentration (B) was increased in the hippocampus of CD200$^{-/-}$, compared with wildtype, mice (*p<0.05; Student's *t* test for independent means; Figure 5.16). IP-10 mRNA expression (C), but not its concentration (D), was also increased in the hippocampus of CD200$^{-/-}$, compared with wildtype, mice (*p<0.05; Student's t test for independent means; Figure 5.16).
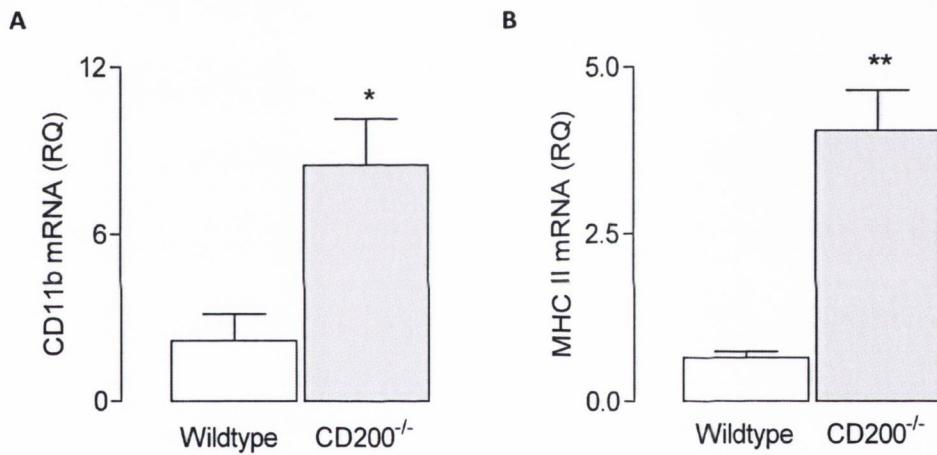
Figure 5.1. CD11b and MHC class II mRNA expression was increased in the hippocampus of CD200$^{-/-}$ mice

Expression of CD11b (A) and MHC II (B) was significantly increased in the hippocampus of CD200$^{-/-}$ mice compared with wildtype mice (*p<0.05; **p<0.01; Student's t test for independent means). Values are presented as means ± SEM expressed as a relative quantity (RQ) calculated with respect to endogenous control, β-actin.

  A. *p=0.0353; 2.181 ± 0.9576; n=3 vs. 8.478 ± 1.665; n=5
  B. **p=0.0016; 0.6570 ± 0.08938; n=4 vs. 4.064 ± 0.6004; n=5

A
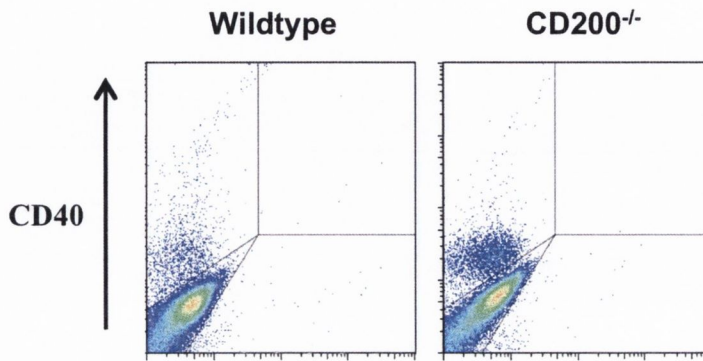
B
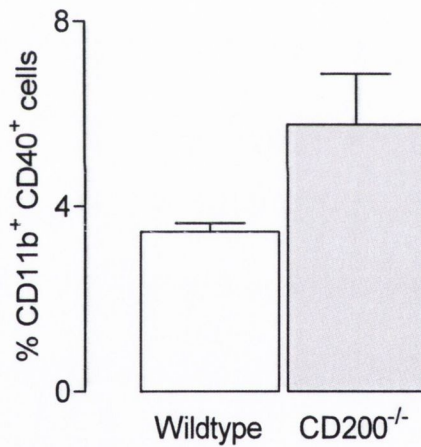
Figure 5.2 CD40 was increased on CD11b+ cells prepared from the brains of CD200-/- mice

CD11b+ cells were isolated from the brains of wildtype and CD200-/- mice. Representative FACS plots for CD11b+ cells expressing CD40 from wildtype and CD200-/- mice are shown (A). There was an apparent increase in CD40 expression on CD11b+ cells prepared from CD200-/-, compared with wildtype, mice, however this failed to reach statistical significance (p=0.0687; One-tailed Student's t test for independent means; 3.446 ± 0.1890, n=3 v. 5.765 ± 1.101, n=4). Values are presented as means ± SEM.
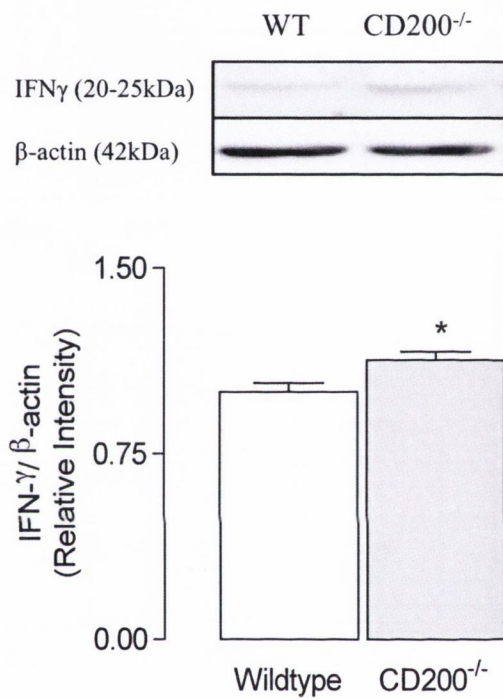
Figure 5.3. IFNγ was increased in the hippocampus of CD200$^{-/-}$ mice

A sample immunoblot indicates that IFNγ was increased in the hippocampus of CD200$^{-/-}$, compared with wildtype, mice, and mean data from densitometric analysis revealed a significant genotype-related difference (*$p < 0.05$; 1.000 ± 0.03527; n=4 vs. 1.129 ± 0.03312; n=5; Students t test for independent means).
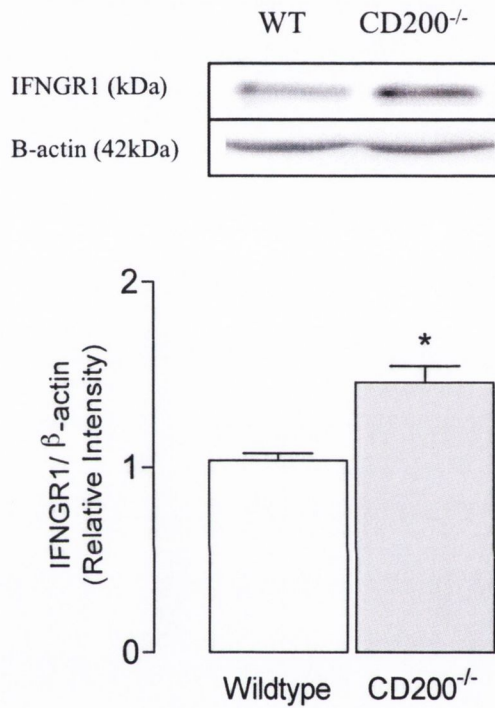
Figure 5.4. IFNγ receptor 1 was increased in the hippocampus of CD200$^{-/-}$ mice

A sample immunoblot indicates that IFNγ receptor 1 (IFNGR1) was increased in the hippocampus of CD200$^{-/-}$, compared with wildtype, mice, and mean data from densitometric analysis revealed a significant genotype-related difference (*p<0.05; 1.038 42 ± 0.03798; n=3 vs. 1.459 ± 0.08936; n=3; Student's *t* test for independent means).
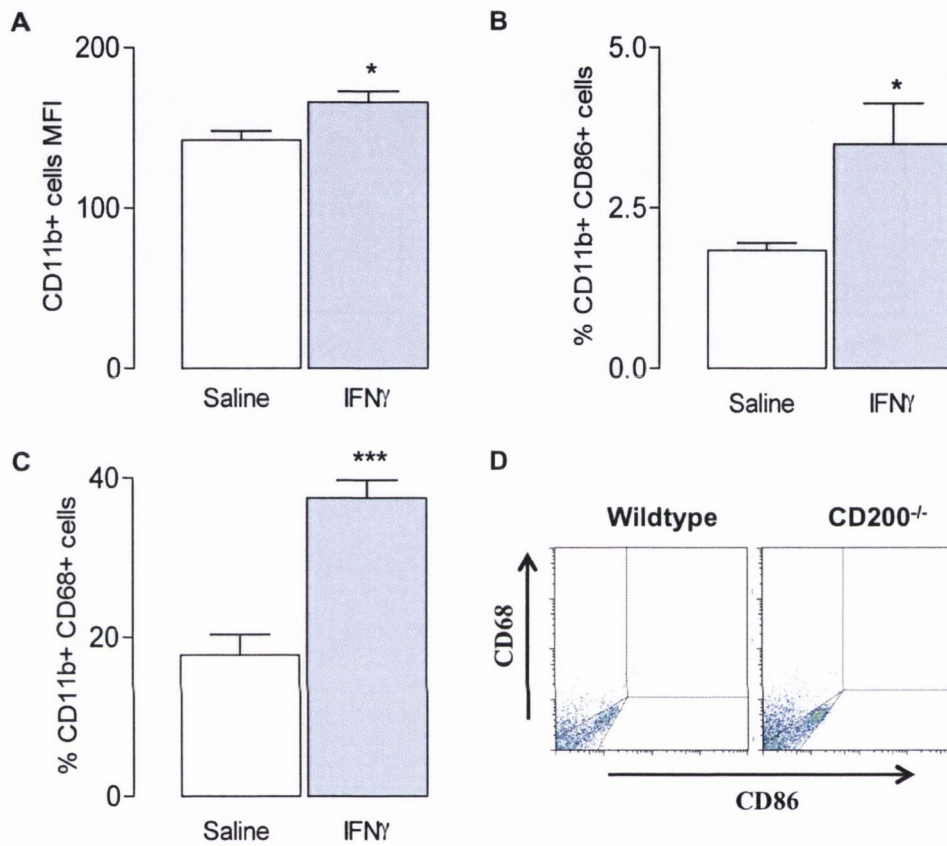
Figure 5.5. IFNγ (i.c.v) increased CD11b, CD86 and CD68 on cells prepared from the cortex of wildtype mice

Cells were prepared from the cortices of wildtype mice injected with saline or IFNγ (50ng/ml). (A) Mean florescence intensity of CD11b was increased in cells prepared from IFNγ treated animals compared with saline controls (*p=0.0261; 142.3 ± 5.806; n=6 vs. 165.8 ± 6.892; n=6; student's t test for independent means). The expression of CD86 (B) and CD68 (C) were increased on CD11b$^+$ cells prepared from IFNγ treated animals compared with saline controls (B; *p=0.0277; 1.835 ± 0.1178; n=6 vs. 3.492 ± 0.6331; n=6 ; C; ***p=0.0002; 17.78 ± 2.594; n=6 vs. 37.52 ± 2.215; n=6; student's *t* test for independent means). Representative FACS plots are shown (D). Values are presented as mean ± SEM.
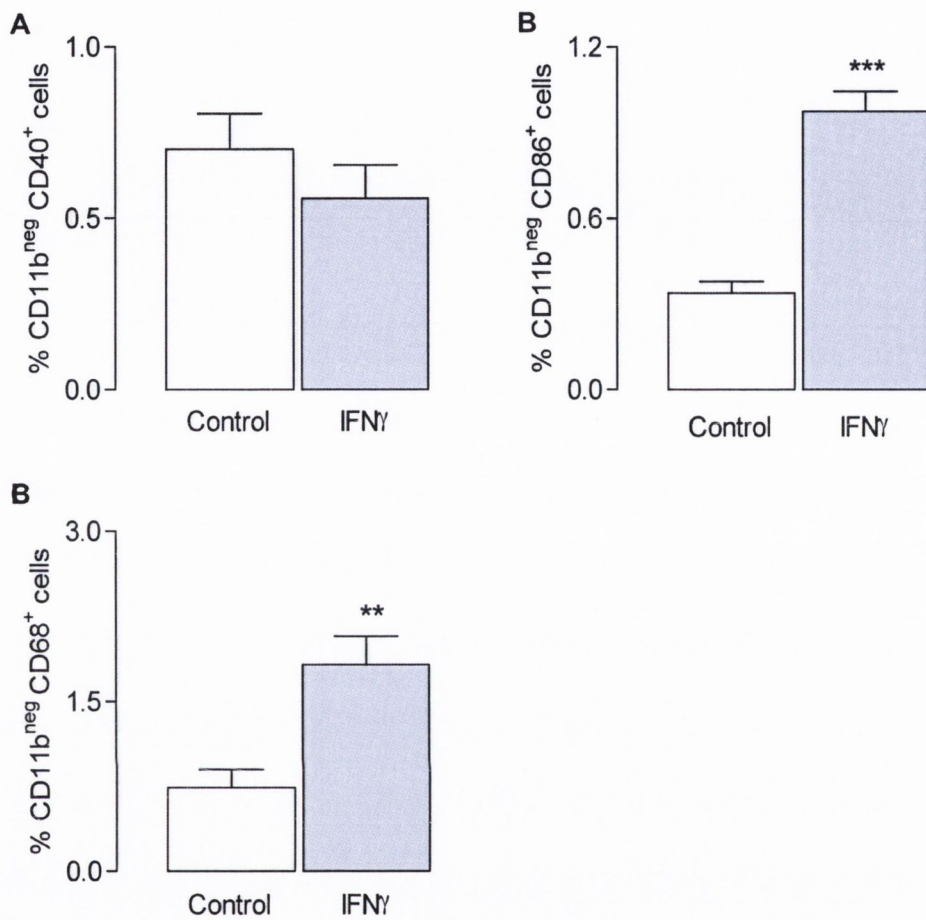
Figure 5.6. IFNγ (i.c.v) increased CD86 and CD68 on CD11b negative cells prepared from the cortex of wildtype mice

Cells were prepared from the cortices of wildtype mice injected with saline or IFNγ (50ng/ml). CD40 expression (A) was similar on CD11b^{negative} prepared from saline and IFNγ treated animals. The expression of CD86 (B) and CD68 (C) was increased on CD11b$^-$ cells prepared from IFNγ treated animals compared with saline controls (B; **p=0.0045; 0.7403 ± 0.1600; n=6 vs. 1.825 ± 0.2511; n=6; C; ***p<0.0001; 0.3383 ± 0.0408; n=6 vs. 0.9742 ± 0.06948; n=6; student's t test for independent means).

A

Young   Middle Aged   Aged

CD8

CD4

Wildtype

CD200⁻/⁻

B
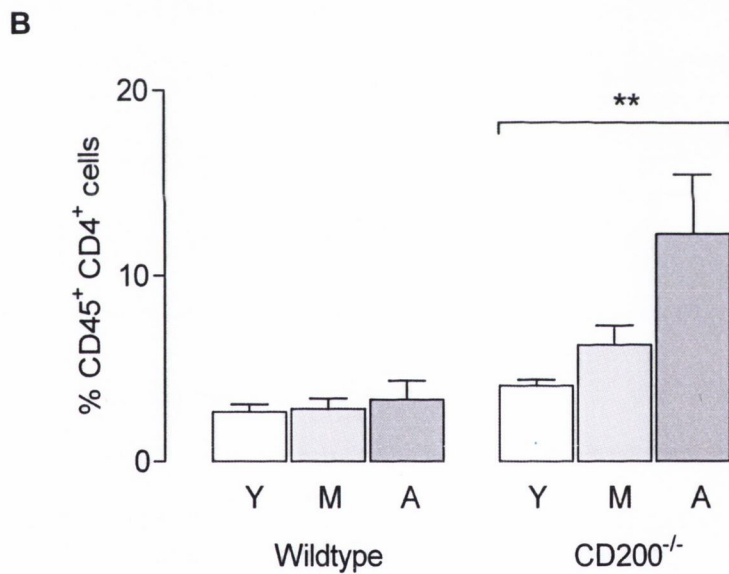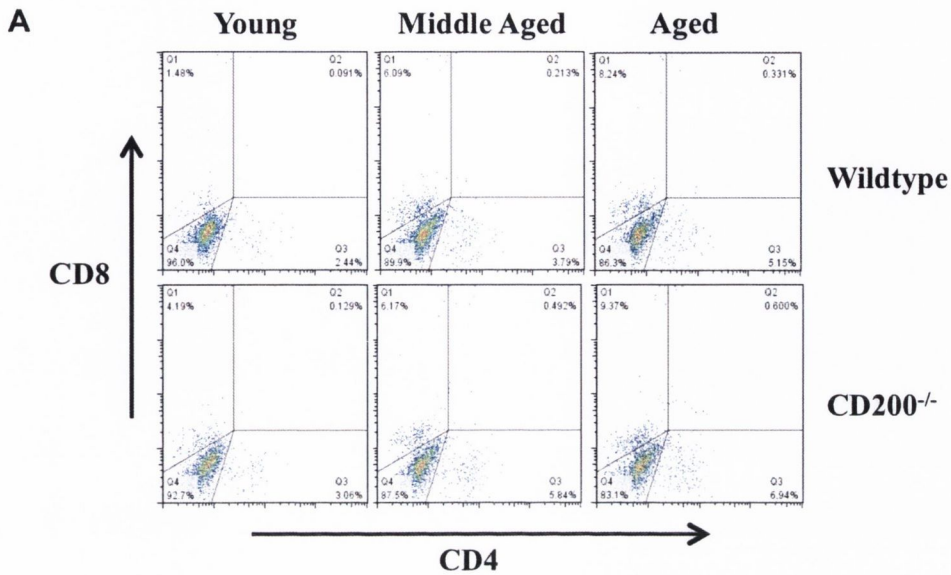
Figure 5.7. Infiltration of CD4+ T cells was increased in the brains of CD200$^{-/-}$ mice

Cells were isolated from the brains of 3 (Y), 12 (M) and 17-24 (A) month old perfused wildtype and CD200$^{-/-}$ mice. Cells were gated on CD45^{+} cells and the percentage of CD8^{+} and CD4^{+} T cells were investigated, representative FACS plots from each experimental group are shown (A). The percentage of CD45^{+} CD4^{+} T cells was increased in cells prepared from CD200$^{-/-}$, compared with wildtype, mice (**p<0.01; 2-way ANOVA). Values are presented as means ± SEM.

2-way ANOVA: Age $_{effect}$ $F(2,22)=3.182$; p=0.0611, Genotype $_{effect}$ $F(1,22)=8.881$; **p=0.0069, Interaction $_{effect}$ $F(2,22)=2.275$; p=0.1265
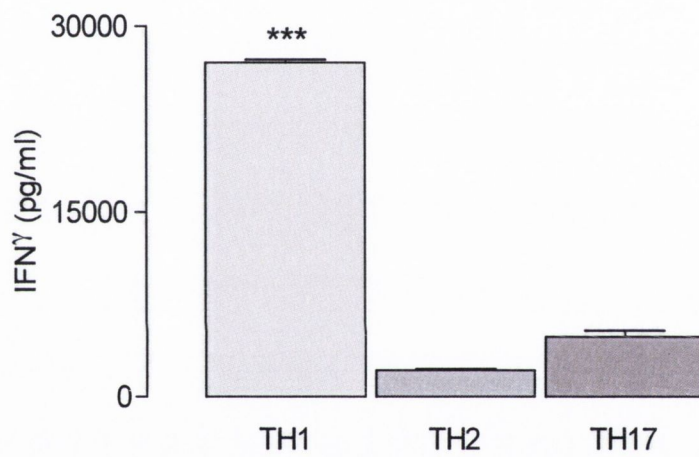
Figure 5.8. IFNγ is produced by Th1 CD4+ T cells

CD4$^+$ T cells were isolated from the spleens of wildtype mice and polarized into specific T cell subsets . Th1's, as opposed to Th2's or Th17's, produce IFNγ (***p<0.001; 1-way ANOVA).
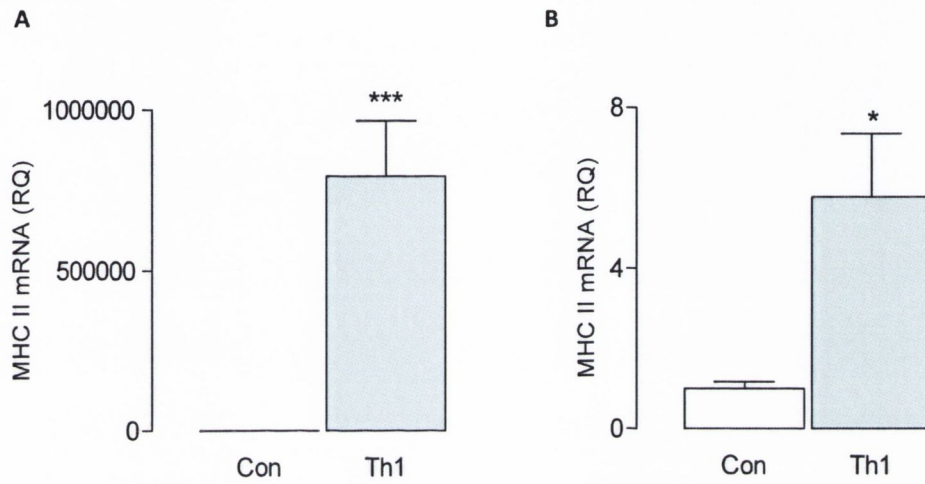
Figure 5.9. Co-incubation of Th1 cells with mixed glia and purified microglia increased MHC class II expression

CD4$^+$ T cells were isolated from the spleens of wildtype mice and polarized into specific T cell subsets. Th1 cells (2:1 ratio of glia to Th1 cells) increased MHCII expression in mixed glia (A) and purified microglia (B) prepared from wildtype mice co-incubated for 24 hours (*p<0.05; ***p<0.001; Student's *t* test for independent means). Values are presented as means ± SEM.

A. ***p=0.001; 1.000 ± 0.6474; n=6 vs. 793600 ± 172900; n=6
B. *p=0.0104; 1.000 ± 0.1669; n=7 vs. 5.784 ± 1.567; n=7
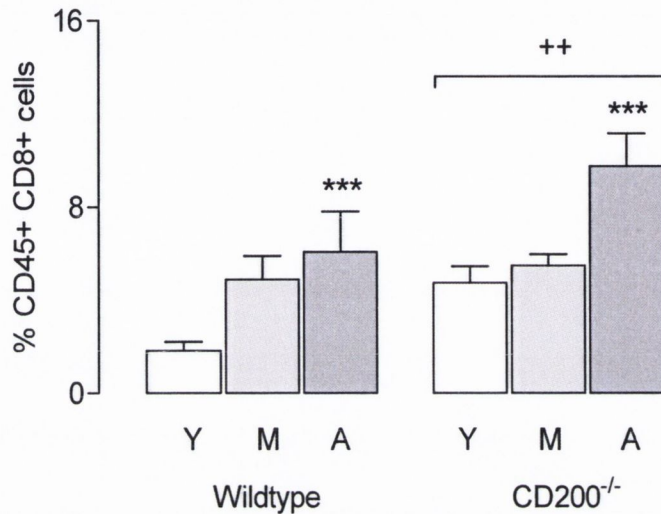
Figure 5.10. Infiltration of CD8$^+$ T cells was increased in the brains of CD200$^{-/-}$ mice

Cells were isolated from the brains of 3 (Y), 12 (M) and 17-24 (A) month old perfused wildtype and CD200$^{-/-}$ mice. Cells were gated on CD45$^+$ cells and the percentage of CD8$^+$ and CD4$^+$ T cells were investigated, see figure 5.3 for representative FACS plots from each experimental group (A). The percentage of CD45$^+$ CD8$^+$ T cells was increased with age in cells prepared from wildtype and CD200$^{-/-}$ mice (***$p<0.001$; 2-way ANOVA), CD200$^{-/-}$ mice had increased CD45$^+$ CD8$^+$ cells compared with wildtype mice (**$p<0.01$; 2-way ANOVA). Values are presented as means ± SEM.

2-way ANOVA: Age $_{effect}$ $F_{(2,21)}=12.13$; ***$p=0.0003$, Genotype $_{effect}$ $F_{(1,21)}=8.767$; **$p=0.0075$, Interaction $_{effect}$ $F_{(2,21)}=1.153$; $p=0.3348$

A

B
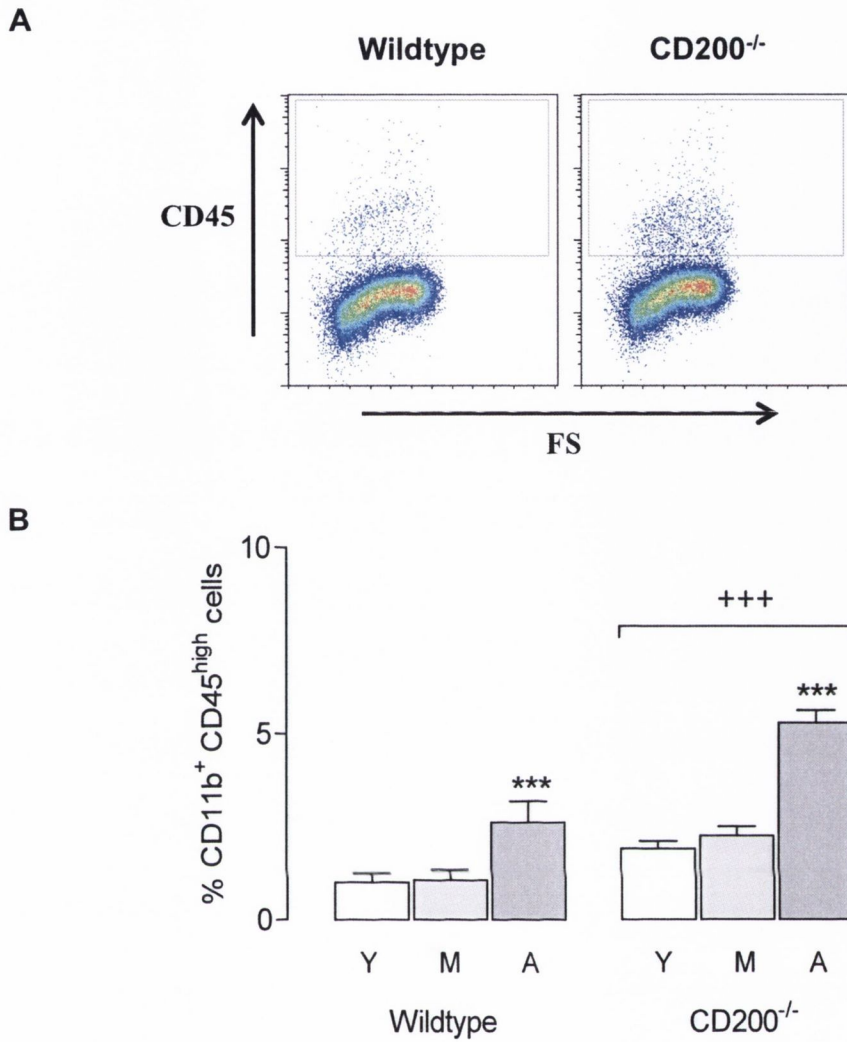
Figure 5.11. Infiltration of CD11b$^+$ CD45^{high} cells were increased in in the brains of CD200$^{-/-}$ mice

Cells were isolated from the brains of 3 (Y), 12 (M) and 17-24 (A) month old perfused wildtype and CD200$^{-/-}$ mice. Cells were gated on CD11b$^+$ cells and the percentage of CD45^{high} cells were investigated, representative FACS plots from young wildtype and CD200$^{-/-}$ mice are shown (A). The percentage of CD11b$^+$ CD45^{high} cells increased with age in cells prepared from wildtype and CD200$^{-/-}$ mice (***$p<0.0001$; 2-way ANOVA); CD200$^{-/-}$ mice had increased CD11b$^+$ CD45^{high} cells compared with wildtype mice ($^{+++}$$p<0.0001$; 2-way ANOVA); further analysis of the data revealed a significant interaction between age and genotype (*$p<0.05$; 2-way ANOVA). Values are presented as means ± SEM.

2-way ANOVA: Age $_{effect}$ F(2,39)=35.13; ***$p<0.0001$, Genotype $_{effect}$ F(1,39)=52.38; ***$p<0.0001$, Interaction $_{effect}$ F(2,39)=4.257; *$p=0.0415$

A

Wildtype   CD200^{-/-}

MHC II

CD40

B
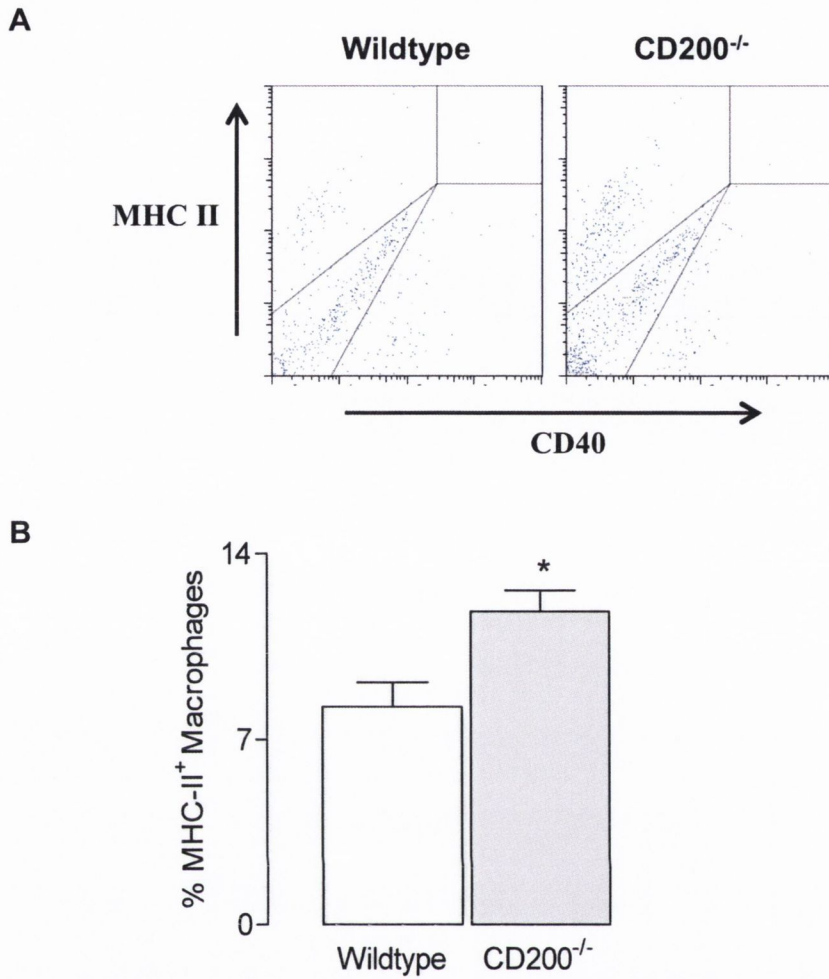
Figure 5.12. MHC II expression was increased on infiltrating CD11b$^+$ CD45^{high} cells prepared from CD200$^{-/-}$ mice

Cells were isolated from the brains of 3 month old perfused wildtype and CD200$^{-/-}$ mice. Cells were gated on CD11b$^+$ CD45^{high} and the expression of MHC II and CD40 was investigated, representative FACS plots are shown (A). The percentage of MHC II$^+$ CD11b$^+$ CD45^{high} cells was increased in cells prepared CD200$^{-/-}$ mice (*p<0.05; Students t test for independent means). Values are presented as means ± SEM.
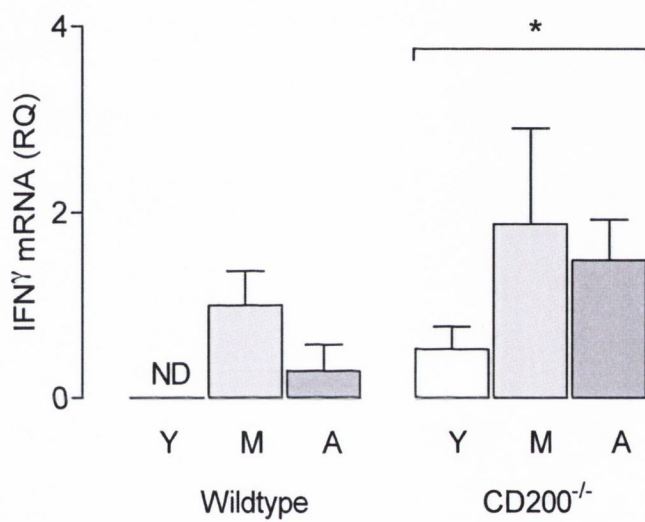
135

Figure 5.13. IFNγ mRNA expression was increased in cells prepared from CD200^{-/-} mice

Cells were isolated from the brains of 3 (Y), 12 (M) and 17-24 (A) month old perfused wildtype and CD200^{-/-} mice. The expression of IFNγ was increased in cells prepared from CD200^{-/-}, compared with wildtype, mice (*p<0.05; 2-way ANOVA). Values are presented as means ± SEM.

2-way ANOVA: Age $_{effect}$ $F(2,22)=4.296$; *p=0.0266, Genotype $_{effect}$ $F(1,22)=6.550$; *p=0.0179, Interaction $_{effect}$ $F(2,22)=0.3828$; p=0.6864
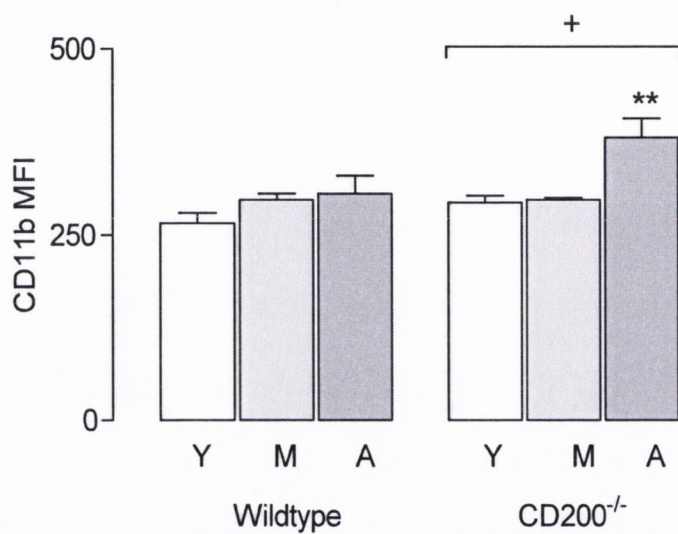
Figure 5.14. Mean florescent intensity of CD11b was increased in cells prepared from CD200$^{-/-}$ mice

Cells were isolated from the brains of 3 (Y), 12 (M) and 17-24 (A) month old perfused wildtype and CD200$^{-/-}$ mice. Mean florescent intensity of CD11b was found to be increased with age in cells prepared from CD200$^{-/-}$, compared with wildtype, mice (**p<0.01; 2-way ANOVA); CD200$^{-/-}$ mice had increased CD11b compared with wildtype mice ($^+$p<0.05; 2-way ANOVA). Values are presented as means ± SEM.

2-way ANOVA: Age $_{effect}$ F(2,18)=9.124; **p=0.0018, Genotype $_{effect}$ F(1,18)=7.174; *p=0.0153, Interaction $_{effect}$ F(2,18)=2.526; p=0.1079
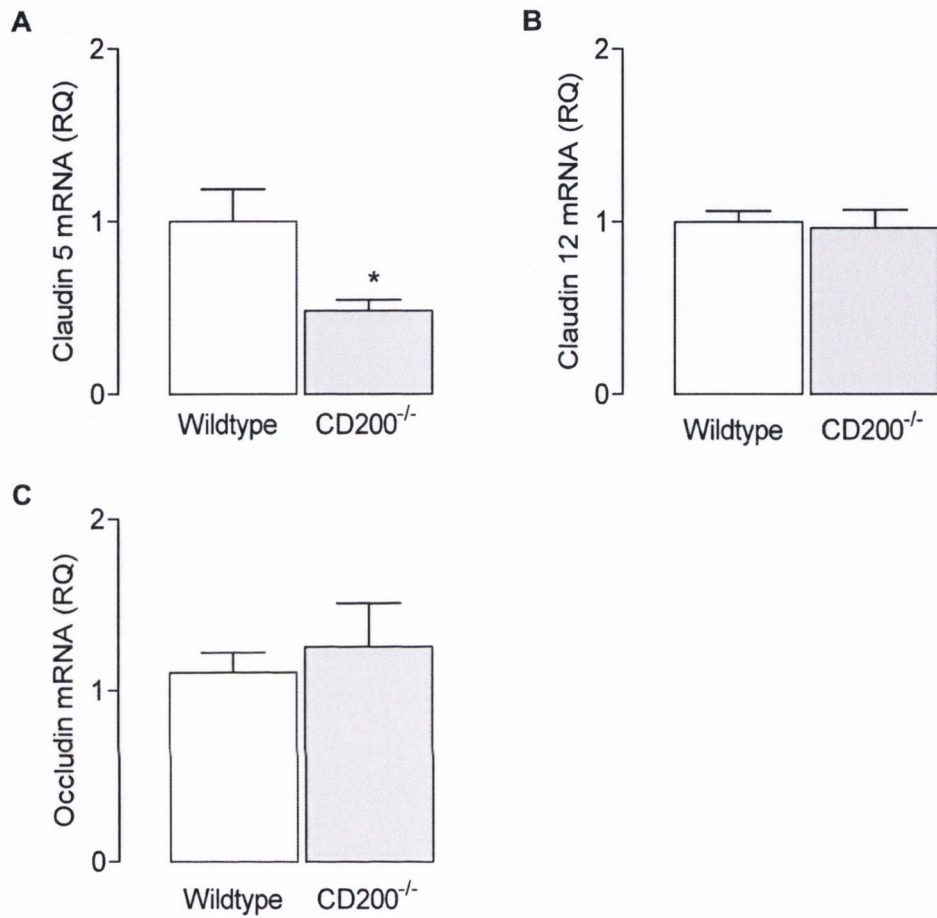
Figure 5.15. Claudin 5 expression was decreased in the hippocampus of CD200$^{-/-}$ mice

Expression of Claudin 5 (A), but not Claudin 12 (B) or Occludin (C), was decreased in the hippocampus of CD200$^{-/-}$ mice compared with wildtype mice (*$p<0.05$; Student's *t* test for unpaired samples). Values are presented as means ± SEM expressed as a relative quantity (RQ) calculated with respect to endogenous control, β-actin.

    A.   *$p=0.0261$; 1.000 ± 0.1872; n=6 vs. 0.4844 ± 0.06302; n=6
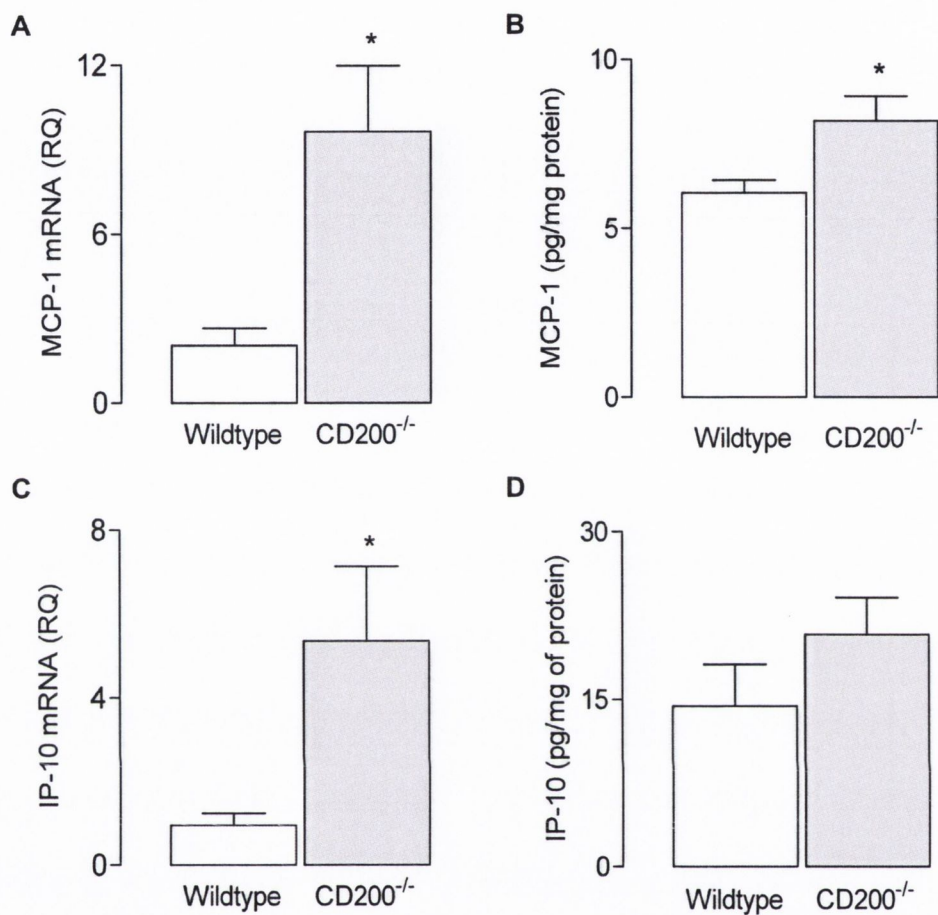
Figure 5.16. MCP1 and IP-10 were increased in the hippocampus of CD200$^{-/-}$ mice

MCP1 expression (A) and release (B) and IP-10 expression (C) was significantly increased in the hippocampus of CD200$^{-/-}$ mice compared with wildtype mice (*$p<0.05$; Student's t test for unpaired samples). Values are presented as means ± SEM.

A. *$p=0.0421$; 2.046 ± 0.6150; n=4 vs. 9.639 ± 2.345; n=7
B. *$p=0.0263$; 6.047 ± 0.3845; n=6 vs. 8.185 ± 0.7253; n=6
C. *$p=0.0334$; 0.9518 ± 0.2910; n=4 vs. 5.359 ± 1.779; n=5; one-tailed t test

5.4 Discussion

The evidence described in this study highlights some of the complexities associated with CD200-deficiency *in vivo*. Specifically microglial activation was found to be increased in CD200$^{-/-}$ mice *in vivo* indicated by increased CD11b, MHC II and CD40 expression even under resting conditions. Interestingly, IFNγ and its receptor were also increased in the hippocampus of CD200$^{-/-}$ mice, perhaps because of the observed increased blood brain barrier permeability and/or the increased chemokine concentration which was evident in the brain and the consequent CD4+ T cells, CD8+ T cells and macrophages. This data show that these cells release IFNγ and the infiltrating macrophage displayed increased MHC class II, which activates microglia and contributes to the inflammatory changes.

An early paper by Streit and colleagues, describes the upregulation of cell surface marker CD11b upon microglial activation (Streit, Walter et al. 1999). In addition such an increase has been described in inflammation which is associated with neurodegeneration (Roy, Fung et al. 2006). Here, CD11b expression was found to be increased in the hippocampus of CD200$^{-/-}$ mice compared with wildtype mice. These results are consistent with previous results which demonstrate that immunological staining of CD11b and CD45 was low in wildtype mice, whereas CD200$^{-/-}$ mice exhibited increased CD11b and CD45 (Hoek, Ruuls et al. 2000). In addition, MHC class II and CD40 were found to be increased in the hippocampus of CD200$^{-/-}$ mice compared with wildtype mice. This is a significant finding as resting state microglia have been shown to display almost undetectable levels of MHC class II, a feature which contributed to the original theory of the "immunologically privileged" brain (Benveniste, Nguyen et al. 2001). Not all microglia are capable of expressing MHC class II and it is presumed that the ones that do express the cell surface marker are acting as APCs. Uncharacteristically high expression of MHC class II in the CNS has been observed in numerous neurodegenerative diseases including MS, AD and EAE (Panek and Benveniste 1995). CD40 has been shown to interact with the CD40 ligand which is expressed predominantly on CD4^{+} T cells, and promote the activation of microglial cells *in vitro* (Ponomarev, Shriver et al. 2006). Its expression has been found to be increased on activated microglia and has therefore been observed with advancing age *in vivo* (Griffin, Nally et al. 2006). These results suggest that CD200-

deficiency is associated with increased microglial activation and that these cells have increased antigen presenting function uncharacteristic of healthy CNS tissue.

In certain pathological conditions IFNγ has been implicated as playing a role in altering glial function to induce active interaction with immune cells (Kawanokuchi, Mizuno et al. 2006). In the previous chapter *in vitro* experiments demonstrated that IFNγ induced TNFα, IL-6 and NOS2 expression and release from purified microglia prepared from wildtype and CD200$^{-/-}$ mice, while CD200$^{-/-}$ mice responded more profoundly to the stimulus compared with wildtype mice. In addition, IFNGR1 was increased on CD11b^{+} microglial cells prepared from CD200$^{-/-}$, compared with wildtype, mice. Here both IFNGR1 and IFNγ protein expression were increased in the hippocampus of CD200$^{-/-}$ mice compared with wildtype mice. This discovery was particularly significant as IFNγ is known to be one of the most potent activators of microglial cells (Benveniste and Benos 1995) and could account for the increased microglial activation observed in CD200$^{-/-}$ mice.

In order to examine the effects of IFNγ *in vivo*, cells were prepared from the cortices of wildtype mice injected with saline or IFNγ. Microglial activation was assessed by CD11b, CD68 and CD86. CD68 is highly expressed by phagocytic microglia (Croisier, Moran et al. 2005). Although predominantly an intracellular protein localized in the lysosome, flow cytometry of intact cells of the monocyte lineage shows significant surface expression upon stimulation of the cells (Ramprasad, Terpstra et al. 1996). Mean florescent intensity of CD11b was increased on cells prepared from IFNγ-treated animals, while CD68 and co-stimulatory molecule CD86 were increased on CD11b^{+} cells from IFNγ-treated animals compared with saline-treated mice. In addition, CD11b^{-} population of cells which manly comprise astrocytes were assessed and the data show that these cells also expressed increased CD68 and CD86. These data illustrate the profound effects of a pathophysiological dose of IFNγ not only on microglia but also on other CNS-associated immune cells, resulting in the induction of an immune response.

Increased concentrations of IFNγ have been detected in the CSF and brain parenchyma during infections and in inflammatory disorders, and have been associated with increases in infiltrates of activated NK cells and T cells (De Simone,

Levi et al. 1998). Here the infiltration of CD4^{+} and CD8^{+} T cells into the CNS was investigated. The percentage of CD45^{+}CD4^{+} and CD45^{+}CD8^{+} T cells was increased in CD200^{-/-}, compared with wildtype, mice. CD4^{+} T cells can differentiate into different lineages of T helper (Th) cells with distinct biological functions, here it is confirmed that Th1 cells, as opposed to Th2 or Th17 cells, produce significant levels of IFNγ. In addition to their cytotoxic activities, CD8^{+} T cells are also capable of producing IFNγ, which enables these cells to combat viral and mycobacterial infection (Szabo, Sullivan et al. 2002; Ngai, McCormick et al. 2007).

IFNγR is known to be expressed on microglia and these cells are known to respond to IFNγ, but IFNγ release from CNS-associated cell types is a matter of controversy. In contrast production of IFNγ by IL-12-stimulated macrophage and dendritic cells is well known. There was an age-related increase in infiltrating macrophages observed in cells prepared from wildtype and CD200^{-/-} mice; furthermore cells prepared from CD200^{-/-} mice had increased percentage of macrophage infiltrates. Interestingly these macrophages expressed increased levels of MHC class II.

It is well established that there are differences between the inflammatory responses in the CNS and peripheral systems (Chang, Chiu et al. 2009). Under normal circumstances the CNS environment is highly controlled, with minimal expression of MHC class II and co-stimulatory molecules CD40 and CD86. MHC class II interacts with the T cell receptor provided the co-stimulatory molecules are also present. It is anticipated that increased MHC class II expression in CD200^{-/-} mice and is indicative of increased T cell-microglia and -macrophage interactions. Here the data demonstrate that Th1 cells, IFNγ-producing CD4^{+} T cells, are capable of increasing MHC class II expression on mixed glia and microglia. This is consistent with previous data which have established IFNγ as the primary inducer of MHC class II, and with *in vitro* experiments which have demonstrated that IFNγ potently stimulates MHC class II expression on both microglia and astrocytes (Panek and Benveniste 1995; Kawanokuchi, Mizuno et al. 2006).

The concept of an immune-privileged CNS gained credence in the 19th century on the back of a number of observations which suggested a physical and immunological

separation and clear distinction between the rest of the body. The presence of the BBB, the lack of a lymphatic drainage system and the negligible levels of MHC expression contributed to this idea, however the separation is by no means absolute and immunological surveillance is routinely carried out. Leukocytes of all types have the ability to enter the CNS (Hickey 1999). Interestingly, the entry of T-lymphocytes into the parenchyma of the CNS is one of the earliest features of the pathogenesis of MS and EAE and is critical for the progression of the disease (Hickey, Hsu et al. 1991). The first critical step in the movement of T cells into the brain parenchyma is penetration of the BBB. One study by Hickey and colleagues concluded that T cells in their activated state, regardless of antigen specificity, had the ability to penetrate the BBB (Hickey, Hsu et al. 1991); however their continued presence was dependent on expression of MHC (Hickey 1999). While routine leukocyte surveillance is detected in the CNS, the relative numbers of T cells are much higher in organs lacking a blood-tissue barrier like the CNS. In this study the integrity of the BBB was investigated with the aim of establishing whether or not its permeability was altered which might offer as a possible mechanism for the increased infiltration of peripheral immune cells observed in CD200^{-/-} mice.

Tight junctions between brain capillary endothelial cells play a key role in the formation of the BBB and play an important role in maintaining cell-to-cell adhesion sealing the intercellular space in the endothelial cellular sheets of the BBB (Saitou, Furuse et al. 2000). Three distinct types of membrane proteins are known to be localised in the tight junctions; occludin, junctional adhesion molecule (JAM), and claudins (Wen, Watry et al. 2004). Here, claudin-5 and -12, as the primary components of the tight junctions in the brain blood vessels, and occludin, shown to be a functional component of tight junctions, were investigated (Saitou, Furuse et al. 2000; Nitta, Hata et al. 2003). A significant decrease in claudin-5, but not claudin-12 or occludin, expression was detected in the hippocampus of CD200^{-/-} mice. These observations are interesting as previous work on occludin^{-/-} mice demonstrated no obvious morphological or barrier function changes in tight functions of intestinal epithelium (Saitou, Furuse et al. 2000); however claudin-5^{-/-} mice displayed significant alterations in BBB permeability, with tracer experiments and MRI revealing a size-selective loosening of the BBB (Nitta, Hata et al. 2003). This is also supportive of experiments carried out in this laboratory investigating BBB

permeability to gadolinium-based contrast agent in saline- and LPS-treated wildtype and CD200$^{-/-}$ mice; increased BBB permeability was observed in CD200$^{-/-}$ mice demonstrated by increased signal intensity in the hippocampus, cortex and thalamus (unpublished data). It is widely accepted that the numbers of T cells and infiltrating macrophages are low in the healthy brain but can increase dramatically under inflammatory conditions. Thus it is plausible that the upregulation of microglial activation observed in the brains of CD200$^{-/-}$ mice may contribute to BBB permeability.

Chemokines play an established role in attracting T cells and macrophage. Much work has been carried out investigating the role of chemokines in EAE. For instance MCP-1 receptor, CCR2, is expressed at high levels on inflammatory monocytes and is required to permit these cells, but not T cells, to enter the CNS. Genetic deletion or blockade of CCR2 protected from EAE owing to a significant decrease in macrophages accumulation in the CNS. These results established a clear correlation between monocytic infiltration and disease progression (Fife, Kennedy et al. 2001; Ajami, Bennett et al. 2011). CXCR3, the receptor for IP-10, is expressed primarily on activated T cells. IP-10 and CXCR3 have been shown to be expressed in the CNS during the development of EAE, whereas anti-IP-10 treatment decreased acute EAE severity by preventing mononuclear cell accumulation (Fife, Kennedy et al. 2001). Here, MCP-1 and IP-10 were investigated as chemo-attractants of macrophage and activated T cells. Both MCP-1 and IP-10 were found to be increased in the hippocampus of CD200$^{-/-}$ mice compared with wildtype mice. It is possible that these increases contributed to the increased T cell and macrophages infiltration seen in CD200$^{-/-}$ mice, however future work should investigate chemokine receptor expression of the infiltrating cells to establish a correlation between increased peripheral cell infiltration and increased chemokine expression.

The data demonstrate that in the normal healthy CNS microglia display a down-regulated phenotype with low expression of markers of microglial activation CD11b, MHC II and CD40. However the loss of CD200 results in increased expression of markers of microglial activation and an increase in the concentration of potent inflammatory mediator, IFNγ. The infiltration of IFNγ-producing cells, CD4^{+} T cells, CD8^{+} T cells and macrophages, thought to be mediated via increased BBB

permeability and chemokine expression, are likely to contribute to the IFNγ-induced activation of microglia and contribute to the inflammatory changes. A significant finding of this study is there was an age-related infiltration of peripheral immune cells which was exaggerated in CD200$^{-/-}$ mice. This is interesting as age is the primary risk factor for many neurodegenerative diseases including AD and decreases in CD200 expression have been demonstrated in the aged brain (Griffin, Nally et al. 2006) and the human AD brain (Walker, Dalsing-Hernandez et al. 2009).

Chapter 6

Discussion and Future Studies

6.1. Discussion and future studies

The overall objective of this study was to assess the inflammatory phenotypes of microglia; to investigate the role of CD200 in modulating LPS-, IFNγ- and IL-4-induced microglia activation; and to evaluate the changes which accompany the loss of CD200 *in vivo* with the objective of increasing our understanding of the mechanisms that modulate microglial function. It was predicted that glia prepared from CD200-deficient mice would respond more profoundly to LPS and IFNγ. The data show that LPS and IFNγ exert a greater effect in glia prepared from CD200-deficient mice. In contrast, the response to IL-4 was similar in glia prepared from wildtype and CD200$^{-/-}$ mice. Increased cell surface expression of TLR4 and IFNGR1, and increased activation of NFκB and STAT1, observed in cells prepared from CD200$^{-/-}$ mice suggest that the regulatory systems which control LPS- and IFNγ-induced inflammation in the normal healthy CNS, were altered in that of CD200$^{-/-}$ mice. The present findings demonstrate that the loss of CD200 increased the vulnerability of microglia to inflammatory challenge. Another significant finding reported here is that the microglial activation, which occurs in the hippocampus of CD200-defcient mice, was associated with an increase in BBB permeability. This was associated with infiltration of T cells and macrophages, which may account for the increased IFNγ, providing the trigger for microglial activation.

LPS increased TNFα, IL-1β and IL-6 mRNA expression and supernatant concentration in mixed glia prepared from wildtype mice consistent with previously-described effects (Lyons, McQuillan et al. 2009; Watson, Costello et al. 2010). This effect was greater in mixed glia prepared from CD200$^{-/-}$ mice. These results are broadly consistent with previous data demonstrating LPS-induced proinflammatory cytokine release was inhibited when glia were co-cultured with neurons and this effect was attributed to CD200-CD200R interaction since it was blocked by addition of anti-CD200 antibody to the cultures (Lyons, McQuillan et al. 2009). These findings and others have focused on the complimentary expression of CD200 and CD200R on neurons and microglia, respectively, in modulating microglial activity. In the current study, mixed glial preparations comprising of approximately 70% astrocytes and 30% microglia were used (Costello, Lyons et al. 2011). The profound LPS-induced

responses observed in mixed glia prepared from CD200$^{-/-}$ mice, and the observed expression of CD200 on astrocytes, demonstrate the importance of astrocytes in modulating microglial activity. Further, the data suggest that the interaction between CD200 and CD200R modulates TLR4-induced proinflammatory cytokine production and release. Although previous studies have confirmed that the interaction of CD200 and its receptor modulates microglial activation (Hoek, Ruuls et al. 2000), the underlying mechanisms for this have remained unclear.

The current data demonstrate that there was an increase in the expression of TLR2 and TLR4 in mixed glia prepared from CD200$^{-/-}$, compared with wildtype mice. This identifies a possible explanation for the increased responsiveness of cells prepared from CD200$^{-/-}$ mice to LPS. Consistent with this explanation, results from the laboratory have demonstrated increased responsiveness to TLR2 agonist Pam$_3$Csk$_4$ in mixed glia prepared from CD200$^{-/-}$, compared with wildtype, mice (Costello, Lyons et al. 2011).

Interestingly, TLR4 mRNA expression was found to be increased on both purified microglia and purified astrocytes prepared from CD200$^{-/-}$, compared with wildtype, mice and interestingly, astrocytes prepared from CD200$^{-/-}$ mice responded more profoundly to LPS compared with wildtype mice. One possible explanation for the enhanced LPS-induced responses of astrocytes prepared from CD200$^{-/-}$, compared with wildtype, mice, is the increased expression of endogenous ligand HMGB1 found in mixed glia prepared from CD200$^{-/-}$ mice. HMGB1 is released from activated astrocytes (Chen, Ward et al. 2004) and, here, the data suggest that HMGB1 may act synergistically with LPS, delivering a stronger signal to the TLR4 receptor resulting in enhanced inflammatory output. The results demonstrate that the consequences of CD200-deficiency altered the inflammatory responses of both microglia and astrocytes. The mechanism by which HMGB1 enhances and prolongs the effects of LPS remain unknown, future experiments may investigate the activity of the HMGB1/LPS complex by adding neutralising antibodies for TLR4 in order to indicate that the complex is acting through the TLR4 receptor.

TLR2 and TLR4 activation lead to NFκB activation, evaluated in this study by assessing phosphorylation of IκKβ and IκBα. The data indicate that unstimulated

mixed glia prepared from CD200$^{-/-}$ mice showed increased phosphorylated IκKβ and IκBα compared with wildtype mice, indicating that NFκB activation was increased in cells prepared from CD200$^{-/-}$ mice. Thus increased receptor expression and activation of downstream signalling present a plausible explanation for the profound responses of cells prepared from CD200$^{-/-}$ mice to LPS.

Interestingly, the CD200/CD200R interaction has been shown to inhibit excessive inflammation induced by TLR, NOD-like receptor (NLR) and inflammasome activation (Mukhopadhyay, Pluddemann et al. 2010). It was suggested that TLR and NLR activation induces CD200 initiating a negative regulatory loop, in turn regulating TLR- and NLR-mediated inflammatory responses. The importance of this was evident from findings in which CD200-deficient mice succumbed to infection with *Neisseria meningitides* more readily than their wildtype counterparts, as they were unable to limit TNFα and IL-6 production. How CD200R activation limits TLR function is still unknown, however it has been suggested that DOK2, which has been shown to be crucial in initiating CD200R signaling, is a potent regulator of TLRs (Shinohara, Inoue et al. 2005; Mukhopadhyay, Pluddemann et al. 2010; Lyons, Downer et al. 2012).

It has been proposed that microglia in the diseased and aging brain are "primed"; this state is characterised by chronic low-level inflammation and increased microglia reactivity. Recent evidence has demonstrated that these "primed" microglia are capable of switching their phenotype to produce neuro-toxic molecules when they respond to systemic inflammatory signals, evoking an exaggerated response which may contribute to disease progression (Perry, Cunningham et al. 2007). Murine ME7-induced prion disease is a model of chronic neurodegeneration that displays chronic microglial activation. Peripheral LPS challenge during pre-symptomatic neurodegeneration in these animals resulted in exaggerated CNS inflammation and sickness behaviour responses compared with controls. Further, a single peripheral challenge was sufficient to exacerbate and accelerate disease progression (Combrinck, Perry et al. 2002; Cunningham, Campion et al. 2009). In fact systemic infection has been shown to accelerate cognitive decline in patients with AD (Holmes, El-Okl et al. 2003), and evidence suggests it is a risk factor that can precipitate relapse in MS patients (Sibley, Bamford et al. 1985). These findings indicate that individuals with

activated or primed microglia are at increased risk of severe neuro-behavioural deficits and neuropathology during and following systemic infection (Godbout, Chen et al. 2005). Interestingly aging has been suggested as one physiological event that may prime microglial cells for an exaggerated response (Barrientos, Higgins et al. 2006).

Age-related changes in microglial activation have been implicated in the pathogenesis of neurodegenerative diseases of aging. While age itself is clearly not a disease it is associated with significant alterations in microglial activation. Expression of CD11b and MHC class II were found to be increased in the brains of aged rodents (Frank, Barrientos et al. 2006), along with other cell surface markers including CD80 and CD86 (Griffin, Nally et al. 2006; Clarke, O'Connell et al. 2007). Furthermore elevation in proinflammatory cytokines IL-1β, TNFα and IL-6, has been observed in the brain of aged rodents (Godbout, Chen et al. 2005), along with a decreased expression of anti-inflammatory cytokines such as IL-4 and IL-10 (Ye and Johnson 2001; Lyons, Downer et al. 2007). Evidence from this laboratory has suggested that CD200 expression is decreased in the hippocampus of aged animals and that this may be a contributing factor to the associated increase in microglial activation (Lyons, Downer et al. 2007). The present data demonstrate that the loss of CD200 in mixed glial cells results in increased expression and responsiveness of TLR2 and TLR4. Expression of TLR2 and TLR4 has been shown to be increased in the aging brain (Letiembre, Hao et al. 2007) and age-related alterations in innate immune receptors have been suggested as playing a role in the development of age-related neurodegenerative diseases (Letiembre, Liu et al. 2009).

The current data provide evidence that microglia are capable of responding to endogenous and exogenous factors which dictate microglial function. However, in aged individuals the impact of exogenous stimuli, such as a peripheral immune challenge, becomes increasingly important. Together these results suggest that the loss of CD200 in the aged brain may lead to a lack of control in the immune response, exemplified by increased TLR expression and microglial activation, yielding an inappropriate, dysregulated response when the system is challenged. Of particular interest is the finding that CD200Fc attenuated the age-related increase in markers of microglial activation, including MHC class II and CD40 in aged, compared with

young, rats (Cox, Carney et al. 2012). Thus the addition of CD200 may prove an attractive therapeutic target in regaining control of age-associated microglial activation.

It has become apparent that the activation of microglia, like that of macrophages, can result in diverse phenotypes (Hanisch and Kettenmann 2007). While many of the published studies have focused on the activation of macrophages, here the focus was on the activation states adopted by microglia, specifically the differential induction of microglial phenotypes by Th1 and Th2 cell-derived cytokines, IFNγ and IL-4 respectively, and the modulatory role of CD200 on these activation states.

The data demonstrate that microglia stimulated with IFNγ resulted in increased expression of TNFα, IL-6, and NOS2, while it inhibited mannose receptor expression, a marker of alternative activation. These results are consistent with previous investigations of macrophages that identified classically-activated macrophages by a pronounced production of TNFα and NOS2 (Ma, Chen et al. 2003; Mosser 2003), and a selective down-regulation of mannose receptor expression (Mokoena and Gordon 1985). In contrast, the expression of mannose receptor, and two other markers of alternative activation, arginase I and chitinase 3-like 3, was increased in mixed glia incubated in the presence of IL-4, IL-4 also decreased expression of the classical activation markers, TNFα and NOS2. These results are consistent with the original description of alternatively activated macrophages arising from the upregulation of mannose receptor expression in the presence of IL-4 (Stein, Keshav et al. 1992; Martinez, Helming et al. 2009; Gordon and Martinez 2010). Interestingly, cells prepared from CD200^{-/-} mice resulted in an amplified response to IFNγ, signified by increased expression of TNFα, IL-6 and NOS2, however cells prepared from wildtype and CD200^{-/-} mice had a similar response to IL-4. These results demonstrate the ability of microglia to respond to adaptive, as well as innate, immune stimuli in a similar fashion to that of macrophages. Furthermore, the data demonstrate the loss of CD200 has a selective significant impact on IFNγ-induced classical activation of microglia.

To investigate a possible explanation for the increased responsiveness of cells prepared from CD200^{-/-} mice to IFNγ, expression of the IFNγR was assessed. An

increase was observed in cell surface expression of IFNGR1, the ligand-binding subunit of the receptor, on microglia prepared from CD200$^{-/-}$, compared with wildtype, mice. Furthermore, STAT1 activation was increased in unstimulated mixed glial cells prepared from CD200$^{-/-}$, compared with wildtype mice. These results demonstrate that the loss of CD200 results in dysfunction of the negative regulators of IFNγ signalling, resulting in greater increases in IFNγ-responsive genes. The data represent a novel mechanism by which the amplified response to IFNγ in cells prepared from CD200$^{-/-}$ mice might be explained. Interestingly, an increase in IL-4Rα was observed in microglia prepared from CD200$^{-/-}$, compared with wildtype, mice; however the data show that this did not result in an increased responsiveness to IL-4.

Recent evidence has suggested that chronic inflammation can result from an imbalance between the levels of inflammatory mediators and inflammatory regulators during immune responses. Functional dysregulation of the IFNγ pathway has been implicated in a variety of inflammatory disorders (Mukhopadhyay, Pluddemann et al. 2010; Varnum and Ikezu 2012). Whereas IFNγ is increased in the brains of aged rodents, a decrease in IL-4 expression has been observed (Maher, Nolan et al. 2005; Nolan, Maher et al. 2005; Lyons, Downer et al. 2007). These data suggest a skew towards a classical activation state in the aged brain. Interestingly, IL-4 is capable of inducing increased expression of CD200 and this may be one mechanism by which it down-regulates microglial activation (Lyons, Downer et al. 2007). In the aged brain, the decrease in both CD200 and responsiveness to IL-4 may allow activated microglia to retain a predominant classical activation state (Fenn, Henry et al. 2012). Microglial phenotypes have been demonstrated to switch from an alternative activation state to a classical activation state in the human AD brain (Varnum and Ikezu 2012). The present data demonstrate that CD200Fc attenuated IFNγ-induced classical activation in mixed glial cells prepared from wildtype mice. Taken together these results demonstrate the possible therapeutic potential of CD200 in controlling inflammation and future studies should investigate whether the loss of CD200, observed in the aged brain (Frank, Barrientos et al. 2006) and the post-mortem brain of patients who suffered from AD (Walker, Dalsing-Hernandez et al. 2009), correlates with a switch from an alternative activation state to the prominent classical activation state observed.

Under normal circumstances, the inflammatory responses within the CNS are tightly regulated. A number of factors contribute to this including the presence of the BBB, low levels of MHC, a lack of professional APCs including dendritic cells and macrophages, and limited T cell entry (Forrester, Xu et al. 2008). These features allow the resident microglia to mount a controlled response to infection (Streit 2002). While cells of the peripheral immune system also contribute to the immunity of the CNS, the migration and infiltration of peripheral immune cells is tightly controlled at the level of the BBB and is relatively low in the healthy CNS (Rezai-Zadeh, Gate et al. 2009).

Here, CD200$^{-/-}$ mice exhibited increased expression of CD11b, MHC class II and CD40 in the hippocampus, compared with wildtype mice. These findings are supportive of experiments carried out in CD200$^{-/-}$ mice which have shown an accelerated microglial response in the facial nerve transection model, compared with wildtype mice (Hoek, Ruuls et al. 2000; Wang, Ye et al. 2007). In addition, the symptoms in MOG-induced EAE appeared earlier in CD200$^{-/-}$, compared with wildtype mice (Hoek, Ruuls et al. 2000); while, CD200$^{-/-}$ animals showed an increased susceptibility to CIA (Hoek, Ruuls et al. 2000; Nimmerjahn, Kirchhoff et al. 2005). However, despite the extensive evidence, presented here and in the literature, linking interaction between CD200 and CD200R with preservation of microglia in a quiescent state, it remains unclear what basal level alterations, if any, contribute to their profound responses to activating stimuli in vivo.

The data presented here demonstrate that IFNGR1 and IFNγ protein expression were increased in the hippocampus of CD200$^{-/-}$ mice compared with wildtype mice. This discovery was particularly significant as IFNγ is known to be one of the most potent activators of microglial cells (Benveniste and Benos 1995) and could account for the increased microglial activation observed in the brains of CD200$^{-/-}$ mice.

The cell source of IFNγ within the brain is unclear. One group has highlighted microglia as a candidate to produce IFNγ (Kawanokuchi, Mizuno et al. 2006), however these results are not corroborated in the literature. Peripheral immune cells CD4$^+$ and CD8$^+$ T cells, and NK cells, are the primary producers of IFNγ (Farrar and Schreiber 1993) and macrophages release IFNγ following infection with

Mycobacterium tuberculosis (Fenton, Vermeulen et al. 1997), in response to LPS (Fultz, Barber et al. 1993) and in the presence of IL-12 and IL-18 (Wang, Wakeham et al. 1999). A central finding of the work presented here is that CD200-deficiency results in increased CD4$^+$ and CD8$^+$ T cells, and MHC class II$^+$ macrophage infiltration. These changes were associated with increased BBB permeability and increased chemokine concentration, offering a possible mechanism for the increased infiltration of peripheral IFNγ-producing immune cells observed in CD200$^{-/-}$ mice.

EAE is a well-studied mouse model of the human disorder MS and is characterized by extensive infiltration of the CNS by inflammatory immune cells (Ajami, Bennett et al. 2011). Many studies have highlighted the importance of the CD200-CD200R signaling pathway in the clinical course of EAE. The *Wld* mouse is a spontaneously-occurring mutant with the unique phenotype of protection against several forms of axonal injury, including a reduced susceptibility to EAE associated with enhanced neuronal expression of CD200 (Chitnis, Imitola et al. 2007). A study by Meuth *et al.*, demonstrated that in vivo disruption of the CD200-CD200R signaling pathway by antibody treatment lead to an aggravated clinical course of EAE (Meuth, Simon et al. 2008). This was associated with double the absolute number of infiltrating immune cells and, caused an increase in the relative number of activated iNOS-expressing macrophages and T cells found in the spinal cord EAE-lesions. Blockade of CD200R led to enhanced IFNγ-induced IL-6 release (Meuth, Simon et al. 2008). These results directly implicate CD200 in the development and progression of EAE. The present data demonstrate that even in the absence of stimuli CD200$^{-/-}$ mice display increased and activated inflammatory cell infiltration, priming the CNS for inflammatory challenge and providing a plausible explanation for increased susceptibility to EAE observed in CD200$^{-/-}$ mice.

Throughout this study the evidence has described the expression of CD200 by astrocytes in the maintenance of microglia homeostasis. However, CD200 is expressed on a wide variety of cells including endothelial cells (Barclay 1981; Webb and Barclay 1984; Clark, Gagnon et al. 1985) and while the primary role of the CD200-CD200R interaction may be to reduce the activation of macrophages and microglia, a second role in T cell adhesion and migration into tissues has been suggested (Ko, Chien et al. 2009). Anti-CD200 antibody blocked the adhesion of T

cells to endothelial cells but did not affect the adhesion of macrophages (Ko, Chien et al. 2009). MS is thought to be mediated by inflammatory CD4^{+} T cells that infiltrate the brain and spinal cord, activate microglia and recruit inflammatory macrophages, resulting in demyelination and degeneration of axons (Prendergast and Anderton 2009). In light of this evidence future studies may target enhanced levels of CD200 as a potential therapeutic strategy in the treatment of disorders exemplified by T cell infiltration.

In this study, it was shown that glia from CD200^{-/-} mice exhibited many features of activation, including increased expression of CD11b and MHC class II in the hippocampus, compared with wildtype mice. These results demonstrate the importance of the CD200-CD200R interaction in maintaining homeostasis in the healthy CNS. Cells prepared from CD200^{-/-} mice respond more profoundly to inflammatory stimuli, LPS and IFNγ; associated with these changes are increased expression of TLR4 and IFNγR and downstream activation of NFκB and STAT1, respectively.

Deficiencies in the CD200-CD200R interaction have been reported in the brain with age and in neurodegenerative diseases including AD (Frank, Barrientos et al. 2006; Walker, Dalsing-Hernandez et al. 2009). Regulatory systems are in place in the CNS to control the inflammatory response are less effective during aging and indeed AD pathogenesis resulting in an imbalance between inflammatory mediators and inflammatory regulators (Walker, Dalsing-Hernandez et al. 2009). The present data show that the loss of CD200 is associated with an increase in potent inflammatory mediator IFNγ. The infiltration of IFNγ-producing cells thought to be mediated via increased BBB permeability and chemokine expression, are likely to contribute to the activation of microglia and contribute to the inflammatory changes. The results demonstrate a specific role for CD200R signaling in the modulation of classical activation of microglia and present a potential approach for therapeutic intervention in disorders associated with inflammatory alterations and immune cell infiltration such as AD and MS.

References

Ajami, B., J. L. Bennett, et al. (2011). "Infiltrating monocytes trigger EAE progression, but do not contribute to the resident microglia pool." Nat Neurosci **14**(9): 1142-1149.

Akira, S. and S. Sato (2003). "Toll-like receptors and their signaling mechanisms." Scand J Infect Dis **35**(9): 555-562.

Alexander, W. S., R. Starr, et al. (1999). "SOCS1 is a critical inhibitor of interferon gamma signaling and prevents the potentially fatal neonatal actions of this cytokine." Cell **98**(5): 597-608.

Baker, B. J., L. N. Akhtar, et al. (2009). "SOCS1 and SOCS3 in the control of CNS immunity." Trends Immunol **30**(8): 392-400.

Barclay, A. N. (1981). "Different reticular elements in rat lymphoid tissue identified by localization of Ia, Thy-1 and MRC OX 2 antigens." Immunology **44**(4): 727-736.

Barclay, A. N. (2001). "Biochemical analysis of the lymphocyte cell surface--from alloantisera to the role of membrane proteins." Immunol Rev **184**: 69-81.

Barclay, A. N. (2003). "Membrane proteins with immunoglobulin-like domains--a master superfamily of interaction molecules." Semin Immunol **15**(4): 215-223.

Barclay, A. N., G. J. Wright, et al. (2002). "CD200 and membrane protein interactions in the control of myeloid cells." Trends Immunol **23**(6): 285-290.

Barrientos, R. M., E. A. Higgins, et al. (2006). "Peripheral infection and aging interact to impair hippocampal memory consolidation." Neurobiol Aging **27**(5): 723-732.

Bechmann, I., I. Galea, et al. (2007). "What is the blood-brain barrier (not)?" Trends Immunol **28**(1): 5-11.

Benveniste, E. N. and D. J. Benos (1995). "TNF-alpha- and IFN-gamma-mediated signal transduction pathways: effects on glial cell gene expression and function." FASEB J **9**(15): 1577-1584.

Benveniste, E. N., V. T. Nguyen, et al. (2001). "Immunological aspects of microglia: relevance to Alzheimer's disease." Neurochem Int **39**(5-6): 381-391.

Bianchi, M. E. (2009). "HMGB1 loves company." J Leukoc Biol **86**(3): 573-576.

Bianchi, M. E. and A. A. Manfredi (2007). "High-mobility group box 1 (HMGB1) protein at the crossroads between innate and adaptive immunity." Immunol Rev **220**: 35-46.

Billingham, R. E. and T. Boswell (1953). "Studies on the problem of corneal homografts." Proc R Soc Lond B Biol Sci **141**(904): 392-406.

Boudakov, I., J. Liu, et al. (2007). "Mice lacking CD200R1 show absence of suppression of lipopolysaccharide-induced tumor necrosis factor-alpha and mixed leukocyte culture responses by CD200." Transplantation **84**(2): 251-257.

Brambilla, R., V. Bracchi-Ricard, et al. (2005). "Inhibition of astroglial nuclear factor kappaB reduces inflammation and improves functional recovery after spinal cord injury." J Exp Med **202**(1): 145-156.

Brodie, C., N. Goldreich, et al. (1998). "Functional IL-4 receptors on mouse astrocytes: IL-4 inhibits astrocyte activation and induces NGF secretion." J Neuroimmunol **81**(1-2): 20-30.

Byrnes, A. P., R. E. MacLaren, et al. (1996). "Immunological instability of persistent adenovirus vectors in the brain: peripheral exposure to vector leads to renewed inflammation, reduced gene expression, and demyelination." J Neurosci **16**(9): 3045-3055.

Capaldo, C. T. and A. Nusrat (2009). "Cytokine regulation of tight junctions." Biochim Biophys Acta **1788**(4): 864-871.

Castiglioni, A., V. Canti, et al. (2011). "High-mobility group box 1 (HMGB1) as a master regulator of innate immunity." Cell Tissue Res **343**(1): 189-199.

Chang, R. C., K. Chiu, et al. (2009). "Modulation of neuroimmune responses on glia in the central nervous system: implication in therapeutic intervention against neuroinflammation." Cell Mol Immunol **6**(5): 317-326.

Chen, G., M. F. Ward, et al. (2004). "Extracellular HMGB1 as a proinflammatory cytokine." J Interferon Cytokine Res **24**(6): 329-333.

Cherwinski, H. M., C. A. Murphy, et al. (2005). "The CD200 receptor is a novel and potent regulator of murine and human mast cell function." J Immunol **174**(3): 1348-1356.

Chitnis, T., J. Imitola, et al. (2007). "Elevated neuronal expression of CD200 protects Wlds mice from inflammation-mediated neurodegeneration." Am J Pathol **170**(5): 1695-1712.

Clark, M. J., J. Gagnon, et al. (1985). "MRC OX-2 antigen: a lymphoid/neuronal membrane glycoprotein with a structure like a single immunoglobulin light chain." EMBO J **4**(1): 113-118.

Clarke, R. M., F. O'Connell, et al. (2007). "The HMG-CoA reductase inhibitor, atorvastatin, attenuates the effects of acute administration of amyloid-beta1-42 in the rat hippocampus in vivo." Neuropharmacology **52**(1): 136-145.

Colton, C. A. (2009). "Heterogeneity of microglial activation in the innate immune response in the brain." J Neuroimmune Pharmacol **4**(4): 399-418.

Colton, C. A., R. T. Mott, et al. (2006). "Expression profiles for macrophage alternative activation genes in AD and in mouse models of AD." J Neuroinflammation **3**: 27.

Colton, C. A. and D. M. Wilcock (2010). "Assessing activation states in microglia." CNS Neurol Disord Drug Targets **9**(2): 174-191.

Combrinck, M. I., V. H. Perry, et al. (2002). "Peripheral infection evokes exaggerated sickness behaviour in pre-clinical murine prion disease." Neuroscience **112**(1): 7-11.

Costello, D. A., A. Lyons, et al. (2011). "Long term potentiation is impaired in membrane glycoprotein CD200-deficient mice: a role for Toll-like receptor activation." J Biol Chem **286**(40): 34722-34732.

Cox, F. F., D. Carney, et al. (2012). "CD200 fusion protein decreases microglial activation in the hippocampus of aged rats." Brain Behav Immun **26**(5): 789-796.

Croisier, E., L. B. Moran, et al. (2005). "Microglial inflammation in the parkinsonian substantia nigra: relationship to alpha-synuclein deposition." J Neuroinflammation **2**: 14.

Cunningham, C., S. Campion, et al. (2009). "Systemic inflammation induces acute behavioral and cognitive changes and accelerates neurodegenerative disease." Biol Psychiatry **65**(4): 304-312.

Damani, M. R., L. Zhao, et al. (2011). "Age-related alterations in the dynamic behavior of microglia." Aging Cell **10**(2): 263-276.

De Simone, R., G. Levi, et al. (1998). "Interferon gamma gene expression in rat central nervous system glial cells." Cytokine **10**(6): 418-422.

Deckert, M., J. D. Sedgwick, et al. (2006). "Regulation of microglial cell responses in murine Toxoplasma encephalitis by CD200/CD200 receptor interaction." Acta Neuropathol **111**(6): 548-558.

Degryse, B. and M. de Virgilio (2003). "The nuclear protein HMGB1, a new kind of chemokine?" FEBS Lett **553**(1-2): 11-17.

Derouiche, A. and M. Frotscher (2001). "Peripheral astrocyte processes: monitoring by selective immunostaining for the actin-binding ERM proteins." Glia **36**(3): 330-341.

Dimitriou, I. D., L. Clemenza, et al. (2008). "Putting out the fire: coordinated suppression of the innate and adaptive immune systems by SOCS1 and SOCS3 proteins." Immunol Rev **224**: 265-283.

Dong, Y. and E. N. Benveniste (2001). "Immune function of astrocytes." Glia **36**(2): 180-190.

Dorman, S. E. and S. M. Holland (1998). "Mutation in the signal-transducing chain of the interferon-gamma receptor and susceptibility to mycobacterial infection." J Clin Invest **101**(11): 2364-2369.

Doyle, A. G., G. Herbein, et al. (1994). "Interleukin-13 alters the activation state of murine macrophages in vitro: comparison with interleukin-4 and interferon-gamma." Eur J Immunol **24**(6): 1441-1445.

Dumitriu, I. E., M. E. Bianchi, et al. (2007). "The secretion of HMGB1 is required for the migration of maturing dendritic cells." J Leukoc Biol **81**(1): 84-91.

Farina, C., F. Aloisi, et al. (2007). "Astrocytes are active players in cerebral innate immunity." Trends Immunol **28**(3): 138-145.

Farrar, M. A. and R. D. Schreiber (1993). "The molecular cell biology of interferon-gamma and its receptor." Annu Rev Immunol **11**: 571-611.

Fenn, A. M., C. J. Henry, et al. (2012). "Lipopolysaccharide-induced interleukin (IL)-4 receptor-alpha expression and corresponding sensitivity to the M2 promoting effects of IL-4 are impaired in microglia of aged mice." Brain Behav Immun **26**(5): 766-777.

Fenton, M. J., M. W. Vermeulen, et al. (1997). "Induction of gamma interferon production in human alveolar macrophages by Mycobacterium tuberculosis." Infect Immun **65**(12): 5149-5156.

Fife, B. T., K. J. Kennedy, et al. (2001). "CXCL10 (IFN-gamma-inducible protein-10) control of encephalitogenic CD4+ T cell accumulation in the central nervous system during experimental autoimmune encephalomyelitis." J Immunol **166**(12): 7617-7624.

Filipe-Santos, O., J. Bustamante, et al. (2006). "Inborn errors of IL-12/23- and IFN-gamma-mediated immunity: molecular, cellular, and clinical features." Semin Immunol **18**(6): 347-361.

Forrester, J. V., H. Xu, et al. (2008). "Immune privilege or privileged immunity?" Mucosal Immunol **1**(5): 372-381.

Frank, M. G., R. M. Barrientos, et al. (2006). "mRNA up-regulation of MHC II and pivotal pro-inflammatory genes in normal brain aging." Neurobiol Aging **27**(5): 717-722.

Friedl, P. and M. Gunzer (2001). "Interaction of T cells with APCs: the serial encounter model." Trends Immunol **22**(4): 187-191.

Fultz, M. J., S. A. Barber, et al. (1993). "Induction of IFN-gamma in macrophages by lipopolysaccharide." Int Immunol **5**(11): 1383-1392.

Galea, I., I. Bechmann, et al. (2007). "What is immune privilege (not)?" Trends Immunol **28**(1): 12-18.

Garden, G. A. and T. Moller (2006). "Microglia biology in health and disease." J Neuroimmune Pharmacol **1**(2): 127-137.

Godbout, J. P., J. Chen, et al. (2005). "Exaggerated neuroinflammation and sickness behavior in aged mice following activation of the peripheral innate immune system." FASEB J **19**(10): 1329-1331.

Godbout, J. P. and R. W. Johnson (2004). "Interleukin-6 in the aging brain." J Neuroimmunol **147**(1-2): 141-144.

Gorczynski, R., Z. Chen, et al. (2004). "CD200 is a ligand for all members of the CD200R family of immunoregulatory molecules." J Immunol **172**(12): 7744-7749.

Gorczynski, R. M., Z. Chen, et al. (2001). "CD200 immunoadhesin suppresses collagen-induced arthritis in mice." Clin Immunol **101**(3): 328-334.

Gordon, S. (2003). "Alternative activation of macrophages." Nat Rev Immunol **3**(1): 23-35.

Gordon, S. and F. O. Martinez (2010). "Alternative activation of macrophages: mechanism and functions." Immunity **32**(5): 593-604.

Graeber, M. B. and W. J. Streit (2010). "Microglia: biology and pathology." Acta Neuropathol **119**(1): 89-105.

Greenlund, A. C., M. A. Farrar, et al. (1994). "Ligand-induced IFN gamma receptor tyrosine phosphorylation couples the receptor to its signal transduction system (p91)." EMBO J **13**(7): 1591-1600.

Griffin, R., R. Nally, et al. (2006). "The age-related attenuation in long-term potentiation is associated with microglial activation." J Neurochem **99**(4): 1263-1272.

Guillemin, G. J. and B. J. Brew (2004). "Microglia, macrophages, perivascular macrophages, and pericytes: a review of function and identification." J Leukoc Biol **75**(3): 388-397.

Hanisch, U. K. and H. Kettenmann (2007). "Microglia: active sensor and versatile effector cells in the normal and pathologic brain." Nat Neurosci **10**(11): 1387-1394.

Hayden, M. S. and S. Ghosh (2004). "Signaling to NF-kappaB." Genes Dev **18**(18): 2195-2224.

Hickey, W. F. (1999). "Leukocyte traffic in the central nervous system: the participants and their roles." Semin Immunol **11**(2): 125-137.

Hickey, W. F., B. L. Hsu, et al. (1991). "T-lymphocyte entry into the central nervous system." J Neurosci Res **28**(2): 254-260.

Hoek, R. M., S. R. Ruuls, et al. (2000). "Down-regulation of the macrophage lineage through interaction with OX2 (CD200)." Science **290**(5497): 1768-1771.

Holmes, C., M. El-Okl, et al. (2003). "Systemic infection, interleukin 1beta, and cognitive decline in Alzheimer's disease." J Neurol Neurosurg Psychiatry **74**(6): 788-789.

Hreggvidsdottir, H. S., T. Ostberg, et al. (2009). "The alarmin HMGB1 acts in synergy with endogenous and exogenous danger signals to promote inflammation." J Leukoc Biol **86**(3): 655-662.

Hu, X., C. Herrero, et al. (2002). "Sensitization of IFN-gamma Jak-STAT signaling during macrophage activation." Nat Immunol **3**(9): 859-866.

Igarashi, K., G. Garotta, et al. (1994). "Interferon-gamma induces tyrosine phosphorylation of interferon-gamma receptor and regulated association of protein tyrosine kinases, Jak1 and Jak2, with its receptor." J Biol Chem **269**(20): 14333-14336.

Jenmalm, M. C., H. Cherwinski, et al. (2006). "Regulation of myeloid cell function through the CD200 receptor." J Immunol **176**(1): 191-199.

Jurgens, H. A. and R. W. Johnson (2010). "Dysregulated neuronal-microglial cross-talk during aging, stress and inflammation." Exp Neurol.

Kawai, T. and S. Akira (2007). "TLR signaling." Semin Immunol **19**(1): 24-32.

Kawanokuchi, J., T. Mizuno, et al. (2006). "Production of interferon-gamma by microglia." Mult Scler **12**(5): 558-564.

Ko, Y. C., H. F. Chien, et al. (2009). "Endothelial CD200 is heterogeneously distributed, regulated and involved in immune cell-endothelium interactions." J Anat **214**(1): 183-195.

Kong, L. Y., M. K. McMillian, et al. (1997). "Inhibition of lipopolysaccharide-induced nitric oxide and cytokine production by ultralow concentrations of dynorphins in mixed glia cultures." J Pharmacol Exp Ther **280**(1): 61-66.

Koning, N., D. F. Swaab, et al. (2009). "Distribution of the immune inhibitory molecules CD200 and CD200R in the normal central nervous system and multiple sclerosis lesions suggests neuron-glia and glia-glia interactions." J Neuropathol Exp Neurol **68**(2): 159-167.

Lang, T. J., P. Nguyen, et al. (2002). "In vivo CD86 blockade inhibits CD4+ T cell activation, whereas CD80 blockade potentiates CD8+ T cell activation and CTL effector function." J Immunol **168**(8): 3786-3792.

Lee, E., S. Chanamara, et al. (2012). "IFN-gamma signaling in the central nervous system controls the course of experimental autoimmune encephalomyelitis independently of the localization and composition of inflammatory foci." J Neuroinflammation 9: 7.

Letiembre, M., W. Hao, et al. (2007). "Innate immune receptor expression in normal brain aging." Neuroscience 146(1): 248-254.

Letiembre, M., Y. Liu, et al. (2009). "Screening of innate immune receptors in neurodegenerative diseases: a similar pattern." Neurobiol Aging 30(5): 759-768.

Liu, B. and J. S. Hong (2003). "Role of microglia in inflammation-mediated neurodegenerative diseases: mechanisms and strategies for therapeutic intervention." J Pharmacol Exp Ther 304(1): 1-7.

Loke, P., M. G. Nair, et al. (2002). "IL-4 dependent alternatively-activated macrophages have a distinctive in vivo gene expression phenotype." BMC Immunol 3: 7.

Lotze, M. T. and K. J. Tracey (2005). "High-mobility group box 1 protein (HMGB1): nuclear weapon in the immune arsenal." Nat Rev Immunol 5(4): 331-342.

Lyons, A., E. J. Downer, et al. (2012). "Dok2 mediates the CD200Fc attenuation of Abeta-induced changes in glia." J Neuroinflammation 9(1): 107.

Lyons, A., E. J. Downer, et al. (2007). "CD200 ligand receptor interaction modulates microglial activation in vivo and in vitro: a role for IL-4." J Neurosci 27(31): 8309-8313.

Lyons, A., A. M. Lynch, et al. (2009). "Fractalkine-induced activation of the phosphatidylinositol-3 kinase pathway attentuates microglial activation in vivo and in vitro." J Neurochem 110(5): 1547-1556.

Lyons, A., K. McQuillan, et al. (2009). "Decreased neuronal CD200 expression in IL-4-deficient mice results in increased neuroinflammation in response to lipopolysaccharide." Brain Behav Immun 23(7): 1020-1027.

Ma, J., T. Chen, et al. (2003). "Regulation of macrophage activation." Cell Mol Life Sci 60(11): 2334-2346.

Madonna, S., C. Scarponi, et al. (2008). "Suppressor of cytokine signaling 1 inhibits IFN-gamma inflammatory signaling in human keratinocytes by sustaining ERK1/2 activation." FASEB J 22(9): 3287-3297.

Maher, F. O., Y. Nolan, et al. (2005). "Downregulation of IL-4-induced signalling in hippocampus contributes to deficits in LTP in the aged rat." Neurobiol Aging 26(5): 717-728.

Martinez, F. O., L. Helming, et al. (2009). "Alternative activation of macrophages: an immunologic functional perspective." Annu Rev Immunol **27**: 451-483.

Matyszak, M. K. (1998). "Inflammation in the CNS: balance between immunological privilege and immune responses." Prog Neurobiol **56**(1): 19-35.

Matyszak, M. K. and V. H. Perry (1995). "Demyelination in the central nervous system following a delayed-type hypersensitivity response to bacillus Calmette-Guerin." Neuroscience **64**(4): 967-977.

McBride, W. H., J. S. Economou, et al. (1990). "Influences of interleukins 2 and 4 on tumor necrosis factor production by murine mononuclear phagocytes." Cancer Res **50**(10): 2949-2952.

McMaster, W. R. and A. F. Williams (1979). "Identification of Ia glycoproteins in rat thymus and purification from rat spleen." Eur J Immunol **9**(6): 426-433.

Medawar, P. B. (1948). "Immunity to homologous grafted skin; the fate of skin homografts transplanted to the brain, to subcutaneous tissue, and to the anterior chamber of the eye." Br J Exp Pathol **29**(1): 58-69.

Meuth, S. G., O. J. Simon, et al. (2008). "CNS inflammation and neuronal degeneration is aggravated by impaired CD200-CD200R-mediated macrophage silencing." J Neuroimmunol **194**(1-2): 62-69.

Mihrshahi, R., A. N. Barclay, et al. (2009). "Essential roles for Dok2 and RasGAP in CD200 receptor-mediated regulation of human myeloid cells." J Immunol **183**(8): 4879-4886.

Minas, K. and J. Liversidge (2006). "Is the CD200/CD200 receptor interaction more than just a myeloid cell inhibitory signal?" Crit Rev Immunol **26**(3): 213-230.

Miyake, K. (2007). "Innate immune sensing of pathogens and danger signals by cell surface Toll-like receptors." Semin Immunol **19**(1): 3-10.

Mokoena, T. and S. Gordon (1985). "Human macrophage activation. Modulation of mannosyl, fucosyl receptor activity in vitro by lymphokines, gamma and alpha interferons, and dexamethasone." J Clin Invest **75**(2): 624-631.

Mosser, D. M. (2003). "The many faces of macrophage activation." J Leukoc Biol **73**(2): 209-212.

Mosser, D. M. and J. P. Edwards (2008). "Exploring the full spectrum of macrophage activation." Nat Rev Immunol **8**(12): 958-969.

Mukhopadhyay, S., A. Pluddemann, et al. (2010). "Immune inhibitory ligand CD200 induction by TLRs and NLRs limits macrophage activation to protect the host from meningococcal septicemia." Cell Host Microbe **8**(3): 236-247.

Murphy, A. C., S. J. Lalor, et al. (2010). "Infiltration of Th1 and Th17 cells and activation of microglia in the CNS during the course of experimental autoimmune encephalomyelitis." Brain Behav Immun **24**(4): 641-651.

Murphy, J. B. a. S., E. (1923). "Conditions determining the transplantability of tissues in the brain. ." *J. Exp. Med*(38): 183-197.

Nabavi, N., G. J. Freeman, et al. (1992). "Signalling through the MHC class II cytoplasmic domain is required for antigen presentation and induces B7 expression." Nature **360**(6401): 266-268.

Nathan, C. and W. A. Muller (2001). "Putting the brakes on innate immunity: a regulatory role for CD200?" Nat Immunol **2**(1): 17-19.

Nedergaard, M., B. Ransom, et al. (2003). "New roles for astrocytes: redefining the functional architecture of the brain." Trends Neurosci **26**(10): 523-530.

Neumann, H. (2001). "Control of glial immune function by neurons." Glia **36**(2): 191-199.

Ngai, P., S. McCormick, et al. (2007). "Gamma interferon responses of CD4 and CD8 T-cell subsets are quantitatively different and independent of each other during pulmonary Mycobacterium bovis BCG infection." Infect Immun **75**(5): 2244-2252.

Nguyen, V. T. and E. N. Benveniste (2000). "IL-4-activated STAT-6 inhibits IFN-gamma-induced CD40 gene expression in macrophages/microglia." J Immunol **165**(11): 6235-6243.

Nimmerjahn, A., F. Kirchhoff, et al. (2005). "Resting microglial cells are highly dynamic surveillants of brain parenchyma in vivo." Science **308**(5726): 1314-1318.

Nitta, T., M. Hata, et al. (2003). "Size-selective loosening of the blood-brain barrier in claudin-5-deficient mice." J Cell Biol **161**(3): 653-660.

Nolan, Y., F. O. Maher, et al. (2005). "Role of interleukin-4 in regulation of age-related inflammatory changes in the hippocampus." J Biol Chem **280**(10): 9354-9362.

Oh, C. K., G. P. Geba, et al. (2010). "Investigational therapeutics targeting the IL-4/IL-13/STAT-6 pathway for the treatment of asthma." Eur Respir Rev **19**(115): 46-54.

Panek, R. B. and E. N. Benveniste (1995). "Class II MHC gene expression in microglia. Regulation by the cytokines IFN-gamma, TNF-alpha, and TGF-beta." J Immunol **154**(6): 2846-2854.

Park, J. S., D. Svetkauskaite, et al. (2004). "Involvement of toll-like receptors 2 and 4 in cellular activation by high mobility group box 1 protein." J Biol Chem **279**(9): 7370-7377.

Perry, V. H., C. Cunningham, et al. (2007). "Systemic infections and inflammation affect chronic neurodegeneration." Nat Rev Immunol **7**(2): 161-167.

Ponomarev, E. D., L. P. Shriver, et al. (2006). "CD40 expression by microglial cells is required for their completion of a two-step activation process during central nervous system autoimmune inflammation." J Immunol **176**(3): 1402-1410.

Ponomarev, E. D., L. P. Shriver, et al. (2005). "Microglial cell activation and proliferation precedes the onset of CNS autoimmunity." J Neurosci Res **81**(3): 374-389.

Prendergast, C. T. and S. M. Anderton (2009). "Immune cell entry to central nervous system--current understanding and prospective therapeutic targets." Endocr Metab Immune Disord Drug Targets **9**(4): 315-327.

Preston, S., G. J. Wright, et al. (1997). "The leukocyte/neuron cell surface antigen OX2 binds to a ligand on macrophages." Eur J Immunol **27**(8): 1911-1918.

Qin, Y. H., S. M. Dai, et al. (2009). "HMGB1 enhances the proinflammatory activity of lipopolysaccharide by promoting the phosphorylation of MAPK p38 through receptor for advanced glycation end products." J Immunol **183**(10): 6244-6250.

Ramprasad, M. P., V. Terpstra, et al. (1996). "Cell surface expression of mouse macrosialin and human CD68 and their role as macrophage receptors for oxidized low density lipoprotein." Proc Natl Acad Sci U S A **93**(25): 14833-14838.

Rezai-Zadeh, K., D. Gate, et al. (2009). "CNS infiltration of peripheral immune cells: D-Day for neurodegenerative disease?" J Neuroimmune Pharmacol **4**(4): 462-475.

Rio-Hortega, D. (1932). "Cytology and cellular pathology of the nervous system." Microglia: 483-534.

Roy, A., Y. K. Fung, et al. (2006). "Up-regulation of microglial CD11b expression by nitric oxide." J Biol Chem **281**(21): 14971-14980.

Saijo, K. and C. K. Glass (2011). "Microglial cell origin and phenotypes in health and disease." Nat Rev Immunol **11**(11): 775-787.

Saitou, M., M. Furuse, et al. (2000). "Complex phenotype of mice lacking occludin, a component of tight junction strands." Mol Biol Cell **11**(12): 4131-4142.

Sarangi, P. P., S. R. Woo, et al. (2009). "Control of viral immunoinflammatory lesions by manipulating CD200:CD200 receptor interaction." Clin Immunol **131**(1): 31-40.

Sawada, M., Y. Itoh, et al. (1993). "Expression of cytokine receptors in cultured neuronal and glial cells." Neurosci Lett **160**(2): 131-134.

Schroder, K., P. J. Hertzog, et al. (2004). "Interferon-gamma: an overview of signals, mechanisms and functions." J Leukoc Biol **75**(2): 163-189.

Schroder, K. and R. Jaster (2004). "Interferon-alpha inhibits interleukin-3-induced proliferation of Ba/F3 cells in a protein kinase R-dependent manner." Cell Signal **16**(2): 167-174.

Sedgwick, J. D., S. Schwender, et al. (1991). "Isolation and direct characterization of resident microglial cells from the normal and inflamed central nervous system." Proc Natl Acad Sci U S A **88**(16): 7438-7442.

Sha, Y., J. Zmijewski, et al. (2008). "HMGB1 develops enhanced proinflammatory activity by binding to cytokines." J Immunol **180**(4): 2531-2537.

Shinohara, H., A. Inoue, et al. (2005). "Dok-1 and Dok-2 are negative regulators of lipopolysaccharide-induced signaling." J Exp Med **201**(3): 333-339.

Shirai, Y. (1921). "On the transplantation of the rat sarcoma in adult heterogenous animals." *Jap. Med. World*(1): 14-15.

Sibley, W. A., C. R. Bamford, et al. (1985). "Clinical viral infections and multiple sclerosis." Lancet **1**(8441): 1313-1315.

Snelgrove, R. J., J. Goulding, et al. (2008). "A critical function for CD200 in lung immune homeostasis and the severity of influenza infection." Nat Immunol **9**(9): 1074-1083.

Somjen, G. G. (1988). "Nervenkitt: notes on the history of the concept of neuroglia." Glia **1**(1): 2-9.

Stein, M., S. Keshav, et al. (1992). "Interleukin 4 potently enhances murine macrophage mannose receptor activity: a marker of alternative immunologic macrophage activation." J Exp Med **176**(1): 287-292.

Stevenson, P. G., S. Hawke, et al. (1997). "The immunogenicity of intracerebral virus infection depends on anatomical site." J Virol **71**(1): 145-151.

Streit, W. J. (2002). "Microglia as neuroprotective, immunocompetent cells of the CNS." Glia **40**(2): 133-139.

Streit, W. J., S. A. Walter, et al. (1999). "Reactive microgliosis." Prog Neurobiol **57**(6): 563-581.

Szabo, S. J., B. M. Sullivan, et al. (2002). "Distinct effects of T-bet in TH1 lineage commitment and IFN-gamma production in CD4 and CD8 T cells." Science **295**(5553): 338-342.

Takeuchi, O., K. Hoshino, et al. (1999). "Differential roles of TLR2 and TLR4 in recognition of gram-negative and gram-positive bacterial cell wall components." Immunity **11**(4): 443-451.

Tan, J., T. Town, et al. (2000). "CD45 opposes beta-amyloid peptide-induced microglial activation via inhibition of p44/42 mitogen-activated protein kinase." J Neurosci **20**(20): 7587-7594.

Tate, M. D., D. L. Pickett, et al. (2010). "Critical role of airway macrophages in modulating disease severity during influenza virus infection of mice." J Virol **84**(15): 7569-7580.

Theele, D. P. and W. J. Streit (1993). "A chronicle of microglial ontogeny." Glia **7**(1): 5-8.

Triantafilou, M., F. G. Gamper, et al. (2006). "Membrane sorting of toll-like receptor (TLR)-2/6 and TLR2/1 heterodimers at the cell surface determines heterotypic associations with CD36 and intracellular targeting." J Biol Chem **281**(41): 31002-31011.

Triantafilou, M. and K. Triantafilou (2002). "Lipopolysaccharide recognition: CD14, TLRs and the LPS-activation cluster." Trends Immunol **23**(6): 301-304.

Tritsch, N. X. and D. E. Bergles (2007). "Defining the role of astrocytes in neuromodulation." Neuron **54**(4): 497-500.

Tsan, M. F. and B. Gao (2004). "Endogenous ligands of Toll-like receptors." J Leukoc Biol **76**(3): 514-519.

Tsan, M. F. and B. Gao (2007). "Pathogen-associated molecular pattern contamination as putative endogenous ligands of Toll-like receptors." J Endotoxin Res **13**(1): 6-14.

Varnum, M. M. and T. Ikezu (2012). "The classification of microglial activation phenotypes on neurodegeneration and regeneration in Alzheimer's disease brain." Arch Immunol Ther Exp (Warsz) **60**(4): 251-266.

Volterra, A. and J. Meldolesi (2005). "Astrocytes, from brain glue to communication elements: the revolution continues." Nat Rev Neurosci **6**(8): 626-640.

Walker, D. G., J. E. Dalsing-Hernandez, et al. (2009). "Decreased expression of CD200 and CD200 receptor in Alzheimer's disease: a potential mechanism leading to chronic inflammation." Exp Neurol **215**(1): 5-19.

Wang, J., J. Wakeham, et al. (1999). "Macrophages are a significant source of type 1 cytokines during mycobacterial infection." J Clin Invest **103**(7): 1023-1029.

Wang, X. J., M. Ye, et al. (2007). "CD200-CD200R regulation of microglia activation in the pathogenesis of Parkinson's disease." J Neuroimmune Pharmacol **2**(3): 259-264.

Watson, M. B., D. A. Costello, et al. (2010). "SIGIRR modulates the inflammatory response in the brain." Brain Behav Immun **24**(6): 985-995.

Webb, M. and A. N. Barclay (1984). "Localisation of the MRC OX-2 glycoprotein on the surfaces of neurones." J Neurochem **43**(4): 1061-1067.

Wen, H., D. D. Watry, et al. (2004). "Selective decrease in paracellular conductance of tight junctions: role of the first extracellular domain of claudin-5." Mol Cell Biol **24**(19): 8408-8417.

Wilson, E. H., W. Weninger, et al. (2010). "Trafficking of immune cells in the central nervous system." J Clin Invest **120**(5): 1368-1379.

Wood, M. J., H. M. Charlton, et al. (1996). "Immune responses to adenovirus vectors in the nervous system." Trends Neurosci **19**(11): 497-501.

Woodland, D. L. and R. W. Dutton (2003). "Heterogeneity of CD4(+) and CD8(+) T cells." Curr Opin Immunol **15**(3): 336-342.

Wright, G. J., H. Cherwinski, et al. (2003). "Characterization of the CD200 receptor family in mice and humans and their interactions with CD200." J Immunol **171**(6): 3034-3046.

Wright, G. J., M. J. Puklavec, et al. (2000). "Lymphoid/neuronal cell surface OX2 glycoprotein recognizes a novel receptor on macrophages implicated in the control of their function." Immunity **13**(2): 233-242.

Yang, H., H. Wang, et al. (2002). "HMGB1 as a cytokine and therapeutic target." J Endotoxin Res **8**(6): 469-472.

Ye, S. M. and R. W. Johnson (2001). "An age-related decline in interleukin-10 may contribute to the increased expression of interleukin-6 in brain of aged mice." Neuroimmunomodulation **9**(4): 183-192.

Zhang, D., G. Zhang, et al. (2004). "A toll-like receptor that prevents infection by uropathogenic bacteria." Science **303**(5663): 1522-1526.

Appendix I

List of Publications to date

Costello DA, Lyons A, **Denieffe S**, Browne T, Cox FF, Lynch MA. (2011) Long-term potentiation is impaired in CD200-deficient mice: a role for Toll-like receptor activation. The Journal of Biological Chemistry, 286, 34722-34732

Stephanie Denieffe*, Ronan J. Kelly*, Anthony Lyons and Marina A. Lynch. Classical activation of microglia in CD200-deficient mice is a consequence of blood brain barrier permeability and infiltration of peripheral cells. (Submitted for review, The Journal of Biological Chemistry; MS ID# JBC/2012/448035).

Conference Presentations

S. Denieffe, M.A. Lynch (2012). Modulation of Microglial phenotypes by CD200. Poster presentation delivered at International society of Neuroimmunology, Boston, Massachusetts, November 2012

S. Denieffe, R.J. Kelly, A. Lyons, M.A. Lynch (2012). Increased responsiveness to LPS in CD200-deficient mice is associated with increased blood brain barrier permeability and infiltration of peripheral cells. Poster presentation delivered at International society of Neuroimmunology, Boston, Massachusetts, November 2012

S. Denieffe, M.A. Lynch (2011). The effect of CD200 fusion protein on LPS- and IFNγ-induced changes in microglial activation. Poster presentation delivered at the 4th School of Medicine Postgraduate Research Day, Bioscience Building, Trinity College, Dublin, September 2011

S. Denieffe, M.A. Lynch (2011). CD200 fusion protein suppresses IFNγ- but not LPS-induced changes in microglial activation. Poster presentation delivered at Neuroscience Ireland, Maynooth, September 2011

S. Denieffe, M.A. Lynch (2011). CD200-CD200R interaction suppresses the IFNγ induced classical activation of microglia. Poster presentation delivered at British neuroscience association, Harrogate, UK. April 2011

S. Denieffe, M.A. Lynch (2011). Increased TLR4 in CD200KO mice is responsible for the exaggerated response to LPS in vitro and in vivo. Oral presentation delivered at Masterclass meeting "Cytokines in the brain: the good, the bad and the ugly" in the Science Gallery, Trinity College Dublin, February 2011

S. Denieffe, M.A. Lynch (2010). The increase of TLR4 in CD200$^{-/-}$ mice is responsible for the exaggerated response to LPS in vitro. Poster presentation delivered at Neuroscience Ireland, University College Dublin, September 2010

S. Denieffe, M.A. Lynch (2010). Increased NFκB signaling in CD200$^{-/-}$ mice is responsible for the exaggerated response to LPS in vitro. Poster presentation

delivered at the 3th School of Medicine Postgraduate Research Day, Bioscience Building, Trinity College, Dublin, September 2010

Grants and Awards

Awarded travel bursary from Trinity College in order to attend the British Neuroscience Association, Harrogate, April 2011

AbD Serotec

Medical Supply Ltd.
Damastown,
Mulhuddart,
Dublin 15
Ireland

Applied Biosystems

Applied Biosystems
Frankfurter street 129b
64293 Darmstadt
Germany

BD Bioscience

BD Pharmingen
10975 Torreyana Road
San Diego
CA 92121
US

Beckman Coulter

Beckman Coulter Inc.
4300 N Harbour Boulevard
PO Box 3100
Fullerton
CA 92834
US

Biolegend

Medical Supply Ltd.
Damastown
Mulhuddart
Dublin 15
Ireland

Biosciences

Biosciences Ltd.
3 Charlemont Terrace
Crofton Road
Dun Laoghaire
Co. Dublin
Ireland

Dako

Alere Ltd.
Pepper road
Hazel Grove
Stockport SK7 SBW
UK

eBioscience	eBioscience 2nd Floor Titan Court 3 Bishop Square Hatfield AL 10 9NA UK
Fisher Scientific	Fisher Scientific Suit 3, Plaza Q12 Blanchardstown Corporate park Ballycoolin Dublin 15 Ireland
Gibco	Gibco Ltd. 3 Fountain drive Linchinnan Drive Paisley PA4 9RF Scotland UK
Hycult Biotech	Frontstraat 2A 5405 PB UDEN Netherlands
Invitrogen	Invitrogen Ltd. 3 Fountain drive Linchinnan Drive Paisley PA4 9RF Scotland UK
Macherey-Nagel	Labquip Ireland 12 The Business Centre Fonthill Industrial Park Clondalkin Dublin 22 Ireland
Miltenyi Biotech	Miltenyi Biotech Almac House Church Lane Surrey GU24 9DR UK

Long Term Potentiation Is Impaired in Membrane Glycoprotein CD200-deficient Mice

A ROLE FOR Toll-LIKE RECEPTOR ACTIVATION*

Derek A. Costello[1,2], Anthony Lyons[1], Stephanie Denieffe, Tara C. Browne, F. Fionnuala Cox, and Marina A. Lynch
From the Department of Physiology and the Trinity College Institute of Neuroscience, Trinity College, Dublin 2, Ireland

The membrane glycoprotein CD200 is expressed on several cell types, including neurons, whereas expression of its receptor, CD200R, is restricted principally to cells of the myeloid lineage, including microglia. The interaction between CD200 and CD200R maintains microglia and macrophages in a quiescent state; therefore, CD200-deficient mice express an inflammatory phenotype exhibiting increased macrophage or microglial activation in models of arthritis, encephalitis, and uveoretinitis. Here, we report that lipopolysaccharide (LPS) and Pam3CysSerLys4 exerted more profound effects on release of the proinflammatory cytokines, interleukin (IL)-1β, IL-6, and tumor necrosis factor-α (TNFα), in glia prepared from CD200$^{-/-}$ mice compared with wild type mice. This effect is explained by the loss of CD200 on astrocytes, which modulates microglial activation. Expression of Toll-like receptors 4 and 2 (TLR4 and -2) was increased in glia prepared from CD200$^{-/-}$ mice, and the evidence indicates that microglial activation, assessed by the increased numbers of CD11b$^+$ cells that stained positively for both MHCII and CD40, was enhanced in CD200$^{-/-}$ mice compared with wild type mice. These neuroinflammatory changes were associated with impaired long term potentiation (LTP) in CA1 of hippocampal slices prepared from CD200$^{-/-}$ mice. One possible explanation for this is the increase in TNFα in hippocampal tissue prepared from CD200$^{-/-}$ mice because TNFα application inhibited LTP in CA1. Significantly, LPS and Pam3CysSerLys4, at concentrations that did not affect LTP in wild type mice, inhibited LTP in slices prepared from CD200$^{-/-}$ mice, probably due to the accompanying increase in TLR2 and TLR4. Thus, the neuroinflammatory changes that result from CD200 deficiency have a negative impact on synaptic plasticity.

CD200 is a type-1 membrane glycoprotein which has been identified as an immunosuppressive molecule, consistent with its expression on cells of the immune system, including dendritic cells, T and B cells, and endothelial and epithelial cells (1). Diverse immunomodulatory roles for CD200 have been reported; these include antigen-specific T cell responses, suppression of regulatory T cells (2), cytotoxic T cell-mediated tumor suppression (3), graft survival (4), and apoptosis-associated immune tolerance (5).

In the brain, CD200 is expressed on neurons (6) and oligodendrocytes (7) but not on microglia (8). A recent report has indicated that CD200 is expressed on reactive astrocytes in lesions from post-mortem multiple sclerosis brains (7). Expression of CD200R is mainly restricted to cells of the myeloid lineage and therefore, in the brain, has been identified on microglia (6, 7) but not on neurons (8). The complementary expression of ligand and receptor on neurons and microglia, respectively, suggests that their interaction may play a role in modulating microglial activation, and recent evidence has supported this contention. The LPS-induced increases in expression of cell surface markers of microglial activation and inflammatory cytokine production were inhibited by the addition of neurons, and this attenuating effect of neurons was blocked by an anti-CD200 antibody (8). This finding suggests that interaction of CD200 with its receptor has the capacity to modulate microglial activation.

In CD200-deficient mice, increased microglial and/or macrophage activation has been described in several models of inflammation (e.g. facial nerve transection, experimental autoimmune encephalomyelitis, an animal model of arthritis (9), and experimental autoimmune uveoretinitis (10)). Conversely, administration of a CD200 fusion protein ameliorates the inflammatory changes observed in collagen-induced arthritis (11, 12), whereas the decrease in experimental autoimmune encephalomyelitis-like symptoms in Wld^s mice has been attributed to increased expression of CD200 on spinal cord neurons (13).

Reduced expression of CD200 is coupled with increased microglial activation in hippocampus of aged and β-amyloid (Aβ)^3-treated rats (8, 14), and synaptic plasticity, specifically long term potentiation (LTP), is impaired when microglial activation is increased (15, 16). Therefore, we predicted that glia prepared from CD200-deficient mice would respond more profoundly to LPS and that this would be coupled with evidence of impaired LTP. The data show that LPS and Pam3Csk4 exert a greater effect on glia prepared from CD200$^{-/-}$ mice, presumably due to the observed increase in expression of TLR4 and TLR2 on these cells. In addition, LTP was markedly reduced at

[3] The abbreviations used are: Aβ, β-amyloid; LTP, long term potentiation; Pam3Csk4, Pam3CysSerLys4; EPSP, excitatory postsynaptic potential; TLR, Toll-like receptor; TBS, θ-burst stimulation; ANOVA, analysis of variance; PE, phycoerythrin; GFAP, glial fibrillary acidic protein; GLAST, L-glutamate/L-aspartate transporter.

CA1 synapses of hippocampal slices prepared from CD200$^{•/•}$, compared with wild type, mice. LPS and Pam$_3$Csk$_4$ further attenuated LTP in slices prepared from CD200$^{•/•}$ mice. The data provide further evidence for an important immunomodulatory role for CD200 and couple the loss of CD200 with a deficit in synaptic function and with increased expression of TLR2 and -4.

EXPERIMENTAL PROCEDURES

Animals—1-day-old and 2–6-month-old C57BL/6 or CD200$^{•/•}$ mice were used for preparation of glial cultures or for preparation of hippocampal slices, respectively. Tissue from 2–6-month-old mice was also used for analysis of expression of TLR2 and -4. All experiments were performed under license (Department of Health and Children, Ireland) and with ethical approval (BioResources, Trinity College, Dublin) in accordance with local guidelines. Animals were housed under controlled conditions (20–22 °C, food and water ad libitum) and maintained under veterinary supervision.

Preparation and Treatment of Primary Glial Cultures—Mixed glial cultures were prepared from 1-day-old C57BL/6 mice or CD200$^{•/•}$ mice as described previously (8). These cultures contained • 70% astrocytes and 30% microglia as assessed by expression of CD11b using FACS. We used mixed glia because CD200 is expressed on astrocytes but not microglia. This means that knocking out CD200 will have no impact on microglia unless they are in culture with astrocytes, and, in this case, the effect can be attributed to the loss of signaling through CD200R. In the context of this study, isolated microglia prepared from wild type and CD200$^{•/•}$ are essentially the same.

In one series of experiments, cells were harvested for flow cytometric analysis to evaluate expression of cell surface markers of microglial activation, for GLAST to identify astrocytes, or for PCR to evaluate expression of TLR2 and -4. In a second series of experiments, cells were incubated in the presence or absence of LPS (100 ng/ml; Alexis Biochemical) or Pam$_3$Csk$_4$ (100 ng/ml; InvivoGen), and, 24 h later, supernatant was collected and assessed for concentration of IL-1β, IL-6, and TNFα.

Purified astrocytes were prepared as described previously, using the shaking method to remove microglia (17), and membranes were isolated using a subcellular protein fractionation kit (Thermo Scientific). Cells were incubated in trypsin-EDTA (1 ml, 15 min, 37 °C), centrifuged (500 • g, 5 min), washed with ice-cold PBS, resuspended in PBS, and centrifuged (500 • g, 5 min). The pellet was resuspended in ice-cold Cytoplasmic Extraction Buffer containing protease inhibitors (Thermo Scientific), incubated (4 °C, 10 min), and centrifuged (3,000 • g, 5 min); the supernatant provided the cytosolic fraction, whereas the pellet, which contained the membrane fraction, was resuspended in ice-cold Membrane Extraction Buffer containing protease inhibitors (Thermo Scientific), incubated (4 °C, 10 min), and centrifuged (3,000 • g, 5 min). The resultant supernatant provided the membrane fraction.

To prepare microglia, cells were initially seeded onto 25-cm^2 flasks, and, after 24 h, medium was replaced with cDMEM containing GM-CSF (10 ng/ml) and M-CSF (20 ng/ml). After 10–14 days in culture, non-adherent microglia were harvested by shaking (110 rpm, 2 h, room temperature), tapping, and centrifuging (2,000 rpm, 5 min). The pellet was resuspended in cDMEM, and the microglia were plated onto 24-well plates at a density of 1 • 10^5 cells/ml and maintained at 37 °C in a 5% CO$_2$ humidified atmosphere for up to 3 days prior to treatment.

Flow Cytometry—Glial cells were trypsinized (0.25% trypsin-EDTA; Sigma) and washed three times in FACS buffer (2% FBS, 0.1% NaN$_3$ in PBS). Whole brain tissue was harvested and passed through a cell strainer (70 μm) and centrifuged (170 • g, 10 min). The pellet was resuspended in PBS containing collagenase D (1 mg/ml) and DNase I (200 μg/ml), incubated at 37 °C for 30 min, and centrifuged (170 • g, 5 min). Pellets were resuspended in 1.088 g/ml Percoll (9 ml), underlaid with 1.122 g/ml Percoll (5 ml), and overlaid with 1.072 and 1.030 g/ml (9 ml each) Percoll and PBS (9 ml) and centrifuged (1,250 • g, 45 min). The mononuclear cells (between 1.088:1.072 g/ml and between 1.072:1.030 g/ml) were centrifuged, and the pellets were washed. All cells were blocked for 15 min at room temperature in FACS block (Mouse BD Fc Block (BD Pharmingen); 1:500 in FACS buffer). Cells were incubated with PE-Cy7- or allophycocyanin-rat anti-mouse CD11b (BD Biosciences), FITC-rat anti-mouse CD40 (BD Biosciences), PE-rat anti-mouse MHCII (BD Biosciences), allophycocyanin-rat anti-mouse CD200 (BD Biosciences), PE-rat anti-mouse CD200R (Serotec), FITC-rat anti-mouse TLR2 (Cambridge Biosciences), FITC-rat anti-mouse TLR4 (Cambridge Biosciences), PE-Cy7-anti-mouse CD45 (BD Biosciences), and allophycocyanin-rat anti-mouse GLAST (BD Biosciences). Antibodies were diluted (1:400) in FACS buffer. Immunofluorescence analysis was performed on a DAKO Cyan ADP 7 color flow cytometer (DAKO Cytomation) with Summit version 4.3 software.

Real-time PCR Analysis of CD11b, CD40, TLR2, and TLR4—Total RNA was extracted from snap-frozen hippocampal tissue and harvested mixed glial cells using a NucleoSpin® RNAII isolation kit (Macherey-Nagel Inc.), and cDNA synthesis was performed on 1 μg of total RNA using a High Capacity cDNA RT kit (Applied Biosystems); the protocols used were according to the manufacturer's instructions. Real-time PCR was performed as described previously (8) using an ABI Prism 7300 instrument (Applied Biosystems). The primer IDs were as follows: CD11b, Mm01271265_m1; CD40, Mm00441895_m1; TLR2, Mm00442346_m1; TLR4, Mm00445273_m1 (Applied Biosystems). Samples were assayed in duplicate, and gene expression was calculated relative to the endogenous control samples (β-actin) to give a relative quantity value ($2^{•••Ct}$, where Ct is the threshold cycle).

Analysis of IL-1β, IL-6, and TNFα—The concentrations of IL-1β, IL-6, and TNFα were analyzed in triplicate by ELISA in samples of supernatant obtained from in vitro experiments as described previously (8).

Analysis of CD200, GFAP, pIκBα, IL-1α, IL-1β, and TNFα by Western Immunoblotting—Hippocampal lysate was assessed for expression of IL-1α, IL-1β, and TNFα; glial cell lysate was evaluated for expression of pIκBα; and membrane and cytosolic preparations obtained from purified astrocytes were evaluated for expression of CD200 and GFAP using standard Western immunoblotting methods (8, 18). Primary antibodies directed against CD200 (anti-goat; 1:500; Santa Cruz Biotechnology,

Inc., Santa Cruz, CA), GFAP (anti-rabbit; 1:1000; Invitrogen), pIκBα (Ser-32) (anti-rabbit; 1:1000; Cell Signaling), IL-1α (anti-goat; 1:1000; R&D Systems), IL-1β (anti-goat; 1:500; Santa Cruz Biotechnology, Inc.), and TNFα (anti-rabbit; 1:500; Cell Signaling) were incubated overnight at 4 °C. The secondary antibodies were conjugated to horseradish peroxidase (1:5000; Jackson Immunoresearch), and after a 2-h incubation step, membranes were washed, and protein complexes were visualized (Immobilon Western chemiluminescent substrate, Millipore). Membranes were stripped and probed for β-actin (to confirm equal loading) as described previously (8, 18). Images were captured using the Fujifilm LAS-3000 imager, and densitometric analysis was used to quantify expression of the proteins. Values are presented as mean · S.E., normalized to β-actin.

Hippocampal Slice Preparation and LTP Recording—Acute hippocampal slices (400 μm) from C57BL/6 and CD200⁺/⁺ mice were prepared using a McIlwain tissue chopper as described previously (18) and maintained in oxygenated artificial cerebrospinal fluid (125 mM NaCl, 1.25 mM KCl, 2 mM CaCl₂, 1.5 mM MgCl₂, 1.25 mM KH₂PO₄, 25 mM NaHCO₃, and 10 mM D-glucose) at room temperature (21–23 °C) in a holding chamber for a minimum of 1 h before being transferred to a submersion recording chamber. Slices were continuously perfused (2–3 ml/min) with oxygenated artificial cerebrospinal fluid at room temperature (21–23 °C). The Schaffer collateral-commissural pathway was stimulated at 0.033 Hz (0.1-ms duration; 30–50% of maximal excitatory postsynaptic potential (EPSP) amplitude) using a bipolar tungsten stimulation electrode (Advent Materials). Stable field EPSPs were recorded from the CA1 stratum radiatum using a monopolar glass recording electrode filled with artificial cerebrospinal fluid. We assessed input-output response and paired pulse facilitation to evaluate neurotransmission at CA1 synapses and found that there were no differences between slices obtained from wild type and CD200⁺/⁺ mice. In addition, there was no evidence of epileptiform activity in any slice. Stable base line EPSPs were recorded for 20 min prior to application of θ-burst stimulation (TBS; 10 trains (4 pulses at 100 Hz) repeated at 5 Hz (18)). In some experiments, LPS (Alexis Biochemicals) or Pam₃Csk₄ (InvivoGen) was added to the perfusate (10 μg/ml for 20 min or 20 μg/ml for 60 min) prior to TBS. In an additional set of experiments, slices were perfused with mouse recombinant TNFα (R&D Systems; 3 ng/ml in 0.002% BSA) or vehicle alone (0.002% BSA), for 20 min prior to LTP induction. This concentration of TNFα is less than that previously demonstrated to impair LTP in hippocampal slices prepared from rats (19, 20). Data were acquired using WinWCP version 4.0.7 software (Dr. J. Dempster, Strathclyde, UK). Evoked EPSPs were normalized to the slope recorded in the 5-min period prior to LTP induction. The level of LTP was evaluated as the mean percentage EPSP slope during the last 5 min of recording, and data are presented as mean percentage EPSP slope · S.E.

Hippocampal slices not used for electrophysiology were prepared for Western immunoblot analysis of IL-1α, IL-1β, and TNFα expression (described above). These slices were incubated as described for a minimum of 1 h following the slicing procedure plus a further incubation period equivalent to the duration of LTP recording.

Statistical Analysis—Data were analyzed using either Student's t test for independent means or analysis of variance (ANOVA) followed by post hoc Student Newman-Keuls test to determine which conditions were significantly different from each other. Data are expressed as means · S.E.

RESULTS

Loss of CD200 has been associated with evidence of increased inflammatory changes in hippocampal tissue prepared from aged animals as well as LPS- and Aβ-treated animals (8, 21). In this study, the effects of the TLR4 and TLR2 agonists, LPS and Pam₃Csk₄, were assessed on cytokine production in mixed glia prepared from wild type and CD200⁺/⁺ mice. The data indicate that incubation of cells prepared from wild type mice in the presence of LPS (100 ng/ml) increased release of the proinflammatory cytokines, IL-1β, IL-6, and TNFα, and the effect was significant in the case of IL-6 and TNFα (***, p · 0.001; ANOVA; Fig. 1, a–c). The effect of LPS was significantly greater in cells prepared from CD200⁺/⁺ mice (•••, p · 0.001; ANOVA; Fig. 1). Incubation of mixed glia prepared from wild type mice in the presence of Pam₃Csk₄ (100 ng/ml) also significantly increased release of inflammatory cytokines (**, p · 0.01; ***, p · 0.001; ANOVA; Fig. 1, d–f). The effect of Pam₃Csk₄ was greater in mixed glia prepared from CD200⁺/⁺ mice, and this was statistically significant in the case of IL-6 and TNFα (•••, p · 0.001; wild type versus CD200⁺/⁺; ANOVA). Both LPS and Pam₃Csk₄ also increased mRNA expression of these inflammatory cytokines, and the effect was greater in cells prepared from CD200⁺/⁺ mice (data not shown). These data indicate that tonic activation by CD200 modulates cytokine release from glia. Analysis of the effect of LPS on cytokine release prepared from purified microglia obtained from wild type and CD200⁺/⁺ mice revealed no genotype-related change for IL-1β (99.64 · 26.52 pg/ml versus 67.80 · 8.03 pg/ml for wild type and CD200⁺/⁺ cells, respectively), IL-6 (3,837 · 171.8 versus 3,875 · 144.8), and TNFα (1,559 · 88.31 versus 1,533 · 204.5). This is consistent with the view that isolated microglia prepared from CD200⁺/⁺ mice are unaffected, whereas when cultured with astrocytes that are deficient in CD200, an activated phenotype is evident.

Using CD11b as a marker of microglia, we show that the number of CD11b⁺ MHCII⁺ cells and CD11b⁺ CD40⁺ cells was increased in a mixed glial population prepared from CD200⁺/⁺ compared with wild type mice (Fig. 2). These data suggest that CD200 contributes to maintenance of microglia (in a mixed glial preparation) in a quiescent state and therefore suggest that CD200 is expressed on astrocytes. To date, its expression on astrocytes has been reported only on reactive astrocytes in lesions from post-mortem brains of individuals with multiple sclerosis (7). Here, flow cytometry was used to evaluate CD200 expression on GLAST⁺ cells in a purified culture of astrocytes prepared from wild type and CD200⁺/⁺ mice (Fig. 3, a and b). Although CD200 expression was evident on GLAST⁺ cells prepared from wild type mice, expression was absent on GLAST⁺ cells prepared from CD200⁺/⁺ mice. To confirm astrocytic expression of CD200, purified astrocytes were used to prepare membrane and cytosolic fractions for analysis by Western immunoblotting. CD200 was evident in
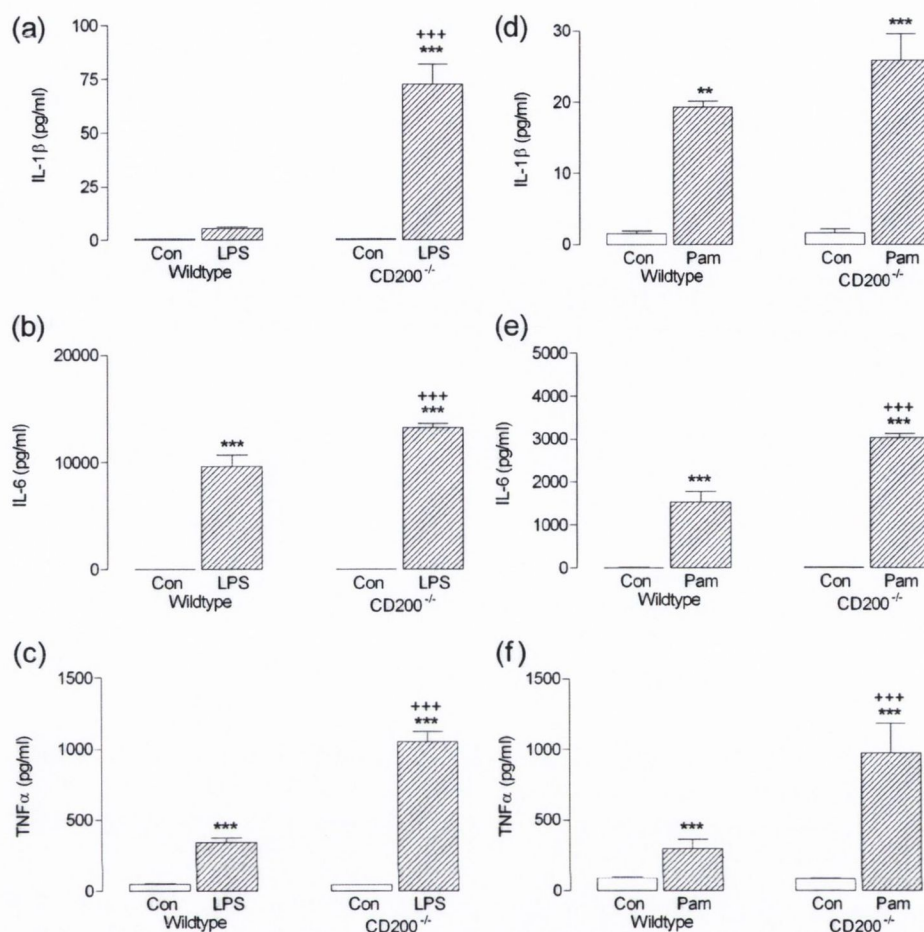
FIGURE 1. **TLR2- and TLR4-induced increases in inflammatory cytokines are enhanced in glia prepared from CD200$^{-/-}$ mice.** Incubation of mixed glia prepared from wild type mice in the presence of LPS (100 ng/ml; *a–c*) or Pam$_3$Csk$_4$ (*Pam*; 100 ng/ml; *d–f*) increased supernatant concentrations of IL-1β, IL-6, and TNFα (**, *p* • 0.01; ***, *p* • 0.001; ANOVA; *n* • 4–8), and the effect of LPS and Pam$_3$Csk$_4$ was significantly greater in cells prepared from CD200$^{• /•}$ mice (• • • , *p* • 0.001; ANOVA; *n* • 4–8). *Error bars*, S.E.

membrane, but not cytosolic, fractions (Fig. 3*c*), whereas GFAP expression was, predictably, largely confined to the cytosolic fractions.

A possible explanation for the increase in responsiveness of cells from CD200$^{• /•}$ mice to LPS and Pam$_3$Csk$_4$ is the significant increase in expression of both TLR2 and TLR4 mRNA in mixed glia prepared from CD200$^{• /•}$ compared with wild type mice (*, p • 0.05; Student's t test for independent means; Fig. 4, *a* and *d*). Flow cytometric analysis demonstrated that cell surface expression of both receptors was increased on CD11b$^•$ cells obtained from CD200$^{• /•}$ compared with wild type mice, but the increase was significant only in the case of TLR2 (**, p • 0.01; Student's t test for independent means; Fig. 4, *b*, *c*, *e*, and *f*). The significant increase in phosphorylated IκBα in cells prepared from CD200$^{• /•}$ compared with wild type mice (*, p • 0.05; Student's t test for independent means; Fig. 4*g*) indicates that signaling through TLR is up-regulated in cells prepared from CD200$^{• /•}$ mice.

CD200 deficiency is accompanied by inflammatory changes (9, 10), and, in the brain, microglial activation is coupled with decreased CD200 in brains of aged animals and also in LPS-treated and Aβ-treated animals (8, 21). To investigate this correlation further, we evaluated expression of surface markers of

microglial activation on cells prepared from CD200$^{• /•}$ and wild type mice using PCR and flow cytometry and show that CD40 mRNA, but not CD11b mRNA, was significantly increased in tissue prepared from CD200$^{• /•}$ compared with wild type mice (*, p • 0.05; Student's t test for independent means; Fig. 5, *a* and *b*). Analysis by flow cytometry indicated that there was no genotype-related change in CD11b$^•$ cells (Fig. 5*c*), but the percentage of CD11b$^•$ cells that were positive for MHCII and CD40 was significantly increased (*, p • 0.05; ***, p • 0.001; Student's t test for independent means; Fig. 5, *d–g*).

CD45 has been used as a means of discriminating between macrophages (which express high levels of CD45) and microglial (which express low levels of CD45 (22)). Flow cytometric analysis revealed that the numbers of CD11b$^•$ CD45^{low} cells were significantly increased in hippocampus of CD200$^{• /•}$ compared with wild type mice (***, p • 0.001; Student's t test for independent means; Fig. 6*a*) and that CD200R expression (*b*), CD40 (*c*), TLR2 (*d*), and TLR4 (*f*) on these cells was greater in tissue prepared from CD200$^{• /•}$ compared with wild type mice. The numbers of macrophages in the brain (i.e. CD11b$^•$ CD45^{high} cells) were negligible in CD200$^{• /•}$ and wild type mice. Analysis of expression of TLR in hippocampus revealed

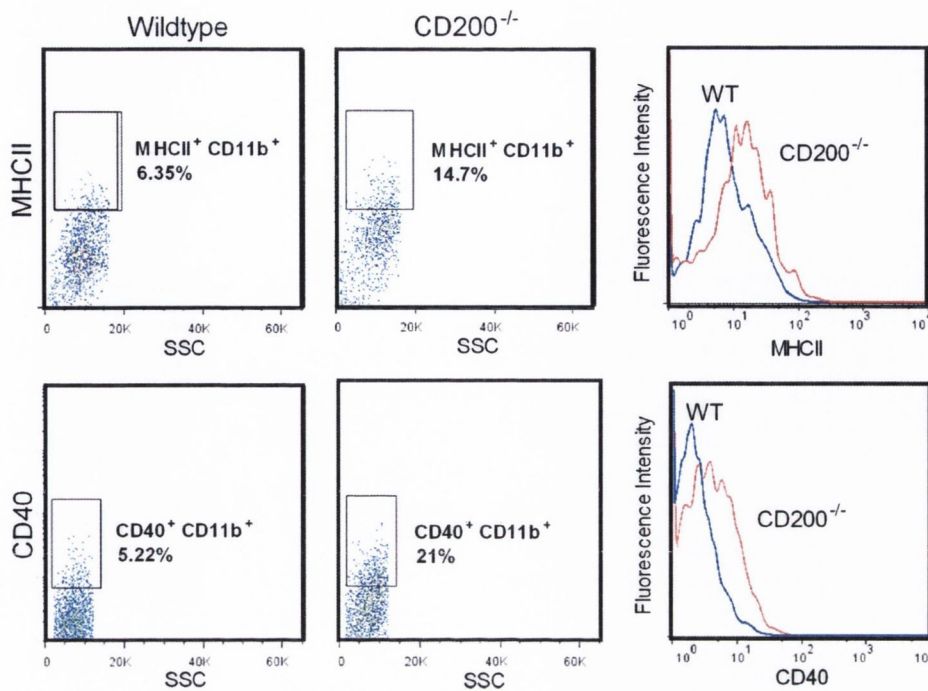FIGURE 2. **MHCII$^+$ CD11b$^+$ and CD40$^+$ CD11b$^+$ cells are increased in glia prepared from CD200$^{-/-}$ mice.** Shown is the mean percentage of CD11b* cells that also stained positively for MHCII* (*top panels*) and CD40 (*bottom panels*). Data are presented as target proteins *versus* side scatter (*SSC*). The *right-hand panels* illustrate representative overlays.
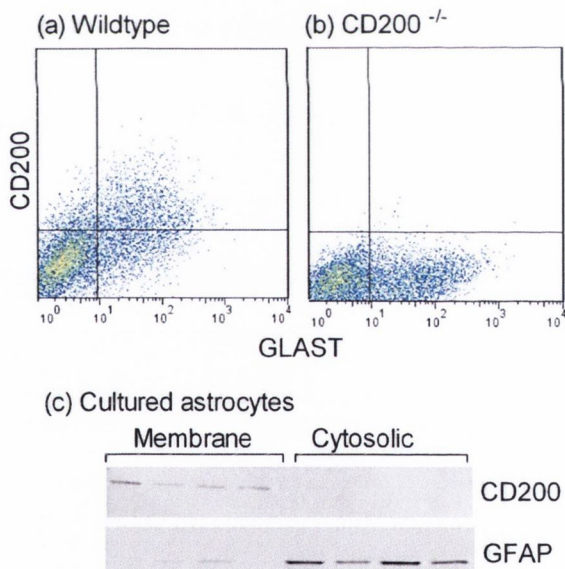

FIGURE 3. **CD200 is expressed on astrocytes.** CD200 expression was observed on GLAST* cells from purified astrocytic cultures obtained from wild type (*a*) but not CD200* /* (*b*) mice. CD200 was observed in membrane, but not cytosolic, fractions prepared from purified astrocytes obtained from wild type mice. GFAP expression was observed in the cytosolic fraction (*c*).

that both TLR2 and -4 were increased in CD200* /* compared with wild type mice (*, p • 0.05; **, p • 0.01; Student's t test for independent means; Fig. 6, e and g). These changes indicate that microglial activation occurs in brain tissue of CD200* /* mice, and therefore the changes in vitro are reflected in vivo, although the increase in expression of TLR2 mRNA in hippocampus is markedly greater than the change observed in cultured cells. Significantly, this was accompanied by a deficit in LTP in CA1

synapses where the response, 60 min following application of TBS, was markedly reduced in slices prepared from CD200* /* mice (12 slices from seven mice) compared with wild type mice (15 slices from 11 mice; p • 0.001; unpaired Student's t test; Fig. 6h). Although a number of inflammatory cytokines released from activated microglia might exert this effect (17–21), here we show that whereas expression of IL-1α and IL-1β were similar in hippocampal tissue prepared from wild type and CD200* /* mice (Fig. 7, a and b), TNFα was increased (p • 0.05; Student's t test for independent means; Fig. 7c). As previously demonstrated in hippocampal slices prepared from rats (19, 20, 23), application of TNFα (3 ng/ml) to mouse hippocampal slices significantly impaired LTP relative to vehicle controls (p • 0.05; unpaired Student's t test; three slices from two mice; Fig. 7d).

Because cells prepared from CD200* /* mice showed increased susceptibility to LPS, we predicted that concentrations of LPS that exerted no effect on LTP in wild type mice may attenuate it in CD200* /* mice. Application of LPS (20 μg/ml) to hippocampal slices from wild type mice for 60 min prior to TBS inhibited LTP (five slices from five mice) compared with controls (15 slices from 11 mice; p • 0.001; Fig. 8a). In contrast, a lower concentration of LPS (10 μg/ml; 20-min pretreatment), which exerted no effect on LTP in slices prepared from wild type mice (seven slices from six mice; Fig. 8b), significantly decreased LTP in slices from CD200* /* mice (13 slices from nine mice) relative to control (12 slices from seven mice; p • 0.05; Fig. 8c).

Like LPS, Pam$_3$Csk$_4$ exerted a greater effect on inflammatory markers in cells prepared from CD200* /* mice, and therefore we predicted that its effect on LTP would be genotype-specific. Application of Pam$_3$Csk$_4$ (20 μg/ml) to hippocampal slices pre-
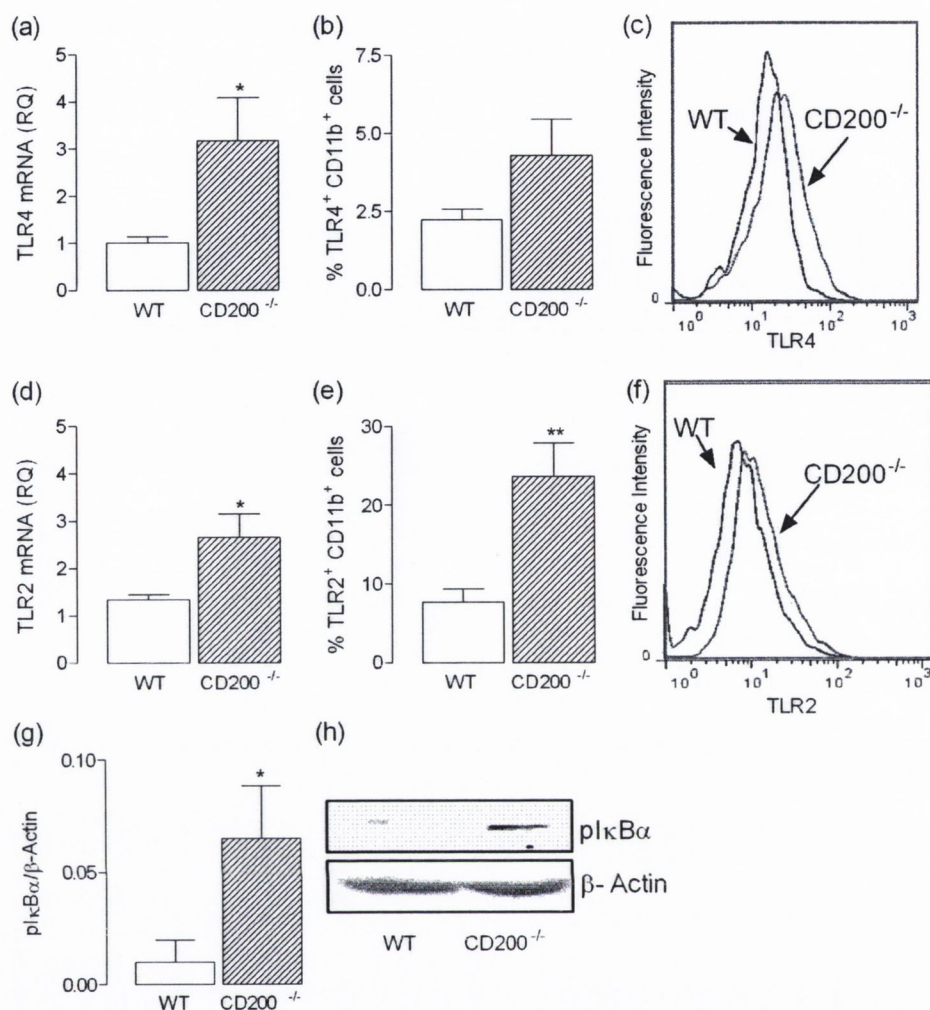
FIGURE 4. **Expression of TLR2 and TLR4 is increased in glia prepared from CD200$^{-/-}$ mice.** TLR4 mRNA (*a*) and TLR2 mRNA (*d*) and the number of CD11b$^+$ cells that stained positively for TLR4 (*b* and *c*) and TLR2 (*e* and *f*) were increased in glia prepared from CD200$^{-/-}$ compared with wild type mice (*, p • 0.05; Student's *t* test for independent means; n • 5). Mean data from densitometric analysis (*g*) and a sample immunoblot (*h*) reveal that phosphorylated IκBα is increased in cells prepared from CD200$^{-/-}$ compared with wild type mice (*, p • 0.05; Student's *t* test for independent means; n • 4–6). Error bars, S.E.

pared from wild type mice for 60 min prior to TBS inhibited LTP (three slices from three mice) compared with untreated controls (15 slices from 11 mice; p • 0.001; Fig. 9a). A lower concentration of Pam$_3$Csk$_4$ (10 μg/ml), applied for 20 min prior to TBS, did not affect LTP in slices prepared from wild type mice (four slices from three mice; Fig. 9b) but significantly reduced LTP in slices prepared from CD200$^{-/-}$ mice (six slices from five mice) compared with control (12 slices from seven mice; p • 0.05; Fig. 9c).

DISCUSSION

The loss of CD200 has a significant impact on activation of microglia in response to inflammatory stimuli, probably because of increased expression of TLR4 and TLR2 in vitro and in vivo. Whereas LTP in Schaffer collateral-CA1 synapses was markedly impaired in slices prepared from CD200-deficient mice under control conditions, activation of TLR4 and TLR2, by LPS and Pam$_3$Csk$_4$, respectively, exerted a more profound effect on LTP in slices prepared from CD200$^{-/-}$ mice. We pro-

pose that the increased expression of TLR4 and TLR2 provides a plausible explanation for the increased responsiveness of CD200$^{-/-}$ mice to inflammatory stimuli.

LPS and Pam$_3$Csk$_4$ increased the release of proinflammatory cytokines, IL-1β, IL-6, and TNFα, from mixed glial cultures, confirming previously described effects of TLR4 and TLR2 (21, 24, 25). Both agonists exerted a greater effect on release of proinflammatory cytokines in mixed glia prepared from CD200$^{-/-}$ mice, compared with wild type mice. Thus, tonic activation of CD200 receptor by CD200 is required to modulate inflammatory cytokine production. This concurs with data indicating that the interaction of neurons and microglia by means of CD200 receptor engagement by CD200 decreased microglial activation and production of IL-1β (8). In the current study, in which a mixed glial preparation was used, we propose that the modulating effect is a consequence of the interaction between microglia and astrocytes, which we demonstrate express CD200. It is known that CD200 is widely expressed on numerous cell types, although, in the case of astrocytes, expres-
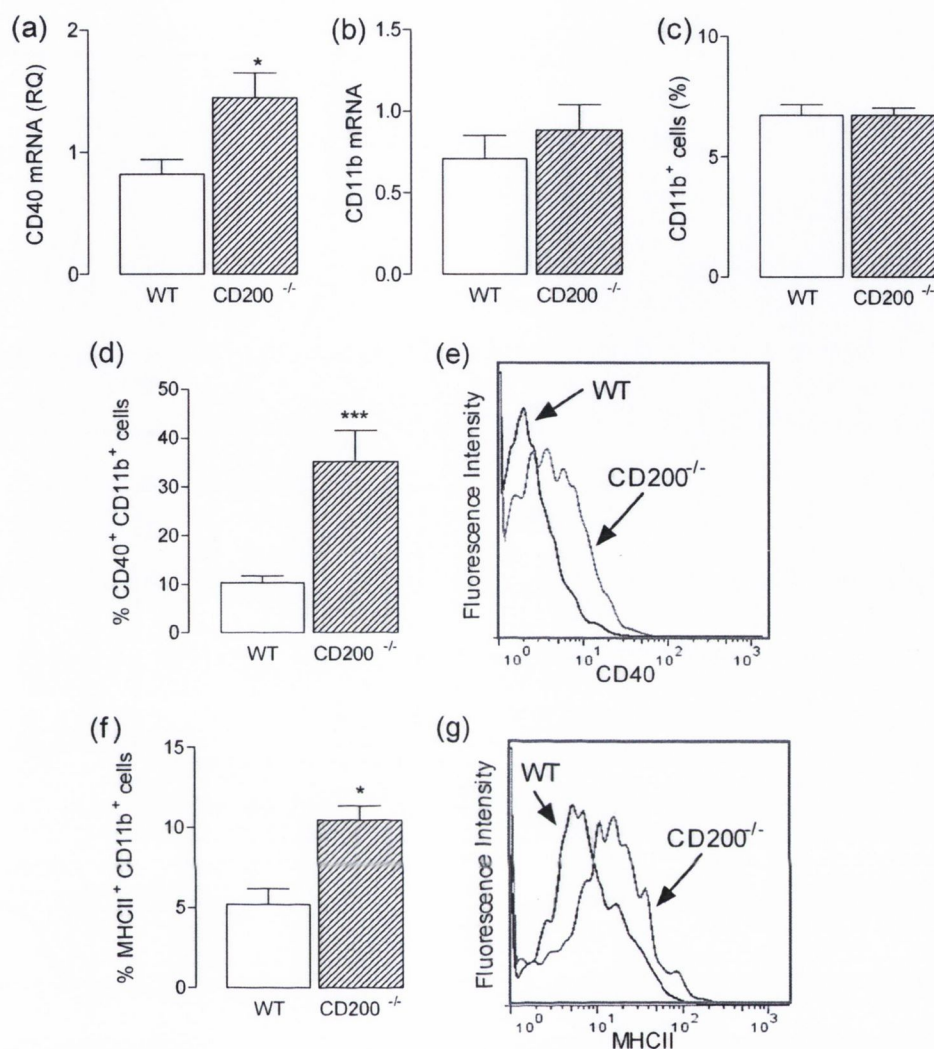
FIGURE 5. **Markers of microglial activation are increased in cells prepared from CD200$^{-/-}$ mice.** *a* and *b*, expression of CD40 mRNA, but not CD11b mRNA, was significantly greater in mixed glia prepared from CD200$^{·/·}$ compared with wild type mice (*, *p* • 0.05; Student's *t* test for independent means; *n* • 4–5). *c–f*, flow cytometric analysis revealed that the percentage of CD11b$^{·}$ cells was similar in wild type and CD200$^{·/·}$ (*c*), but the percentage of CD11b$^{·}$ cells that also stained positively for CD40 (*d* and *e*) and MHCII (*f* and *g*) was significantly greater in mixed glia obtained from CD200$^{·/·}$ compared with wild type mice (*, *p* • 0.05; ***, *p* • 0.001; Student's *t* test for independent means; *n* • 4–8). *Error bars*, S.E.

sion to date has been reported only on reactive astrocytes in lesions from post-mortem brains of individuals with multiple sclerosis (7). An interesting possibility is that the relatively activated state of microglia in a purified microglial culture may be a consequence of the loss of the CD200-controlled modulating effect of astrocytes.

The present findings in glia mirror those observed in peritoneal macrophages; thus, stimulation with LPS and peptidoglycan and also poly(I:C) increased release of TNFα and IL-6 to a greater extent in macrophages prepared from CD200$^{·/·}$ mice compared with wild type mice (26). Similarly, alveolar macrophages prepared from CD200$^{·/·}$ mice, when stimulated ex vivo with LPS or IFNγ, expressed more MHCII and released more inflammatory cytokines than macrophages from wild type mice (27). It has been known for many years that astrocytes are capable of modulating microglial/macrophage function. They have been shown to modulate LPS-induced changes in inducible nitric oxide synthase and NO production (28, 29) and

expression of MHCII (30), effects that have been attributed to astrocytic release of soluble factors like transforming growth factor TGFβ. The present findings uncover another mechanism by which astrocytes can modulate microglial activation.

Several studies have established that responses to insults that induce inflammatory changes are exacerbated in CD200$^{·/·}$ mice. Thus, the symptoms and inflammation associated with experimental autoimmune encephalomyelitis, Toxoplasma encephalitis, experimental autoimmune uveoretinitis, collagen-induced arthritis, and facial nerve transaction are more profound in CD200-deficient mice (9, 10, 31). In addition, the response to an influenza dose of hemagglutination was much more severe (inducing some fatalities) in CD200-deficient compared with wild type mice (27). Although it has been shown that CD200R activation by a CD200Fc ameliorates the symptoms associated with these conditions and although CD200R-mediated regulation of macrophages relies on the binding of Dok2 to the PTB binding motif in the cytoplasmic region of CD200R and
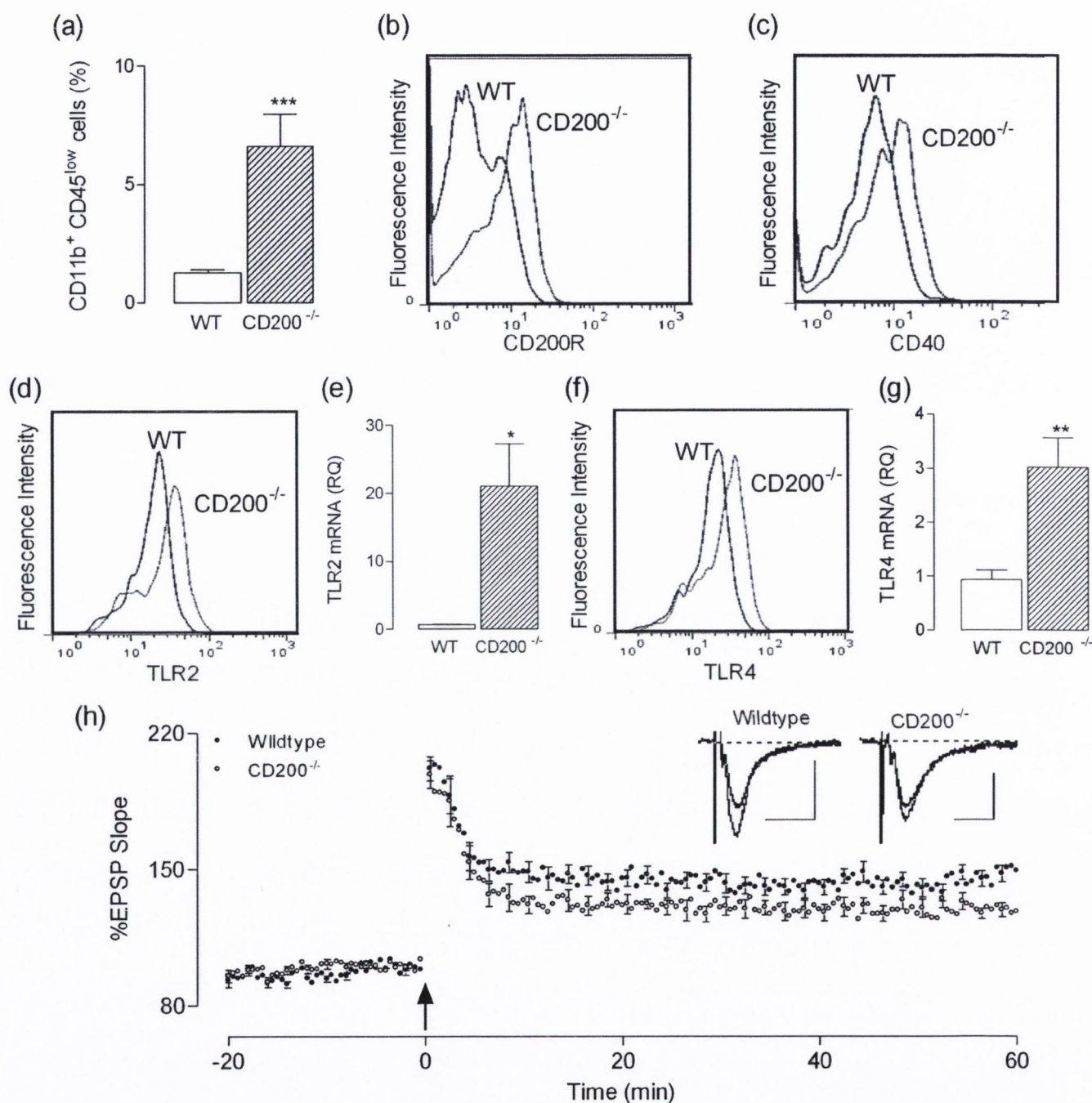
FIGURE 6. **The increase in hippocampal expression of TLR2 and TLR4 in CD200**$^{-/-}$ **mice is coupled with a deficit in LTP.** *a*, greater numbers of CD11b$^+$ CD45^{low} cells were found in the hippocampus of CD200$^{-/-}$ compared with wild type mice (***, $p < 0.001$; Student's t test for independent means), and expression of CD200R expression (*b*) and CD40 (*c*) was greater in tissue prepared from CD200$^{-/-}$ compared with wild type mice. TLR2 (*d*) and TLR4 (*f*) expression on CD11b$^+$ CD45^{low} cells was greater in tissue prepared from CD200$^{-/-}$ compared with wild type mice, whereas TLR2 mRNA (*e*) and TLR4 mRNA (*g*) expression were significantly increased in hippocampal tissue prepared from CD200$^{-/-}$ compared with wild type mice (*, $p < 0.05$; **, $p < 0.01$; Student's t test for independent means; $n = 5$). *h*, TBS (*arrow*) induced LTP in CA1 synapses of hippocampal slices prepared from wild type mice (15 slices from 11 mice). LTP, measured as mean percentage EPSP slope in the last 5 min of the experiment, was significantly reduced in slices prepared from CD200$^{-/-}$ mice relative to wild type mice ($p < 0.001$; 12 slices from seven mice). Sample recordings immediately before and 60 min following TBS are shown for wild type and CD200$^{-/-}$ mice (*scale bars*, 1 mV/20 ms). *Error bars*, S.E.

the subsequent recruitment and activation of RasGAP (32), the mechanism by which these changes lead to dampening the activation of macrophage/microglia remains to be fully explained. In this study, we show that increased expression of both TLR4 and TLR2 was observed in glia prepared from CD200$^{-/-}$ mice, and this may,

at least in part, provide an explanation for the susceptibility of CD200$^{-/-}$ mice to inflammatory stimuli. Both TLR2 and TLR4 ultimately lead to activation of NFκB, and, in this study, the increased receptor expression in glia prepared from CD200$^{-/-}$ mice is coupled with increased expression of phosphorylated IκB,
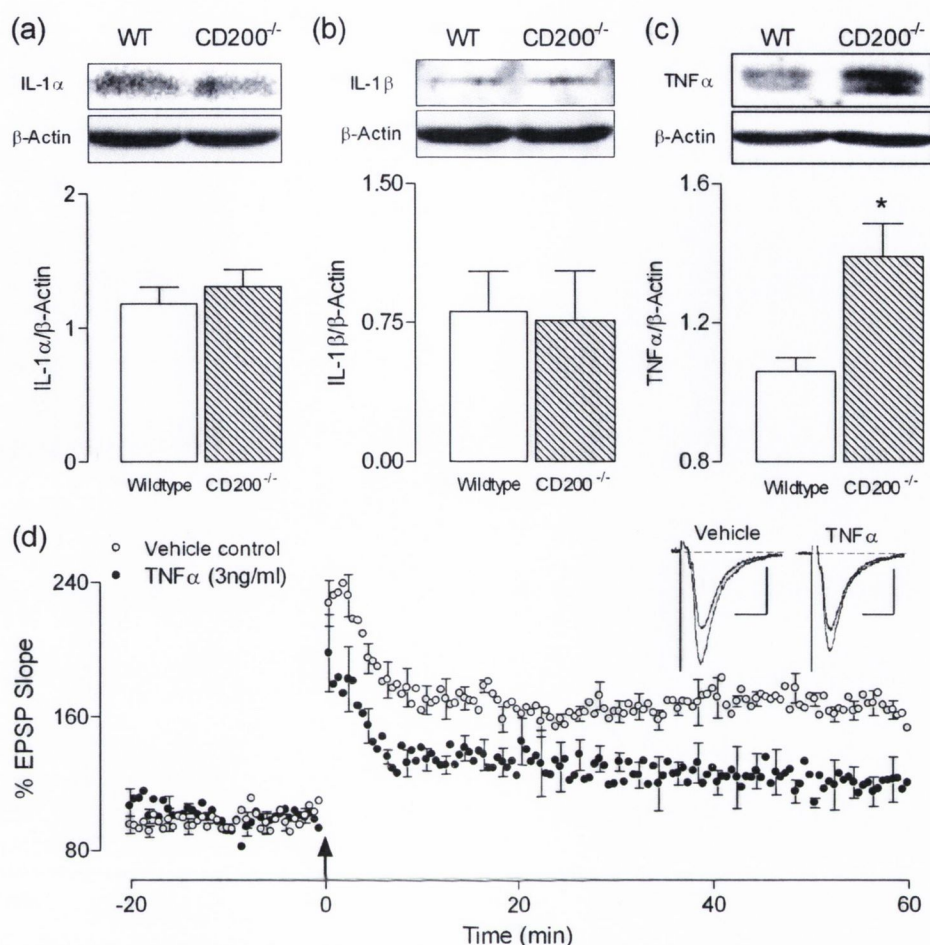
FIGURE 7. **Increased hippocampal expression of TNFα in CD200$^{-/-}$ mice may underlie the associated deficit in LTP.** IL-1α and IL-1β were similar in tissue prepared from wild type and CD200$^{-/-}$ mice (a and b), but TNFα was significantly increased (p • 0.05; Student's t test for independent means; c), as revealed by sample immunoblots and analysis of densitometric data. Application of TNFα (3 ng/ml) to hippocampal slices significantly impaired LTP relative to vehicle controls (p • 0.05; unpaired Student's t test; three slices from two mice; d). Sample EPSP traces immediately prior to and 60 min following TBS are presented (*scale bars*, 1 mV/20 ms). *Error bars*, S.E.

which is indicative of NFκB activation. These changes clearly provide one possible explanation for the increased responsiveness of these cells to LPS and Pam$_3$Csk$_4$ in the present study and perhaps also in other models.

Loss of CD200 increases expression of markers of microglial activation in mixed glial cultures; CD200 deficiency was associated with enhanced expression of CD40 mRNA but not CD11b mRNA. In parallel, flow cytometry revealed that these markers and also MHCII were increased on CD11b-positive cells prepared from CD200$^{-/-}$ mice. Previous studies have highlighted the importance of the interaction between CD200 and CD200R in maintaining the quiescent state of microglia and have revealed that the age-related and Aβ-induced increases in microglial activation are coupled with decreased CD200 expression on neurons (8, 14, 21). The present observations also concur with the findings that under resting conditions, spinal cord microglia adopt an inflammatory morphology expressing more CD11b (9), and the number of CD45$^+$ CD11b$^+$ cells prepared from retina of CD200$^{-/-}$ mice was increased (10).

In the past decade, it has become clear that neuroinflammatory changes, coupled with increased microglial activation,

negatively affect synaptic plasticity in aged, LPS-treated, and Aβ-treated rats (15, 33–35). These observations are corroborated in this study, where we directly associate the loss of CD200 with microglial activation and a deficit in LTP. The evidence indicates that slices prepared from CD200$^{-/-}$ mice do not display LTP to the same degree as slices prepared from wild type mice. One possible explanation for this is that TNFα, which is increased in hippocampal tissue prepared from these mice, is released from activated microglia and inhibits LTP. We demonstrate that TNFα inhibits TBS-induced LTP in mouse Schaffer collateral-CA1 synapses, which concurs with previous evidence indicating that it exerts a similar effect on tetanus-induced LTP in rats in vitro and in vivo (17, 19, 23).

In addition to the decrease in LTP observed in untreated slices prepared from CD200$^{-/-}$ mice, the data indicate that a subthreshold concentration of LPS or Pam$_3$Csk$_4$, which exerts minimal effects on LTP in wild type mice, markedly impairs LTP in slices prepared from CD200$^{-/-}$ mice. These findings show for the first time that activation of TLR2 leads to inhibition of LTP and further emphasize the protective effect of CD200-CD200R interaction, such that a deficit in CD200 leads to increased susceptibility to inflammatory stimuli. At this
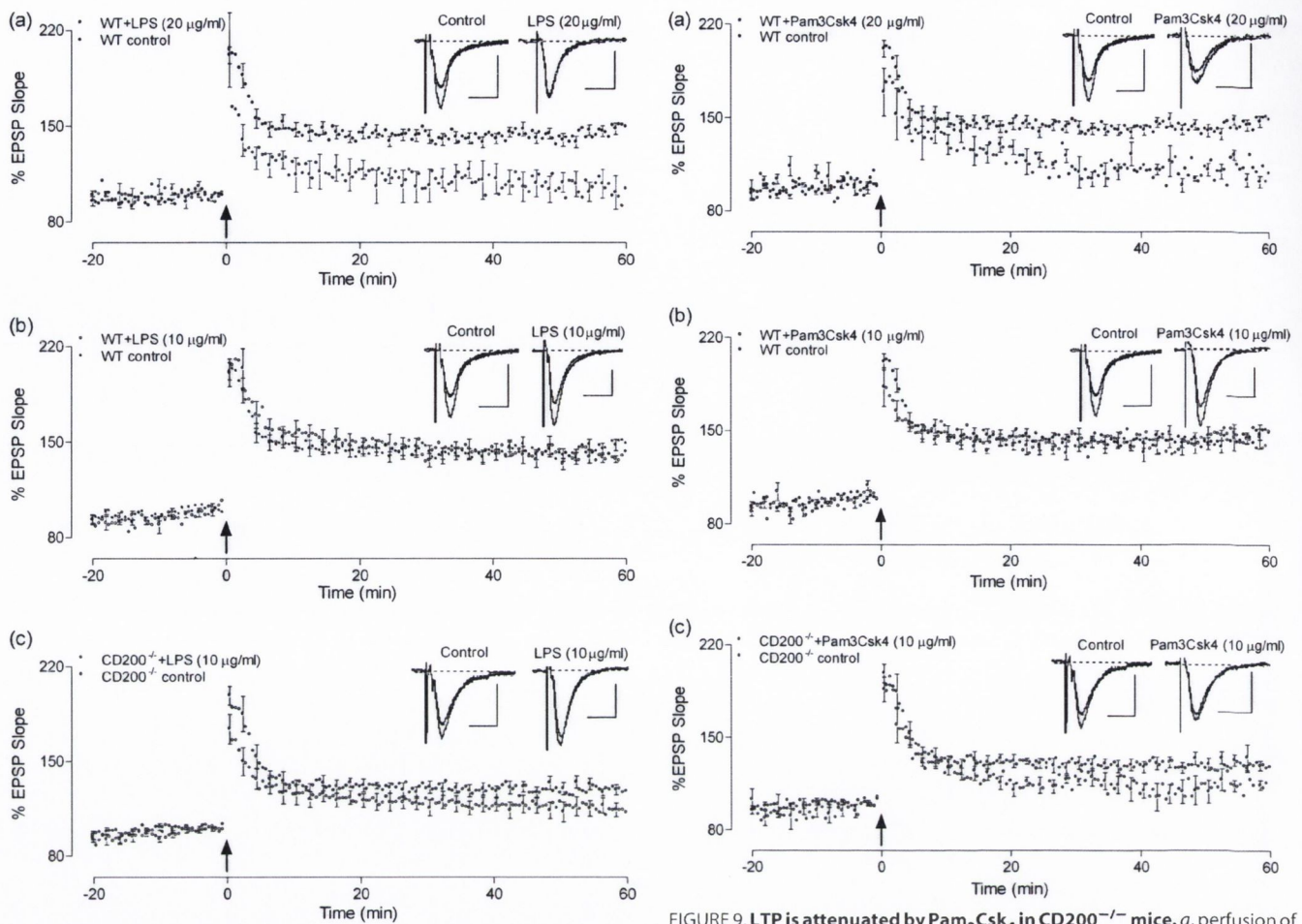
FIGURE 8. **LTP is attenuated by LPS in CD200$^{-/-}$ mice.** *a*, perfusion of LPS (20 μg/ml) for 60 min prior to TBS (*arrow*) decreased LTP in slices prepared from wild type mice (five slices from five mice), and the mean percentage EPSP slope in the last 5 min of the experiment was significantly decreased compared with control slices ($p \cdot$ 0.0001; 15 slices from 11 mice). *b* and *c*, LTP in slices prepared from wild type mice was unaffected by perfusion of 10 μg/ml LPS for 20 min prior to TBS (*b*; seven slices from six mice relative to control 15 slices from 11 mice), but LTP was attenuated in slices from CD200$^{\cdot/\cdot}$ mice (*c*; $p \cdot$ 0.05; 13 slices from nine mice relative to control 12 slices from seven mice). Sample EPSP traces immediately prior to and 60 min following TBS are presented (*scale bars*, 1 mV/20 ms). *Error bars*, S.E.

FIGURE 9. **LTP is attenuated by Pam$_3$Csk$_4$ in CD200$^{-/-}$ mice.** *a*, perfusion of Pam$_3$Csk$_4$ (20 μg/ml) for 60 min prior to TBS (*arrow*) decreased LTP in slices prepared from wild type mice (three slices from three mice), and the mean percentage EPSP slope in the last 5 min of the experiment was significantly decreased compared with control slices (15 slices from 11 mice; $p \cdot$ 0.001). *b* and *c*, LTP in slices prepared from wild type mice was unaffected by perfusion of 10 μg/ml Pam$_3$Csk$_4$ for 20 min prior to TBS (*b*; four slices from three mice relative to control 15 slices from 11 mice). However, LTP was attenuated in slices from CD200$^{\cdot/\cdot}$ mice following treatment with 10 μg/ml Pam$_3$Csk$_4$ (*c*; six slices from five mice relative to control 12 slices from seven mice; $p \cdot$ 0.05). Sample EPSP traces immediately prior to and 60 min following TBS are presented (*scale bars*, 1 mV/20 ms). *Error bars*, S.E.

point, it is unclear whether the effects of LPS or Pam$_3$Csk$_4$ on LTP are secondary to changes in glia or are a consequence of a direct effect on neuronal TLR4 and TLR2. In this regard, it is important to note that although some groups have reported neuronal expression of most TLRs both in vitro and in vivo (36, 37), others have been unable to demonstrate expression of TLR2 on neurons (38). The implication of this finding for the present study is that the mechanism underlying the Pam$_3$Csk$_4$-induced depression in LTP may result from its ability to release IL-1β, IL-6, and TNFα from glia; each of these inflammatory cytokines has been shown to inhibit LTP (17, 39, 40).

Although there is an accumulating body of evidence indicating that CD200 deficiency is associated with increased inflammatory changes in several tissues, including the brain, the effect on neuronal function is relatively unexplored. Here we report that activation of TLR4 and -2 exacerbates neuroinflammatory changes in the absence of CD200 and, importantly, demon-

strate that CD200 deficiency also exerts a negative effect on LTP. A key factor underlying these changes is increased expression of these receptors. The findings highlight the importance of CD200 as a potential therapeutic target in disorders that are characterized by neuroinflammatory changes, coupled with loss of synaptic function.

REFERENCES

1. Barclay, A. N. (1981) Immunology **44,** 727–736
2. Pallasch, C. P., Ulbrich, S., Brinker, R., Hallek, M., Uger, R. A., and Wendtner, C. M. (2009) Leuk. Res. **33,** 460–464
3. Siva, A., Xin, H., Qin, F., Oltean, D., Bowdish, K. S., and Kretz-Rommel, A. (2008) Cancer Immunol. Immunother. **57,** 987–996
4. Gorczynski, R. M., Yu, K., and Clark, D. (2000) J. Immunol. **165,**

4854–4860

5. Rosenblum, M. D., Olasz, E., Woodliff, J. E., Johnson, B. D., Konkol, M. C., Gerber, K. A., Orentas, R. J., Sandford, G., and Truitt, R. L. (2004) Blood **103**, 2691–2698

6. Barclay, A. N., Wright, G. J., Brooke, G., and Brown, M. H. (2002) Trends Immunol. **23**, 285–290

7. Koning, N., Swaab, D. F., Hoek, R. M., and Huitinga, I. (2009) J. Neuropathol. Exp. Neurol. **68**, 159–167

8. Lyons, A., Downer, E. J., Crotty, S., Nolan, Y. M., Mills, K. H., and Lynch, M. A. (2007) J. Neurosci. **27**, 8309–8313

9. Hoek, R. M., Ruuls, S. R., Murphy, C. A., Wright, G. J., Goddard, R., Zurawski, S. M., Blom, B., Homola, M. E., Streit, W. J., Brown, M. H., Barclay, A. N., and Sedgwick, J. D. (2000) Science **290**, 1768–1771

10. Broderick, C., Hoek, R. M., Forrester, J. V., Liversidge, J., Sedgwick, J. D., and Dick, A. D. (2002) Am. J. Pathol. **161**, 1669–1677

11. Gorczynski, R. M., Chen, Z., Yu, K., and Hu, J. (2001) Clin. Immunol. **101**, 328–334

12. Gorczynski, R. M., Chen, Z., Lee, L., Yu, K., and Hu, J. (2002) Clin. Immunol. **104**, 256–264

13. Chitnis, T., Imitola, J., Wang, Y., Elyaman, W., Chawla, P., Sharuk, M., Raddassi, K., Bronson, R. T., and Khoury, S. J. (2007) Am. J. Pathol. **170**, 1695–1712

14. Downer, E. J., Cowley, T. R., Lyons, A., Mills, K. H., Berezin, V., Bock, E., and Lynch, M. A. (2010) Neurobiol Aging **31**, 118–128

15. Lynch, A. M., Loane, D. J., Minogue, A. M., Clarke, R. M., Kilroy, D., Nally, R. E., Roche, O. J., O'Connell, F., and Lynch, M. A. (2007) Neurobiol. Aging **28**, 845–855

16. Nolan, Y., Maher, F. O., Martin, D. S., Clarke, R. M., Brady, M. T., Bolton, A. E., Mills, K. H., and Lynch, M. A. (2005) J. Biol. Chem. **280**, 9354–9362

17. Cowley, T. R., O'Sullivan, J., Blau, C., Deighan, B. F., Jones, R., Kerskens, C., Richardson, J. C., Virley, D., Upton, N., and Lynch, M. A. (2010) Neurobiol. Aging, in press

18. Costello, D. A., Watson, M. B., Cowley, T. R., Murphy, N., Murphy Royal, C., Garlanda, C., and Lynch, M. A. (2011) J. Neurosci. **31**, 3871–3879

19. Butler, M. P., O'Connor, J. J., and Moynagh, P. N. (2004) Neuroscience **124**, 319–326

20. Cunningham, A. J., Murray, C. A., O'Neill, L. A., Lynch, M. A., and O'Connor, J. J. (1996) Neurosci. Lett. **203**, 17–20

21. Lyons, A., McQuillan, K., Deighan, B. F., O'Reilly, J. A., Downer, E. J., Murphy, A. C., Watson, M., Piazza, A., O'Connell, F., Griffin, R., Mills, K. H., and Lynch, M. A. (2009) Brain Behav. Immun. **23**, 1020–1027

22. Carson, M. J., Reilly, C. R., Sutcliffe, J. G., and Lo, D. (1998) Glia **22**, 72–85

23. Tancredi, V., D'Arcangelo, G., Grassi, F., Tarroni, P., Palmieri, G., Santoni, A., and Eusebi, F. (1992) Neurosci. Lett. **146**, 176–178

24. Lin, H. Y., Tang, C. H., Chen, J. H., Chuang, J. Y., Huang, S. M., Tan, T. W., Lai, C. H., and Lu, D. Y. (2010) J. Cell Physiol. **226**, 1573–1582

25. Lotz, M., Ebert, S., Esselmann, H., Iliev, A. I., Prinz, M., Wiazewicz, N., Wiltfang, J., Gerber, J., and Nau, R. (2005) J. Neurochem **94**, 289–298

26. Mukhopadhyay, S., Plüddemann, A., Hoe, J. C., Williams, K. J., Varin, A., Makepeace, K., Aknin, M. L., Bowdish, D. M., Smale, S. T., Barclay, A. N., and Gordon, S. (2010) Cell Host Microbe **8**, 236–247

27. Snelgrove, R. J., Goulding, J., Didierlaurent, A. M., Lyonga, D., Vekaria, S., Edwards, L., Gwyer, E., Sedgwick, J. D., Barclay, A. N., and Hussell, T. (2008) Nat. Immunol. **9**, 1074–1083

28. Vincent, V. A., Tilders, F. J., and Van Dam, A. M. (1997) Glia **19**, 190–198

29. Vincent, V. A., Van Dam, A. M., Persoons, J. H., Schotanus, K., Steinbusch, H. W., Schoffelmeer, A. N., and Berkenbosch, F. (1996) Glia **17**, 94–102

30. Hailer, N. P., Heppner, F. L., Haas, D., and Nitsch, R. (1998) Brain Pathol. **8**, 459–474

31. Deckert, M., Sedgwick, J. D., Fischer, E., and Schlüter, D. (2006) Acta Neuropathol. **111**, 548–558

32. Mihrshahi, R., Barclay, A. N., and Brown, M. H. (2009) J. Immunol. **183**, 4879–4886

33. Hauss-Wegrzyniak, B., Lynch, M. A., Vraniak, P. D., and Wenk, G. L. (2002) Exp. Neurol. **176**, 336–341

34. Rosi, S., Vazdarjanova, A., Ramirez-Amaya, V., Worley, P. F., Barnes, C. A., and Wenk, G. L. (2006) Neuroscience **142**, 1303–1315

35. Griffin, R., Nally, R., Nolan, Y., McCartney, Y., Linden, J., and Lynch, M. A. (2006) J. Neurochem. **99**, 1263–1272

36. Tang, S. C., Arumugam, T. V., Xu, X., Cheng, A., Mughal, M. R., Jo, D. G., Lathia, J. D., Siler, D. A., Chigurupati, S., Ouyang, X., Magnus, T., Camandola, S., and Mattson, M. P. (2007) Proc. Natl. Acad. Sci. U.S.A. **104**, 13798–13803

37. Mishra, B. B., Mishra, P. K., and Teale, J. M. (2006) J. Neuroimmunol. **181**, 46–56

38. Lehnardt, S., Henneke, P., Lien, E., Kasper, D. L., Volpe, J. J., Bechmann, I., Nitsch, R., Weber, J. R., Golenbock, D. T., and Vartanian, T. (2006) J. Immunol. **177**, 583–592

39. Tancredi, V., D'Antuono, M., Cafè, C., Giovedì, S., Buè, M. C., D'Arcangelo, G., Onofri, F., and Benfenati, F. (2000) J. Neurochem. **75**, 634–643

40. Murray, C. A., and Lynch, M. A. (1998) J. Neurosci. **18**, 2974–2981